Transport Canada
Development

Transports Canada
Développement

TP 5232E

Modelling of Heat Flow in Ships

Summary Report

Prepared for
Transportation
Development Centre

MARCH 1984

CA1
DTC 845
84
M63S
c.2

Canada

85-2370/

TP5232E

THE MODELLING OF HEAT FLOW IN SHIPS

SUMMARY REPORT

by

Dr. A. Firmin

H.G. Engineering Ltd.
260 Lesmill Rd., Don Mills, Ontario
(in association with Hooper and Angus Ltd.)

March 1984

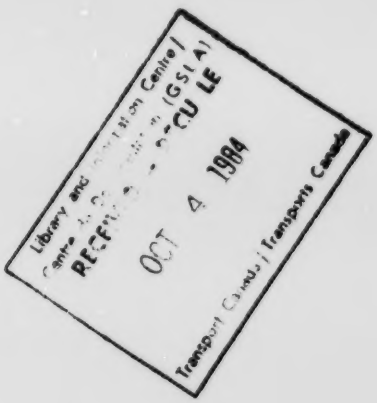

The contents of this report reflect the views of the contractor and not necessarily the official views or policies of the Transportation Development Centre of Transport Canada.

REPORT DOCUMENTATION FORM

1. Transport Canada Report No.	2. TDC Project No.	3. Recipient's Catalogue No.
TP 5232E	4555, 8953	

4. Title and Subtitle	5. Report Date
MODELLING OF HEAT FLOW IN SHIPS, Summary	MARCH 1984
	6. Performing Organization Report No.

7. Author(s)	8. Transport Canada File No.
Dr. A. Firmin	D1460-129-3

9. Performing Organization Name and Address	10. DSS File No.
H.G, Engineering Ltd. 260 Lesmill Road Don Mills, Ontario M3B 2T5	17SV.T8200-8-8559
	11. DSS or Transport Canada Contract No. OSV79-00044 OST81-00108

12. Sponsoring Agency Name and Address	13. Type of Report and Period Covered
Transportation Development Centre (TDC) 1000 Sherbrooke Street West Suite 2421 Montreal, Quebec H3A 2R3	Summary; Nov. 79-Sept. 83
	14. Sponsoring Agency Code TDC 4555, 8953

15. Supplementary Notes	16. TDC Project Officer
Summary of TP5001E "Modelling of Heat Flow in Ships" (September 1983)	I.M. Bayly

17. Abstract

Various analytical models have been developed for studying the heat flow in ship's structures. A finite element program, ASASHEAT, has been adapted to deal with the particular problems associated with fabricated plate structures. Several different ship's sections have been analyzed using this program and the results reported for the extreme temperature conditions anticipated in the Arctic. More detailed analyses of typical cells from the section of a ship's hull have been made to illustrate how non-linear, local temperature variations and transient conditions may be handled.

Also included is a report on temperature measurements taken aboard the M.V. Arctic during a July crossing of the Atlantic from Antwerp to Nanisivik.

18. Key Words	19. Distribution Statement
Heat Flow in Ships, Thermal, Conduction, Radiation, Modelling, Ship, Finite Element, Flow Heat	Limited number of copies available from TDC

20. Security Classification (of this report)	21. Security Classification (of this page)	22. No. of Pages	23. Price
Unclassified	Unclassified	26	

TDC/CDT 79-005

FORMULE DE DOCUMENTATION POUR RAPPORT

1. Nº du rapport Transports Canada	2. Nº de l'étude — CDT	3. Nº de catalogue du destinataire
4. Titre et sous-titre		5. Date du rapport
		6. Nº du rapport de l'organisme exécutant
7. Auteur(s)		8. Nº de dossier Transports Canada
9. Nom et adresse de l'organisme exécutant		10. Nº de dossier — ASC
		11 Nº de contrat — ASC ou Transports Canada
12. Nom et adresse de l'organisme parrain		13 Genre de rapport et période visée
		14 Code de l'organisme parrain
15. Remarques additionnelles		16 Agent de projet — CDT

17. Résumé

18. Mots-clés	19. Diffusion

20. Classification de sécurité (de ce rapport)	21. Classification de sécurité (de cette page)	22. Nombre de pages	23. Prix

CDT/ TDC 79-005

FORMULE DE DOCUMENTATION POUR RAPPORT

1. Nº du rapport Transports Canada	2. Nº de l'étude — CDT	3. Nº de catalogue du destinataire
TP 5232E	4555, 8953	

4. Titre et sous-titre	5. Date du rapport
MODELLING OF HEAT FLOW IN SHIPS, Summary	mars 1984
	6. Nº du rapport de l'organisme exécutant

7. Auteur(s)	8. Nº de dossier Transports Canada
Dr. A. Firmin	D1460-129-3

9. Nom et adresse de l'organisme exécutant	10. Nº de dossier — ASC
H.G. Engineering Limitée 260 Lesmill Road Don Mills, Ontario M3B 2T5	17SV.T8200-8-8559
	11. Nº de contrat — ASC ou Transports Canada OSV79-00044 OST81-00108

12. Nom et adresse de l'organisme parrain	13. Genre de rapport et période visée
Centre de développement des transports (CDT) 1000 ouest, rue Sherbrooke Suite 2421 Montréal, Québec H3A 2R3	Sommaire; nov. 79-sept. 83
	14. Code de l'organisme parrain CDT 4555, 8953

15. Remarques additionnelles	16. Agent de projet — CDT
Sommaire de TP5001E "Modelling of Heat Flow in Ships" (Septembre 1983)	I.M. Bayly

17. Résumé

Les échanges thermiques qui peuvent se produire dans la structure des navires ont pu être étudiés grâce à divers modèles analytiques, notamment le programme ASASHEAT qui fait appel à la méthode des éléments finis et qui a été adapté aux particularités des structures mécano-soudées. Ce programme peut s'appliquer à diverses parties d'un navire et prendre en compte les températures extrêmes régnant dans l'Arctique. Des analyses plus poussées de cellules types faisant partie de la coque ont été faites, montrant la voie à suivre pour maîtriser les fluctuations aléatoires et ponctuelles des températures ainsi que les conditions transitoires.

Le rapport présente, en outre, un relevé des températures mesurées à bord de l'Arctic durant son périple de juillet, entre Anvers et Nanisivik.

18. Mots-clés	19. Diffusion
Echanges thermiques, propagation de la chaleur, conduction, convection, radiation, modélisation, navires, méthode des éléments finis	Le CDT dispose d'un nombre limité d'exemplaires

20. Classification de sécurité (de ce rapport)	21. Classification de sécurité (de cette page)	22. Nombre de pages	23. Prix
non-classifié	non-classifiée	26	

CDT/TDC 79-005

REPORT DOCUMENTATION FORM

1. Transport Canada Report No.	2. TDC Project No.	3. Recipient's Catalogue No.
4. Title and Subtitle		5. Report Date
		6. Performing Organization Report No.
7. Author(s)		8. Transport Canada File No.
9. Performing Organization Name and Address		10. DSS File No.
		11. DSS or Transport Canada Contract No.
12. Sponsoring Agency Name and Address		13. Type of Report and Period Covered
		14. Sponsoring Agency Code
15. Supplementary Notes		16. TDC Project Officer

17. Abstract

18. Key Words	19. Distribution Statement

20. Security Classification (of this report)	21. Security Classification (of this page)	22. No. of Pages	23. Price

SUMMARY REPORT ON THE MODELLING OF HEAT FLOW IN SHIPS

CONTENTS

		Page No.
1.	INTRODUCTION	1
2.	HEAT TRANSFER IN PLATE FABRICATED STRUCTURES	4
	2.1 Heat Flow Mechanisms	4
	2.2 Heat Flux in a Typical Cell	4
	2.3 Computer Based Numerical Methods	7
	2.4 Evaluation of Plate Convection Coefficients	8
	2.5 Programs for Heat Transfer	8
3.	HEAT FLOW MODELS IN SHIP'S HULLS	9
	3.1 Multi-Compartment Models	9
	3.2 Single Cell Models	13
	3.3 Transient Thermal Solutions of a Cell from the M.V. Arctic	16
4.	M.V. ARCTIC TEMPERATURE MODELLING	18
5.	CONCLUSIONS	19
6.	REFERENCES	20

1. INTRODUCTION

The Canadian Arctic holds tremendous potential for providing Canada with energy and other mineral resources. As yet these reserves have been largely untapped due to the obvious engineering difficulties faced in these frontier regions. One mode of transportation that is available and highly valued is shipping. Experience in the operation of bulk carriers in the arctic environment is small compared with that in warmer waters, and consequently research into the special problems associated with arctic transportation has to be carried out to assist in the design of suitable ships.

A major design study underway at the time of the writing of this report is the Arctic Pilot Project whose goal is to prove the feasibility of shipping liquid natural gas (LNG) from Melville Island to the Canadian east coast by large ice breaking vessels. These ships are expected to carry 140,000 cubic meters capacity and be constructed of as much as 60,000 tons of steel. If built they will be the most sophisticated ice breakers in the world and the most powerful.

Clearly one of the major problems to be reckoned with in arctic transportation is the impact of the ship with the ice encountered in its voyage. An associated problem is the cold temperatures to which the ship will be subjected, because in general ship steels exhibit unacceptably brittle behavior at low temperatures. In addition extreme thermal gradients may give rise to local stresses that are significant compared to primary design loads and hence could affect design decisions. Finally, the energy losses through the outer skin of the ship's hull are an important consideration as the freezing of the ballast water must be prevented, or limited. Other temperature related problems are likely to become apparent as the number of arctic voyages increases and a broader experience is gained. It is important, therefore, to have a flexible and reliable means of predicting structural temperatures in any part of a ship given its environmental conditions.

The modelling of heat flow in ship's report describes work done to fulfill the requirement for temperature and heat flow predictions in typical ship hull construction under the conditions of the arctic environment. The work centered around the use of the computer to provide solutions to numerical models based on the equations of heat transfer. Because of the geometrical complexity of the ship's structure the finite element method was originally proposed for the representation of the conduction through the steel platework. In view of the large liquid or

vapor spaces within the ship's hull, it was realized that convection and radiation may also play an important role in the total heat transport mechanism and hence considerable attention was given to estimating these effects.

The initial part of the study involved the modification of an existing finite element code (ASASHEAT) to accomodate the appropriate boundary conditions for heat transfer from a plate's surface. At the same time an investigation was made of the convection of fluid within the typical cells of a ship's hull as it was felt that this provided a significant part of the total heat transport between the inside and outside plates. The numerical procedures used to obtain a solution to this fluid mechanics problem proved inadequate, and no good alternative has yet been identified. Classical semi-empirical methods were therefore used to estimate these plate heat transfer coefficients.

Following this initial development work a number of typical hull structures were modelled and used to calculate temperature distributions under a variety of boundary temperature conditions. It was concluded that the facility developed was adequate for the analysis of large sections of the hull but that in many cases such an analysis would be unnecessary as the heat transfer mechanism was dominated by the action of a single cell.

A study of the heat transfer within a typical cell bounded by frames and longitudinal members was conducted in more detail by two approaches. First by the use of a 2-D model which was able to handle the non-linear effects. This was prepared using a thermal network analysis program (THETA) that was simpler in its geometrical modelling facilities but more sophisticated in its ability to handle temperature dependent boundary conditions. The second model using ASASHEAT was able to study the cell as a three-dimensional assemblage of plates. In this case the sensitivity of the solution to varying surface conditions was tested.

Whilst the numerical techniques mentioned above are very powerful, the solutions they produce are only as good as the quality of the original data. It was realized early on that the weakness of the work was the inability to provide any calibration from real experience against which to measure the accuracy of the assumptions made in the model. An investigation was made into the possibility of conducting experimental work as back-up to this project and it was concluded that laboratory work at less than full scale was inappropriate and that measurements on a real ship were preferable. A parallel project was therefore undertaken to instrument typical sections of the M.V. Arctic, a bulk carrier designed for use in arctic waters. Temperature measurements were taken during a trip from Antwerp to Nanisivik in July

1981. A further set of measurements planned for November 1981 were unfortunately prevented by the destruction of part of the measuring apparatus. Thus although the first trip was successful the temperature differentials encountered were not those anticipated under winter conditions and were only of partial interest. Further experimental work will therefore be needed to verify the accuracy of the theoretical work reported here.

The main report (Modelling of Heat Flow in Ships, TP 5001E, September 1983) is divided into sections covering the following topics:

A review of past work
Technical considerations
Multi-compartment heat flow models
Single cell heat flow models
M.V. Arctic temperature monitoring

In addition a number of Appendices in the main report cover the theoretical foundation for the various analytical models used, validation of the ASASHEAT program, a summary of preferred units for the heat transfer calculation, useful conversion coefficients and some commonly used values for the key physical parameters. Finally, summary proposals are made for the re-instrumentation of the ship and for a possible laboratory apparatus.

2. HEAT TRANSFER IN PLATE FABRICATED STRUCTURES

2.1 Heat Flow Mechanisms

A typical section of an Arctic going vessel's hull is an assemblage of cells, large and small, surrounded by steel plate. These cells are not usually self contained but have cutouts that link them with the spaces of adjacent cells. Clearly, much of the interior of a ship used for transportation of goods is going to be open space, the majority of the steel being confined to the surrounding hull structure. In the double skin construction of typical ships designed for use in arctic waters, the space between the two skins is filled with cells that arise from the intersection of the hull plates, frames and longitudinal members. A typical section is shown in figure 1.

The heat flow through the hull is therefore a combination of the following mechanisms:

a) conduction through the steel plate surrounding the cells
b) natural convection in the fluid contained in the cavities which includes local convection in pockets and possibly large scale convection through several cells
c) radiation across air-filled regions
d) potentially, forced convection involving heat transfer through mass transport could also play a part.

The first step in the consideration of the total heat flow model must be to examine which of these mechanisms is important. Can any be ignored and under what circumstances will one dominate? In order to focus attention on a particular example, a typical cell encountered in the wall of a ship's hull is considered and the heat flux calculated for conduction, radiation and convection. The example is a rectangular cell of dimensions similar to those proposed for an LNG tanker and is shown in figure 2.

2.2 Heat Flux in a Typical Cell

If it is assumed a typical cell is bounded above and below by cells of similar proportions having similar temperature distributions, then the walls between the cells can be considered adiabatic. This simplifying assumption permits the approximate calculation of the three components of heat transfer in an air-filled cell. The values are as follows.

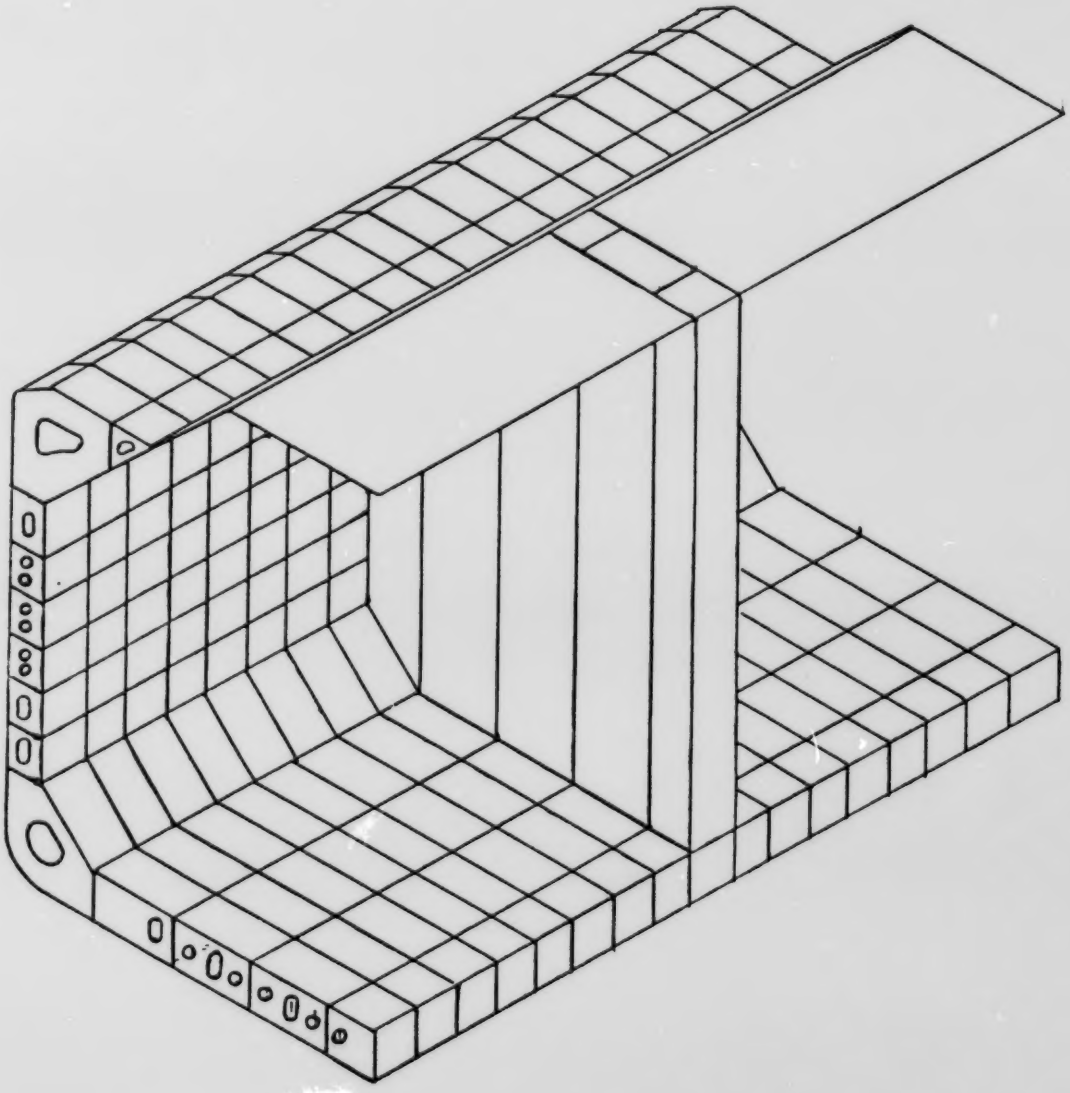

Figure 1 TYPICAL HULL CONSTRUCTION

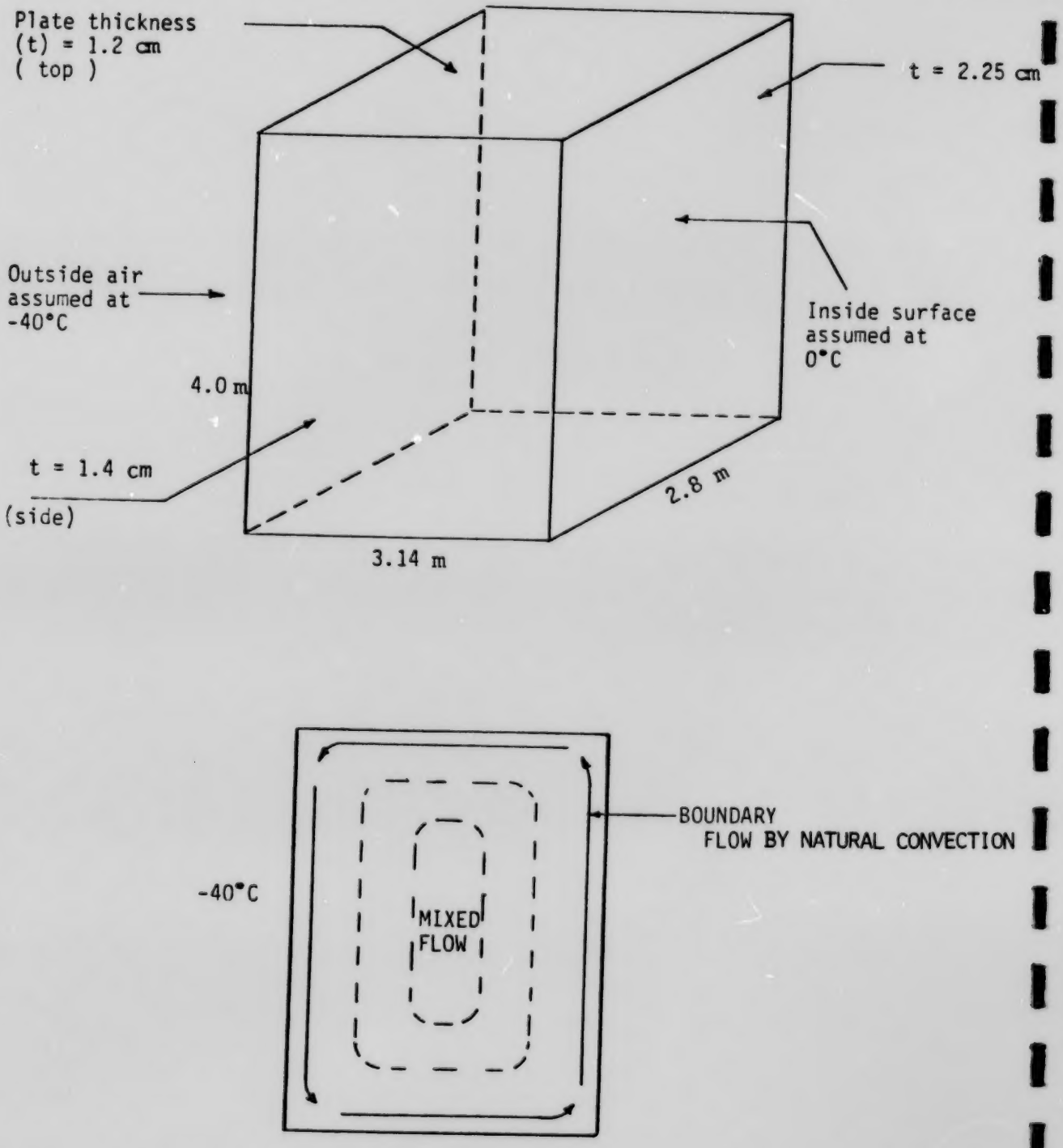

Figure 2 TYPICAL CELL

	Heat Flux	%
Radiation	74. W/M^2	49.5
Convection	70. W/M^2	47.0
Conduction	5.3 W/M^2	3.5
		100.0

From this it can be seen that under the circumstances postulated and in an air filled cell, the convection and radiation are going to play a large part in the determination of the heat flux. It is obviously important, therefore, to accurately estimate the heat transfer from the plate surfaces in addition to representing conduction.

2.3 Computer Based Numerical Methods

Finite difference and finite element methods are commonly used to solve problems in heat transfer. The finite element method has advantages when complex geometric shapes are involved which is typical of the plate assemblages of a ship's hull. The mechanics of finite element analysis involves the modelling of the structure as a number of discrete regions (finite elements) which satisfy the heat balance equations only at discrete points which are called "nodes". The behavior of the idealized model is described by the temperatures at every node. This method was chosen as the basis for the solution of the heat transfer in ship's hulls.

In contrast to the finite element method which is well suited to developing conduction models of two and three dimensional continua a simplified, less sophisticated approach is used in thermal network analysis. In this case links in the mesh must be specified explicitly. The real physical structure is idealized as a network of nodes connected by links that have thermal properties representing a variety of heat flux mechanisms. The main advantage of adopting such an approach is that non-linear phenomena may be more easily incorporated in the model. As radiation and convection both have a non-linear behavior it may be necessary to employ a non-linear solution where a linearized approximation to these effects is not appropriate. This approach has been used to complement the facilities of the linear finite element model.

In addition to the problem of heat flow the process of natural convection of the fluid (air, water or fuel oil) internal to the cells requires computation. The finite element technique can be adapted to solve fluid flow problems of this type however attempts made in this project proved numerically inadequate. Finite difference programs now exist that may be able to adequately model this type of flow.

2.4 Evaluation of Plate Convection Coefficients

The estimation of the surface heat transfer coefficients has been made following the assumption that the fluid boundary layer is thin compared to the major dimensions of the cell and that the central area of the cell is well mixed and at a uniform temperature. This assumption implies that each plate may be considered separately and a value calculated from the semi-empirical data already available in the literature. Calculations performed on this basis are contained in the program called FILMC which is included in the main report.

2.5 Programs for Heat Transfer

An existing finite element program, ASASHEAT, was taken in preference to developing a new code. At the commencement of the project this program was not capable of handling plate surface heat transfer and this extension to the program was made as part of the work undertaken. Subsequent revisions to the program now permit the inclusion of non-linear links for radiation or convective heat transfer. The ASASHEAT program is available for general use and can model the heat transfer processes in any type of hull configuration. Some examples of the use of this program are given in the report.

A non-linear thermal network program, THETA, was used to model the effects of radiation. This program is also commercially available. The approach adopted in this code is not appropriate for developing complex plate models.

3. HEAT FLOW MODELS IN SHIP'S HULLS

3.1 Multi-Compartment Models

The major temperature differences on a ship's hull are through the wall of the hull or vertically down the side. The heat flow analysis of a typical hull may therefore be represented by two typical models, one at the centre of a tank or hold and one at a major bulkhead. If it is assumed that the ambient conditions are symmetric about the longitudinal centre line of the ship, then it is possible to model only one half of a typical section.

Three different ship's hulls were studied with the intention of determining the extremes of steel plate temperatures that might be encountered in the Arctic. It was also assumed that local temperature variations were at this stage of secondary importance. The ships studied were a preliminary Arctic LNG carrier design; a bulk carrier, the M.V. Arctic and a Coast Guard icebreaker, the Pierre Radisson. Figures 3-5 illustrate finite element models representing the sections chosen.

In all cases it was assumed that the ambient air temperature was $-55^{o}C$ and the sea temperature was $-2^{o}C$. Various temperatures internal to the hull were assumed dependent on the ship in question. The external plate surface convective heat transfer coefficients were based on the best estimates available but were, in general, one or two orders of magnitude higher than the internal plate coefficients. Radiative solar heating was ignored as this would always seek to raise the plate temperatures, radiative cooling was included in the estimate of the external plate coefficients.

The calculation of the surface transfer from the internal plate surfaces by natural convection was the area of greatest uncertainty. The surface coefficients calculated were dependent on the mean cell temperature and the temperature drop assumed in the boundary layer. Apart from this the nature of the orientation of the stiffeners (vertical or horizontal) affects the surface transfer. It is believed that the real values would not differ significantly from those calculated from the semi-empirical methods adopted.

The overall conclusions reached in the analysis are that the external hull plates under steady-state conditions are going to follow the external ambient temperatures because the heat transfer rates on the external surfaces are so much higher than those internally. Internal

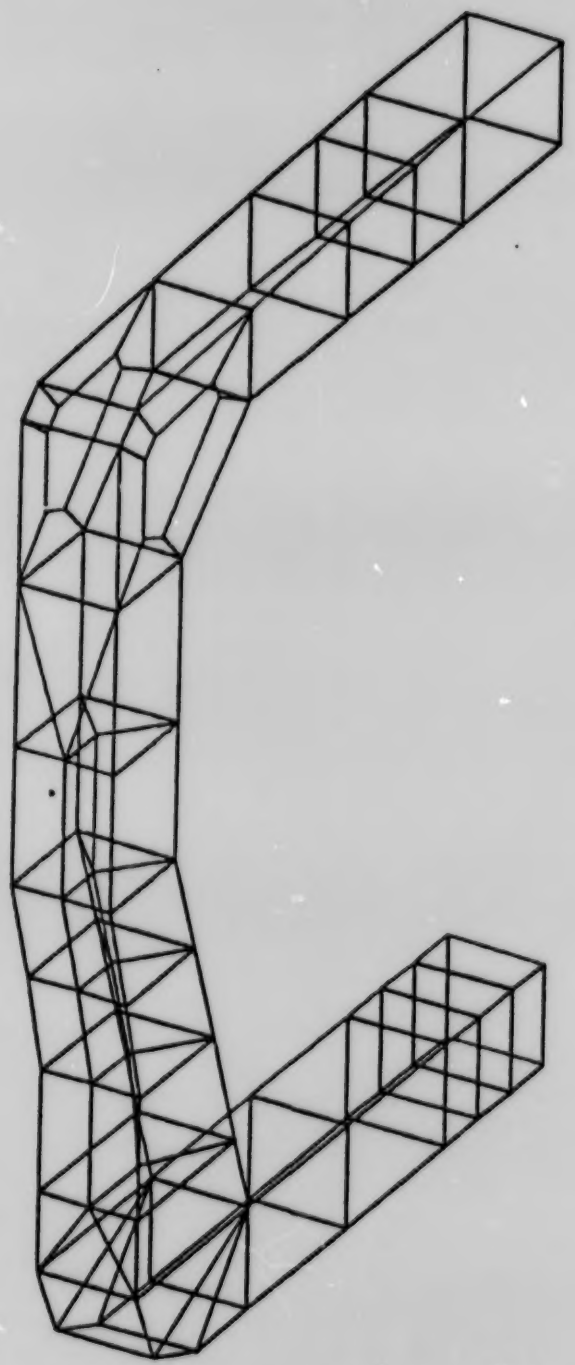

Figure 3

TWO FRAME FINITE ELEMENT MESH OF THE LNG CARRIER

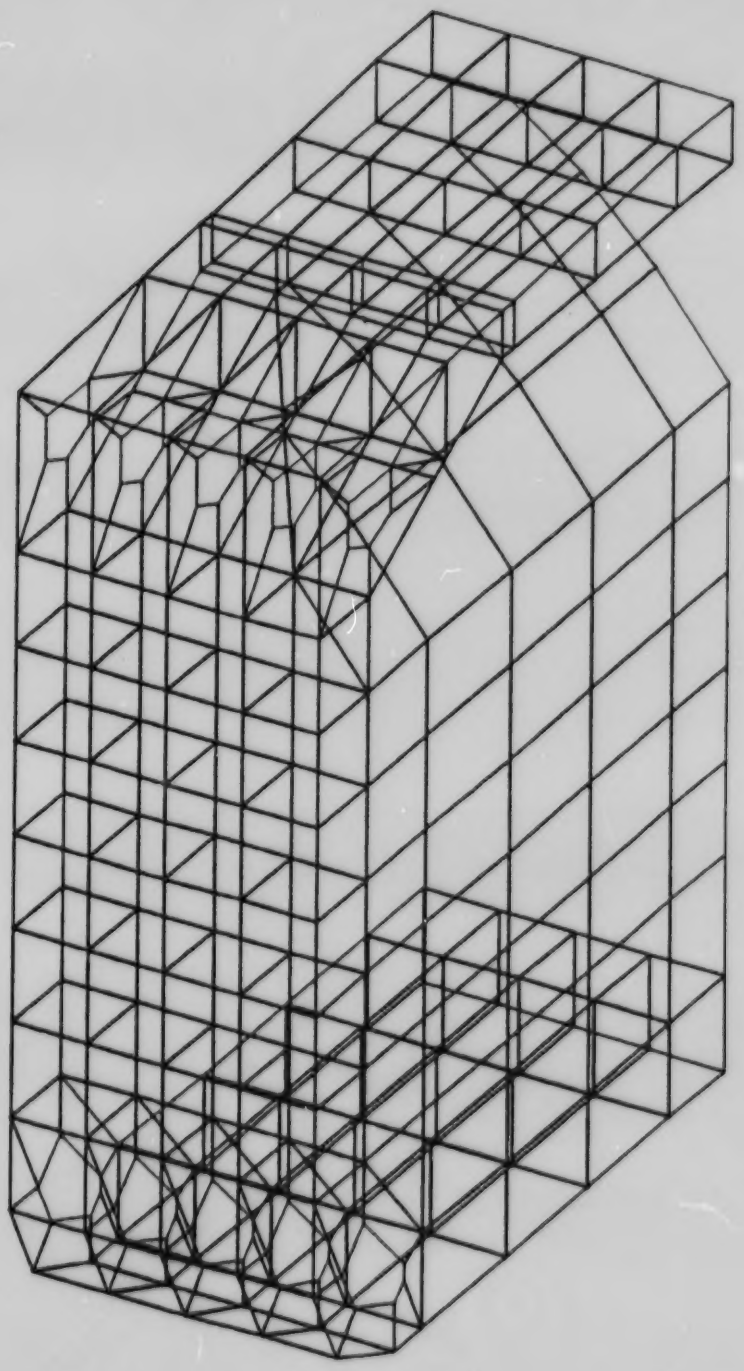

Figure 4 FIVE FRAME FINITE ELEMENT MESH INCLUDING BULKHEAD OF THE M.V. ARTIC

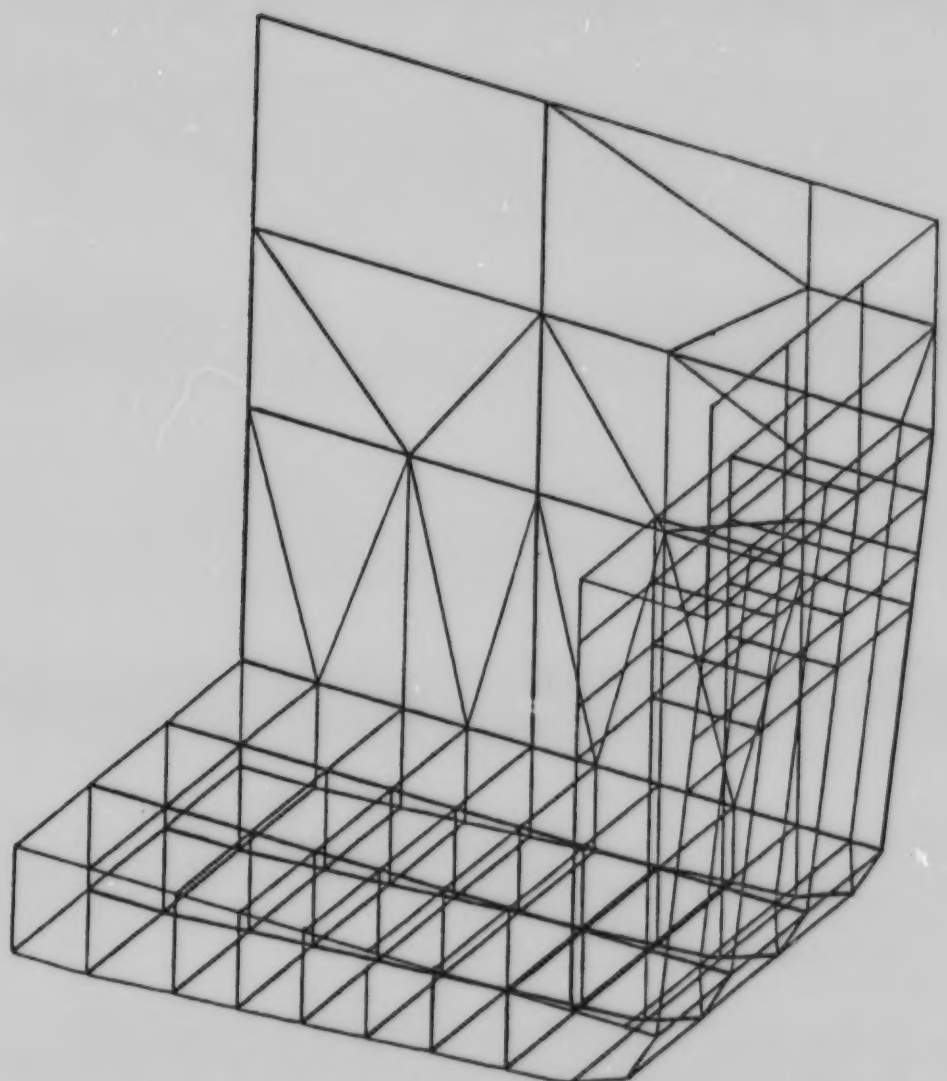

Figure 5 P. RADISSON

FINITE ELEMENT MESH

INCLUDING BULKHEAD

plate temperatures, on the other hand, can vary considerably depending on circumstances. For the purpose of establishing structural temperatures in the average sense, it is felt that the macro finite element models are sufficiently accurate. Such models can be used for establishing the quality of structural steels needed and for examining gross thermal stress effects that may be created internal to the hull. None of the models in the report have considered any other than the minimum external temperature conditions, however the same form of model could be used to establish temperature differences across the hull caused by wind cooling or solar heating.

In order to study the micro-thermal effects causing local temperature changes and to examine in more detail the heat flux through a typical cell, other models are more appropriate.

3.2 Single Cell Models

The heat transfer across a typical cell in a double skin hull has been shown to depend heavily on the convection and radiation components in addition to the conduction through the surrounding steel. The two former effects are non-linear due to the dependency of the surface coefficients on the surrounding temperatures.

A simple thermal network model (see Figure 6) using the non-linear THETA program was set up to study the single cell used in the original hand calculated estimates. The balance between the three heat transfer mechanisms differed from the original estimates. The non-linear solution computed more accurately the convective flow based on a lower temperature difference and hence a lower convective coefficient. The radiation component was lower for the same reason. The results indicate that for the particular example chosen, the balance of the heat flows is

	%
Radiation	17.39
Convection	58.95
Conduction	23.66
	100.00

A closer examination of the local temperature variations across a single cell was also made using a refined finite element model shown in Figure 7. The model was constructed to run on the ASASHEAT program with the same quadrilateral plate element. A variation of the surface coefficient was imposed on the model to represent the assumption that most of the heat transfer takes place at the centre of the plate and only 25% at the edges. A

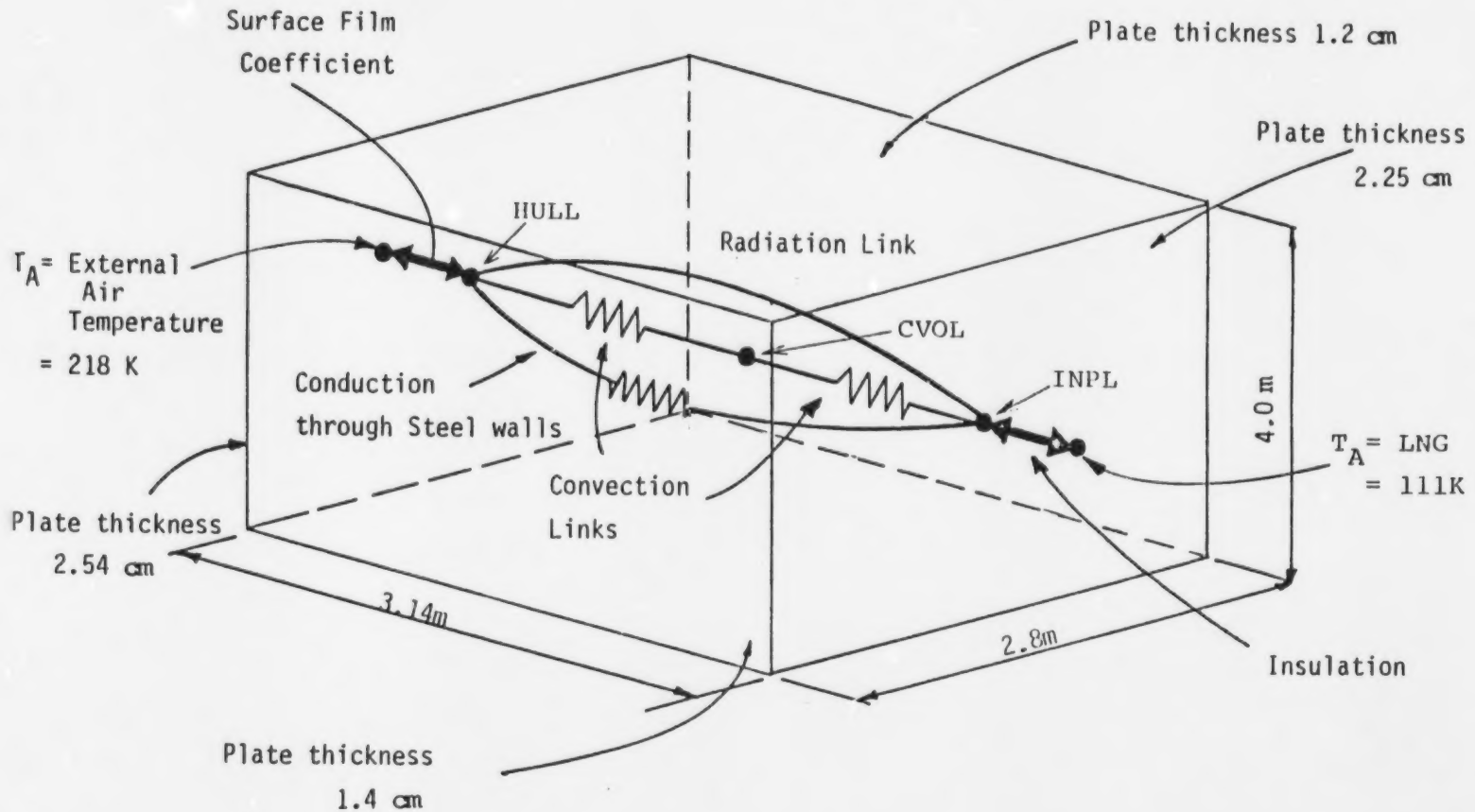

Figure 6 SINGLE CELL FROM PROPOSED LNG TANKER

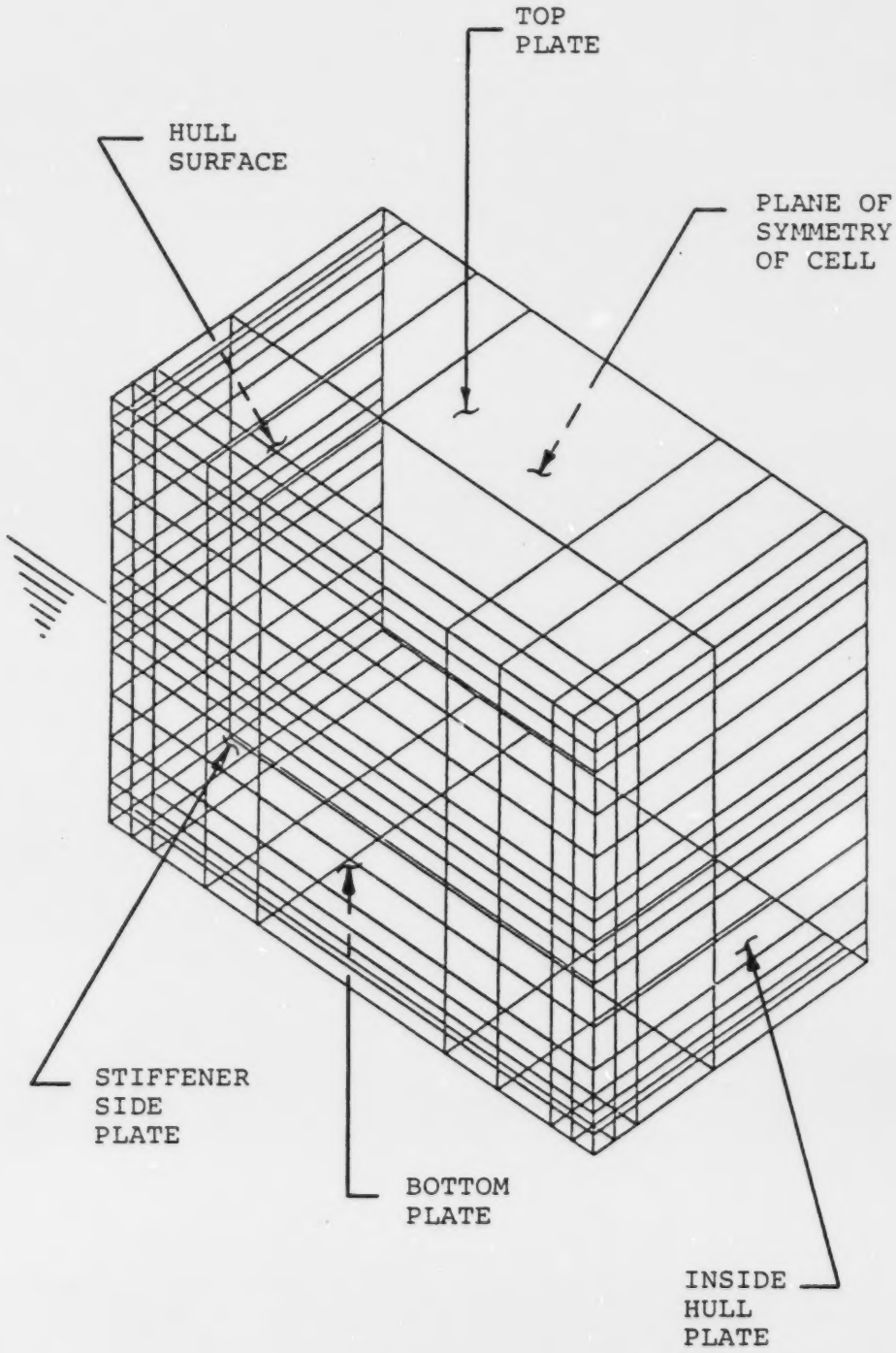

Figure 7

FINITE ELEMENT IDEALIZATION OF THE CELL

range of values for the internal conditions was taken assuming the cell was air, water or oil filled and assuming a variation of the calculated coefficients from +100% to -50% of the mean value. A steady-state solution was found for each case.

Varying the surface coefficients between wide limits demonstrated that the steady-state temperature solution for the case studied provides essentially the same mean plate temperatures. It was also discovered that changing the coefficients considerably effected the variation across the plate. The most important difference was the identification of steep temperature gradients near the edges of the plates and frames. This is worthy of further investigation as such temperature gradients may cause undesirable thermal stresses in the plates. Finally it should be noted that variations of the internal coefficients from +100% to -50% will have a marked effect on the time of the transient thermal solution.

3.3 Transient Thermal Solution of a Cell from the M.V. Arctic

During the progress of the analytical study a parallel project was undertaken to measure temperatures and heat flux values in cells of the M.V. Arctic. One successful voyage was undertaken and temperatures gathered, however before a run could be made at really low external temperatures the cables from the sensors to the monitoring equipment were destroyed. The data gathered in the first voyage served as a comparison for a thermal transient model of a single cell at the waterline. The nature of the idealization is shown in Figure 8.

Two analysis runs were made, the first used the external temperature transient measured during a voyage of the M.V. Arctic from Antwerp to Nanisivik, the second assumed the same transatlantic crossing, but with the external air and sea temperatures dropping to -55°C and -2°C respectively. The results from the analytical model followed closely the measured values recorded. This indicates that when taken over a long time scale, the surface coefficients chosen are sufficiently accurate to predict the response and that the characteristic time for the response of the cell is short. The temperature of the ballast water lags, by a few hours, the changing environmental temperatures.

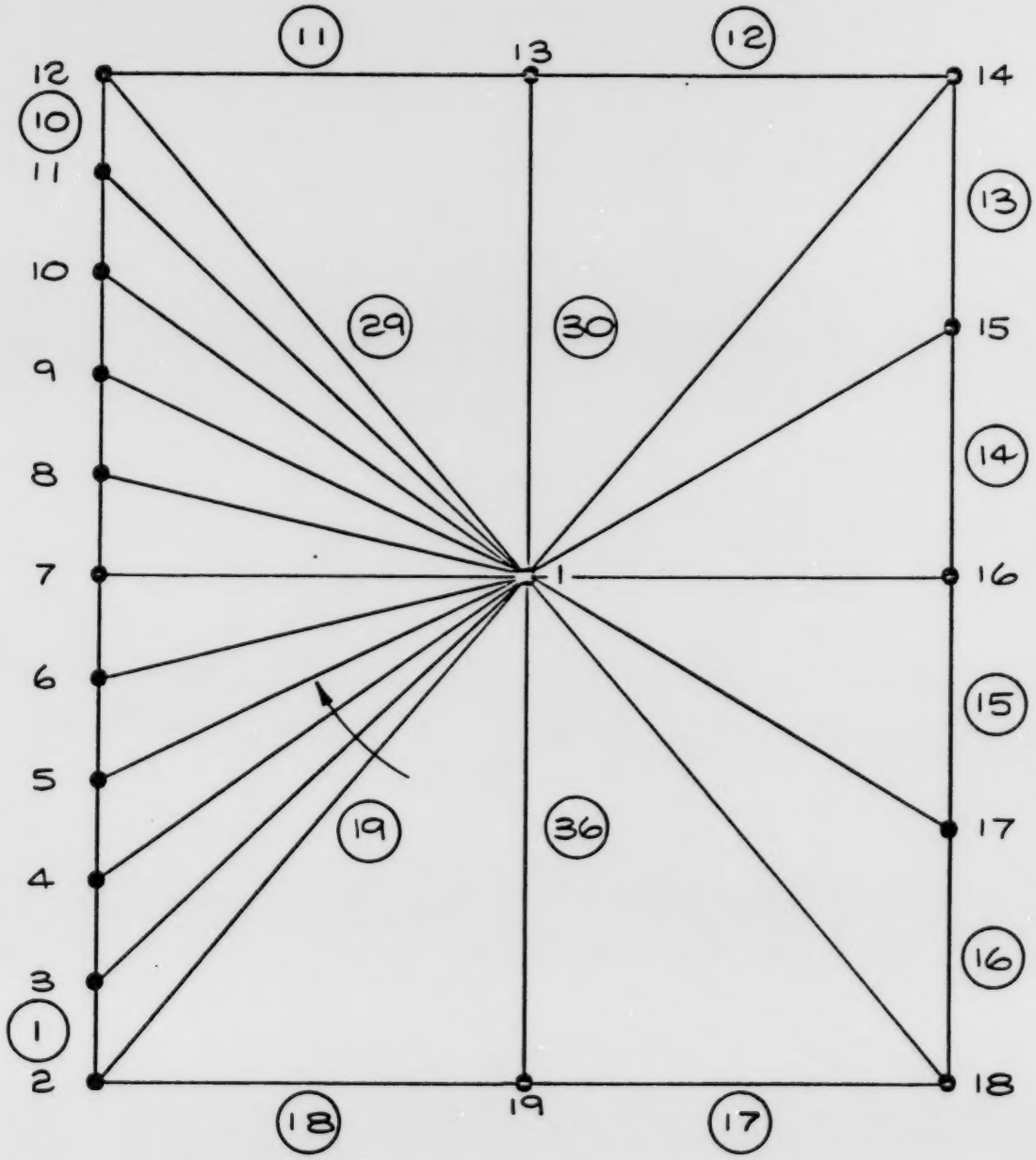

Figure 8

THERMAL NETWORK MODEL OF M.V. ARCTIC CELL

4. M.V. ARCTIC TEMPERATURE MONITORING

Following the numerical difficulties encountered in establishing the internal plate surface coefficients it was decided to monitor the thermal response of an actual vessel in Arctic service. An opportunity arose to participate in an on-going test program aboard the M.V. Arctic during the period July to November 1981.

The objective was to measure temperatures in the outside ballast tanks in a region removed from the engine room, and where the structure is typical of the standard hull construction. It was decided to monitor all the plates within two cells at the same horizontal level and two cells above and below the fully monitored cells. For one of the two cells the openings were covered by plates to prevent free motion of the fluid through the cell. The temperature measurements were made using precision thermistors mounted directly on the steel surfaces.

The ship sailed to Nanisivik from Antwerp under full ballast on June 26. The ballast tanks were purposely voided and refilled on entering the Gulf Stream on June 28. The maximum water temperature at that time was 12^{o}C. The sea and air temperatures fell continuously until the ship encountered ice on July 3, 1981.

The temperature values were recorded on magnetic tape and subsequently processed for display in a graphical form both as a transient and in a positional format as a plan of the layout on the cells. The following conclusions were drawn from a review of the recorded temperatures.

1) A stable temperature gradient is set up in the ballast water such that the upper levels are considerably warmer than the lower.

2) The outside plate temperature was maintained, at most, a couple of degrees above the sea temperature as the vessel sailed through Arctic waters.

3) The higher temperature of the ballast water in the upper cell is assumed to have been caused by daytime heating of the upper deck plates.

4) The air temperature measured in the hold is maintained 4^{o}C above the sea temperature and 2^{o}C above the average outside air temperature.

5. CONCLUSIONS

The overall conclusion of this report, concisely stated, is that a satisfactory analytical methodology has been demonstrated for the prediction of the temperature distributions throughout the hull of a ship in Arctic waters. However the numerical values predicted are dependent upon a knowledge of the physical data including the convective heat transfer surface coefficients. There are three future alternatives for investigating the real values of the latter more accurately, ship board monitoring; laboratory testing; and state of the art numerical analysis. The main report includes summary proposals as to how the experimental work might be conducted. It is recommended that the three alternatives be pursued as they all have the potential of adding to the understanding of the heat transfer through the cells under varied conditions. The prediction of local variations of temperature and such effects as ice build-up in the ballast water above the water line will be most affected by the accurate knowledge of the surface heat transfer effects.

REFERENCES

1. Basic Heat Transfer, M.N. Ozisik, McGraw-Hill, New York, 1977

2. Heat Transfer, A.J. Chapman, MacMillan Co., New York, 1960

3. Thermal Insulation Report, Society of Naval Architects, New York, TRB 4-7, 1974

4. Heat Transfer in an Oil Tank on Board the Danish Motor Tanker "Esso Aarkus", Danish Ship Research Institute, December 1971

5. Thermal Analysis for Complex Structural Systems, J.F. Cox, D.F. Cameal, Marine Technology Vol. 8, No. 4, Oct. 1971

6. Structural Analysis Including Thermal Effects for Icebreakers, E.W. Kiesling, Southwest Research Institute TCG 17961-A, June 1967

7. Heat Losses from Oil Tanker Cargoes, R.J. Saunders, C.Eng., British Ship Research Association

8. The Heating of High Viscosity Oils by Natural Convection using Horizontal Tubular Grids, C.B. Lamb, British Ship Research Association, J. Inst. of Petroleum, Vol. 57, Sept. 1971

9. Experimental Studies on Heat Transfer Coefficients and Effective Length of Tank Heating Coils in Vessels, Kurihara, Armagata and Mackowa, J.S.N.A. West Japan No. 40, July 1970

10. Finite Element Analysis of Free Convection Flows, B. Tabarrok and R.C. Lin, Int. J. Heat and Mass Transfer, Vol. 20 #9, 1977

11. Maximum Density Effects in the Free Convection of Liquids in a Closed Cell, Robillard and Vasseur, Can. J. Civil Eng., December 1979

12. ASASHEAT User's Manual, H.G. Engineering Ltd., June 1982

13. THETA User's Manual, H.G. Engineering Ltd., April 1982

14. THETA: A Desktop Computer Solution for Non-Linear Time Dependent Heat Flow Problems, P.J. Moir and J.R. Stoker (copies available from H.G. Engineering Ltd.)

15. Arctic Resources by Sea, Northern Associates Holdings Ltd., 1973

16. Heat Transmission, W.H. McAdams, 3rd ed. McGraw Hill Book Company, New York, 1954

17. An Analysis of Turbulent Free Convection Heat Transfer, F.J. Bayley, Proc. Inst. Mech. Eng. London 168: 361 (1955)

18. An Investigation of Turbulent Natural Convection in Air at Low Pressure Along a Vertical Heated Plate, C.Y. Warner and V.S. Arpaci, Int. J. Heat Mass Transfer 11: 347-406 (1968)

19. Heat Transfer and Flow Instability of Natural Convection over Upward-Facing Horizontal Surfaces, R. Ishiguro and T. Abe, Proc. Sixth International Heat Transfer Conference, Toronto, August 1978

20. The Influence of Aging Factors on the Emissivity of Reflective Insulations, F.C. Hooper and W.T. Moroz, A.S.T.M. Bulletin, #182, May 1952.

TP 5001 E

MODELLING OF HEAT FLOW IN SHIPS

PREPARED FOR:
TRANSPORT CANADA
TRANSPORTATION DEVELOPMENT CENTRE

BY:
H. G. ENGINEERING LIMITED
(in association with HOOPER & ANGUS LIMITED)

DSS CONTRACT NO: 17SV.T8200-8-8559

SEPTEMBER 1983

CA1
DTC 845
83
M63
c.2

MODELLING OF HEAT FLOW IN SHIPS

by

Dr. A. Firmin

H.G. Engineering Ltd.
260 Lesmill Rd., Don Mills, Ontario
(in association with Hooper and Angus Ltd.)

September 1983

The contents of this report reflect the views of the contractor and not necessarily the official views or policies of the Transportation Development Centre of Transport Canada.

The Project Team consisted of: -

H.G. Engineering
- Dr. A. Firmin
- Mr. D.J. Sandison
- Mr. D. Ruby

Hooper & Angus
- Prof. F. Hooper

University of Toronto
- Prof. B. Tabarrok

Others
- Mr. E. Bustard

REPORT DOCUMENTATION FORM

1. Transport Canada Report No.	2. TDC Project No.	3. Recipient's Catalogue No.
TP 5001E	4555, 8953	

4. Title and Subtitle	5. Report Date
MODELLING OF HEAT FLOW IN SHIPS	SEPTEMBER 1983
	6. Performing Organization Report No.

7. Author(s)	8. Transport Canada File No.
Dr. A. Firmin	D1460-129-3

9. Performing Organization Name and Address	10. DSS File No.
H.G. Engineering Ltd. 260 Lesmil Road Don Mills, Ontario M3B 2T5	17SV.T8200-8-8559
	11. DSS or Transport Canada Contract No. OSV 79-00044 OST 81-00108

12. Sponsoring Agency Name and Address	13. Type of Report and Period Covered
Transportation Development Centre (TDC) 1000 Sherbrooke Street West Suite 2421 Montreal, Quebec H3A 2R3	Final; Nov. 79 - Sept. 83
	14. Sponsoring Agency Code TDC 4555-8953

15. Supplementary Notes	16. TDC Project Officer
	I.M. Bayly

17. Abstract

Various analytical models have been developed for studying the heat flow in ship's structures. A finite element program, ASASHEAT, has been adapted to deal with the particular problems associated with fabricated plate structures. Several different ship's sections have been analyzed using this program and the results reported for the extreme temperature conditions anticipated in the Arctic. More detailed analyses of typical cells from the section of a ship's hull have been made to illustrate how non-linear, local temperature variations and transient conditions may be handled.

Also included is a report on temperature measurements taken aboard the M.V. Arctic during a July crossing of the Atlantic from Antwerp to Nanisivik.

18. Key Words	19. Distribution Statement
Heat Flow in Ships, Thermal, Conduction, Radiation, Modelling, Ship, Finite Element, Flow Heat	Limited number of copies available from TDC

20. Security Classification (of this report)	21. Security Classification (of this page)	22. No. of Pages	23. Price
Unclassified	Unclassified		

TDC/CDT 79-005

FORMULE DE DOCUMENTATION POUR RAPPORT

1. N° du rapport Transports Canada	2. N° de l'étude — CDT	3. N° de catalogue du destinataire
TP 5001E	4555, 8953	

4. Titre et sous-titre	5. Date du rapport
MODELLING OF HEAT FLOW IN SHIPS	septembre 1983
	6. N° du rapport de l'organisme exécutant

7. Auteur(s)	8. N° de dossier Transports Canada
Dr. A. Firmin	D1460-129-3

9. Nom et adresse de l'organisme exécutant	10. N° de dossier — ASC
H.G. Engineering Limitée 260 Lesmill Road Don Mills, Ontario M3B 2T5	17SV.T8200-8-8559
	11. N° de contrat — ASC ou Transports Canada OSV 79-00044 OST 81-00108

12. Nom et adresse de l'organisme parrain	13. Genre de rapport et période visée
Centre de développement des transports (CDT) 1000 ouest, rue Sherbrooke Suite 2421 Montréal, Québec H3A 2R3	Final; nov. 79 - sept. 83
	14. Code de l'organisme parrain CDT 4555, 8953

15. Remarques additionnelles	16. Agent de projet — CDT
	I.M. Bayly

17. Résumé

Les échanges thermiques qui peuvent se produire dans la structure des navires ont pu être étudiés grâce à divers modèles analytiques, notamment le programme ASASHEAT qui fait appel à la méthode des éléments finis et qui a été adapté aux particularités des structures mécano-soudées. Ce programme peut s'appliquer à diverses parties d'un navire et prendre en compte les températures extrêmes régnant dans l'Arctique. Des analyses plus poussées de cellules types faisant partie de la coque ont été faites, montrant la voie à suivre pour maîtriser les fluctuations aléatoires et ponctuelles des températures ainsi que les conditions transitoires.

Le rapport présente, en outre, un relevé des températures mesurées à bord de l'Arctic durant son périple de juillet, entre Anvers et Nanisivik.

18. Mots-clés	19. Diffusion
Echanges thermiques, propagation de la chaleur, conduction, convection, radiation, modélisation, navires, méthode des éléments finis	Le CDT dispose d'un nombre limité d'exemplaires

20. Classification de sécurité (de ce rapport)	21. Classification de sécurité (de cette page)	22. Nombre de pages	23. Prix
non-classifié	non-classifiée		

CDT/TDC 79-005

ACKNOWLEDGEMENTS

H.G. Engineering wishes to thank Profs. Taborrak and Bains of the University of Toronto for their assistance early in this project and for the continuing and enthusiastic support of Prof. Hooper (Hooper and Angus) whose vast experience in all aspects of heat transfer provided a guiding light through the many problems encountered during the project. We are also grateful to Mr. E. Bustard who provided expert assistance on issues of naval architecture that arose during the construction of the computer models. Finally, thanks are also due to the staff of H.G. Engineering who patiently endured through the physical preparation of the report and whose continued good spirits made the author's life an easier one.

TABLE OF CONTENTS

1.	INTRODUCTION	1
2.	A REVIEW OF PAST WORK	4
3.	TECHNICAL CONSIDERATIONS	6
3.1	Heat Transfer in Plate Fabricated Structures	6
3.1.1	Discussion of Heat Flow Mechanisms	6
3.1.1.1	Typical Cell for Estimation of Heat Flux	6
3.1.1.2	Natural Convection	8
3.1.2	Solution by Numerical Methods	12
3.1.2.1	Finite Elements	12
3.1.2.2	Thermal Network	13
3.1.3	Numerical Modelling of the Convection Process	16
3.1.3.1	Introduction	16
3.1.4	Evaluation of Convection Coefficients from Existing Theory	21
3.1.4.1	Surface Coefficients for a Vertical Wall	27
3.1.4.2	Surface Coefficients for Horizontal Plates	29
3.1.4.3	Surface Coefficients for Inclined Surfaces	31
3.1.5	Equivalent Surface Coefficient for Radiation Heat Transfer	32
3.1.6	Environmental Conditions	35
4.	HEAT FLOW MODELS - MULTI-COMPARTMENT MODELS	37
4.1	Model of a Proposed LNG Carrier	37
4.1.1	Introduction	37
4.1.2	The Analytical Model	41
4.1.3	Construction of the Computer Models	42
4.1.4	Results for a Typical Mid-hold Section	45
4.1.5	Results for a Section Including the Bulkhead	50
4.2	Model for the 'M.V. Arctic' Bulk Carrier	54
4.2.1	Introduction	54
4.2.2	The Finite Element Models	54
4.2.3	Results from the Analysis	60
4.3	Model of a Section of the Pierre Radisson Icebreaker	63
4.3.1	Introduction	63
4.3.2	The Finite Element Model	63
4.3.3	Results from the Analysis	73
4.4	Conclusions	76

5. HEAT FLOW MODELS - SINGLE CELL MODELS 78
5.1 Model of a Single Cell from the Proposed LNG Carrier 78
5.1.1 Introduction 78
5.1.2 Steady-State Thermal Network Model 78
5.1.3 Discussion of the Results 80
5.2 Finite Element Model of a Single Cell from the M.V. Arctic 83
5.2.1 Introduction 83
5.2.2 Steady-State Finite Element Model 83
5.2.3 Discussion of the Results 88
5.3 Transient Thermal Model of a Cell from the M.V. Arctic 107
5.3.1 Introduction 107
5.3.2 Transient Thermal Network Model 107
5.3.3 Discussion of the Results 117
5.4 Conclusions 126

6. M.V. ARCTIC TEMPERATURE MONITORING 127
6.1 Introduction 127
6.2 Description of the Monitoring Procedure 131
6.3 The Voyage 131
6.4 Discussion of the Results 136
6.5 Conclusions 148

7. GENERAL DISCUSSION AND RECOMMENDATIONS 163
7.1 General Discussion 163
7.2 Overall Conclusions 164
7.3 Recommendations for Future Work 164

REFERENCES 166

APPENDICES

A. Formulation of the Solution of the Heat Flow Model Using the F.E. Method 169

B. Steps in the Preparation of the ASASHEAT Program for the Solution of the Fabricated Plate Structure 178

C. Validation Model for ASASHEAT Update 181

D. Theoretical Background to Modelling Closed Cell Convection 188

E. Detail of Calculation for Cell Surface Coefficients for LNG Model 194

F. Program for the Evaluation of Plate Convection Coefficients by Classical Methods 198

G. Description of the Thermal Network Modelling Program and its Non-Linear Solution 206

H. Preferred Units and Commonly Used Values 210

I. Summary of a Proposal for a Long Term Temperature Monitoring System on Board the M.V. Arctic 220

J. Recommendations for the Design of a Laboratory Apparatus for the Determination of the Heat Transfer Coefficients in a Ship's Hull 223

LIST OF FIGURES

		Page No.
Figure 1	Typical Hull Construction	7
Figure 2	Typical Cell	9
Figure 3	Natural Convection Flow	9
Figure 4	Free Convection from a Hot Vertical Wall	21
Figure 5	Temperature and Velocity Profiles for Free Convection from a Hot Vertical Plate	26
Figure 6	Heat Flux Across an Inclined Surface	31
Figure 7	Rectangular Parallelopiped Cell	34
Figure 8	Typical Section of the LNG Carrier	38
Figure 9	Two Frame Finite Element Mesh of the LNG Carrier	39
Figure 10	Two Frame Finite Element Mesh of the LNG Carrier Including Bulkhead	40
Figure 11	Typical Cross-Section of a Cell	41
Figure 12	LNG Carrier Major Cell Dimensions & Plate Thicknesses	43
Figure 13	Film Coefficients and Ambient Temperatures	44
Figure 14	LNG Heat Flow Model Temperature Results Run 1	46
Figure 15	LNG Heat Flow Model Temperature Results Run 2	47
Figure 16	LNG Heat Flow Model Temperature Results Run 3	48
Figure 17	LNG Heat Flow Model Temperature Results Run 4	49
Figure 18	LNG Heat Flow Model Bulkhead in Place, First Frame	52
Figure 19	LNG Heat Flow Model Bulkhead in Place, Second Frame	53
Figure 20	Typical Section of the M.V. Arctic	55
Figure 21	Two Frame Finite Element Mesh of the M.V. Arctic	56
Figure 22	Five Frame Finite Element Mesh Including Bulkhead of the M.V. Arctic	57
Figure 23	Major Cell Dimensions & Plate Thicknesses M.V. Arctic	58
Figure 24	M.V. Arctic Surface Coefficients	59
Figure 25	Five Frames with Bulkhead, Resulting Temperatures Run 1	61
Figure 26	2 Frames Without Bulkhead, Resulting Temperatures Run 1	62
Figure 27	P. Radisson Engine Rooms & Casing	64
Figure 28	P. Radisson Bulkheads	65
Figure 29	P. Radisson Sea Bay & Oil Fuel Wing Tanks	66
Figure 30	P. Radisson Accommodation	67

Figure 31	P. Radisson Finite Element Mesh Including Bulkhead	68
Figure 32	P. Radisson Major Dimensions & Plate Thicknesses	69
Figure 33	P. Radisson Ambient Temperatures	71
Figure 34	P. Radisson Surface Coefficients	74
Figure 35	P. Radisson Plate Temperatures (^{o}C)	75
Figure 36	Single Cell From Proposed LNG Tanker	79
Figure 37	Thermal Network Analysis - Input Data for Steady State Solution	81
Figure 38	THETA1 Thermal Network Analysis - Steady State Solution(s)	82
Figure 39	M.V. Arctic Cell Model	84
Figure 40	Finite Element Idealization of the Cell	85
Figure 41	Variation of the Surface Coefficients at the Internal Surfaces	86
Figure 42	Film Coefficients for Water Filled Cell	90
Figure 43	Film Coefficients for Water Filled Cell	91
Figure 44	Film Coefficients for Air Filled Cell	92
Figure 45	Film Coefficients for Oil Filled Cell	93
Figure 46	Temperature Distribution for Oil Filled Cell -55, 0, 20 - High Coefficients	94
Figure 47	Temperature Distribution for Water Filled Cell -40, 0, 20 - Low Coefficients	95
Figure 48	Temperature Distribution for Water Filled Cell -55, 0, 20 - High Coefficients	96
Figure 49	Temperature Distribution for Air Filled Cell -55, 0, 20 - High Coefficients	97
Figure 50	Temperature Distribution for Air Filled Cell -55, 0, 20 - Low Coefficients	98
Figure 51	Temperature Distribution for Air Filled Cell 0, 9, 20 - Low Coefficients	99
Figure 52	Temperature Distribution for Air Filled Cell 0, 9, 20 - High Coefficients	100
Figure 53	Temperature Distribution for Water Filled Cell 0, 9, 20 - High Coefficients	101
Figure 54	Temperature Distribution for Water Filled Cell 0, 9, 20 - Low Coefficients	102
Figure 55	Temperature Distribution for Water Filled Cell -20, 4.5, 20 - Low Coefficients	103
Figure 56	Temperature Distribution for Water Filled Cell -20, 4.5, 20 - High Coefficients	104
Figure 57	Temperature Distribution for Water Filled Cell -40, 0, 20 - High Coefficients	105
Figure 58	Temperature Distribution for Water Filled Cell -55, 0, 20 - Low Coefficients	106
Figure 59	Dimensions of a Single Cell from the M.V. Arctic	108
Figure 60	Thermal Network Model of the M.V. Arctic Cell	109

Figure	61	Input Data for Transient Sequence Solution	113
Figure	62	Input Data (Continued)	114
Figure	63	Input Data (Continued)	115
Figure	64	Input Data (Continued)	116
Figure	65	Ballast Water Temperature Transient	119
Figure	66	Rate of Heat Loss or Gain From the Ballast Water	120
Figure	67	Exterior Hull Plates Temperature Transients	121
Figure	68	Hold Plates Temperature Transients	122
Figure	69	Hull Plates and Ballast Water Temperature Transients	123
Figure	70	Hold Plates Temperature Transients	124
Figure	71	Heat Loss from the Ballast Water	125
Figure	72	M.V. Arctic	128
Figure	73	Location of Test Cells	130
Figure	74	Thermistor Placement Main Cell	132
Figure	75	Thermistor Placement Two Bays Forward of Main Cell	133
Figure	76	Thermistor Placement in Other Than Main Cell	134
Figure	77	Thermistor Mounting Details	135
Figure	78	M.V. Arctic Position Chart	138
Figure	79	Plate Temperature Levels	139
Figure	80	Sea Water Temperature	140
Figure	81	Thermistor Placement for the Closed Cell	141
Figure	82	Closed Cell Temperatures	142
Figure	83	Closed Cell Temperatures	143
Figure	84	Closed Cell Temperatures	144
Figure	85	Closed Cell Temperatures	145
Figure	86	Typical Closed Cell Plate Temperatures	149
Figure	87	Air and Ballast Water Temperatures	150
Figure	88	Air and Ballast Water Temperatures	151
Figure	89	Thermistor Placement Open Cell	152
Figure	90	Open Cell Temperatures	153
Figure	91	Open Cell Temperatures	154
Figure	92	Open Cell Temperatures	155
Figure	93	Open Cell Temperatures	156
Figure	94	Thermistor Placement Above and Below Main Cell	157
Figure	95	Temperatures Above and Below Main Cell	158
Figure	96	Temperatures Above and Below Main Cell	159
Figure	97	Temperatures Above and Below Main Cell	160
Figure	98	Temperatures Above and Below Main Cell	161

Figure 99	Hold Temperature Transient	162
Figure 100	Typical Plate Fabricated Cell	178
Figure 101	Fin Plate	181
Figure 102	Three Finite Element Idealizations of the Fin Plate	184
Figure 103	ASASHEAT Input Data	185
Figure 104	ASASHEAT Input Data and Results	186
Figure 105	A Comparison of the Closed Form and Numerical Solutions for the Plate Test Case	187
Figure 106	The Closed Cell	189
Figure 107	Elements at the Edge of the Mesh	193
Figure 108	A Typical Cell on the Bottom of the Hull	195
Figure 109	A Typical Bilge Cell	196
Figure 110	Temperature Monitoring System	222

LIST OF TABLES

Table 1	Free Convection Program - Results Summary - Variation of Grashof Number	19
Table 2	Free Convection Program (with mods) - Results Summary - Mesh Variation	20
Table 3	Constants c and n for Free Convection from a Vertical Wall at Uniform Temperature	28
Table 4	Values of c and n for Horizontal Plates	30
Table 5	Environmental Conditions	36
Table 6	Surface Coefficient Variation from the Mean Calculated Value	87
Table 7	M.V. Arctic Positional Data	137
Table 8	Preferred Units (SI)	213
Table 9	Heat Transfer Units	214
Table 10	Conversion Between Imperial and SI Units	215
Table 11	Conversion Between Metric and SI Units	216
Table 12	Commonly used Values of Heat Transfer Constants	217
Table 13	Dimensionless Groups used in Thermo Physical Analysis	218
Table 14	Emissivity Values for Various Hull Surfaces	219

1. INTRODUCTION

The Canadian Arctic holds tremendous potential for providing Canada with energy and other mineral resources. As yet these reserves have been largely untapped due to the obvious engineering difficulties faced in these frontier regions. One mode of transportation that is available and highly valued is shipping. Experience in the operation of bulk carriers in the arctic environment is small compared with that in warmer waters, and consequently research into the special problems associated with arctic transportation has to be carried out to assist in the design of suitable ships.

A major design study underway at the time of the writing of this report is the Arctic Pilot Project whose goal is to prove the feasibility of shipping liquid natural gas (LNG) from Melville Island to the Canadian east coast by large ice breaking vessels. These ships are expected to carry 140,000 cubic meters capacity and be constructed of as much as 60,000 tons of steel. If built they will be the most sophisticated ice breakers in the world and the most powerful.

Clearly one of the major problems to be reckoned with in arctic transportation is the impact of the ship with the ice encountered in its voyage. An associated problem is the cold temperatures to which the ship will be subjected, because in general ship steels exhibit unacceptably brittle behavior at low temperatures. In addition extreme thermal gradients may give rise to local stresses that are significant compared to primary design loads and hence could affect design decisions. Finally, the energy losses through the outer skin of the ship's hull are an important consideration as the freezing of the ballast water must be prevented, or limited. Other temperature related problems are likely to become apparent as the number of arctic voyages increases and a broader experience is gained. It is important, therefore, to have a flexible and reliable means of predicting structural temperatures in any part of a ship given its environmental conditions.

The following report describes work done to fulfill the requirement for temperature and heat flow predictions in typical ship hull construction under the conditions of the arctic environment. The work centered around the use of the computer to provide solutions to numerical models based on the equations of heat transfer. Because of the geometrical complexity of the ship's structure the finite element method was originally proposed for the representation of the conduction through the steel platework. In view of the large liquid or

vapor spaces within the ship's hull, it was realized that convection and radiation may also play an important role in the total heat transport mechanism and hence considerable attention was given to estimating these effects.

The initial part of the study involved the modification of an existing finite element code (ASASHEAT) to accomodate the appropriate boundary conditions for heat transfer from a plate's surface. At the same time an investigation was made of the convection of fluid within the typical cells of a ship's hull as it was felt that this provided a significant part of the total heat transport between the inside and outside plates. The numerical procedures used to obtain a solution to this fluid mechanics problem proved inadequate, and no good alternative has yet been identified. Classical semi-empirical methods were therefore used to estimate these plate heat transfer coefficients.

Following this initial development work a number of typical hull structures were modelled and used to calculate temperature distributions under a variety of boundary temperature conditions. It was concluded that the facility developed was adequate for the analysis of large sections of the hull but that in many cases such an analysis would be unnecessary as the heat transfer mechanism was dominated by the action of a single cell.

A study of the heat transfer within a typical cell bounded by frames and longitudinal members was conducted in more detail by two approaches. First by the use of a 2-D model which was able to handle the non-linear effects. This was prepared using a thermal network analysis program (THETA) that was simpler in its geometrical modelling facilities but more sophisticated in its ability to handle temperature dependent boundary conditions. The second model using ASASHEAT was able to study the cell as a three-dimensional assemblage of plates. In this case the sensitivity of the solution to varying surface conditions was tested.

Whilst the numerical techniques mentioned above are very powerful, the solutions they produce are only as good as the quality of the original data. It was realized early on that the weakness of the work was the inability to provide any calibration from real experience against which to measure the accuracy of the assumptions made in the model. An investigation was made into the possibility of conducting experimental work as back-up to this project and it was concluded that laboratory work at less than full scale was inappropriate and that measurements on a real ship were preferable. A parallel project was therefore undertaken to instrument typical sections of the M.V. Arctic, a bulk carrier designed for use in arctic waters. Temperature measurements were taken during a crip from Antwerp to Nanisivik in July

of 1981. A further set of measurements planned for November of 1981 were unfortunately prevented by the destruction of part of the measuring apparatus. Thus although the first trip was successful the temperature differentials encountered were not those anticipated under winter conditions and were only of partial interest. Further experimental work will therefore be needed to verify the accuracy of the theoretical work reported here.

2. A REVIEW OF PAST WORK

During the course of this work an attempt has been made to collect data from any similar studies that may have been conducted into heat transfer in ships' structures. A computer search was made on the NTIS, ENERGYLINE COMPENDEX, COLD REGIONS DATABASE and CONFERENCE PAPERS DATABASE using all sensible combinations of the key words ship; vessel; tank; carrier; hull; heat flow; transfer; balance or loss; thermal and analysis. A similar search was separately conducted on the Maritime Research Information Service. These searches produced approximately seventy references, not one of which was directly concerned with heat transfer in ships travelling in arctic waters. The subjects covered included:

- computer programs for thermal analysis
- insulation
- cryogenic storage
- thermal stress
- heat transfer in oil tankers

A request for information through personal contacts of the people associated with this contract revealed that some work of a proprietary nature had been or was currently being carried out. No published work was forthcoming.

From the reading of several of the references obtained through the above process of enquiry, a general picture of the current state of the art has been established. It appears that considerable work was done in the early 70's on heat transfer in oil tankers both analytically and experimentally. This work centered around the heat transfer from the heating coils to oil and heat losses through the vessel walls. Similarly, the design of LNG vessels necessitated the thermal analysis of various containment systems. Leakage of the LNG causing locally cold temperatures of portions of the ship's hull has also been considered. However none of these studies are particularly relevant to the broad objective of this study.

The analysis models currently in use are based on finite element, finite difference or thermal network models. The only program identified in the literature that has been written specifically for ships' structures is the GNATS program developed by Newport News Shipbuilding. This code, written in the late 60's, is based on a finite difference approach and solves two and three dimensional problems in transient and steady state heat flow. Conduction, convection and radiation effects can be included in the same model. The rise of the finite element method as a tool for solving large structural and heat flow problems has led to a number of other commercial programs such as ASAS, NASTRAN, ANSYS becoming available, but no papers describing the thermal analysis of ships using these codes have been uncovered.

It is concluded that although there has been some work on specialized aspects of heat flow in certain types of ship, there is little discussion of this work available in the published literature. In particular, no help was found to assist in the estimation of the relevant empirical data associated with the heat transfer in ship's hulls other than that found from conventional texts and no experimental data were available to confirm any assumptions made.

3. TECHNICAL CONSIDERATIONS

3.1 Heat Transfer in Plate Fabricated Structures

3.1.1 Discussion of Heat Flow Mechanisms

A typical section of an Arctic going vessel's hull is an assemblage of cells, large and small, surrounded by steel plate. These cells are not usually self contained but have cutouts that link them with the spaces of adjacent cells. Clearly, much of the interior of a ship used for transportation of goods is going to be open space, the majority of the steel being confined to the surrounding hull structure. In the double skin construction of typical ships designed for use in arctic waters, the space between the two skins is filled with cells that arise from the intersection of the hull plates, frames and longitudinal members. A typical section is shown in figure 1.

The heat flow through the hull is therefore a combination of the following mechanisms:

a) conduction through the steel plate surrounding the cells
b) natural convection in the fluid contained in the cavities which includes local convection in pockets and possibly large scale convection through several cells
c) radiation across air-filled regions
d) potentially, forced convection involving heat transfer through mass transport could also play a part.

The first step in the consideration of the total heat flow model must be to examine which of these mechanisms is important. Can any be ignored and under what circumstances will one dominate? In order to focus attention on a particular example, a typical cell encountered in the wall of a ship's hull is considered and the heat flux calculated for conduction, radiation and convection. The example is a rectangular cell of dimensions similar to those proposed for an LNG tanker and is shown in figure 2.

3.1.1.1 Typical Cell for Estimation of Heat Flux

The cell is assumed to be bounded above and below by cells of similar proportions having similar temperature distributions. Hence the walls to adjacent cells are assumed to have no heat flow normal to them (adiabatic). This assumption is not strictly correct as a small temperature difference will exist due to the natural circulation in the cell.

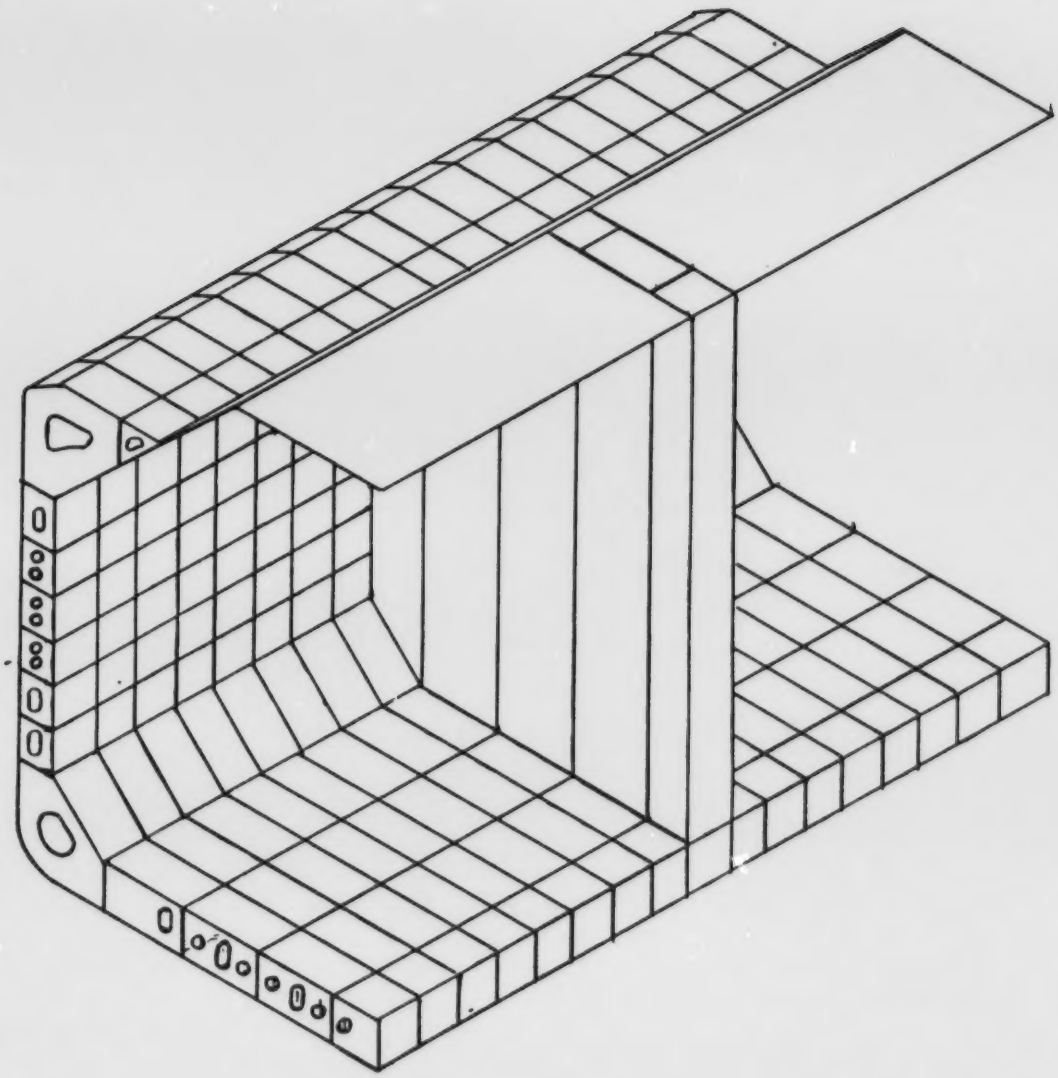

Figure 1 TYPICAL HULL CONSTRUCTION

3.1.1.2 Natural Convection

Natural convection will take place in the cell due to density differences induced in the fluid through the temperature variation of the plates. In our example, a flow pattern as shown in figure 3 might arise. The natural convection process is characterized by two dimensionless variables; the Prandtl and Grashof numbers. In particular the latter determines whether the flow will be laminar or turbulent.

The Grashof number is defined as:

$$G_r = \rho^2 g\beta (T-T_\infty)\, L^3/\mu^2 \qquad (1)$$

Where

ρ = fluid density of air = $1.293\ kg/m^3$

g = gravitational constant = $9.806\ m/s^2$

β = expansion coefficient of air = $0.367 \times 10^{-2}/K$

T = temperature difference (assumed difference between mean and plate temperature) = $20^{\circ}C$

L = typical length (height) = $4.0m$

μ = viscosity of air = $17.08 \times 10^{-6}\ Pa \cdot s$

Hence

$$Gr = \frac{(1.293)^2 \times 9.806 \times 0.367 \times 10^{-2} \times 4^3 \times 20}{(17.08 \times 10^{-6})^2}$$

$$\underline{Gr = 2.64 \times 10^{11}}$$

From this we can deduce that the flow will be turbulent. With this Grashof number the heat transfer through the boundary layer at the cell wall can be estimated. The dimensionless variable that characterizes this is the Nusselt number:

$$Nu = \frac{hL}{k} \qquad (2)$$

Where

h = the surface film coefficient ($W/m^2\ ^{\circ}C$)

k = conductivity of air = $.023\ W/m\ ^{\circ}C$

L = typical length = $4.0m$

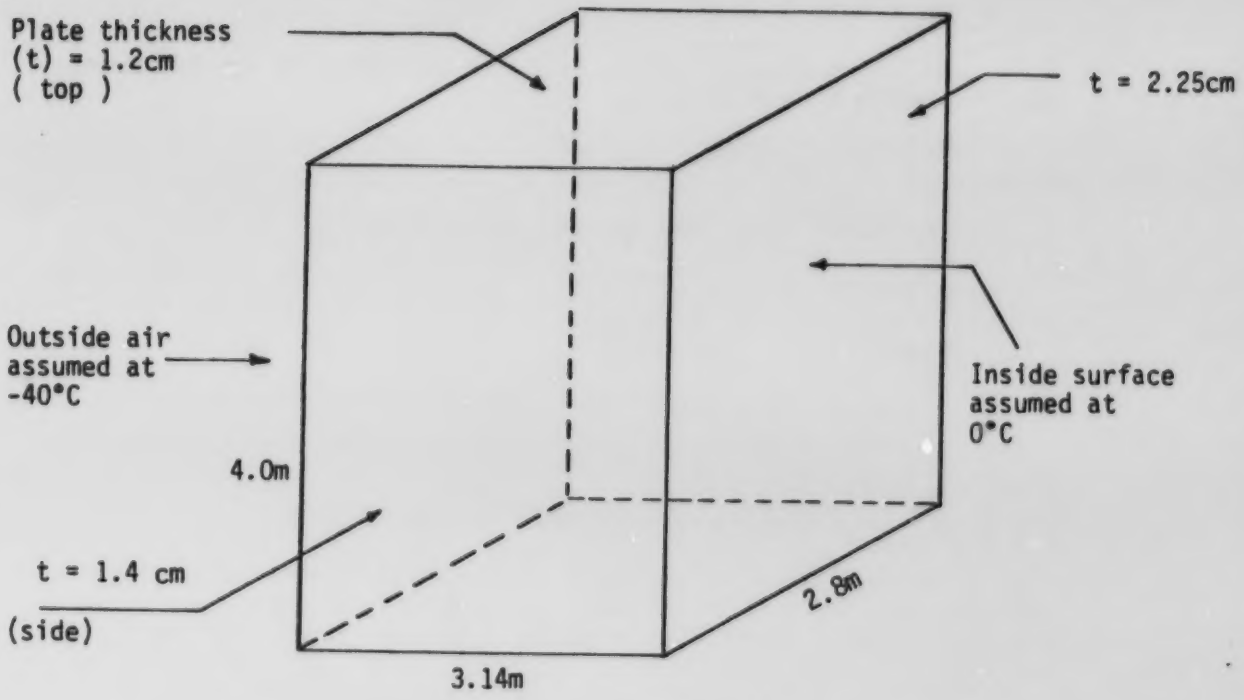

Figure 2 TYPICAL CELL

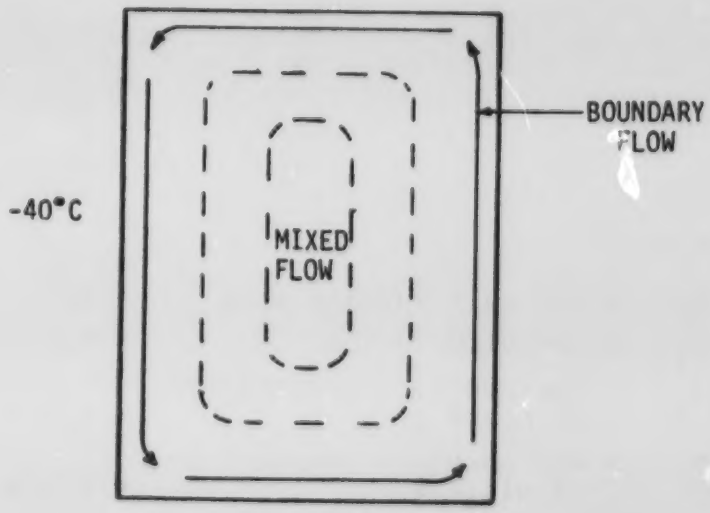

Figure 3 NATURAL CONVECTION FLOW

The Nusselt number can be estimated from sources such as Reference 1. (p 304) from which

$$Nu \doteq 600$$

An approximate value for the convection coefficient may therefore be taken as:

$$h = \frac{600 \times .023}{4} = 3.5 W/m^{2o}C$$

The heat flux may be calculated as:

$$q = hTA \qquad (3)$$

Where

q = the heat flux (W/m^2) over $1m^2$ of the plate

T = the temperature difference between the plate and the air

A = the projected surface of the plate.

If the cell is assumed to be well mixed such that the temperature differential exists only in a layer near the cell wall, then the mean cell temperature can be taken to be -20^oC.

$$q_{cv} = 3.5 \times 1 \times 20$$
$$= 70 \ W/m^2$$

3.1.1.3 Radiation

In the case of our chosen example, the main surface temperature difference is between the inner and outer walls of the cell. The remaining walls will all have roughly the same temperature. The radiation heat flux is therefore given by:

$$q_r = A_1 f_{12} \sigma (T_1^4 - T_2^4) \qquad (4)$$

Where

A_1 = the unit surface area = $1m^2$

f_{12} = the view factor = 0.5

T_1 = the absolute temperature of plate 1 = 233 K

T_2 = the absolute temperature of plate 2 = 273 K

σ = the Stefan-Boltzman constant = $5.67 \times 10^{-8} \ W/m^2K^4$

Hence

$$q_r = 5.67 \times 10^{-8} \times 0.5 \times (2.73^4 - 2.33^4) \times 10^8$$
$$q_r = 73.92 \text{ W/m}^2$$

3.1.1.4 Conduction

The conduction of heat through the walls of steel, as a proportion of the projected area is:

$$q_c = \tfrac{1}{2} \frac{\Sigma Ap}{A} KT/L \qquad (5)$$

Where

$\frac{1}{2}\Sigma Ap$ = half the area of cross-section of the steel plates
= $2.8 \times 0.012 + 4.0 \times .014$
= 0.0896 m^2

A = projected area = $4 \times 2.8 = 11.2\text{m}^2$

k = conductivity of steel = $52 \text{ W/m } ^\circ\text{C}$

L = depth of cell = 3.14m

Hence

$$q_c = \frac{.0895 \times 52 \times 40}{11.2 \times 3.14}$$
$$= 5.29 \text{ W/m}^2$$

From the above estimates of heat flux for the three modes of heat transport, the total heat flux for the cell is:

$$q_T = 5.29 + 73.75 + 70$$
$$= 149.04 \text{ W/m}^2$$

Hence the relative magnitudes for the three components are:

Convection =	47. %
Radiation =	49.5%
Conduction =	3.5%
	100.0%

From this it can be seen that under the circumstances postulated, the convection and radiation are going to play a large part in the determination of the heat flux through the cell. Although there are many reasons why the circumstances may be different, it is unlikely that the conduction effects will ever dominate. It is obviously important, therefore, to accurately estimate the heat transfer from the plate surfaces in a typical cell.

3.1.2 Solution by Numerical Methods

3.1.2.1 Finite Elements

The finite element method can be used to solve the transient or steady-state heat diffusion equations of solid two and three-dimensional continua. Appendix A describes the mathematical background to this model. The mechanics of finite element analysis involves the modelling of the structure as a number of discrete regions (finite elements), which may be thought of as satisfying the global heat balance equations only at discrete points which are called "nodes". The behavior of the idealized model is described by the temperatures at every node. The ability to model a real body and its boundary conditions by this approach is contained in the ASASHEAT computer program.

The process of idealization commences with the analyst assessing in a qualitative sense the type of behavior that is to be modelled. Each finite element has an assumed temperature variation inherent in its formulation. The analyst should be aware of the approximations and should refine the idealization accordingly. Thus, if an element is only capable of reproducing a linear temperature distribution, then several will be needed for modelling an area of rapidly varying temperature. If a transient analysis is required then this also influences the choice. Each element has a characteristic time, which is a function of its size and is incapable of reproducing a transient behavior occurring in a significantly shorter period than this.

ASASHEAT has a library of finite elements which are capable of modelling one, two and three-dimensional problems. The User Manual describes these facilities in detail (12). All the analysis in this report was conducted using plate elements having 3 or 4 nodes, with the ability to conduct heat in the plane of the plate and to absorb or emit heat from their surface.

An analysis model is constructed by preparing the following data. The user is free to choose any consistent set of units.

Nodes - Each node defined for the analysis model must be given a unique positive integer number so that an element can be identified unambiguously by the node numbers on its boundaries. The shape and orientation of an element is determined by the coordinates of these nodes. The coordinates may be defined in any convenient rectangular cartesian, cylindrical polar or spherical polar coordinate system.

Elements - Each finite element must be described by its node numbers, called up from the previously defined set in a clockwise or anti-clockwise order. The material properties of conductivity, density and specific heat are given on an associated material properties card,

There are several types of boundary conditions available in ASASHEAT:

Prescribed Temperature - A known temperature may be given as a prescribed nodal value.

Internal Heat Sources/Sinks - An internal heat source may be specified that varies within an element (negative for heat sink). The source may vary transiently.

Surface Coefficient - The heat flux passing to or from a body across a boundary is often expressed as proportional to the difference between the temperature of the body at the boundary and the ambient temperature of the surrounding medium. In ASASHEAT the constant of proportionality is termed the 'film coefficient'. In the case of a plate which has two surfaces, two coefficients and two associated background ambient temperatures are required. These are labelled EXternal FACE and INternal FACE COEFFICIENTS and EXternal and INternal AMBIENT TEMPeratures respectively in the ASASHEAT data deck.

Surface Radiation - Where the surface flux is through radiation to adjacent matter at a known ambient temperature the value of surface radiation (i.e. emissivity times the Stefan-Boltzmann constant) is given for nodes on the surface (see Appendix A for more details).

Time functions may be used to specify any required transient variation.

The most recent version of ASASHEAT which was under development at the time of writing this report includes the following additional features:

Temperature dependent material properties.
Radiation link between nodes on two surfaces.
Non-linear temperature dependent link between two nodes.

All of these facilities require an iterative means of solution as they are non-linear, being dependent upon the temperature solution. An example of the use of this program is given in Appendix C.

3.1.2.2 Thermal Network

In contrast to the Finite Element method, thermal network analysis is a considerably less sophisticated technique from the point of view of modelling two and three dimensional structural problems. Unlike the F.E. approach, each heat transfer link (conduction, radiation or convection) in the network has to be specified explicitly. The real physical structure is idealized as a network of nodes connected by links that have only thermal properties. The

dimensions of the physical system enter only implicity since they are used in the preparation of node and link properties that are entered as data. The main advantage of such an approach is that non-linear phenomena may more easily be incorporated in the program and complex transient or temperature dependent behavior can be examined using a simpler physical model.

The THETA program performs analysis by this method. Both steady state and transient sequence solutions may be obtained by an iterative solution technique in which all material properties may have non-linear temperature dependence, independent of each other. The modelling facilities allow structure and background nodes to be connected by radiation, convection and conduction links, the latter including non-homogeneous/interface effects. Nodal temperatures may be either constrained at particular values, within certain bounds, or used to trigger temperature dependent heat sources/sinks.

Following is a synposis of the modelling facilities:

Structural Modelling:

Body representation - The body is represented by numbered nodes. Nodal volumes are required for transient solutions in order to calculate thermal capacity effects.

Surface representation - Surface faces may be attached to body nodes, allowing nodes to be connected by radiation links.

Conduction links - Conduction links transmit heat between nodes through material bulk.

Radiation links - Radiation links transmit heat between nodes through free space, depending on the temperatures, properties and relative view factors.

Cooling circuits - A cooling circuit may be defined as a route along which heat transmission is by mass transport independent of the thermal properties of the medium. Heat exchange between structure and coolant is governed by the relative temperatures of connected points, and the formulation of a link.

Thermal Loading:

Thermal loads may be applied directly by either internal or radiant sources, or indirectly by controlling temperatures of model nodes or the background environment.

Internal loads - Applied to nodes independent of material properties or nodal temperatures.

Radiant loads - Gross radiant loads may be applied to various surfaces, the net input depending on the user defined properties of the surface and the temperature of the associated node.

Background links - These links relate the model to an environment, depending on a user specified proportionality constant, background temperature and temperature power. Depending on the values selected either radiation or convection can be modelled.

Temperature constraints - Temperature constraints from the temperature of specified nodes at a specified time.

Transient temperature controls - Temperature bounds may be used to maintain the temperature of a node between limits or trigger heat sources/or sinks.

With the exception of temperature controls, all thermal load types may be varied with time.

3.1.3 Numerical Modelling of the Convection Process

3.1.3.1 Introduction

Following recognition of the important role played by convective heat flow in the transfer of heat through the cells formed by plates in the ship's hull, an effort was made to seek a numerical solution to the fluid convection problem.

Tabarrok and Lin (10) developed a method and program for the solution of two-dimensional incompressible convective flow and used it successfully to predict a number of solutions for flow in a closed rectangular cell. A technical summary of the method is given in Appendix D. In brief, the method involves simultaneously satisfying the energy, momentum and continuity equations. The formulation is expressed in terms of the stream function, vorticity and temperature and requires the iterative solution of three equations. Convergence to a solution is based on a comparison between two consecutive calculations of the vorticity. The finite element approach is used to develop a discrete system of equations for each partial differential equation and a solution is sought for a specific set of boundary conditions. A triangular element shape was chosen which permitted a linear variation of each function.

The non-dimensional form of the equations is given in terms of two major variables, the Prandtl number (Pr) and the Grashof number (Gr). These characterize the fluid (Pr) and the forces within the fluid (Gr) as described in Appendix H. For a given value of viscosity a larger Grashof No. implies larger buoyancy forces and hence, in general, increased flow velocities.

Following a successful solution, the average Nusselt number is calculated by integrating the local temperature gradient at the walls. The Nusselt number leads directly to the value of the surface coefficient required for the plate model.

The program based on the above approach was tested on a number of values of Pr, Gr and mesh sizes and the results compared successfully with those of a number of other researchers (10). Prior to proceeding to the parameters of the problem for the ship's cell, it was confirmed that the version of the program used did in fact reproduce the results originally reported.

In general the aspect ratios of the cavity ranged from 0.2 to 1. Two values of Pr were tried, 0.7 and 7, and values of Gr were taken from 1×10^3 to 2×10^4.

Results for these parameters were reported in Reference 10. During the testing of the program some errors were found and corrected, and some improvements made to speed up the iterative procedure. In addition some new features were added to improve the printed output and to make the input of data more flexible. Finally an automatic procedure was added to calculate the Nusselt number from the temperature data.

The main difficulty with the solution technique lay in the inability of the iterative procedure to converge for high Grashof numbers. Table (1) shows a number of runs that were performed with differing damping factors and varying convergence criteria. It was found impossible to obtain convergence for a Grashof number greater or equal to 5×10^4 for air. For the typical cell in a ship's hull the appropriate Grashof numbers would be

	Pr	Gr
for air	0.733	2.6×10^{11}
for water	6.9	2.8×10^{12}

and these are many orders of magnitude greater than the value for which a solution was achieved. It was therefore concluded that there was no chance of this numerical approach producing a solution for the range of Grashof numbers required in this analysis.

It is believed that the breakdown in the solution is linked to the onset of turbulence in the physical model. Although the transition from laminar to turbulent flow on a single vertical plate does not take place until a value of $Gr = 10^{10}$, the transition in a closed cell is anticipated at a lower value (Ref. 1). It is believed that the flow in a typical ship's cell will be confined to a narrow boundary layer near the plate surface and that the central region will be turbulent and well mixed. Clearly the prediction of such complex flow by a numerical model is difficult, if not impossible.

In an attempt to model the region near the cell wall more accurately, a non-uniform mesh was tried with small elements close to the edge. These numerical experiments are reported in Table 2 and indicate that a worse problem was encountered in trying to obtain convergence for the lower Grashof number.

Since completing this work the author has become aware of other more recent research that has been done in the area of turbulent flow using quite a different approach. It is believed that further work could be done using currently available software to try and achieve the desired

goal, however no firm evidence indicating that the solution is achievable has so far been obtained.

Run #	Prandtl #	Grashof #	Initial Cond. From	Damping Factor	Iterations	Convergence W	Criteria S	Nusselt #
1A	0.733	5000.	Zero	0.5	Converges at 17	0.73E -03	0.22 E-03	1.653
2A	0.733	20000.	Zero	0.5	Oscillating at 25	0.16 E 00	0.25 E 00	2.764
2B	0.733	20000.	1A	0.5	Oscillating at 10	0.25 E 00	0.24 E 00	2.661
2C	0.733	20000.	1A	0.1	Converging at 10	0.74 E-01	0.25 E-01	2.392
3	0.733	10000.	1A	0.25	Converging at 25	0.23 E-02	0.71 E-03	2.103
3A	0.733	10000.	3	0.50	Converging at 5	0.57 E-03	0.40 E-03	2.106
4	0.733	20000.	3A	0.25	Oscillating at 15	0.48 E-01	0.61 E-01	2.732
4A	0.733	20000.	4	0.5	Oscillating at 15	0.51 E-01	0.86 E-01	2.563
4B	0.733	20000.	4	0.1	Converging at 15	0.93 E-02	0.69 E-02	2.595
4C	0.733	20000.	4B	0.2	Oscillating at 15	0.67 E-02	0.11 E-01	-
4D	0.733	20000.	4B	0.1	Converging at 15	0.43 E-02	0.19 E-02	2.630
5	0.733	50000.	4D	0.1	Oscillating at 15	0.43 E-01	0.67 E-01	3.614
5A	0.733	50000.	5	0.2	Diverges at 20	0.43 E-01	0.67 E-01	3.614
5B	0.733	50000.	5	0.075	Oscillating at 20	0.17 E-01	0.17 E-01	3.420

Original Data - 200 Equal Elements

Table 1 FREE CONVECTION PROGRAM - RESULTS SUMMARY - VARIATION OF GRASHOF NUMBER

Run #	Run Description	Prandtl #	Grashof #	Initial Cond.	Damping Factor	Iterations	Convergence W	Criteria S	Nusselt #
B	200 Equal Elements	0.733	5000.	Zero	0.5	Converges at 17	0.93 E-03	0.29 E-03	1.679
C1	200 Unequal	0.733	5000.	Zero	0.5	Diverges at 7	-	-	-
C2	200 Unequal	0.733	5000.	Zero	0.25	Converges at 20	0.82 E-02	0.79 E-02	1.657
C3	200 Unequal	0.733	5000.	C2 Results	0.5	Converges at 9	0.67 E-03	0.35 E-03	1.616
D1	800 Equal Elements	0.733	5000.	Zero	0.5	Diverges at 7	-	-	-
D2	800 Equal Elements	0.733	5000.	Zero	0.25	Converges at 20	0.14 E-01	0.36 E-02	1.672

Table 2 FREE CONVECTION PROGRAM (WITH MODS) - RESULTS SUMMARY - MESH VARIATION

3.1.4 Evaluation of Convection Coefficients from Existing Theory

The following section discusses in more detail the calculation of the film coefficients representing convection. It has been assumed that in the steady state the turbulent boundary layer is thin compared to the major dimensions of the cell and that the central area of the cell is well mixed and at a uniform temperature which is the average of the surrounding wall temperatures. This assumption implies that each plate may be considered separately and a value calculated from semi-empirical data already available in the literature.

Consider first a vertical wall as shown in Figure 4. Suppose the temperature of the wall T_w is higher than the temperature of the fluid. Since the layer of the fluid next to the wall acquires a

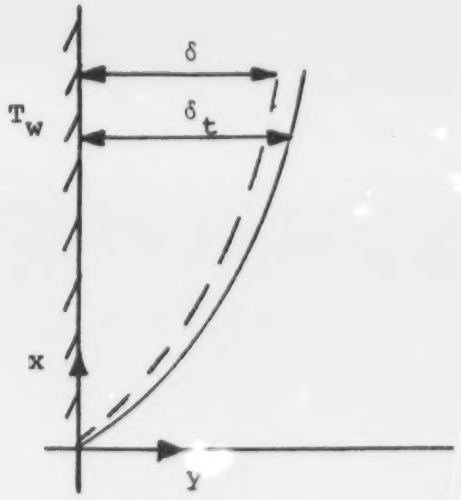

δ = velocity boundary layer thickness

δ_t = thermal boundary layer

Fluid at rest $u = v = 0$,

$\rho = \rho_\infty$,

$T = T_\infty$

Figure 4 FREE CONVECTION FROM A HOT VERTICAL WALL

higher temperature than that of the rest of the fluid, its density will decrease and it will begin to rise. In so doing, it will transfer energy from the hot wall. The mechanism for this energy transfer is referred to as natural or free convection. The factors controlling this movement of the fluid (mass transfer), and the associated heat transfer are: i) Momentum balance for the fluid, ii) Energy balance for the heat and iii) Conservation of mass for the fluid. Denoting components of the fluid

velocity by u, and v and the fluid density by ρ, pressure by P and temperature by T, we can write the governing equations of free convection as

$$\frac{\partial u}{\partial x} + \frac{\partial v}{\partial y} = 0 \qquad \text{mass conservation} \qquad (6)$$

$$\rho \left(u \frac{\partial u}{\partial x} + v \frac{\partial u}{\partial y} \right) = - \rho g - \frac{\partial P}{\partial x} + \mu \frac{\partial^2 u}{\partial y^2} \qquad \text{X momentum} \qquad (7)$$

$$\rho c_p \left(u \frac{\partial T}{\partial x} + v \frac{\partial T}{\partial y} \right) = k \frac{\partial^2 T}{\partial y^2} \qquad \text{energy balance} \qquad (8)$$

where μ is the viscosity; c_p is the specific heat at constand pressure and k is the coefficient of conduction for the fluid. To identify the buoyancy term let us evaluate the x momentum equation along the edge of the boundary layer. Here $u = 0$ and $\rho = \rho_\infty$. Then equation (7) simplifies to

$$\frac{\partial P}{\partial x} = - \rho_\infty g \qquad (9)$$

Using this expression for the pressure gradient we may write the term $\left(- \rho g - \frac{\partial P}{\partial x} \right)$ in equation (7)

as

$$- \rho g - \frac{\partial P}{\partial x} = - \rho g - (- \rho_\infty g)$$

or

$$- \rho g - \frac{\partial P}{\partial x} = = (\rho_\infty - \rho) g \qquad (10)$$

The difference between $\rho\infty$ and ρ is clearly due to the difference of temperatures at the edge of the boundary layer and on the wall. If we let β be the coefficient of thermal expansion for the fluid (at constant pressure) we can relate the density changes to temperature

changes by noting that

$$\frac{\Delta\rho}{\rho} = -\beta\,\Delta T \tag{11}$$

The -ve sign is due to the fact that a +ve ΔT corresponds to a - ve $\Delta\rho$. In our case equation (11) may be written as

$$\rho_\infty - \rho = -\beta\,\rho\,(T_\infty - T) \tag{12}$$

Returning to equation (10) we may write

$$-\rho g - \frac{\partial P}{\partial x} = -\beta\,\rho\,(T_\infty - T)\,g \tag{13}$$

Finally substituting from equation (13) into equation (7) we may write the latter as

$$\left(u\,\frac{\partial u}{\partial x} + v\,\frac{\partial u}{\partial y}\right) = g\beta\,(T - T_\infty) + \nu\,\frac{\partial^2 u}{\partial y^2} \tag{14}$$

where $\nu = \mu/\rho$ is the kinematic viscosity of the fluid.

Now it is worth noting that in the above development while for the buoyancy term the density is considered to vary with small temperature differences, for purposes of momentum balance and mass conservation, the density is considered to be a constant. This inconsistency in the assumptions has negligible effect on the solution problem providing the temperature differences are not very large. For gases quite an accurate estimation can be made for β by using the ideal gas law;

$$\rho = \frac{P}{RT} \qquad R = \text{individual gas constant} \tag{15}$$

where $R = \dfrac{R_u}{N}$

N = molecular weight

R_u = universal gas constant

now

$$\beta = \frac{\rho_\infty - \rho}{\rho} \Big/ (T - T_\infty) \tag{16}$$

or

$$\beta = \frac{\frac{P}{RT_\infty} - \frac{P}{RT}}{\frac{P}{RT}} \Big/ (T - T_\infty)$$

$$\beta = \frac{T - T_\infty}{T_\infty} \Big/ (T - T_\infty) = \frac{1}{T_\infty} \qquad (17)$$

In attempting to solve the governing equations (6), (9) and (8) it is worth casting these equations into non-dimensional form so that results can be used for a large variety of cases. To this end we introduce the following dimensionless parameters:

$$X = \frac{x}{L} \quad Y = \frac{y}{L} \quad U = \frac{u}{U_o} \quad V = \frac{v}{V_o} \quad \theta = \frac{T - T_\infty}{T_w - T_\infty} \qquad (18)$$

where L is a characterizing length and U_o is a reference velocity. In terms of these new parameters the governing equations may be written as

$$\frac{\partial U}{\partial X} + \frac{\partial V}{\partial Y} = 0 \qquad \text{mass conservation (19)}$$

$$U \frac{\partial U}{\partial X} + V \frac{\partial U}{\partial Y} = \theta \frac{Gr}{Re^2} + \frac{1}{Re} \frac{\partial^2 U}{\partial Y^2} \qquad \text{X momentum (20)}$$

$$U \frac{\partial \theta}{\partial X} + V \frac{\partial \theta}{\partial Y} = \frac{1}{Re\ Pr} \frac{\partial^2 \theta}{\partial Y^2} \qquad \text{Energy balance (21)}$$

In equations (19) and (21) three groups of non-dimensional numbers can be noted. These are

$$Re = \frac{U_o L}{\nu} \qquad \text{Reynolds number} \qquad (22)$$

$$Pr = \frac{\nu}{\alpha} \qquad \text{Prandtl number} \qquad (23)$$

$$Gr = \frac{g\beta L^3 \quad (T_w - T_\infty)}{\nu^2} \qquad \text{Grashof number} \qquad (24)$$

Sometimes another dimensionless parameter, called the Rayleigh number, Ra, is defined as

$$Ra = Gr\ Pr = \frac{g\beta L^3\ (T_w - T_\infty)}{\nu\alpha} \qquad (25)$$

The governing equations (19) and (21) can be solved satisfactorily by imposing a number of simplifying assumptions. One of these assumptions is that the thickness of the velocity and thermal boundary layers are the same, that is, $\delta = \delta_t$. The solutions show profiles for the velocity and temperature distributions as shown in Figure 5.

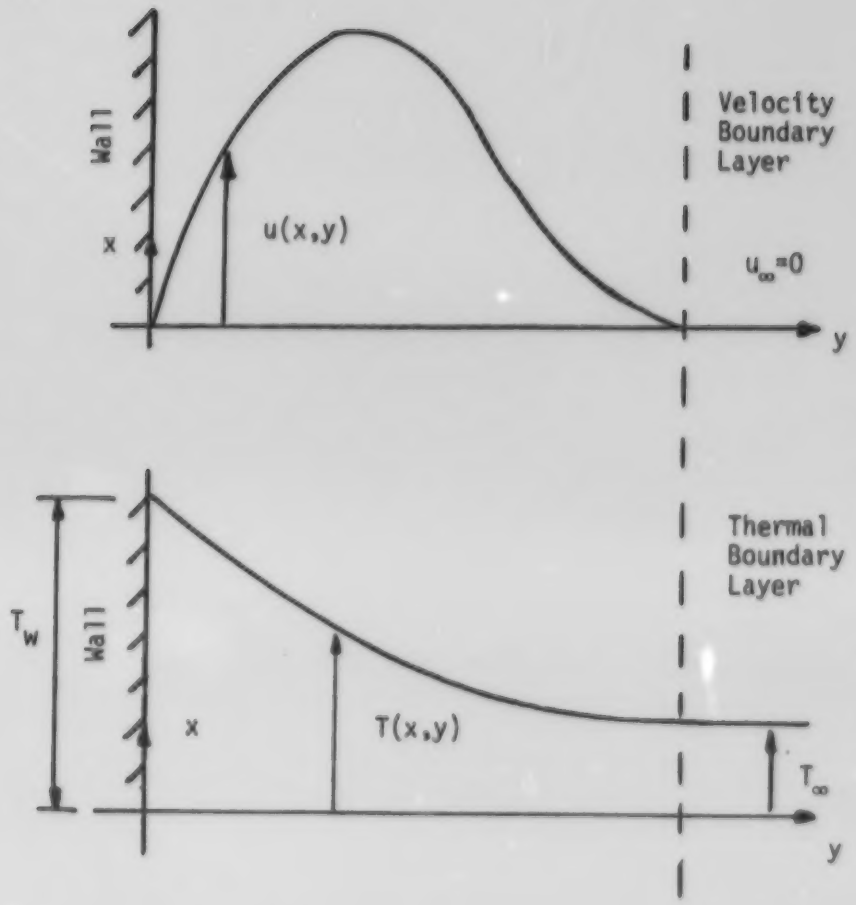

Figure 5

TEMPERATURE AND VELOCITY PROFILES FOR FREE CONVECTION FROM A HOT VERTICAL PLATE

3.1.4.1 Surface Coefficients for a Vertical Wall

To compute the heat transfer between the fluid and the wall surface a heat transfer coefficient h is defined as

$$q = h\,\Delta T \tag{26}$$

where q is the heat flux and ΔT is the difference between the wall surface and the mean fluid temperature i.e. $\Delta T = (T_w - T_\infty)$. Now from Fourier's law the heat flux is related to the temperature gradient by

$$q = - k \left.\frac{\partial T}{\partial y}\right|_{wall} \tag{27}$$

From equations (26) and (27) it follows that

$$h\Delta T = - k \left.\frac{\partial T}{\partial y}\right|_{y=0} \tag{28}$$

Now invoking the dimensionless parameters $Y = y/L$ and $\theta = (T-T_\infty)/\Delta T$ we may write equation (28) as

$$h = - \frac{k}{L} \left.\frac{\partial \theta}{\partial Y}\right|_{wall} \tag{29}$$

It is worth noting that (hL/k) generates another dimensionless number namely the Biot number, the ratio of the internal resistance of the solid to the film coefficient

$$Bi = \frac{hL_w}{k_w} \tag{30}$$

where k_w = conductivity of the wall material

L_w = dimension of the heat flow path into the wall

Note that the Nusselt number is of similar form:

$$Nu = \frac{hL_f}{k_f} \tag{31}$$

where k_f = conductivity of the fluid

L_f = characteristic size of the surface, typically a diameter or length

Although Nu and Bi are similar in form, they are different in significance and in numerical value. Physically, Nu is the ratio of the temperature gradient in the fluid immediately in contact with the surface to a reference temperature gradient, $(T_w - T_\infty)/L_f$. For free convection L_f is usually a vertical dimension.

In solving the governing equations one finds that the average Nusselt number for free convection from a vertical plate under uniform surface temperature can be expressed in the following form

$$Nu = c(Gr \cdot Pr)^n \tag{32}$$

where c and n are some constants. For laminar flow the values of c and n can be analytically calculated. For turbulent flow the values of c and n are usually determined by "best fit" of equation (32) to experimental findings. The values of c and n are tabulated in Table 3 for a wide range of (Gr . Pr).

Type of Flow	Range of (Gr · Pr)	c	n	Reference
Laminar	10^4 to 10^9	0.59	1/4	(16)
Turbulent	10^9 to 10^{13}	0.1	1/3	(17, 18)

Table 3 CONSTANTS c AND n FOR FREE CONVECTION FROM A VERTICAL WALL AT UNIFORM TEMPERATURE

Using equations (32) and (31), and employing the constants c and n from Table 3, we may express the film coefficient h as

Laminar flow $$h = 0.59 \frac{k}{L} \left[\frac{g\beta L^3 \Delta T}{\nu^2} \cdot \frac{\nu}{\alpha} \right]^{\frac{1}{4}} \quad (33)$$

Turbulent flow $$h = 0.1 \frac{k}{L} \left[\frac{g\beta L^3 \Delta T}{\nu^2} \frac{\nu}{\alpha} \right]^{\frac{1}{3}} \quad (34)$$

In the latter case the expression simplifies to

$$h = 0.1 \; k \left[\frac{g\beta \Delta T}{\nu\alpha} \right]^{\frac{1}{3}} \quad (35)$$

which shows h to be independent of the height. Physically, this is true because, over a high wall, many small circulation cells develop, and greater height only introduces more similar cells.

3.1.4.2 Surface Coefficients for Horizontal Plates

The heat transfer coefficient in free convection from a horizontal plate depends on the orientation of the heat transfer surface, namely, whether the surface is facing up or down, and whether the plate is heated or cooled. The mean Nusselt number (i.e. averaged over the entire surface) for free convection from a horizontal surface can again be expressed in the following form

$$Nu = c(Gr \cdot Pr)^n \quad (36)$$

where once again the values of constants depend upon the type of flow. In Table 4 values for c and n for different cases are tabulated.

Type of flow	Orientation of Plate	Range of Gr · Pr	c	n	Reference
Laminar	A cooler upper surface or A warmer lower surface	10^5 to 2×10^7	0.54	$\frac{1}{4}$	(16)
Turbulent	A cooler upper surface or A warmer lower surface	2×10^7 to 3×10^{10}	0.2	$\frac{1}{3}$	(19)
Laminar	A cooler lower surface or A warmer upper surface	3×10^5 to 3×10^{10}	0.27	$\frac{1}{4}$	(16)

Table 4 VALUES OF c AND n FOR HORIZONTAL PLATES

It is worth noting that for the case of a cooler lower surface or a warmer upper surface, the turbulent condition is not reached even at $Gr \cdot Pr = 3 \times 10^{10}$, due to the effects of stratification, and the absence of de-stabilizing forces.

In water filled cells ice may form on the inside of the outer hull surfaces. This has several effects. It holds the surface temperature at the freezing point. It provides a heat sink at the ice surface corresponding to the latent heat of fusion of the frozen layer. It also introduces a further thermal resistance corresponding to the heat flow path through the ice. In the case of a thick ice layer, the shape and size of the liquid volume is altered. All of these are difficult to handle in an analytical model, and are not accounted for in the steady state case treated numerically in this report.

3.1.4.3 Surface Coefficients for Inclined Surfaces

For inclined surfaces the expressions for film coefficients must be modified to account for the direction of heat flux. Indicating the orientation of the surface by the angle measured from the heat flux vector, one can distinguish two different cases depending on the direction of the flux vector.

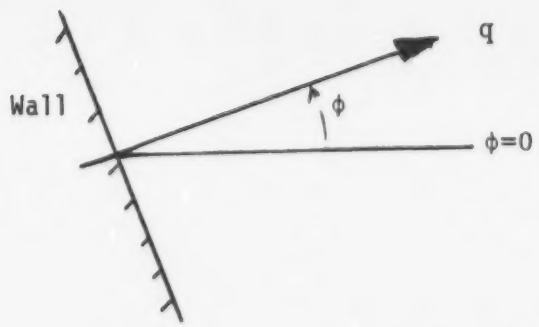

q heat flux vector

ϕ is measured anti-clockwise as positive

Figure 6 HEAT FLUX ACROSS AN INCLINED SURFACE

For surfaces warmer than the fluid, and

$$\text{for } -\frac{\pi}{2} < \phi \leq 0 \qquad h = \frac{k}{L} c \, (Gr \cdot Pr \cos\phi)^n \tag{37}$$

$$\text{for } \frac{\pi}{2} \geq \phi \geq 0 \qquad h = \frac{k}{L} c \, (Gr \cdot Pr \left(\cos\phi + d \sin\phi\right))^n \tag{38}$$

For the turbulent regime the constant d may be taken as 8 and for laminar regime it can be specified as 1.

Note: The density of fresh water goes through a maximum at about 4°C (39°F), and correspondingly the term β, the temperature coefficient of volume expansion, becomes negative below this temperature. Physically this means that for water the buoyancy forces are small, and reverse in this temperature region. It also causes the Gr and Ra numbers to pass through zero, leading to discontinuities and violation of the criteria justifying the approximations implicit in the analysis. For sea water the maximum densities vary both with salinity and temperature, but the same effects with respect to convection are encountered.

3.1.5 Equivalent Surface Coefficient for Radiation Heat Transfer

Radiation heat transfer is fundamentally a function of the fourth power of the absolute temperatures, most simply expressed in terms of the Stefan-Boltzmann equation $q = \alpha T^4$ for the radiation from a black surface of unit area. However, in order to solve simultaneously the heat flow expressions at a given surface by all of the three mechanisms; conduction, convection and radiation, it is very much more convenient to have the radiant component expressed in an equation of the first degree such as $q_r = h_r A\ (T_1 - T_2)$. This is then of the same form as the convection equation $q_c = h_c A\ (T_1 - T_3)$ and the conduction equation $q_K = \frac{kA}{L}\ (T_1 - T_4)$.

The actual radiant interchange between the various surfaces making up an enclosure such as a cell in the hull of a ship involves many factors. These include the temperature and surface properties for each component surface of the enclosure, including the absorptivity and emissivity values which are functions of the material, the surface finish, the angle of incidence or emission, the wavelength of the incident radiation, and the absolute temperature. The geometric relationship between the surfaces is also a basic factor. Computational and analytical methods have been developed which can yield reliable estimates of the radiation heat transfer in given cases.

For our present purpose it will be convenient to utilize the concept of "configuration factors", introduced by Hottel. A factor F_{12} is defined as the proportion of the radiation leaving a black surface (1) which falls directly upon and is absorbed by a second black surface (2) in an enclosure having n surfaces. The factor $\bar{F}_{12}$ is then defined as the fraction of the radiation leaving black surface 1 which reaches and is absorbed by black surface (2) including that passing by reflection from other surfaces in the enclosure, or by absorption and re-radiation from adiabatic surfaces. Finally, a factor $\hat{f}$ is introduced which defines the fraction of the radiation which would have left a black surface (1) (at T_1) which passes from a grey surface (1) directly and indirectly to, and which is absorbed by grey surface (2). This concept allows us to write for the net radiant exchange between surfaces (1) and (2) the simple equation

$$q_{net} = \sigma A_1\ \hat{f}_{12}\ (T_1^4 - T_2^4) \qquad (39)$$

in which σ is the Stefan-Boltzmann constant

$$\sigma = 5.6693 \times 10^{-8} \frac{W}{m^2 K^4}$$

Here all the complexity is taken up in the factor $\hat{f}_{12}$. Using this relation we can write

$$h_r = \frac{\sigma \hat{f}_{12} (T_1^4 - T_2^4)}{(T_1 - T_3)} \tag{40}$$

and so define a radiation coefficient for the first degree expression $q = h_r A(T_1 - T_3)$.

In some cases T_3 can be taken equal to T_2, as in the case of a surface 1 in a large room at uniform temperature T_2. In other cases an appropriate value of T_3 must be taken.

For the class of enclosures having only two active source-sink type surfaces, with the rest essentially inactive or adiabatic, relatively simple relationships exist between F, $\bar{F}$ and $\hat{f}$. For such cases

$$\bar{F}_{12} = \frac{A_2 - A_1 (F_{12})^2}{A_1 + A_2 - 2A_1 F_{12}} \tag{41}$$

and

$$\hat{f}_{12} = \frac{1}{(\frac{1}{\varepsilon_1} - 1) + \frac{A_1}{A_2} (\frac{1}{\varepsilon_2} - 1) + \frac{1}{\bar{F}_{12}}} \tag{42}$$

The emissivity values, ε_1 and ε_2, are properties of the surfaces (1) and (2). Table 14 tabulates values for these emissivities appropriate to various surfaces encountered in the hulls of ships in cold weather service.

The inner surfaces of the outer hull of a ship in Arctic service will often be below the frost point, and white frost will accumulate on these surfaces. This frosting changes the emissivity to a value of about 0.8 as long as

it persists (Reference 20).

Cells that are water filled may accumulate a layer of clear ice on the inside of the outer hull plates while the ship is in ballast. When these cells are pumped dry this ice can remain attached until warmer conditions are encountered. For such conditions emissivities of 0.97, corresponding to clear ice, may be more appropriate.

The evaluation of F_{12} for any given geometry is a detailed computation. For a cell in the shape of a rectangular parallelopiped (Figure 7), with opposed surfaces A_1 and A_2 active sources or sinks, and the other surfaces essentially passive, such as often occurs in the cells of ships' hulls,

putting $X = a/c$

and $Y = b/c$

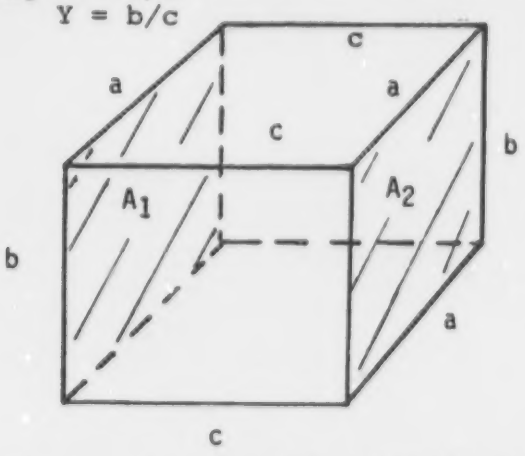

Figure 7 RECTANGULAR PARALLELOPIPED CELL

$$F_{12} = \frac{2}{\pi XY}\left\{ \ln\left[\frac{(1+X^2)(1+Y^2)}{1+X^2+Y^2}\right] + X\sqrt{1+Y^2}\,\tan^{-1}\left(\frac{X}{1+Y^2}\right) + Y\sqrt{1+X^2}\,\tan^{-1}\left(\frac{Y}{1+X^2}\right) - X\tan^{-1}X - Y\tan^{-1}Y \right\} \quad (43)$$

Appropriate values for the emissivity ε for the enclosure surface are tabulated in Table 14 (Appendix H).

3.1.6 Environmental Conditions

For completeness an extract from a 1973 reference is included which shows the typical year-round environmental conditions experienced in various regions of the Arctic (Ref. 15). A table showing temperature and wind conditions is given in Table 5 referring to the chart shown below.

The most significant factor from the standpoint of this study is that the minimum mean air temperature is shown to be -40°C. Our assumption throughout the analysis based on a 'worst case' assumption is that the temperature might drop to -55°C (-67°F). While such temperatures are of short duration, daily means approaching this temperature are not unusual in the high Arctic.

Wind conditions clearly affect the rate of cooling on the outside of the hull. Most of the analysis has been conducted with a steady-state condition assumed and as the external air to surface coefficient is generally much higher than the internal surface transfer coefficients, the effects of wind speed are of little importance. Once again, a conservative assumption was made by taking a coefficient that in dry air is equivalent to a wind speed of approximately 40 m/s.

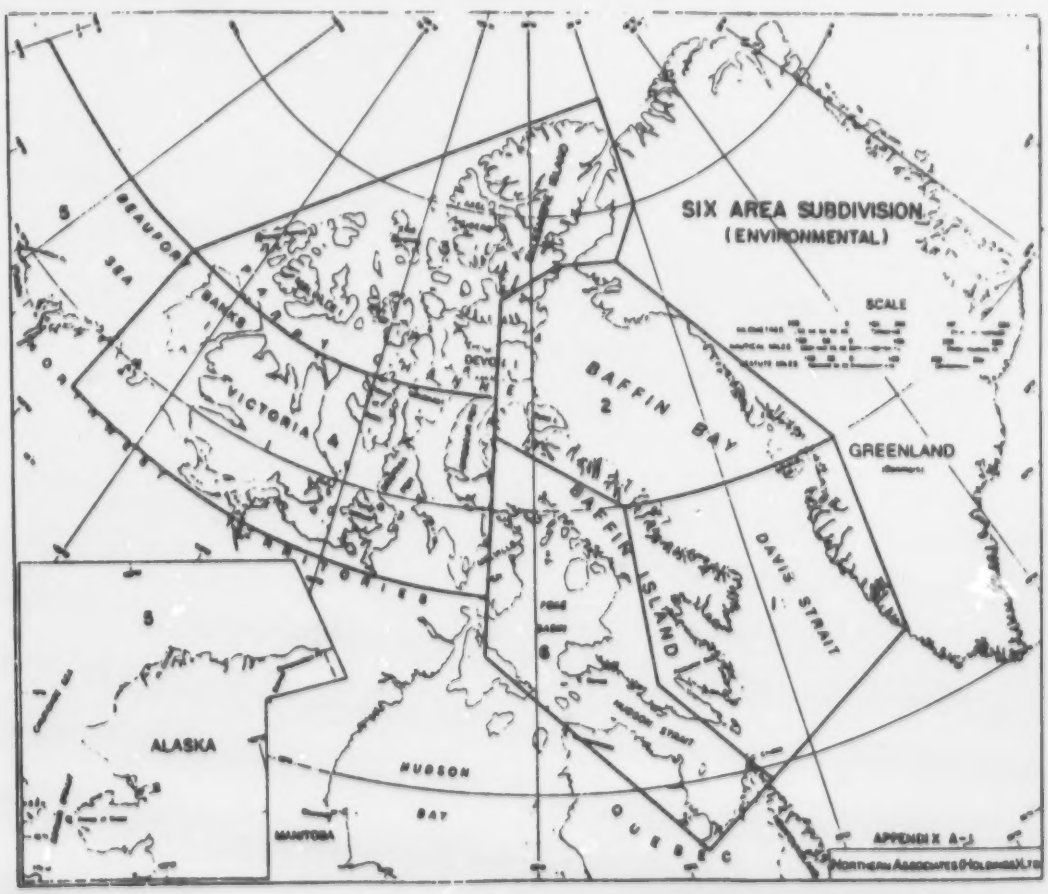

ENVIRONMENTAL FACTORS

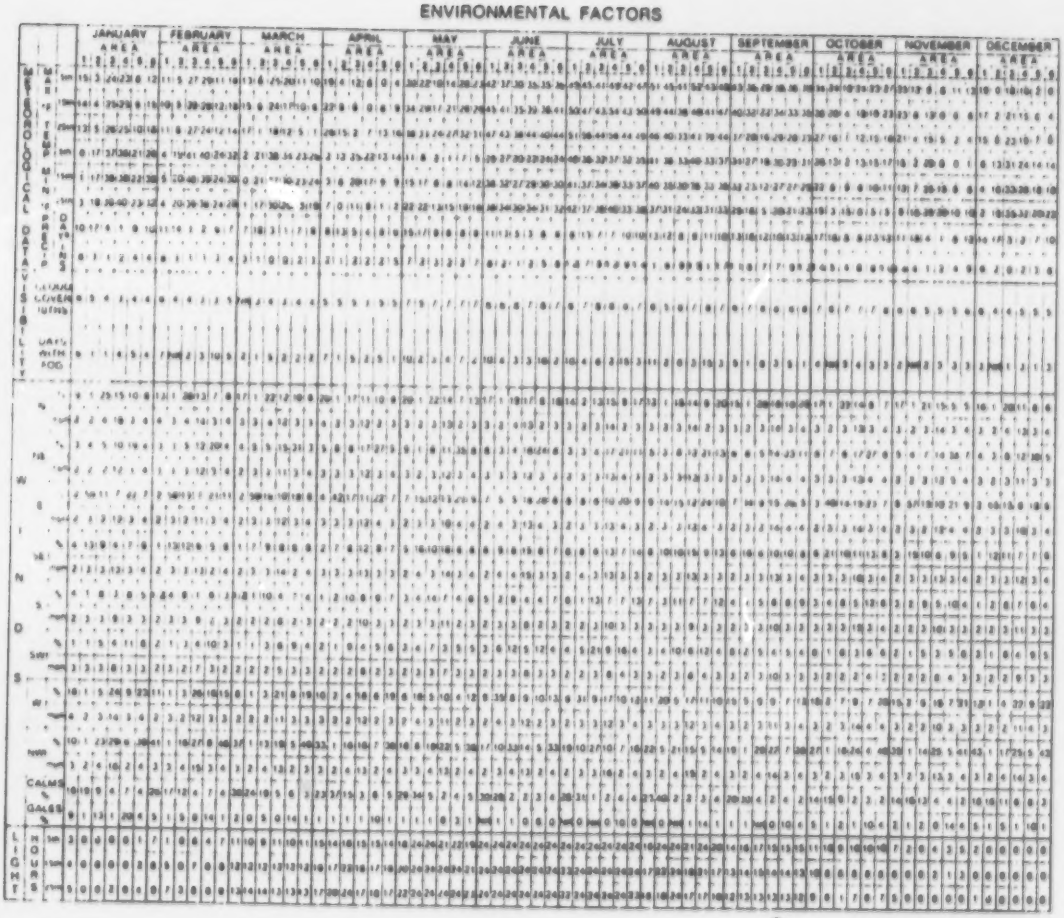

© 1973 Appendix No A6(a) Northern Associates (Holdings) Ltd

Table 5 ENVIRONMENTAL CONDITIONS

4. HEAT FLOW MODELS - MULTI-COMPARTMENT MODELS

4.1 Model of a Proposed LNG Carrier

4.1.1 Introduction

An early design proposed for the arctic LNG vessel featured a prismatic containment system. In a typical tank at the mid-ship section the cross-section remains constant between bulkheads as illustrated in Figure 8 . LNG occupies the entire central space and is separated from the double skin hull by an insulating layer.

The major ambient temperature differences exist either through the wall of the ship or vertically down the side. The heat flow analysis may therefore be covered by two typical models, one at the center of the tank, the other centered on a cofferdam between the tanks. If it is assumed that the ambient conditions are symmetric about the longitudinal center line of the ship, then it is possible to model only one half of a typical section.

A representative section at the center of a tank consists of all the structure between two typical frames. This is typically a series of cells bounded on all sides by plates of varying thickness. These cells form the deck, side and bottom of the hull. It can be assumed that the heat flux between longitudinally adjacent cells is zero. These cells may be air or water filled depending on the state of ballast. Heat flows through this cellular structure by conduction, convection and radiation. The model is modified at the cofferdam by the presence of the steel bulkheads and the air space between them.

The object of the analysis is to determine for the extremes of temperature encountered in the Arctic what the steel plate temperatures would be. In this analysis a macro-solution of the temperature field is required with local variations being considered of secondary importance. Many alternative scenarios could be taken for the ambient conditions and for such factors as hull speed, wind speed and the plate surface conditions. Some heating of the ballast water might also be in effect, or forced convection, in the case of air-filled cells. Out of all alternative possibilities one set of conditions was chosen that it was judged would give the lowest steel temperatures. The ambient air temperature was assumed to be -55^{o}C and the sea water -2^{o}C, no internal energy input was assumed and the temperature of the internal tank was taken to be uniform at -162^{o}C. A steady state solution of the problem was sought for the given boundary conditions.

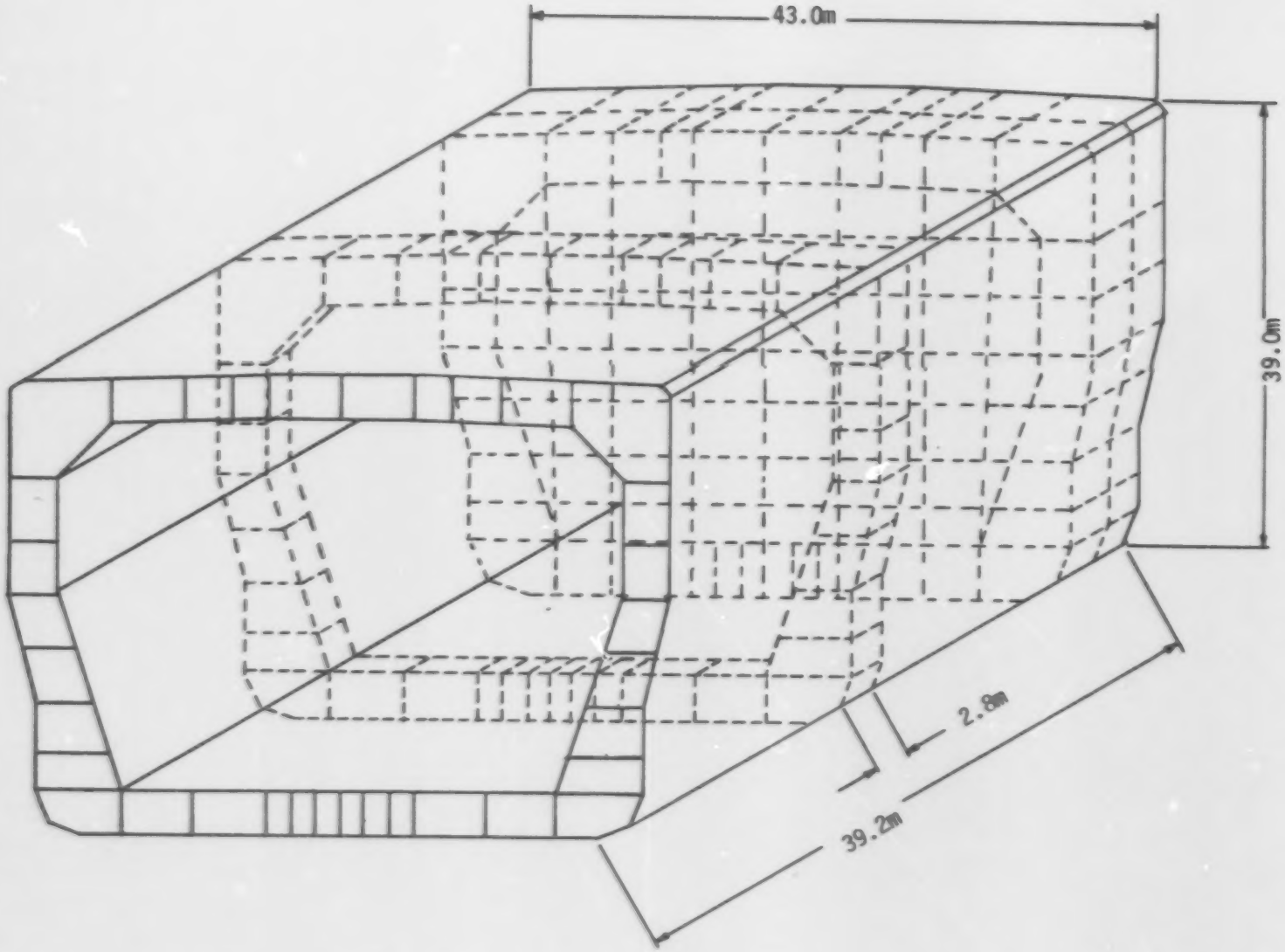

Figure 8 TYPICAL SECTION OF THE LNG CARRIER

Figure 9

TWO FRAME FINITE ELEMENT MESH OF THE LNG CARRIER

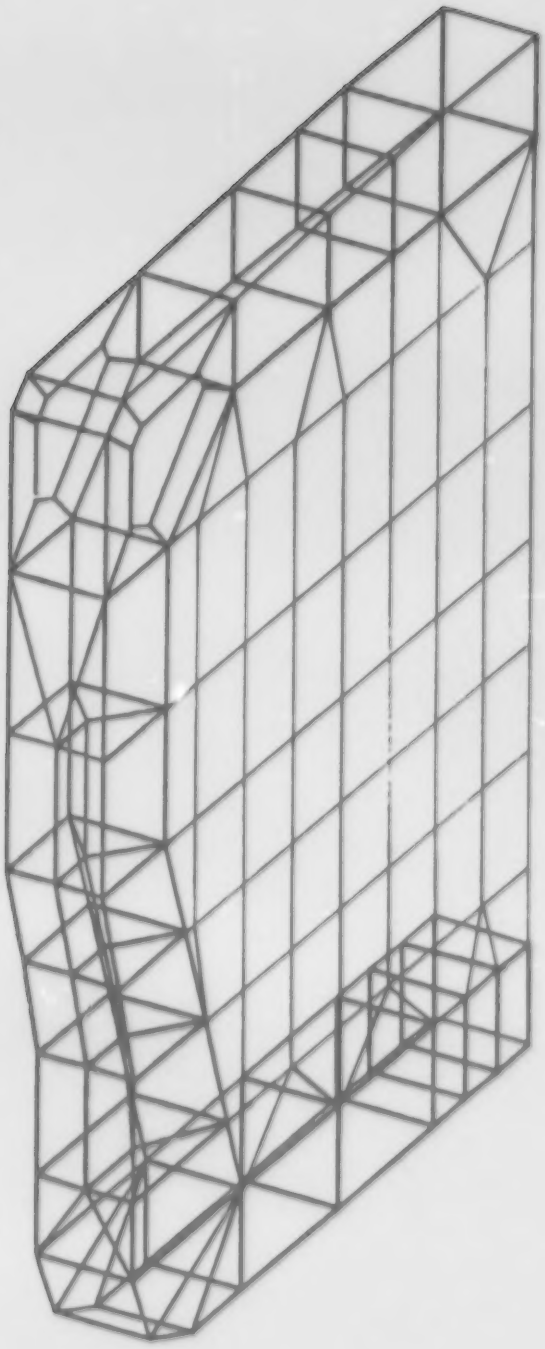

Figure 10

TWO FRAME FINITE ELEMENT MESH OF THE LNG CARRIER INCLUDING BULKHEAD

Many other alternative conditions exist in practice and can be analyzed by the same basic model described in the following sections.

4.1.2 The Analytical Model

Conduction through the steel is represented by a mesh of three and four noded finite elements each having the capability of representing a linear distribution of temperature between nodes. It is reasonable to assume that the temperature distribution along any of the plates in a typical cell will be linear and hence the natural division provided by the major structural members can be used as a basis for the mesh. The mesh used to represent the bulkhead plates is then largely dictated by the position of the longitudinal members. The resulting finite element mesh is shown in Figure 9 for the mid-hold section and Figure 10 for the frames adjacent to the bulkhead.

As shown in section 3.1.1 the heat transfer through convection and radiation are major contributors to the total flux. This effect is represented by prescribing heat transfer coefficients over the surfaces of the plates. The coefficients on the external surfaces, that is to say, those in contact with the sea, external air and LNG, are calculated from well established principles as previously described in section 3.1.3. The surfaces internal to the cell which are subject to natural convection are more difficult to estimate as they depend on the ambient temperature of the cell fluid. In this analysis it is reasonably assumed that the mean cell temperature is midway between the surrounding plate temperatures. As these temperatures are not known in advance, the solution is an iterative one involving a modification of the ambient fluid temperature based on the plate temperatures of the previous solution. This setup is shown in Figure 11 for a typical 2-D cross-section of a cell.

Figure 11 TYPICAL CROSS SECTION OF A CELL

Radiation occurs primarily between the inner and outer plate surfaces and only when the cell is air filled. This non-linear (αT^4) phenomenon requires an iterative solution technique even for the steady state solution, and was not available in the ASASHEAT program when this model was constructed. (The latest version of the program does include such a link). The model reported here simply uses a linearized surface coefficient to represent the effects of radiation (see section 3.1.5).

4.1.3 Construction of the Computer Models

Specification of the finite element analytical data described above requires six basic types of data.

1. Node point coordinates.
2. Element connectivity.
3. Material thermal properties.
4. Plate thicknesses.
5. Surface coefficients.
6. Ambient temperatures associated with the plate surfaces.

An example of how these data are prepared for the ASASHEAT program is given in Appendix C for a simple model. The first two data decks define the geometric model in terms of the element node points, the element types and how they are connected. The thermal conduction requires this element data along with the specification of the steel properties and plate thicknesses. The surface heat transfer requires in addition that the surface coefficients and ambient temperatures be prescribed.

The two models constructed had the following sizes:

	Two frame model	Two frames + bulkhead
Number of nodes	100	148
Number of elements	124	182

The natural skeleton of the ship's structure was used as the basic guide in sizing the finite element model. In other words a single element was taken for each plate bounded by longitudinal and transverse frames. Coordinates were calculated and elements called up as shown in Figure 9 . The major dimensions are shown in Figure 12 . By far the most complex data preparation involved the calculation of the surface coefficients and the specification of the associated ambient temperatures. Bearing in mind that each plate has two surfaces, 250 surface coefficients and 250 values of ambient temperature had to be calculated and entered for the simple model. This process is both tedious and error prone but at this stage hard to automate.

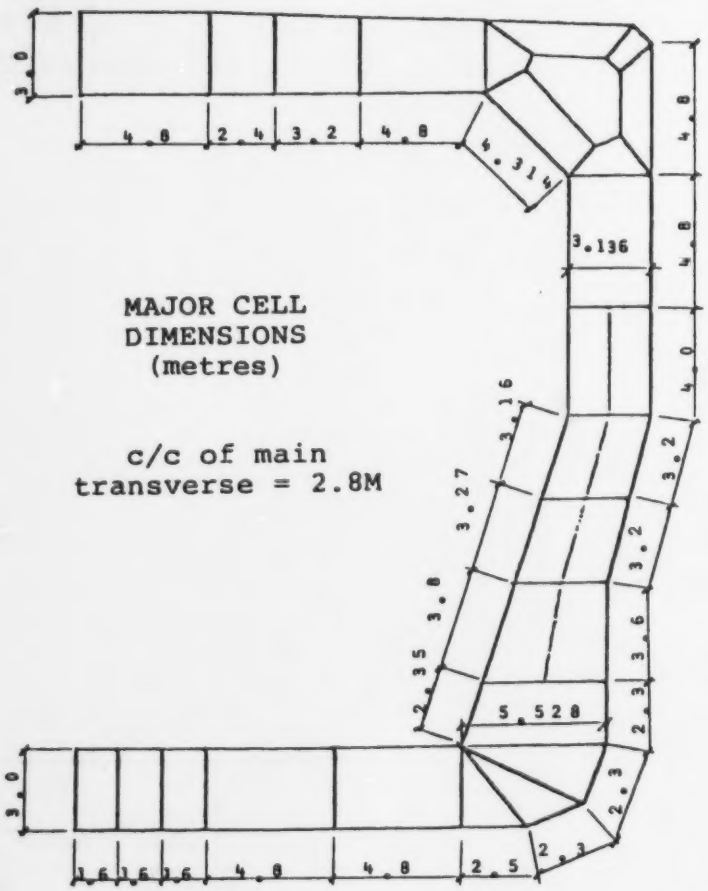

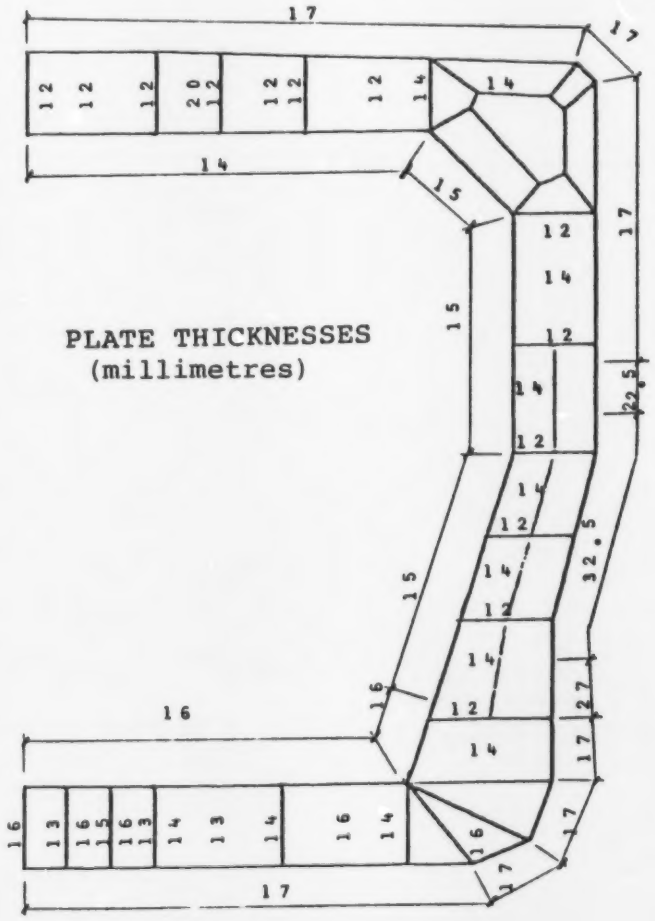

Figure 12

LNG CARRIER

MAJOR CELL DIMENSIONS & PLATE THICKNESSES

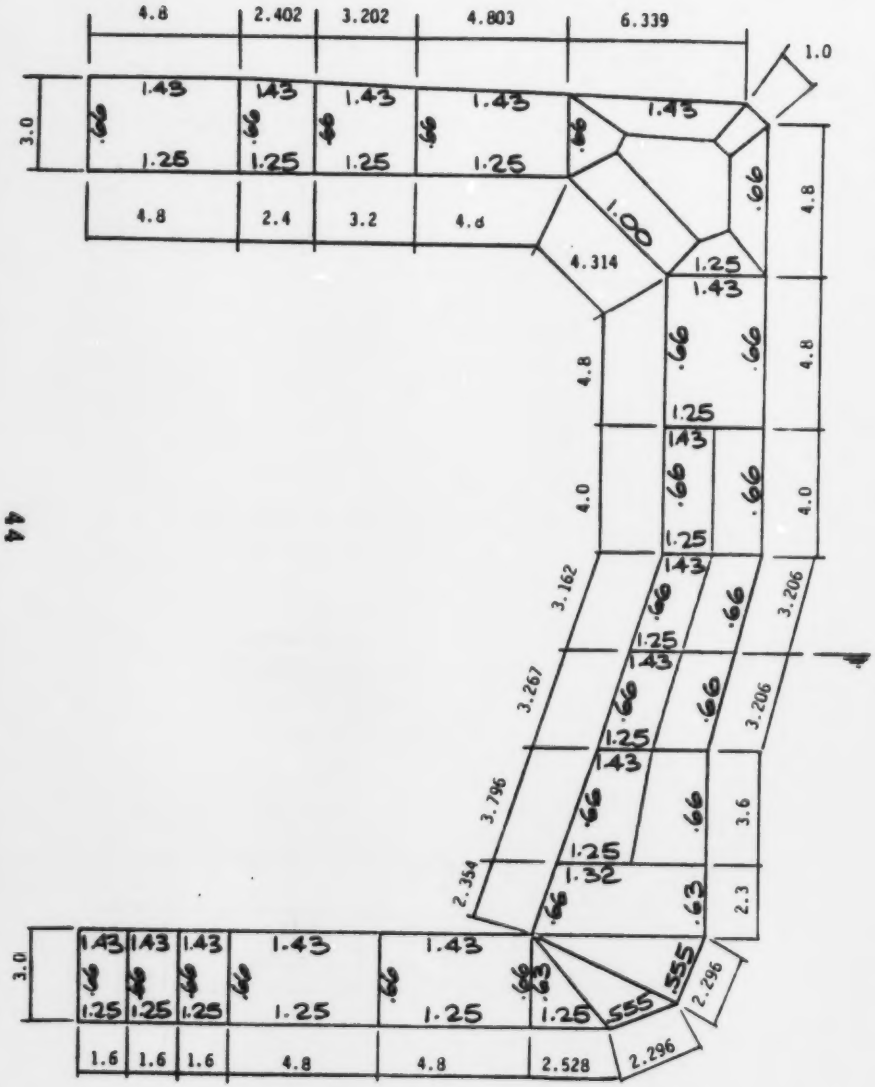

NOTES:

AIR

$T_A = -55^oC$

h_{st}-AIR = 40 W/M^{2o}C

WATER

$T_A = -2^oC$

h_{st}-WATER = 210 W/M^{2o}C

HOLDING TANK

$T_A = -162^oC$

$h_{insulation}$ = .15127 W/M^{2o}C

INTERNAL

T_A - variable

h_{long} = .2 W/M^{2o}C

h_{vert} = AS SHOWN

FILM COEFFICIENTS AND AMBIENT TEMPERATURES

Figure 13 FILM COEFFICIENTS AND AMBIENT TEMPERATURES

The calculation of the surface coefficients was based on the methods laid out in section 3.1.4 and resulted in the distribution of coefficients shown in figure 13 . Subsequent to this model a computer program was written to automate the calculation as reported in Appendix F. However, the details by which the hand calculated values were obtained for this model are given in Appendix E.

It was apparent from these early calculations that the internal surface coeffi[illegible]s were an order of magnitude different from ei[illegible] the external or internal hold values. Further they were dependent to a large extent on the assumptions made about

a) The mean cell temperature.
b) The temperature drop assumed in the boundary layer.

Apart from this, of course, the nature of the stiffeners (vertical or horizontal relative to the cell), also affects the surface transfer. Faced with an almost impossible set of variables to deal with, and believing that the real values would not differ significantly from those calculated, it was decided to run the analysis with these typical values, and examine the sensitivity of the solution to such variations at a later date.

The steel was assumed to have a conductivity of 52 W/mK.

4.1.4 Results for a Typical Mid-hold Section

An initial steady state solution to the model was obtained using an ambient mean cell temperature of -35°C. Temperatures calculated at each node of the mesh are shown in Figure 14. From this first solution a revised mean cell temperature was calculated from the average of the surrounding plates, and the surface coefficient and ambient temperatures modified accordingly. The analysis was re-run in this manner three more times leading to the revised temperature distributions shown in Figures 15-17.

The above iterative procedure was necessary because of the non-linear relationship introduced through the dependency of the internal surface heat transfer on the mean cell temperature. This manual approach, though convergent, proved unwieldy, and in this particular case, slow to converge. Each re-analysis involved the modification of many data cards and was time consuming and error prone. A future addition to the finite element model that would remove this problem would be the ability to include this temperature as a variable. This is a complex requirement that would involve the specification of many more links

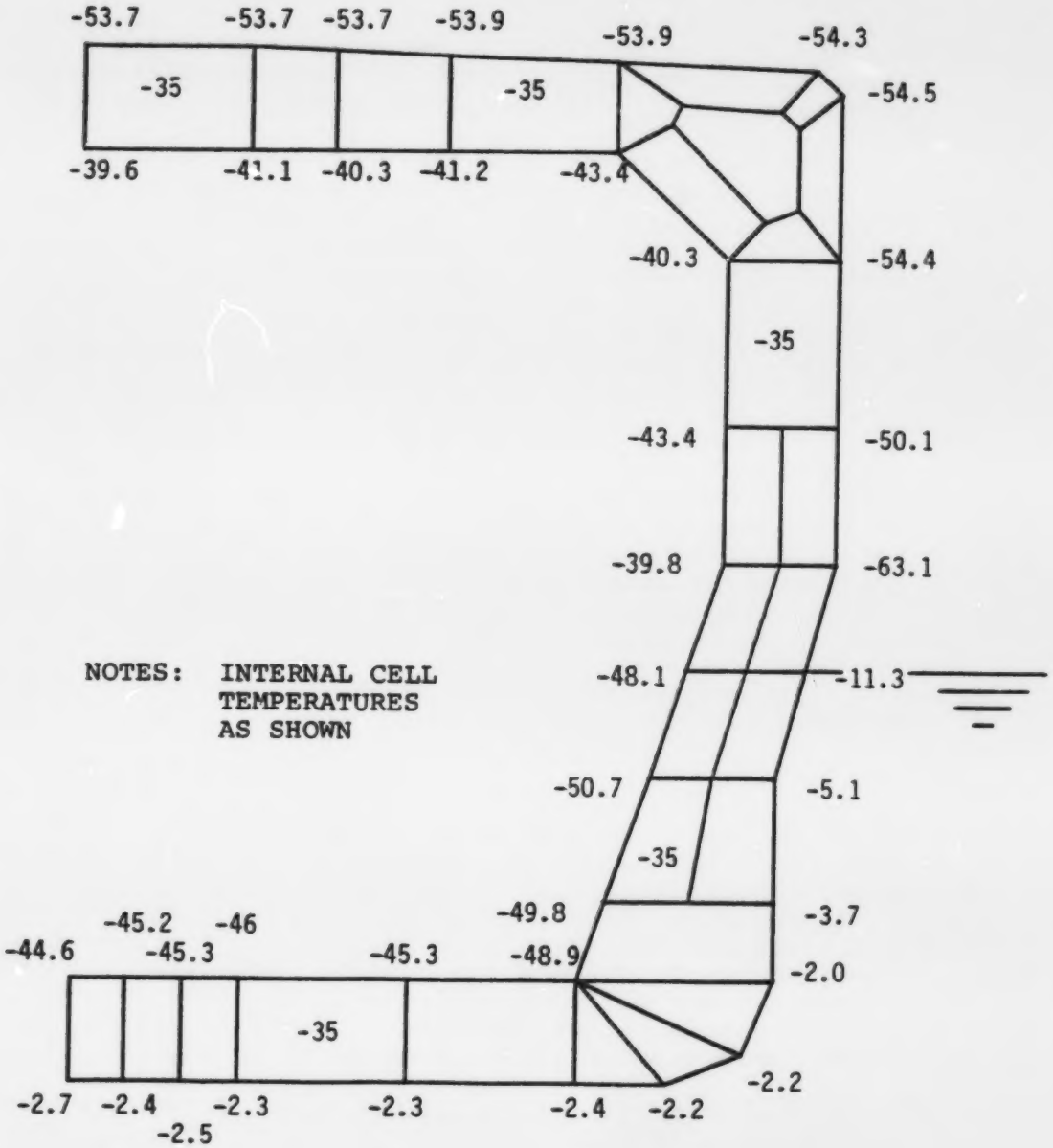

LNG HEAT FLOW MODEL

Figure 14 TEMPERATURE RESULTS

RUN 1

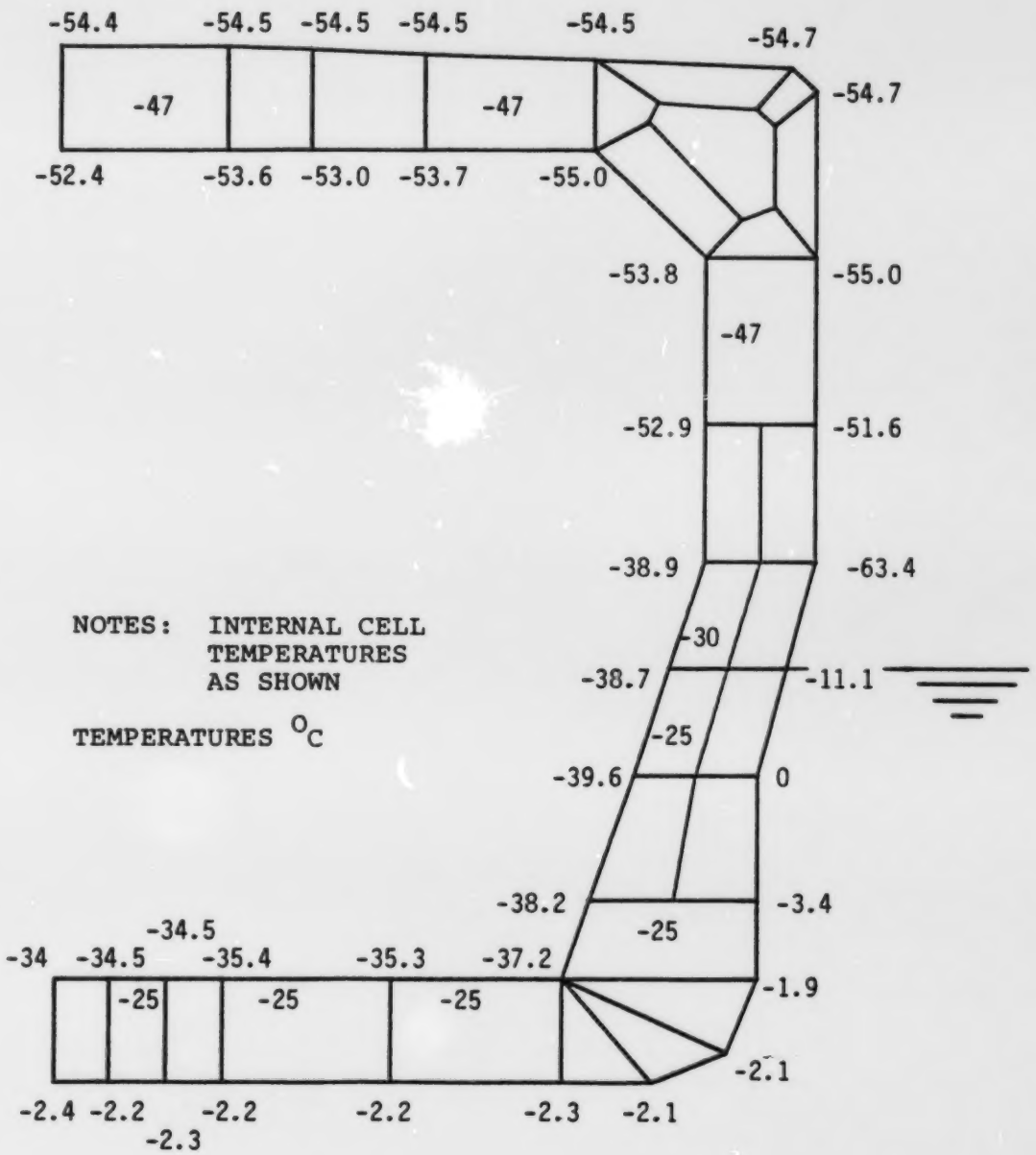

LNG HEAT FLOW MODEL

Figure 15 TEMPERATURE RESULTS RUN 2

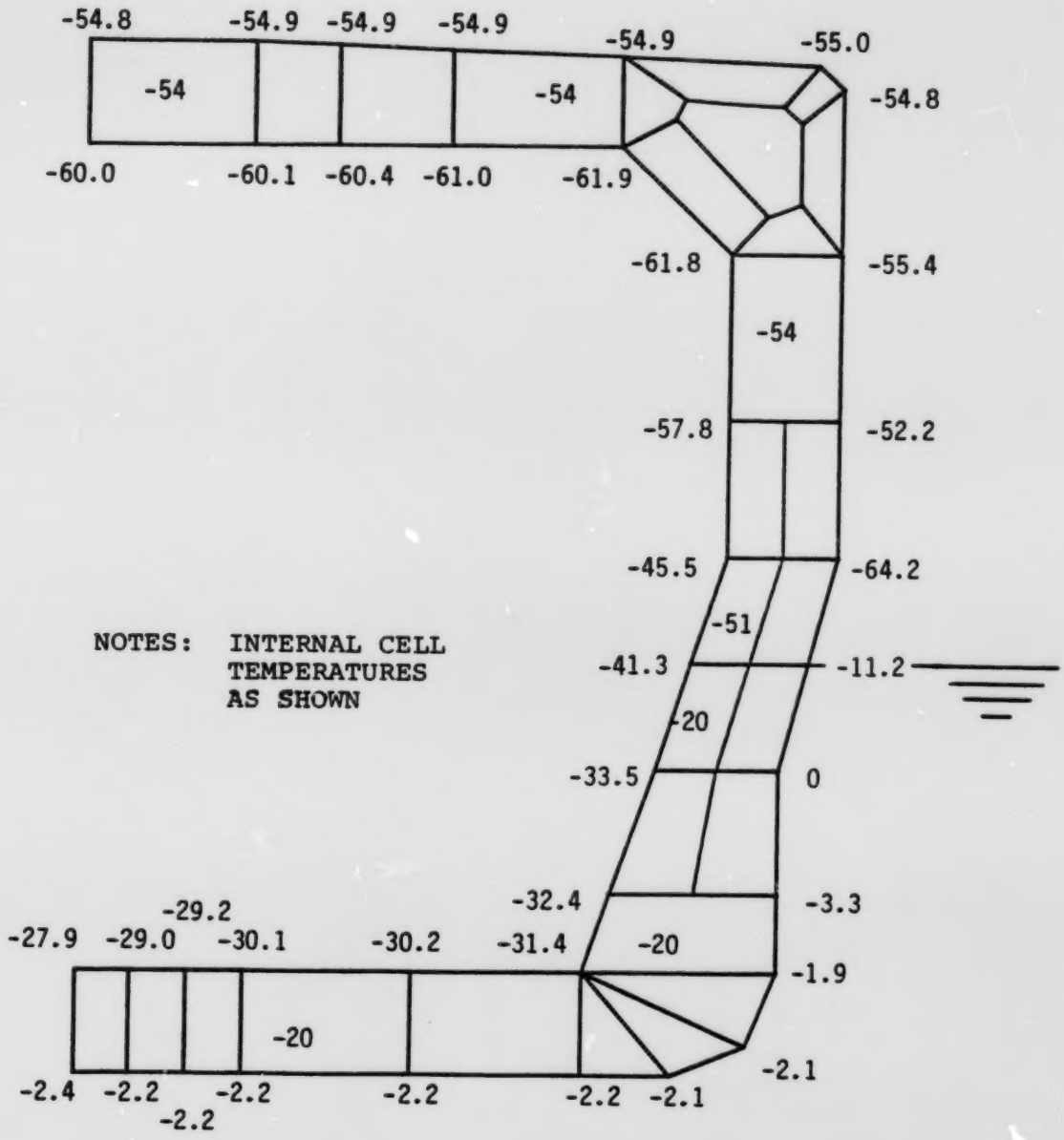

LNG HEAT FLOW MODEL

Figure 16 TEMPERATURE RESULTS RUN 3

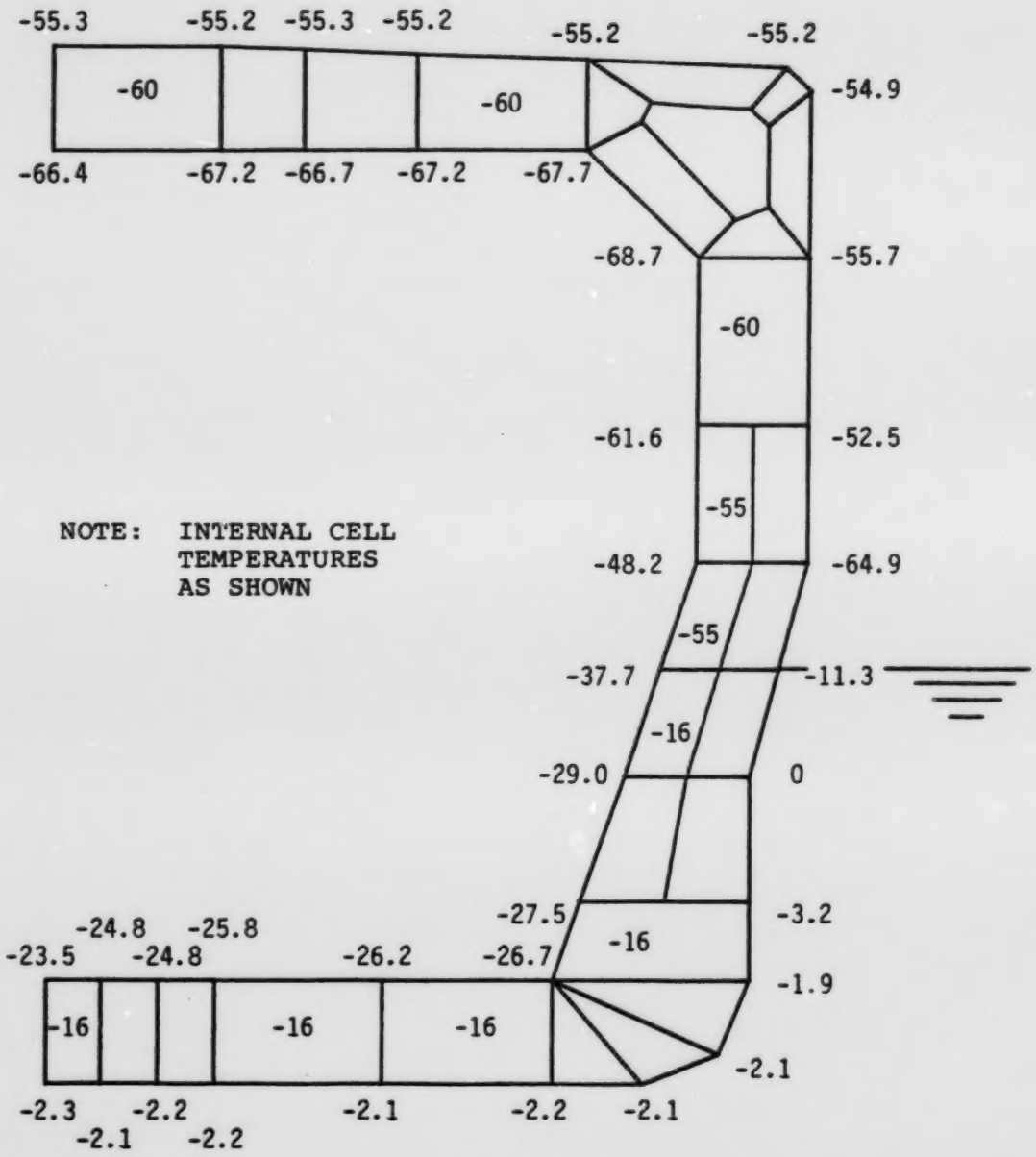

LNG HEAT FLOW MODEL

Figure 17 TEMPERATURE RESULTS RUN 4

between a 'dummy' node at the center of the cell and the surface of each adjacent plate. For this reason it was not possible to conveniently add this facility to the existing ASASHEAT model. Such a model has however been constructed for a single cell using the THETA, thermal network program as described in section 5. Subsequent to the completion of this work a non-linear link element has been added to the ASASHEAT program to permit the modelling of this form of temperature dependent boundary condition. No experience is available as yet to determine the effectiveness of this facility in the solution of the specific problem described here. As suggested, considerable modification of the model would be required to incorporate the additional links. Future modelling could include this approach at the outset.

The solution presented here, albeit crude, is sufficient to provide a good overall level of accuracy for the plate temperatures. The external plates are more accurately modelled as they depend upon surface coefficients that are both large and more accurately assessed.

An inadequacy in the idealization at the waterline is reflected in the temperatures recorded near the waterline. Clearly the temperature of -65^{o}C is unrealistic as it is lower than the ambient, and likewise the temperature below the surface of 0^{o}C is incorrect. This effect results from the sudden step variation in temperature that takes place at the air-water interface, and the fact that elements can only represent a linear variation in temperature. It is shown later in the single cell test (section 5.2) that by using a finer mesh of elements in this region the overshooting of the temperature is avoided. The outside steel temperature can be shown to follow the external air temperature or water temperature very closely.

4.1.5 Results for a Section Including the Bulkhead

The heat flux in the region of the cofferdam is significantly affected by the large surface area of steel in the bulkhead. The cavity within the cofferdam is air filled. In practice, it is anticipated that there would be a number of vertical stiffeners running the height of the tank and thus dividing the space into a number of vertical cells. The manner in which the air circulates through these cells would have a profound effect on the temperature of the bulkhead plates. It is quite possible, for example, that convection currents might be set up around the complete tank. In this analysis a conservative assumption has been made that there is no net heat flux into the cavity in the steady-state condition and hence the surface on the cavity side is adiabatic.

The results are shown in Figure 18 and indicate that under the above assumption, the center of the bulkhead can become as cold as the adjacent LNG fluid. This would suggest a system of forced air convection would be needed to prevent this from happening. The temperatures on the first frame away from the bulkhead are shown in Figure 19.

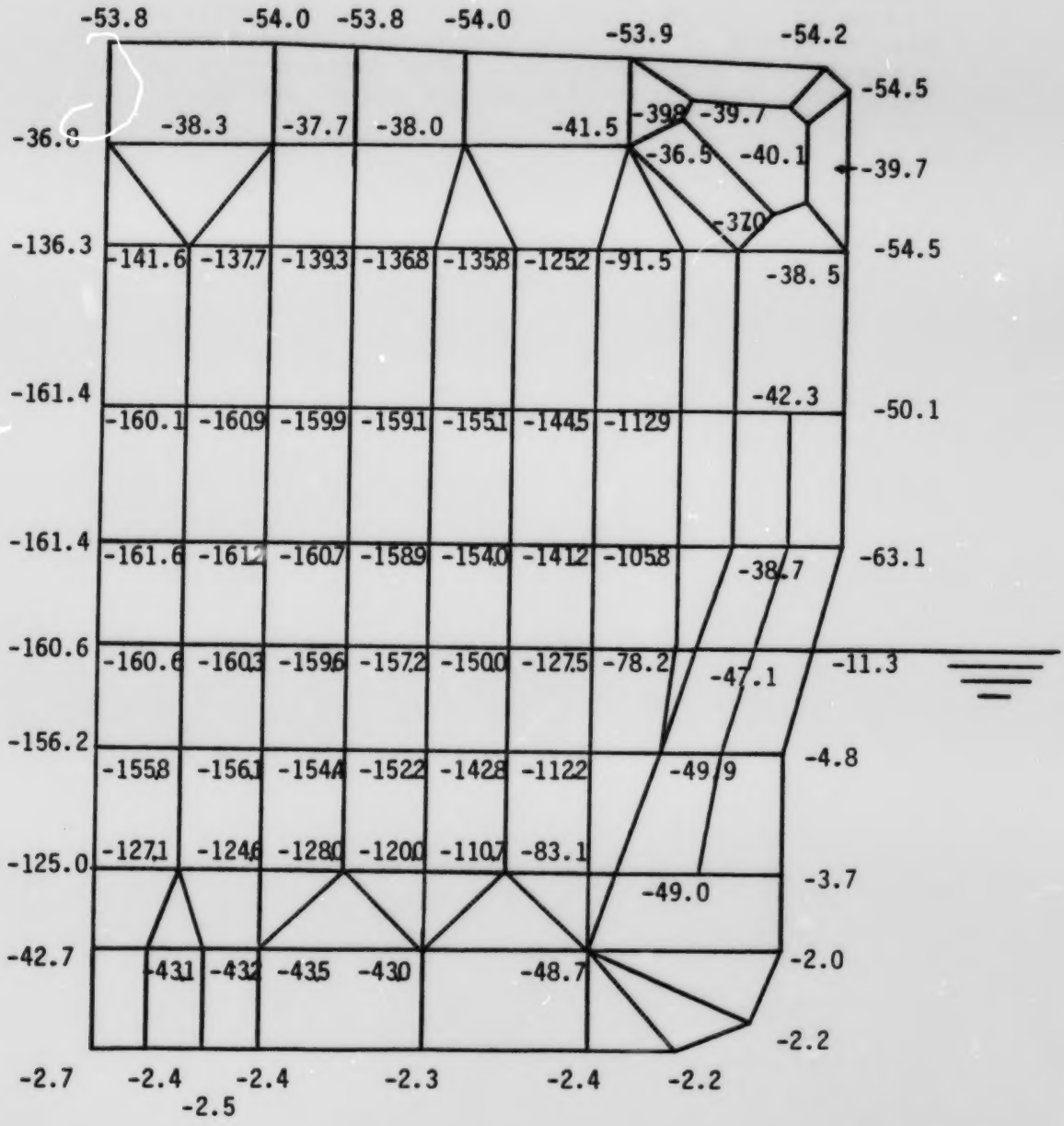

LNG HEAT FLOW MODEL

BULKHEAD IN PLACE

Figure 18 FIRST FRAME

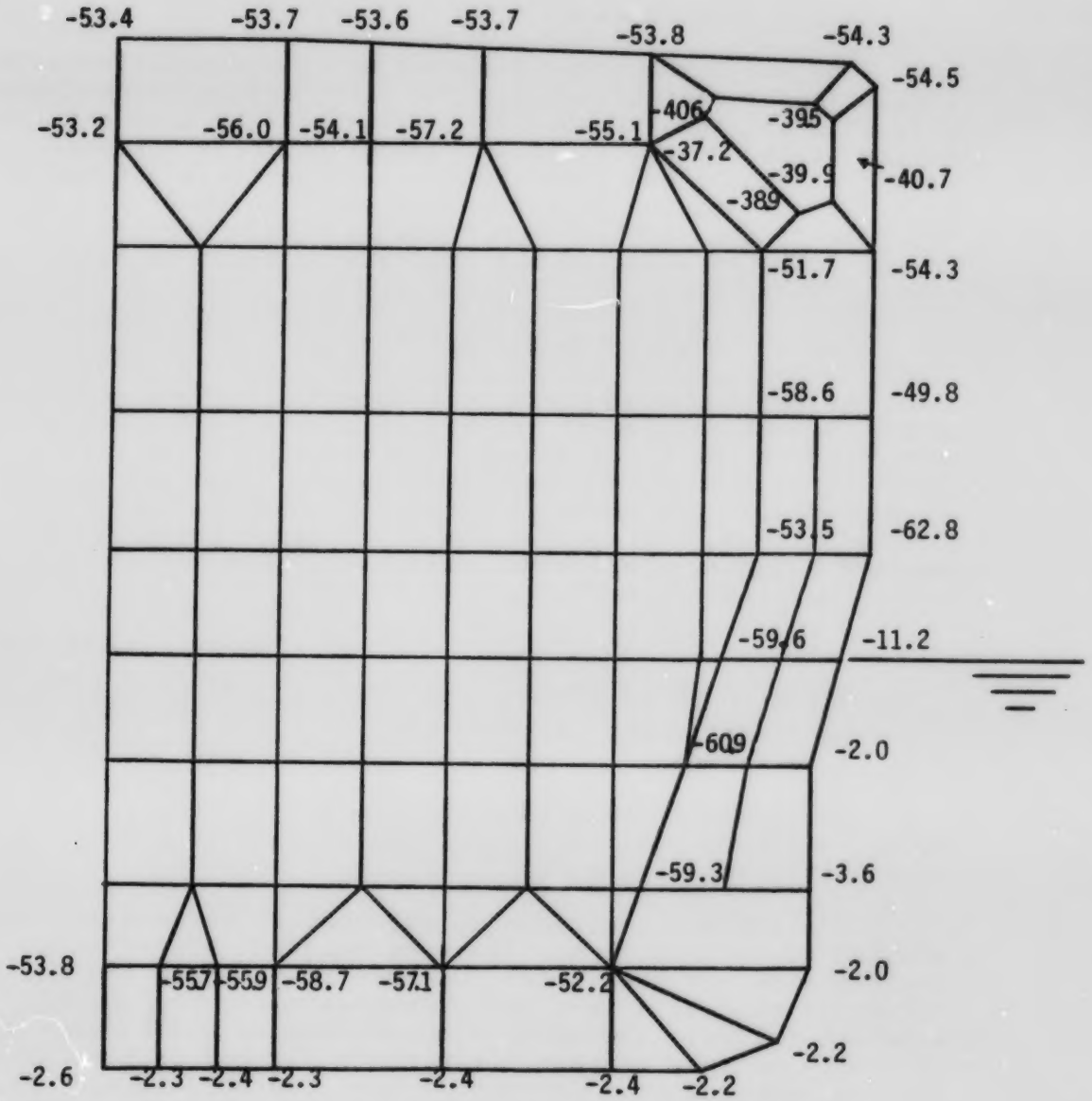

LNG HEAT FLOW MODEL

BULKHEAD IN PLACE

Figure 19 SECOND FRAME

4.2 Model for the 'M.V. Arctic' Bulk Carrier

4.2.1 Introduction

The M.V. Arctic was designed as an ice-breaking bulk carrier and research vessel. The main differences between this ship and the LNG carrier are its smaller size and the nature of the goods carried. Typical cells in the side wall of the hull are approximately 1.5 meters x 2.0 meters with a frame spacing of 1.2 meters which is about 1/3 of the size of the proposed LNG vessel. A mid-ship section of the ship was selected for analysis as shown in Figure 20

4.2.2 The Finite Element Models

As before, two models were constructed, one representing a typical section at the middle of the hold, the other including the bulkhead plates. It was assumed in both models that the hatch cover was in place. The two finite element models are shown in figures 21 and 22. Each cell in the hull was represented and each plate finite element assumed a linear temperature variation. The size of the models were as follows:

	Nodes	Elements
Center hold (2 frames)	152	110
Model including bulkhead and five frames	539	417

The overall dimensions and plate thicknesses are shown in Figure 23. The steel was assumed to have a conductivity of 52 W/m ^{o}C.

The surface coefficients external to the vessel were assumed to have the same values as before. The surface coefficients for the plates internal to the hold and internal to the cells were calculated assuming the spaces were air filled. The mean hold temperature was assumed to be -28^{o}C, mid-way between the minimum air temperature and the sea temperature. In other words, the hold is air-filled and unheated. A variation of the hold air temperature was assumed to exist between the top and bottom of the hold. The surface coefficients used in the analysis and the ambient temperatures assumed are shown in Figure 24 This represents only one of the many circumstances that could exist in practice but illustrates a 'worst case' situation where the metal temperatures should reach their lowest values.

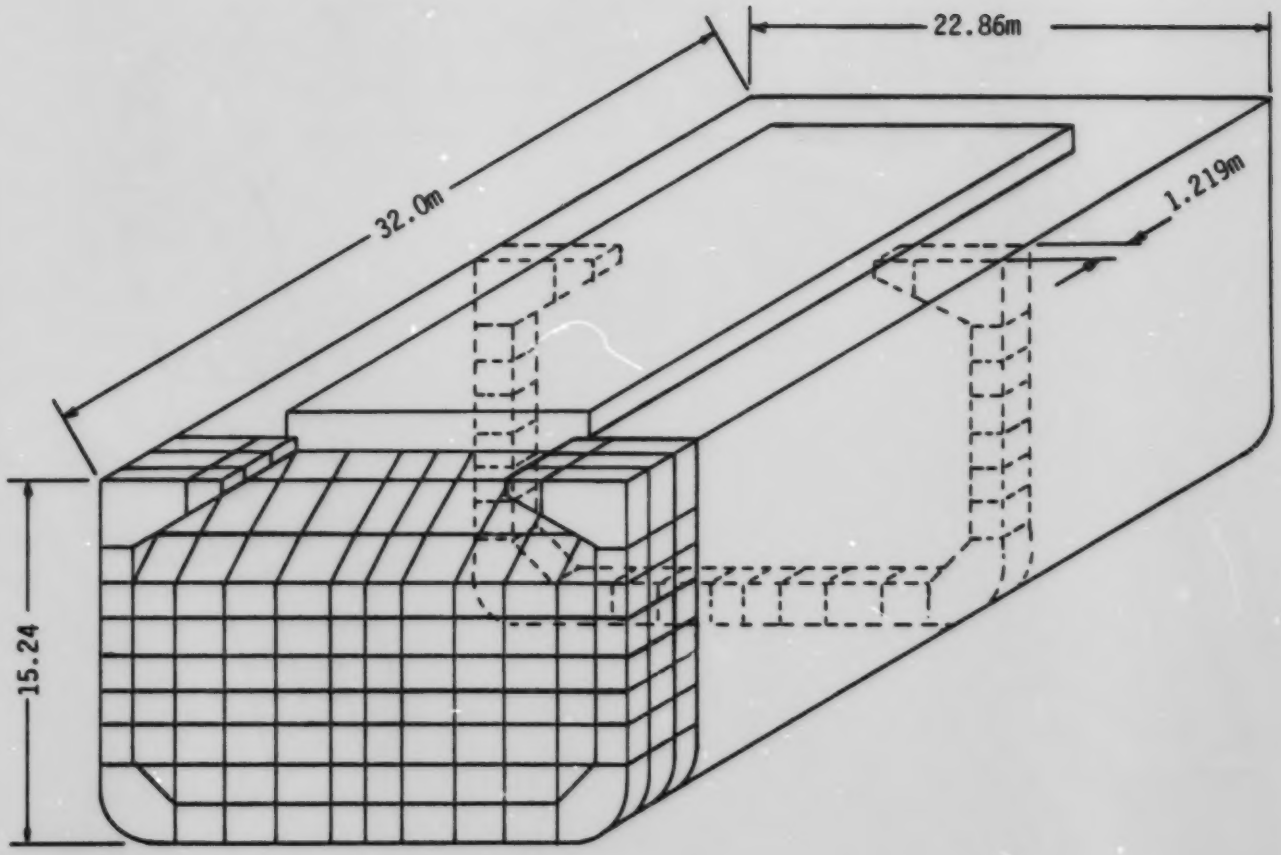

Figure 20 TYPICAL SECTION OF THE M.V. ARTIC

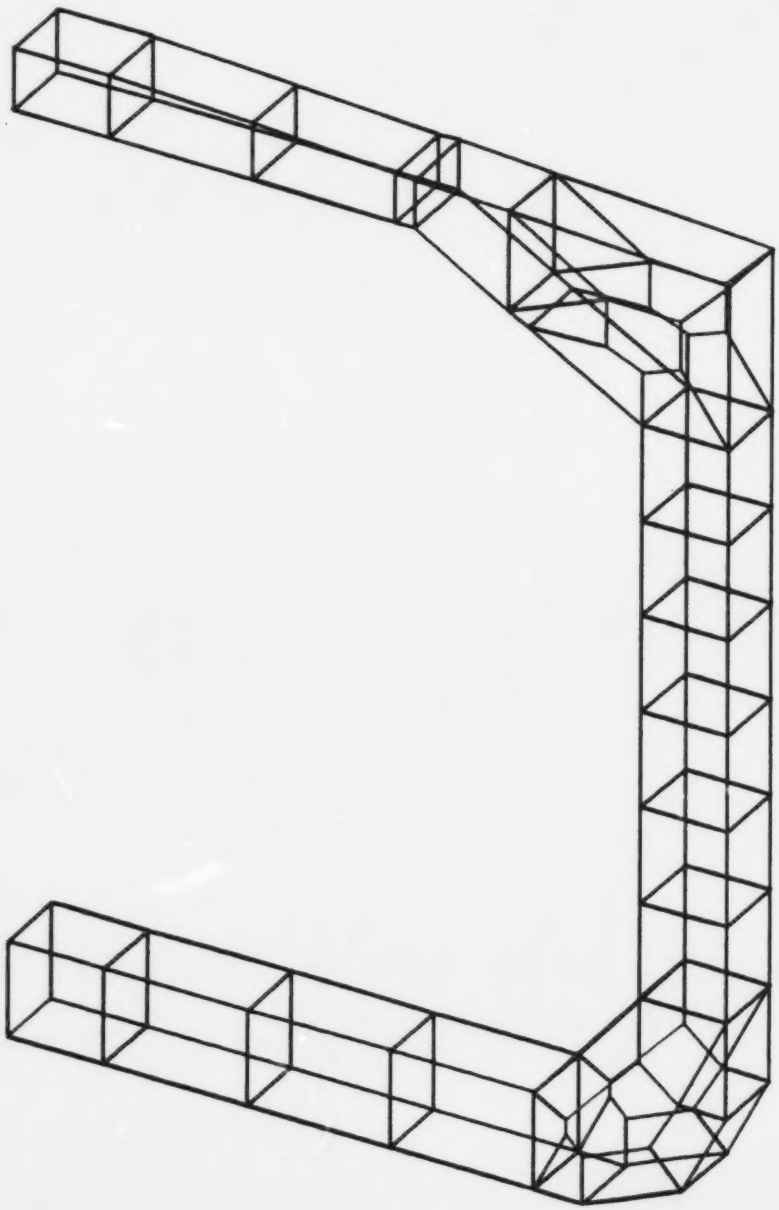

Figure 21 TWO FRAME FINITE ELEMENT MESH OF THE M.V. ARTIC

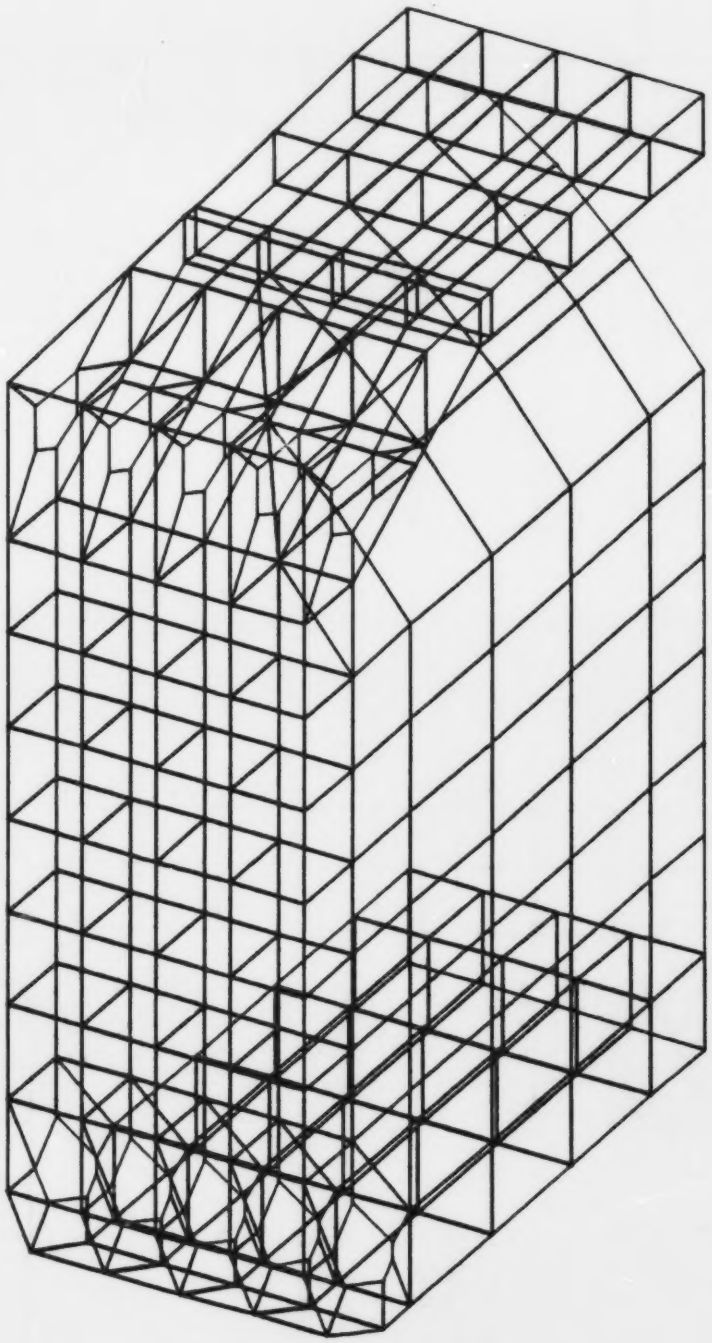

Figure 22 FIVE FRAME FINITE ELEMENT MESH INCLUDING BULKHEAD OF THE M.V. ARTIC

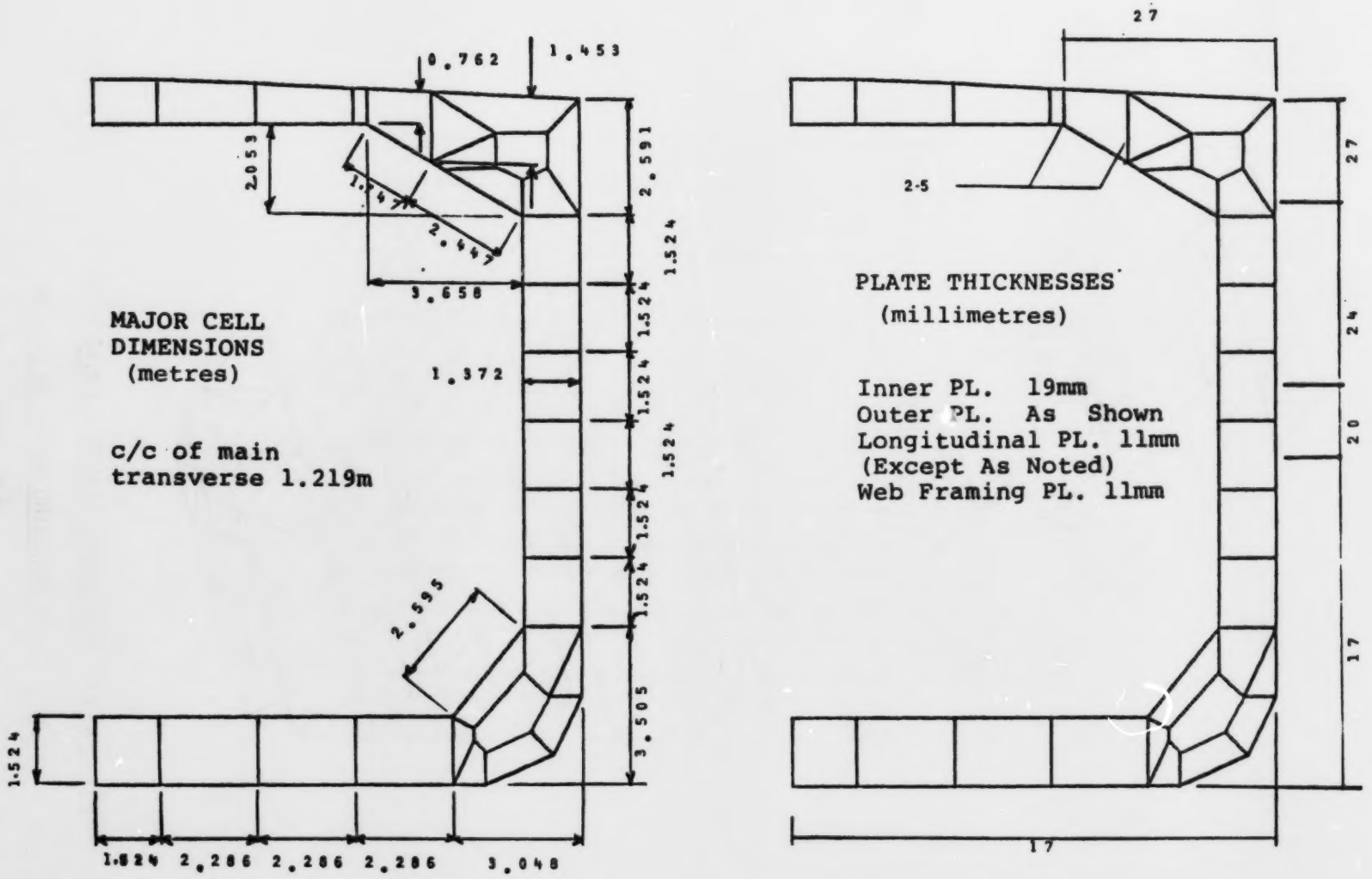

Figure 23 MAJOR CELL DIMENSIONS & PLATE THICKNESSES

M.V. ARTIC

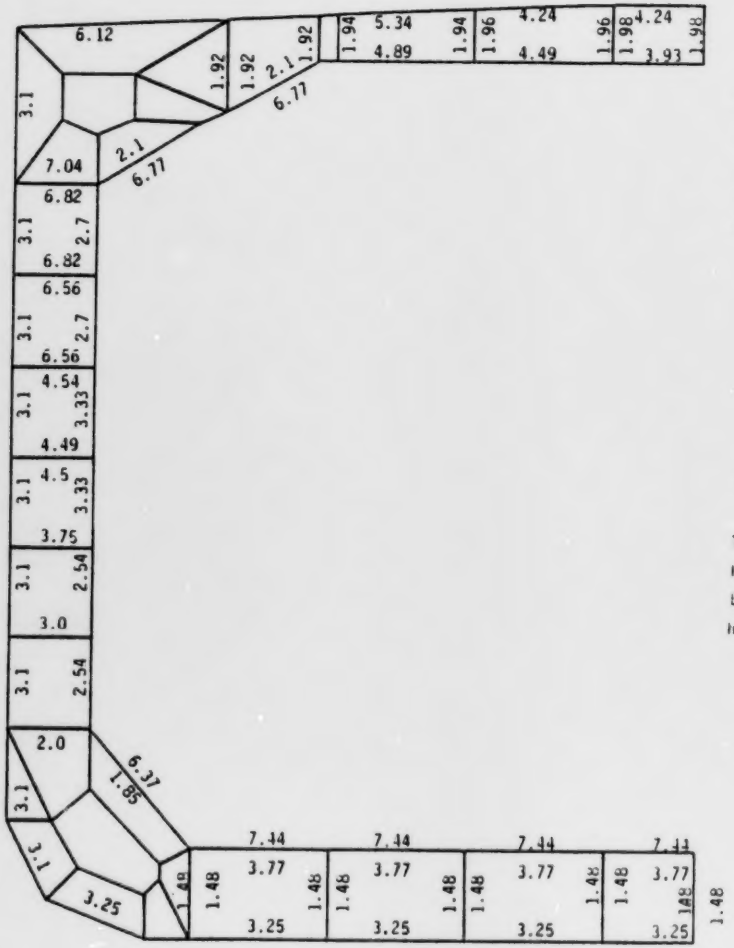

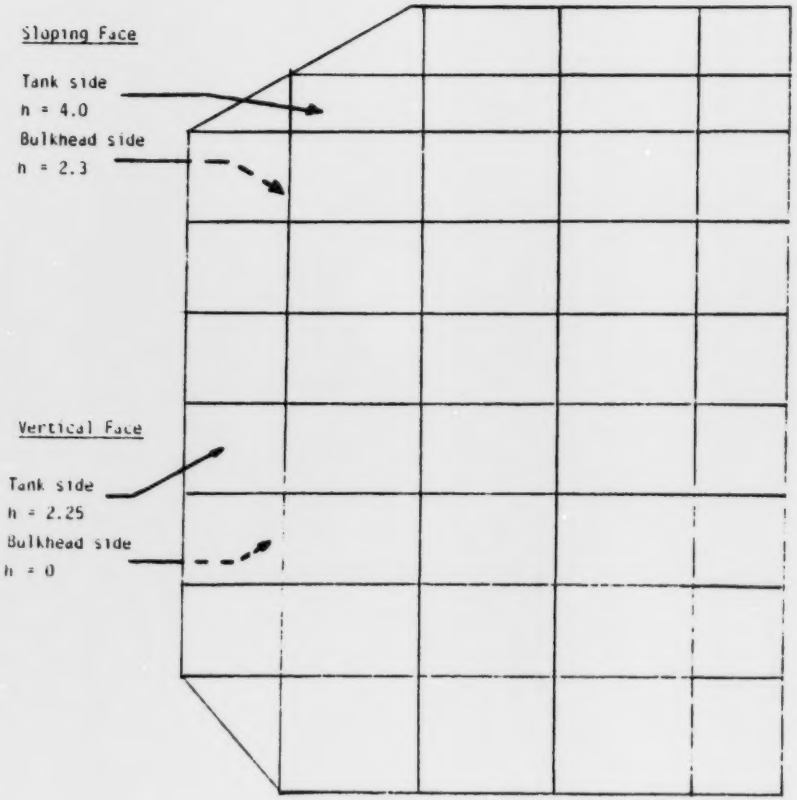

Figure 24 M.V. ARCTIC

SURFACE COEFFICIENTS

4.2.3 Results from the Analysis

The temperatures resulting from the two frame model are shown in Figure 25 and for the frames and bulkhead of the larger model in Figure 26.

Similar deficiencies are observed in the waterline temperatures which are explained as before by the crudeness of the mesh in that region. The outside plate temperatures are clearly those of the environmental conditions and the inner plates on the side of the hold are greatly influenced by the temperature of the hold, which in this case is assumed unheated.

M.V. ARCTIC

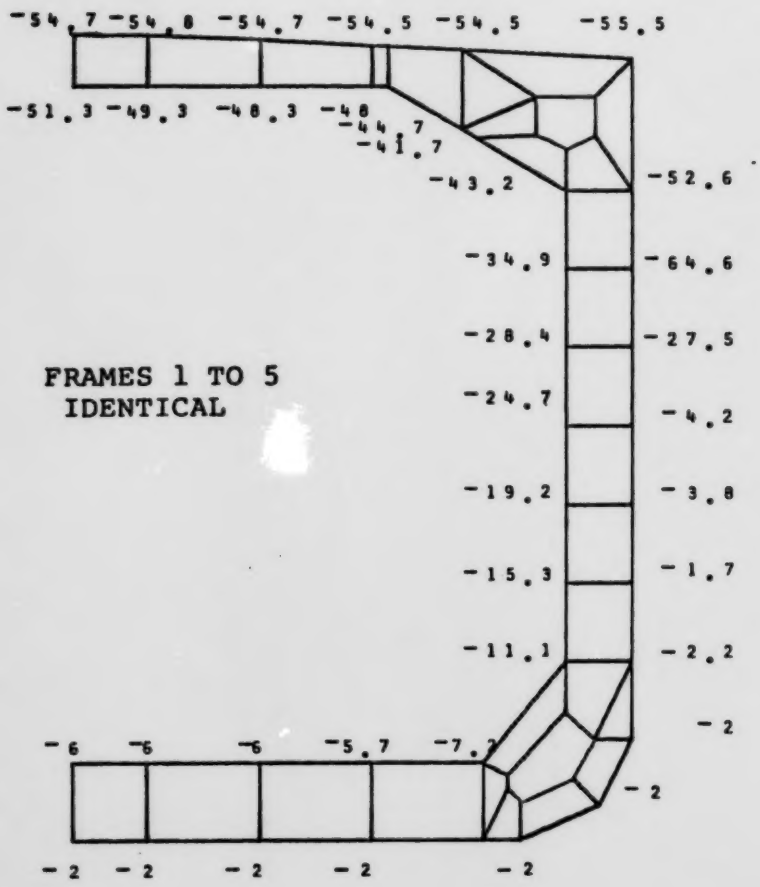

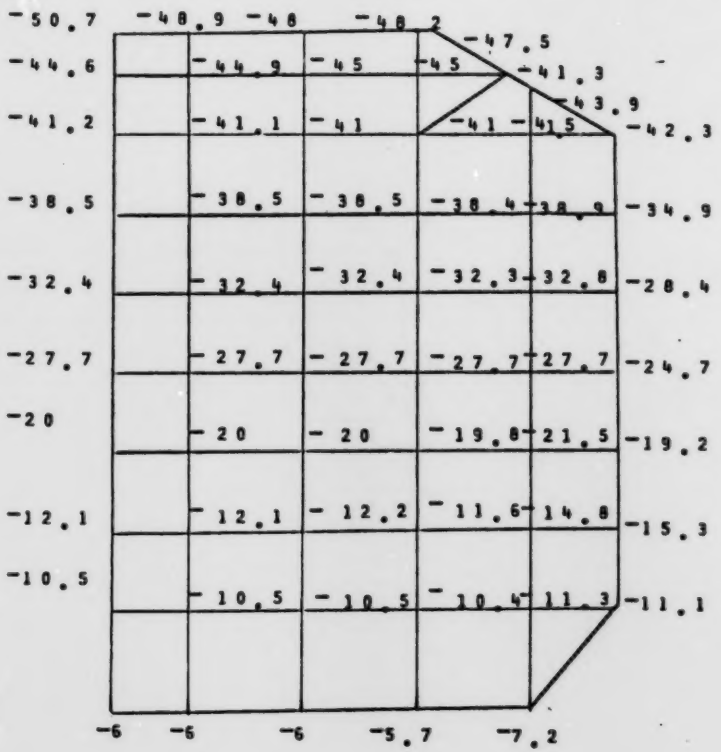

TEMPERATURES ^{o}C

Figure 25 FIVE FRAMES WITH BULKHEAD
RESULTING TEMPERATURES
RUN 1

M.V. ARCTIC

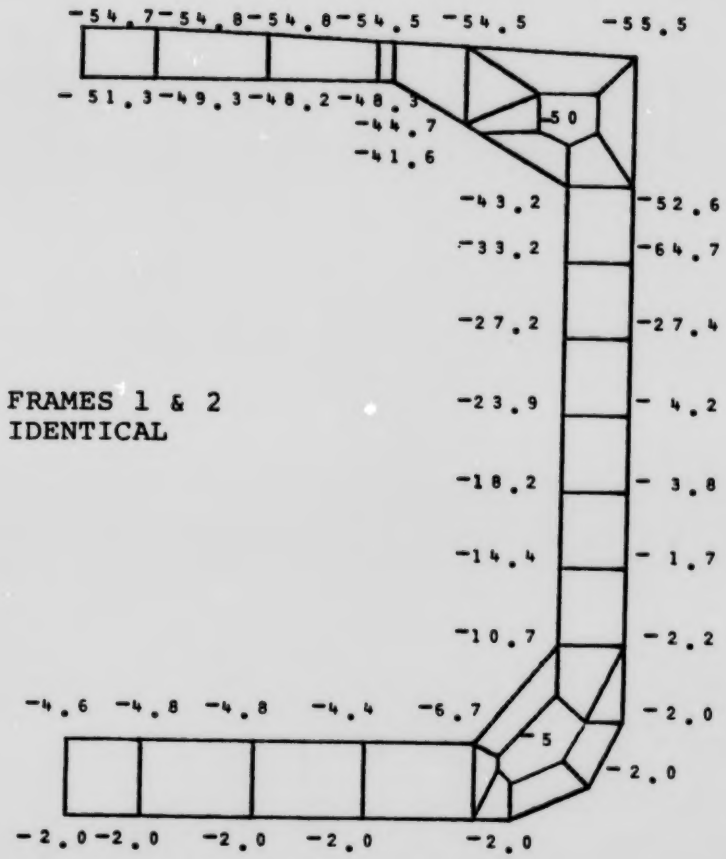

TEMPERATURES ^{o}C

Figure 26 2 FRAMES WITHOUT BULKHEAD
RESULTING TEMPERATURES
RUN 1

4.3 Model of a Section of the Pierre Radisson Icebreaker

4.3.1 Introduction

Unlike the two previous ships modelled, the Pierre Radisson is not a cargo ship but an icebreaker. The internal structure of the vessel is far more complex at the midship section as the engine room and crews' quarters are all located in this area. A three-dimensional sketch of a representative section of the ship is shown in Figures 27-30. Within this framework are cabins, engine room equipment, fuel storage tanks and exhaust ducts. The heat transfer between all these components at first seems impossibly complex to model. In particular the heat transferred through the mass flow of air in and out of the engine room is impossible to calculate without measured data on the mass flow rate and temperature.

The goal of the analysis was to calculate temperature distributions throughout the steel structure of the hull. The main temperature gradients are naturally between the center of the hull and the outside environment. In practice the main air spaces within the hull are divided between living quarters and the engine room. Hence the temperature of a large volume of the interior of the ship can be determined from the knowledge that these areas must be kept within certain limits for the seamen's comfort. The penetration of the colder temperatures through the walls, frames and bulkheads of the ship can then be calculated by a finite element model having suitable heat transfer coefficients specified at the surface of the plates. Interior decking will, in the steady state, be at the temperature of the surrounding air as it has a large surface area exposed to these temperatures.

4.3.2 The Finite Element Model

A finite element plate model was constructed of the essential structure of the center section illustrated in Figure 29 , a plot of the model is shown in Figure 31 .

The major dimensions are given in Figure 32. The model size was as follows:

Number of nodes	151
Number of elements	219

It was assumed the temperature distribution would be symmetric between bulkheads and across the centerline of the hull hence the section modelled extended from a main bulkhead towards the interior of the engine room across four frames. No heat flow was assumed through the

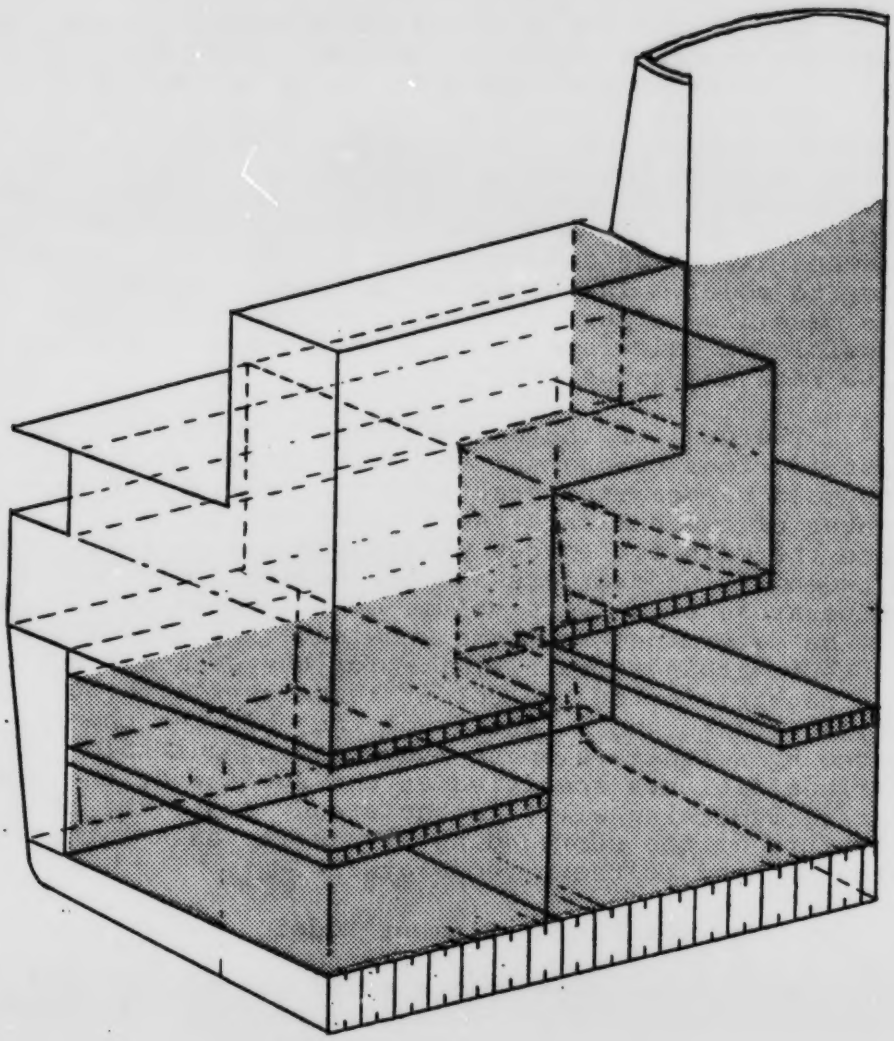

Figure 27 P. RADISSON

ENGINE ROOMS & CASING

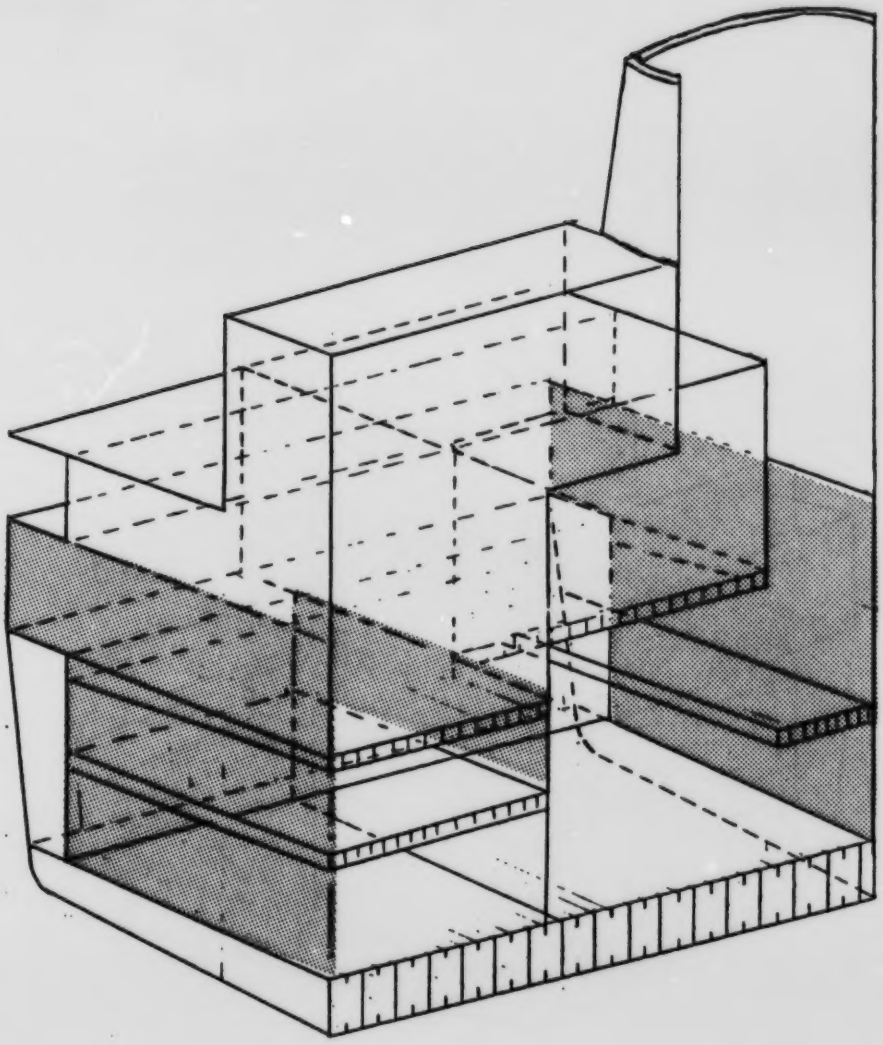

Figure 28 P. RADISSON

BULKHEADS

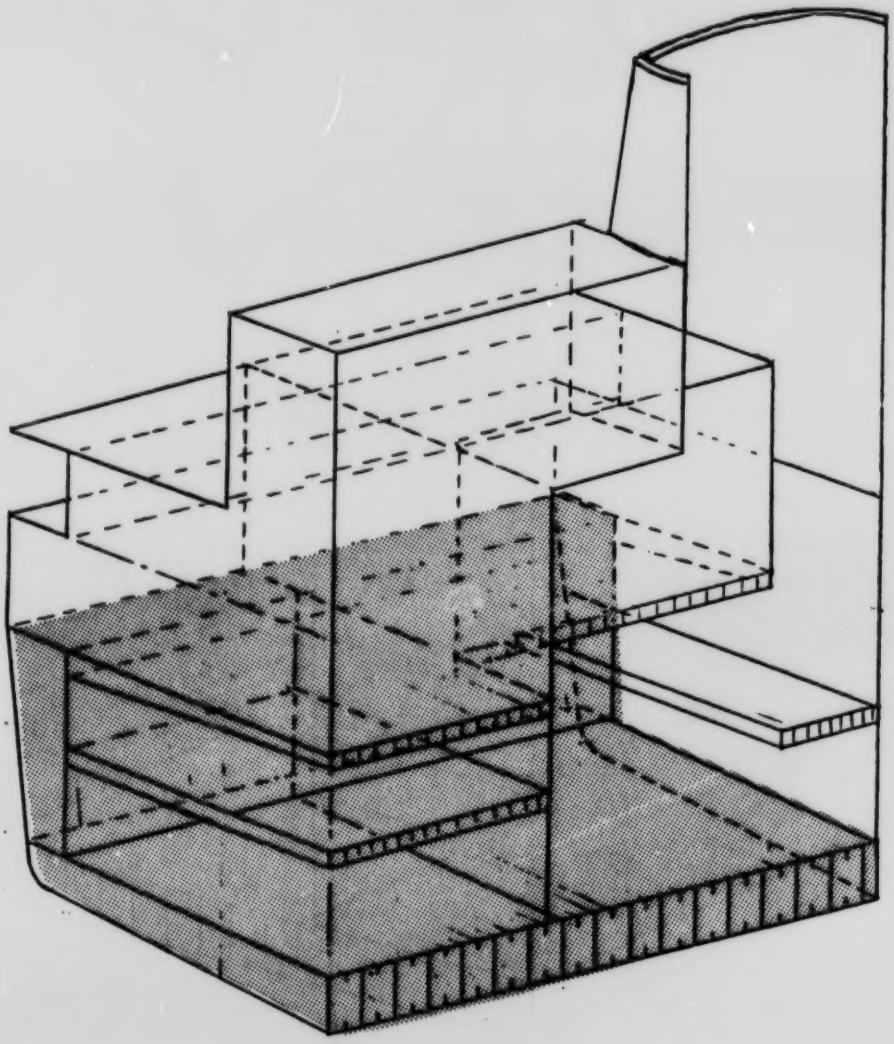

Figure 29 P. RADISSON

SEA BAY & OIL FUEL WING TANKS

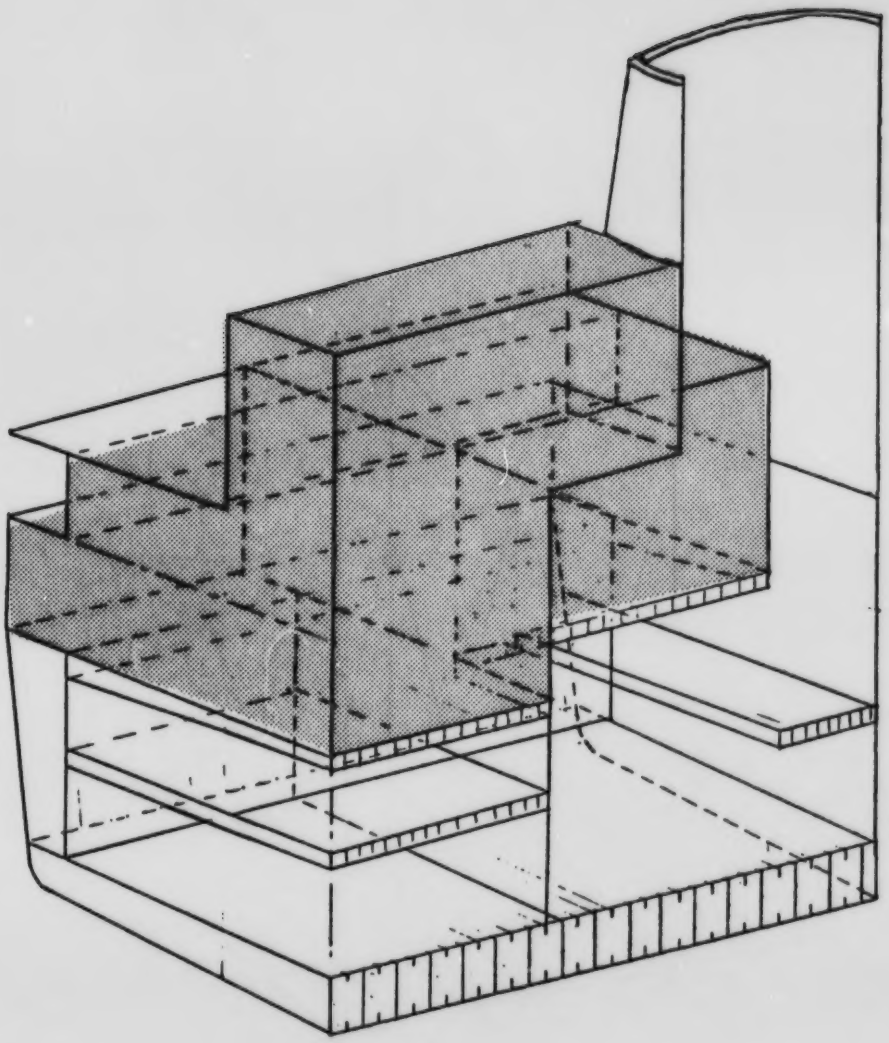

Figure 30 P. RADISSON

ACCOMMODATION

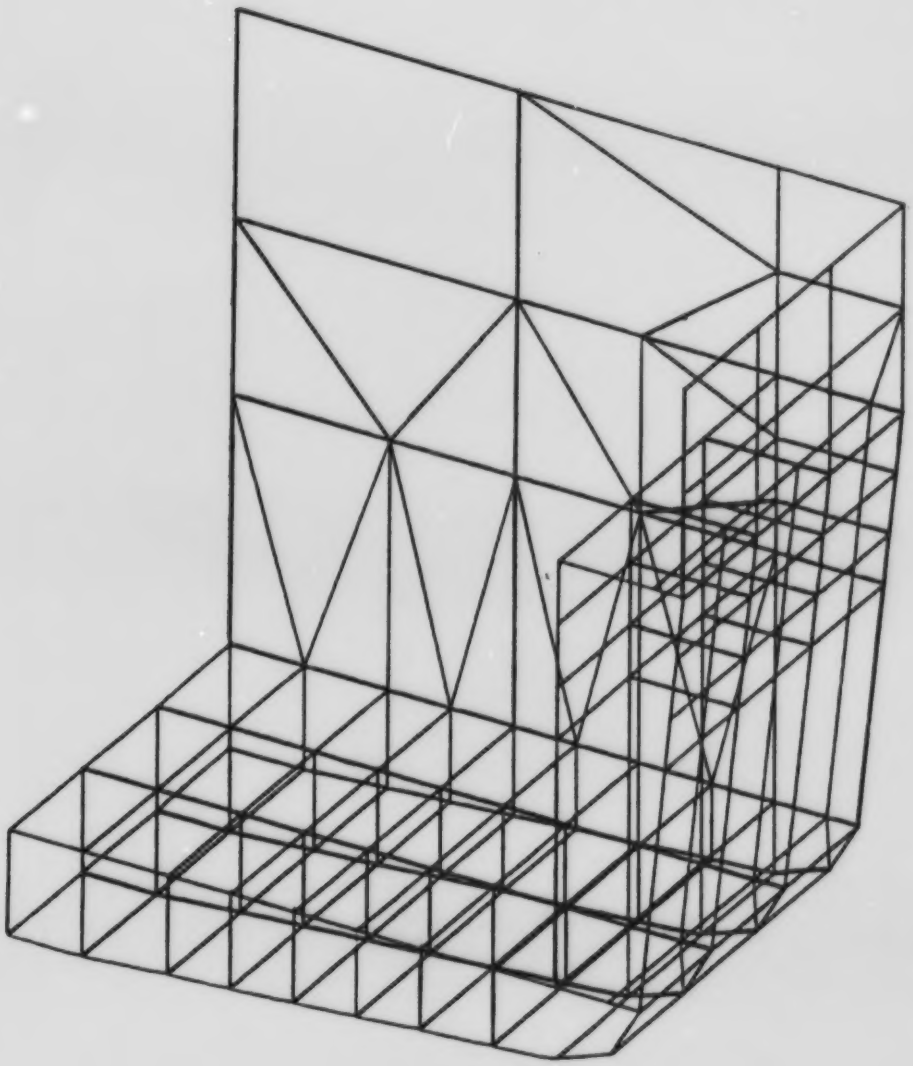

Figure 31 P. RADISSON

FINITE ELEMENT MESH

INCLUDING BULKHEAD

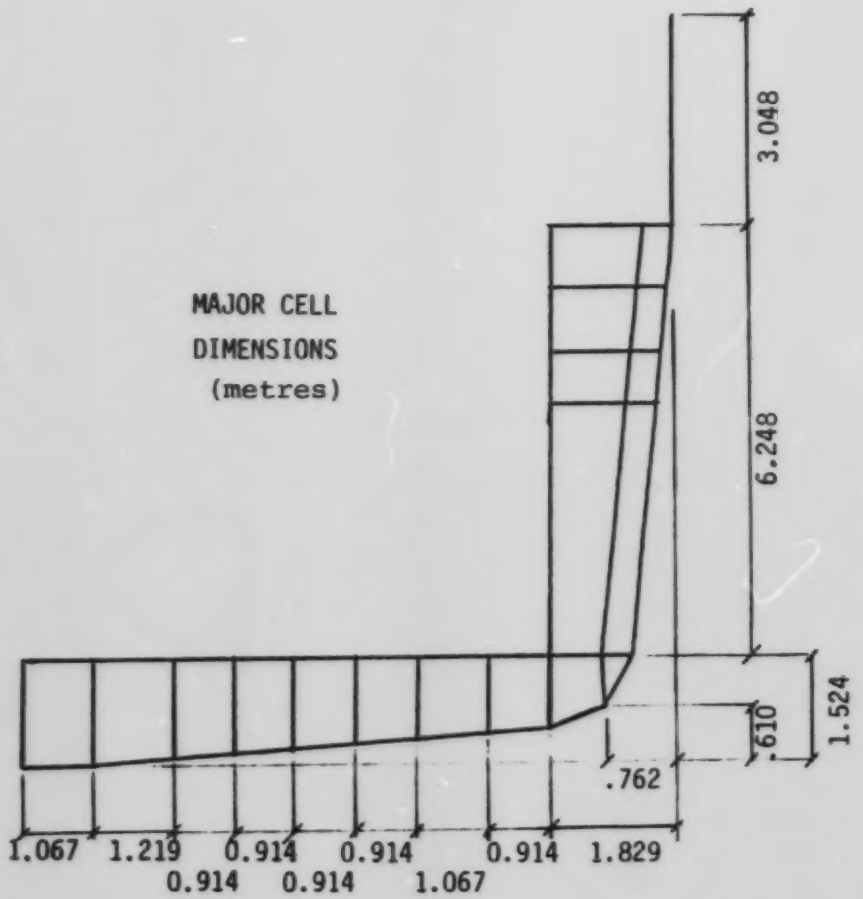

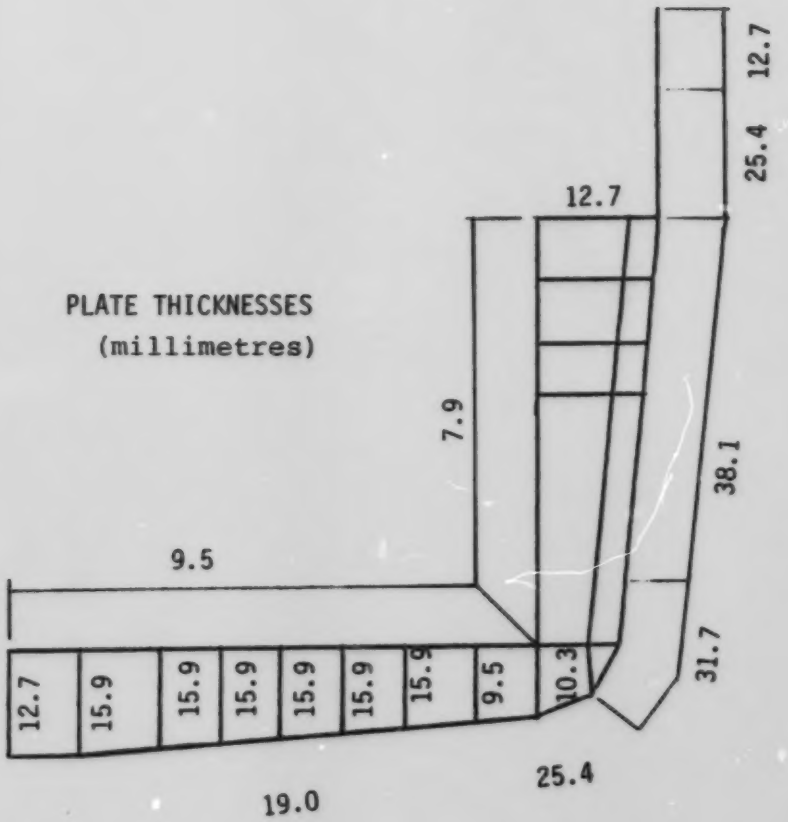

Figure 32

P. RADISSON

MAJOR DIMENSIONS & PLATE THICKNESSES

bulkhead as equivalent conditions were assumed to exist on the opposite side. In this design fuel tanks are situated abreast the engine room and are the main barrier to heat flow through the side of the ship. The sea bay is a complex cellular space consisting of many frames intersected by longitudinal members. It is assumed the space is air filled. The walls of the engine room are insulated but there is no insulation on the steel floor.

For the purpose of this analysis the engine room space was assumed to be at a temperature of 32°C and the living space on the main deck at 20°C. The surface coefficients in the sea bay were calculated, as previously, from an estimate of the inner and outer plate temperatures, and an assumption that natural convection and radiation take place across the cells. It has also been assumed that the fuel tank is air filled. The plate temperatures used as a basis for the calculation are shown in Figure 33.

The effective surface coefficient (h*) due to radiation is approximated by the following expression

$$h^* = \sigma \frac{\hat{f}_{12} (T_1^4 - T_2^4)}{(T_1 - T_3)} \qquad (44)$$

where T_1 & T_2 are estimates of the cell wall temperatures

T_3 is the mean cell temperature

$\hat{f}_{12}$ is the factor that determines the fraction of the heat which passes from grey surface 1 (directly or indirectly) and is absorbed by grey surface 2.

σ is the Stefan-Boltzmann constant =

$$5.67 \times 10^{-8} \text{ W/m}^2\text{K}^4$$

(Note: All temperatures are in absolute K)

For the fuel tank the dimensions are such that the areas radiating between the wall of the ship and the inside plates are considerably greater than the end plate areas. The value of the f factor will therefore be close to 0.25.

Note : Temperatures in °C

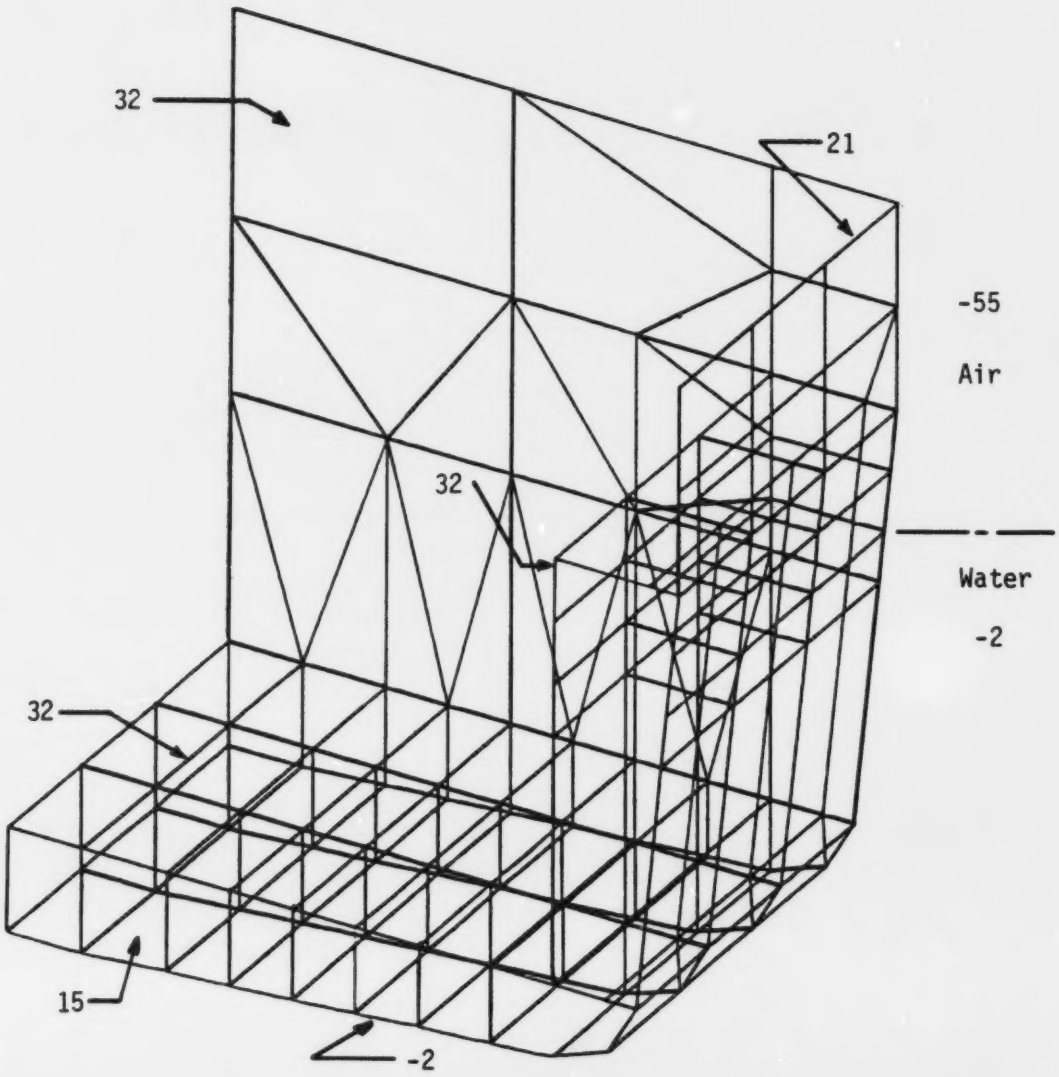

Figure 33 P. RADISSON

AMBIENT TEMPERATURES

In addition

$$T_1 \sim 4 + 273 = 277 \text{ K}$$

$$T_2 \sim 22 + 273 = 295 \text{ K}$$

$$T_3 \sim 10 + 273 = 283 \text{ K}$$

Hence the effective surface coefficient for the tank h^*_{tank} is

$$h^*_{tank} = \frac{5.67 \times 10^{-8} \times 0.25 \times (277^4 - 295^4)}{(277 - 283)}$$

$$\sim \underline{4.0 \text{ W/m}^2 \text{ K}}$$

For the sea bay the cells are approximately cubic hence $\hat{f} = 0.5$. The plate temperatures are estimated to be

$$T_1 \sim 273$$

$$T_2 \sim 293$$

$$T_3 \sim 283$$

Hence the effective surface coefficient for the sea bay cells h^*_{sb} is

$$\underline{h^*_{sb} \sim 5.2 \text{ W/m}^2 \text{ K}}$$

A figure for the surface coefficient of the uninsulated steel floor of the engine room was taken from P59 Table 15, (SNAME - Thermal Insulation Report). (Ref. 3).

$$h_{sf} = \underline{4.0\ W/m^2\ K}$$

From the same reference, the effective surface coefficient for the insulation on the bulkhead (5 cm F.G. Type 335) h_{blk} and engine room wall was recommended as

$$h_{blk} = \underline{0.8\ W/m^2\ K}$$

The inside surface of the upper hull was given as 4 in F.G. Type 335 + 3/4 in T.A.C. board for which the effective surface coefficient was given as

$$h_{upper} = \underline{0.4\ W/m^2\ K}$$

These results are illustrated in Figure 34.

4.3.3 Results from the Analysis

The steady state temperature distribution is shown in Figure 35 . As before an anomalous temperature is recorded at the waterline. It can be seen that the cold external temperatures penetrate very little into the interior of the ship. The heat transfer through the surface of the plates dominates over the conductive flow. Thus plates exposed to the interior air temperatures and insulated from the outside environment by air cavities or cells will be close in temperature to the ambient air. Frames, longitudinals and stiffeners intermediate to these plates will have a temperature distribution varying in an approximately linear manner from the inside to the outside plates. Local temperature distributions in these members can only be found from a more accurate model of a local area which takes into account the variation of natural convective flows around the cells.

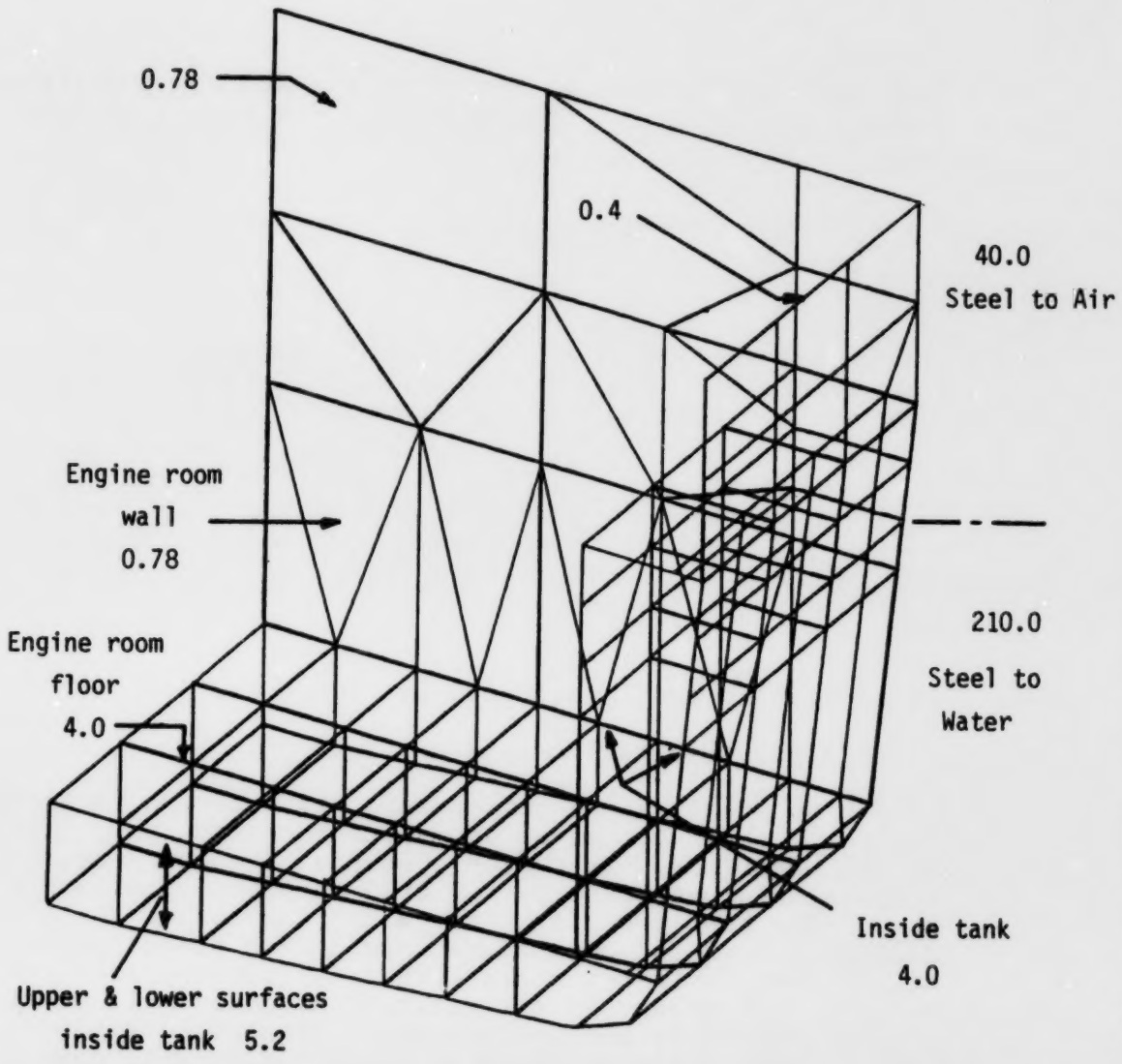

Figure 34 P. RADISSON

SURFACE COEFFICIENTS

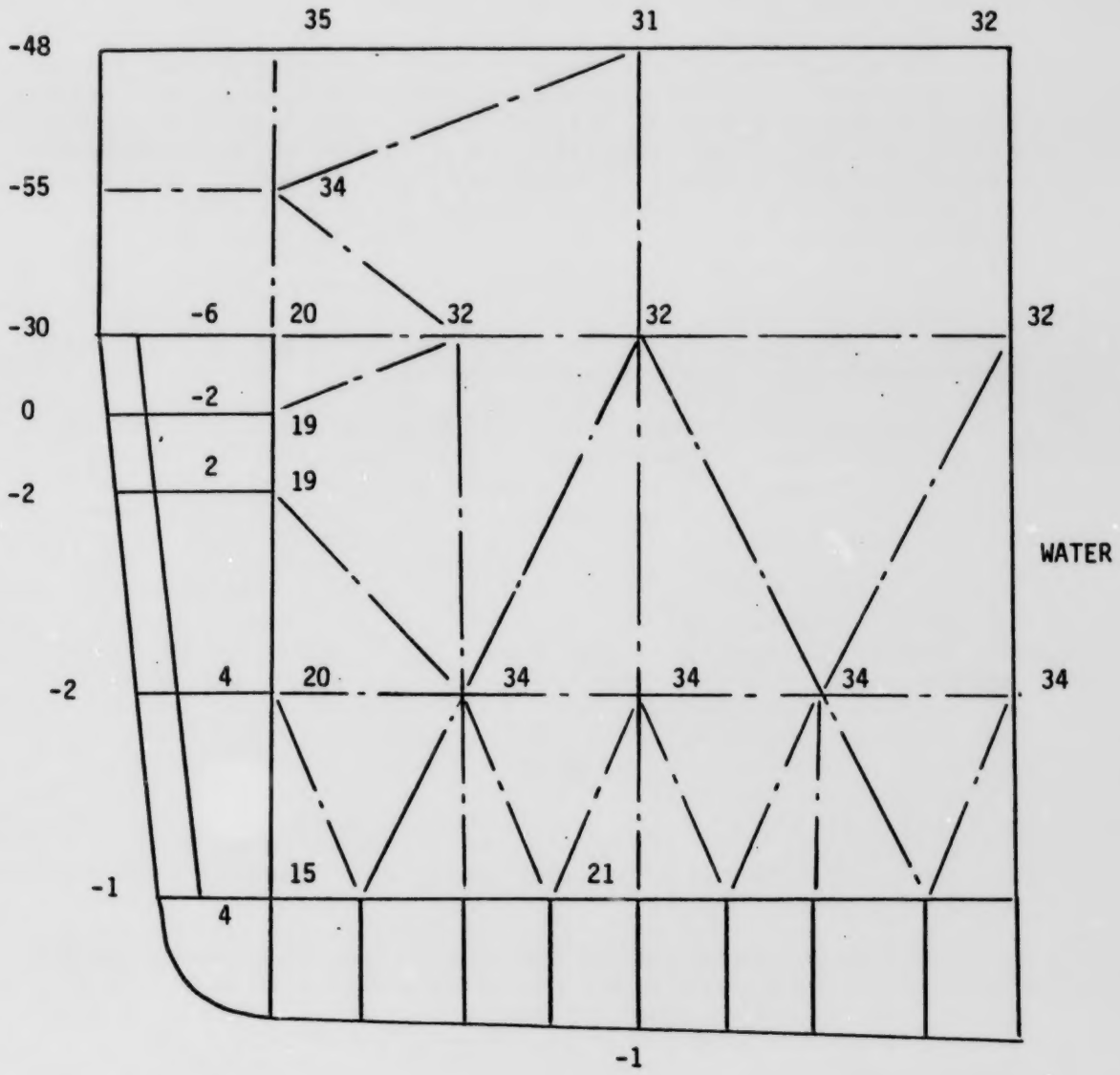

Figure 35 P. RADISSON

PLATE TEMPERATURES (°C)

4.4 Conclusions from the Finite Element Analysis of Multi-Compartment Sections

An attempt has been made in the preceding three models to represent the heat transfer characteristics of hull sections of three quite different ships. The finite element method has been used to formulate a linear model representing conduction through the plates. Environmental temperatures have been taken as the lowest operating conditions anticipated in Arctic waters. Heat flux through the surfaces of the plates in the hull is a combination of convection and radiation and estimates have been made from the best available data as to the nature of the equivalent linear surface coefficients representing these effects and their associated ambient temperatures.

The object of these analyses was two fold. First to investigate the temperature distribution across a central section of each hull under typical Arctic conditions, and second to illustrate the use of this modelling technique for solving problems of this type. In the process of performing the analysis, it was possible to center in on a number of key factors that influence the nature of the solution. Naturally, the different ships presented their own particular problems but these might occur in any other analysis of this type and hence were valuable in demonstrating difficulties. These models represented large sections of the ship and as such could be termed macro-modules. Temperature variations through individual stiffeners, and locally at the corners of the intersections of plates, were ignored, and only average temperatures of the plate sections were obtained. As is shown later such micro-models can be built and local heat transfer effects studied in more detail.

The main advantage of the finite element method is its ability to model arbitrary plate geometries with relative ease. Hence the conduction paths through the hull can be established for complex plate assemblages rather easily. The method, and in particular the computer program, can be used to model any form and section of a ship's hull, and do so in a relatively mechanistic way from the point of view of the user. In the models shown here, for example, the finite element shapes were mostly decided by the real plate sub-divisions of the hull. In theory, if more elements were used to represent the same plate, a more accurate solution to the temperature distribution would be obtained. In practice one has to trade off cost in building and running the computer model against a desired level of accuracy. Unfortunately, even when all aspects of the model are

accurate, the finite element method only provides an approximate solution. This solution improves with increasing numbers of elements, but no proper measure exists to determine the accuracy in any absolute way. For the models of the three ships, the plate temperatures away from areas of rapid temperature change near the waterline should be within 2 - 3°C of the steady-state solution for the model configuration and boundary conditions assumed.

The most inaccurate component of all the models is the choice of the surface coefficients for the plate surfaces internal to the hull. At this time, the error cannot be verified by experiment or by numerical analysis. However, the areas most affected by the potential error can be identified. The external hull plates are clearly going to follow closely the external ambient temperatures because the heat transfer to the external surface of these plates is very much higher than to the internal surfaces. The plates most affected by the error are those of the internal structure. Assuming that the internal ambient temperatures have been correctly chosen, then the errors could be in the 5 - 10°C range. The coarseness of the model in areas of rapid fluid temperature change, or near structural discontinuities, is likely to cause errors of a similar size. For the purpose of establishing structural temperatures in an average sense, it is felt the macro finite element models are sufficiently accurate. Such models can be used for establishing the quality of structural steels needed and for examining gross thermal stress effects that may be created internal to the hull. None of the models illustrated here have considered any other than the minimum external temperature conditions. However, the same form of model could be used to establish temperature differences across the hull caused by, for example, wind cooling on one side and solar heating on the other.

In order to study the micro thermal effects of local temperature changes and to examine in more detail the heat flux through a typical cell in the ship's hull, other models, as described in Section 5, are more appropriate.

5. HEAT FLOW MODELS - SINGLE CELL MODELS

5.1 Model of a Single Cell from the Proposed LNG Carrier

5.1.1 Introduction

Having identified the importance of the heat transfer across a typical cell in a ship's hull, an alternative approach to modelling this complex phenomenon has been attempted using a series of thermal network models. The simplest model represents the case where the surfaces of the inner and outer cell plates are assumed to be at uniform temperature, and the internal fluid is well mixed, and hence also at a uniform but unknown temperature.

The transfer of heat across a typical cell in the LNG carrier has been shown to depend heavily on the convection and radiation components in addition to the conduction through the surrounding steel. The two former effects are essentially non-linear. The THETA heat transfer program is designed to solve non-linear problems that can be expressed as a network of inter-connected nodes.

5.1.2 Steady-state thermal network model

The typical cell selected for this model was the same as in the example used in section 3.1. The idealization is shown in Figure 36. The parameters governing the model are given below and differ slightly from those in the original analysis.

Environmental conditions

External air temperature	218 K
LNG temperature	111 K

Heat transfer links

External surface coefficient	40 W/m^2 K
Internal surface film coefficients L1, L2	0.66 W/m^2 K
Insulation on internal LNG surface	0.151 W/m^2 K
Conduction through cell walls	
Steel conductivity	52 W/m K
Conduction path length	3.14 m
Cross-sectional area	0.1792 m^2
Radiation through cell	
View factor	0.50
Emissivity	0.94

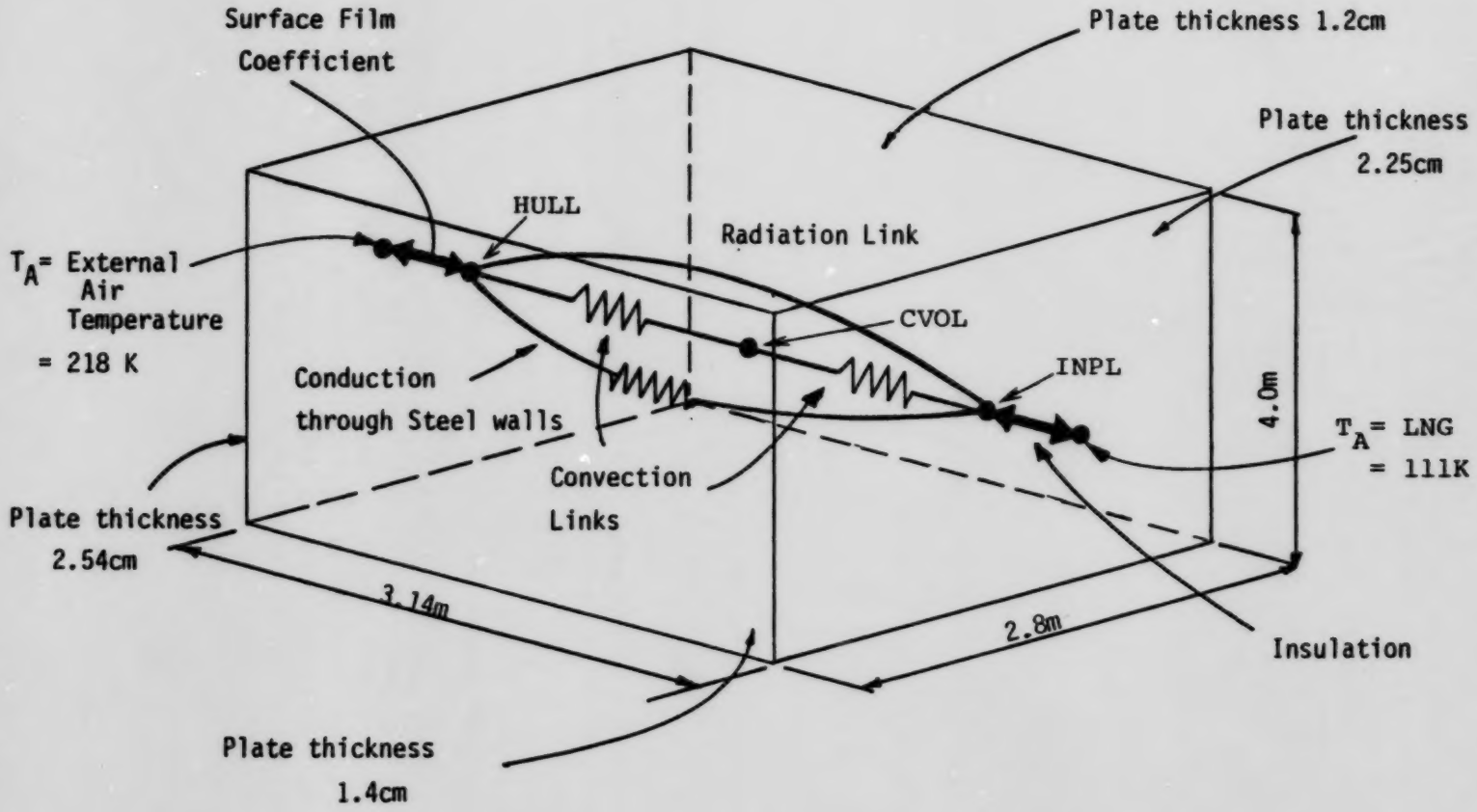

Figure 36 SINGLE CELL FROM PROPOSED LNG TANKER

The data prepared for the THETA model are shown in figure 37 as listed from the program. The node on the external side of the cell is labelled HULL and that on the interior INPL. The node at the center of the volume is labelled CVOL. Conduction, convection and radiation links are used to represent the heat flow through the cell. Surface coefficients representing the interior insulation and external forced air convection are also provided. A non-linear steady-state solution has been obtained for the minimum external air temperature of -55°C and assuming the interior of the ship is filled with LNG at -162°C.

5.1.3 Discussion of the results

A listing of the temperatures and heat fluxes output from THETA are shown in figure 38. The results indicate that for the particular example chosen, the balance of the heat flows is

	Watts	%
Conduction through the steel	33.6	23.66
Radiation	24.7	17.39
Convection	83.7	58.95
		100.00

Thus even with a relatively low convective surface coefficient assumed internally, the convection still dominates the heat transfer.

The balance between the three heat transfer mechanisms differs from that given in Section 3 for two reasons a) the temperature difference across the cell turns out to be less, and b) the convective surface coefficient was computed to be much lower at this smaller temperature difference. The radiation component is lower for the same reason.

The temperature dependence of the surface coefficient representing natural convection could be included in the definition of the model. However, the added complexity could only be justified if this dependence were more accurately defined, and if the temperature range encountered was substantially greater than in the present example.

THERMAL NETWORK ANALYSIS - INPUT DATA FOR STEADY STATE SOLUTION

Engineer ...A.F.
Date ...
Run Identifier ...SIMPLE CELL - LNGS1

DATA SUMMARY

Number of Nodes in Structure	...	3
Number of Conduction Links	...	3
Number of Conduction Link Interfaces	...	2
Number of Radiation Links	...	1
Highest number of Surface Faces for any one Node	...	1
No of Surfaces having Implicit Radiation Losses	...	2
Number of sets of Bulk Material Properties	...	2
Number of sets of Surface Material Properties	...	1
Number of Background Load Points Cases	...	2 1
Solution Type	...	STEADY STATE
Number of Results Outputs	...	1
Problem Bandwidth	...	3
Due to Radiation link no 1 connecting nodes 1 and 3		

BODY DATA

Data set consists of 3 entries

Node Number	Name	Volume	No. of Surface Faces	Bulk Properties Identifier
1	HULL	284000.00	1	SSHIPST
2	CVOL	352000.00	0	AIR
3	INPL	384000.00	1	SSHIPST

SURFACE DATA

Data set consists of 2 entries

Implicit radiation loss background temperature = SUPPRESSED

Node Name	Face Number	Area	Surface Properties Identifier	Sum of Body View Factors
HULL	1	112000.00	SSHIPST	.500
INPL	1	112000.00	SSHIPST	.500

CONDUCTION LINK (HOMOGENOUS) DATA

Data set consists of 1 entries

	Connected Node Names		Link Length	Link Cross Section
1)	HULL	INPL	314.00	895.00

CONDUCTION LINK (INTERFACE) DATA

Data set consists of 2 entries

	Connected Node Names		Link Length	Link Section	Link Length	Link Section	Interface Conductance	Interface Section
1)	HULL	CVOL	0.00	0.00	0.00	0.00	.66	112000.00
2)	CVOL	INPL	0.00	0.00	0.00	0.00	.66	112000.00

RADIATION LINK DATA

Data set consists of 1 entries

	NODE NAME	FACE NO	VIEW FACTOR	NODE NAME	FACE NO	VIEW FACTOR
1)	HULL	1	.5000	INPL	1	.5000

Figure 37

THETA1 THERMAL NETWORK ANALYSIS - STEADY STATE SOLUTION(S)
(Temperatures are output in degrees KELVIN)

OUTPUT NUMBER ... 1 OF ... 1

ENGINEER ... A.F.
DATA PREPARATION DATE ...
RUN IDENTIFIER ... LMG CELL - LMGS1

CONVERGENCE CRITERIA

	Criteria	Value Set	Value Achieved
	Limit on the Number of Iterations	10000	29
***	Limit on ABS of Temperature Differences	1.00E-02	9.17E-03

('***' indicates set value achieved or exceeded)

FULL OUTPUT - TEMPERATURE DISTRIBUTION AND DETAILED HEAT FLOWS

Heat Flow Sign Convention - Into Node POSITIVE

Structure Network Details

Node A	Temp	Node B	Temp	Link Type	Heat Flow (Watts) A to B
HULL	217.68			Background Link	139.3670
		INPL	195.03	Radiation (1,1)	-24.6907
		INPL	195.03	Conduction	-33.9797
		CVOL	206.36	Conduction	-83.7396

				Nodal Heat Balance =	-2.439E-00
CVOL	206.36	HULL	217.68	Conduction	83.7396
		INPL	195.03	Conduction	-83.7396

				Nodal Heat Balance =	-2.352E-05
INPL	195.03			Background Link	-142.3200
		HULL	217.68	Radiation (1,1)	24.6907
		HULL	217.68	Conduction	33.9797
		CVOL	206.36	Conduction	83.7396

				Nodal Heat Balance =	-1.367E-02

Figure 38

5.2 Finite Element Model of a Single Cell

5.2.1 Introduction

Having completed a study of a number of ship hull geometries for macro temperature variations throughout the hull, it was felt that a closer examination of a typical cell was required for a range of internal and external boundary conditions. Such a study in three dimensions should reveal the sensitivity of the solution to the variation of boundary conditions and be capable of determining local temperature variations along the plates.

5.2.2 The Cell Model

The dimensions of the cell chosen were typical of those in the mid-ship section of the M.V. Arctic and are shown in Figure 39. A fully symmetric set of temperature boundary conditions was assumed such that a half model of the cell could be constructed.

It was assumed that this cell was located at the waterline in such a way that the water surface was at the center line of the cell.

The model was constructed using the ASASHEAT program and the same quadrilateral plate element types used in previous analyses. In this case the mesh was refined particularly in the area near the waterline and at the corners of the cell, see Figure 40.

From previous consideration of the nature of the convective circulation within a cell, it was realized that the velocity of flow and hence heat transfer would likely reach a maximum at the center of the cell and die away to perhaps 25% of the maximum at the outside. The value of the maximum was calculated using the simple semi-empirical formulas described in section 3.1.4 and implemented in the program FILMC. The variation was expressed over the surface as a product of two harmonic terms

$$h' = h \left[(1\text{-const}) \sin\left(\frac{\pi z}{H}\right) . \cos \frac{\pi x}{W} + \text{const} \right] \qquad (45)$$

where H - height (z direction)

W - width (x direction)

The value of 'const' has been chosen to be 0.25. This distribution is shown in Figure 41.

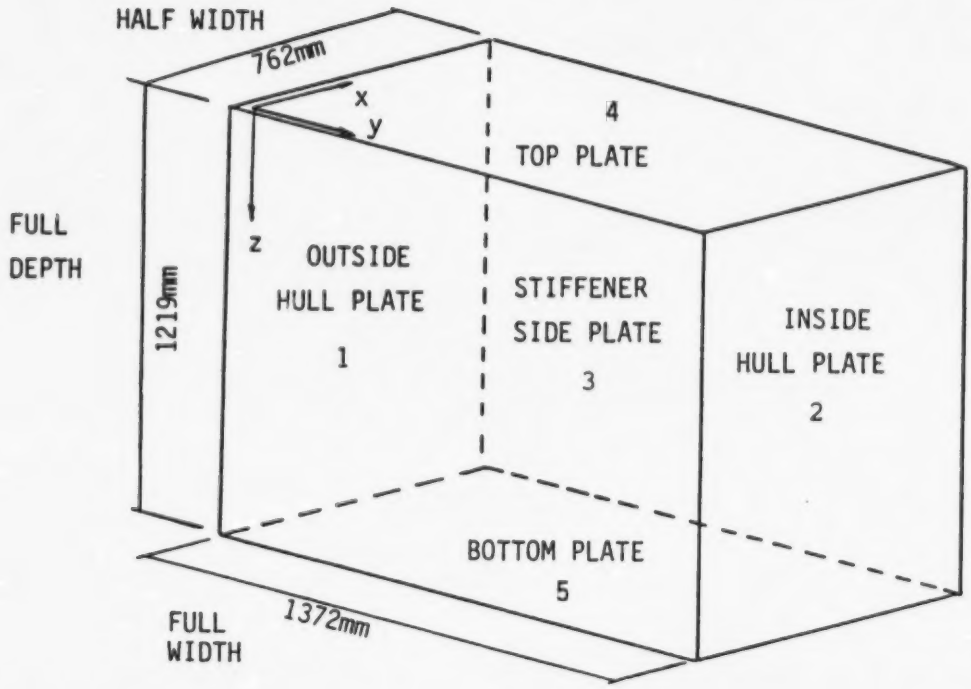

Figure 39 M.V. ARCTIC - CELL MODEL

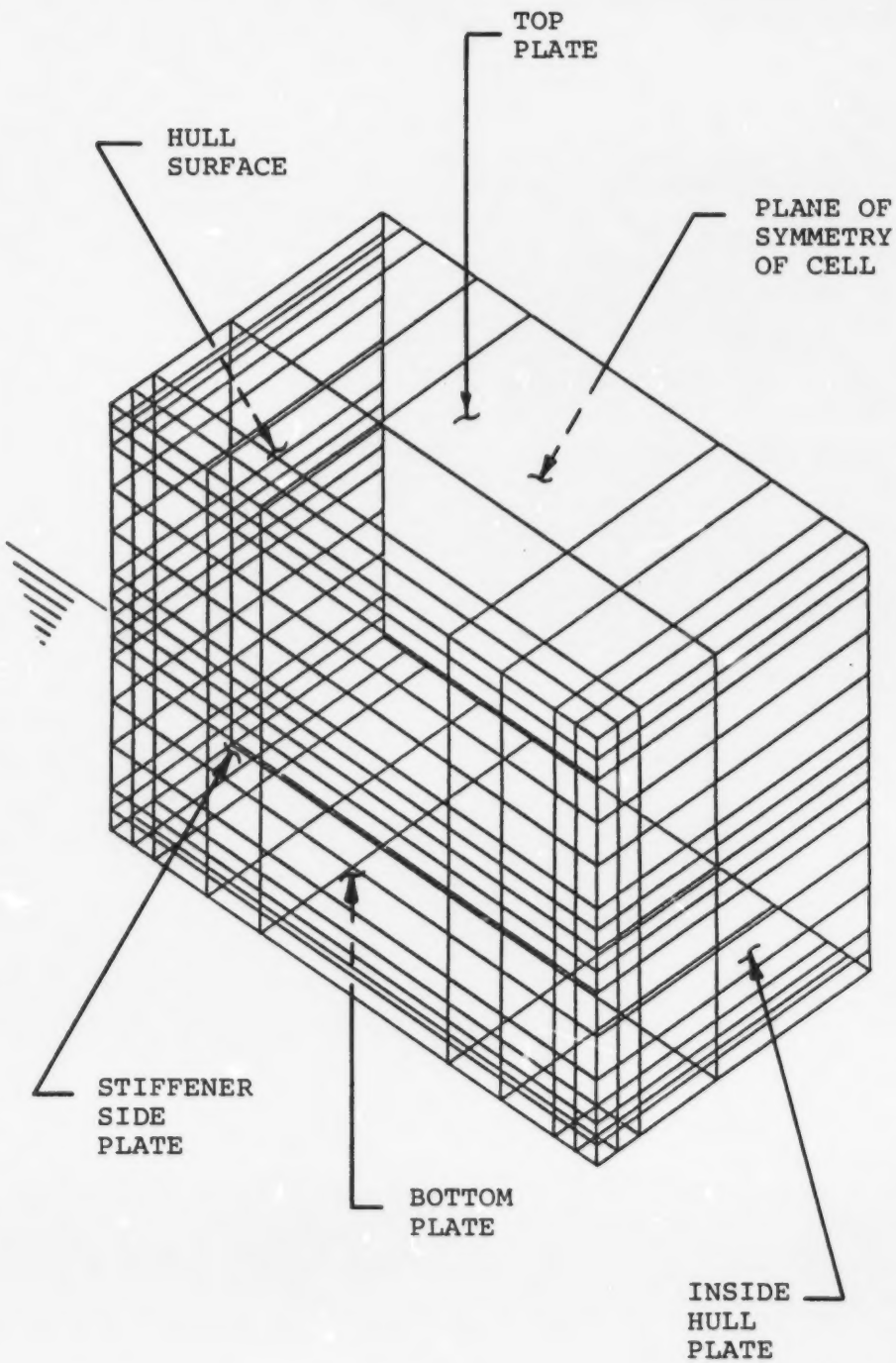

Figure 40

FINITE ELEMENT IDEALIZATION OF THE CELL

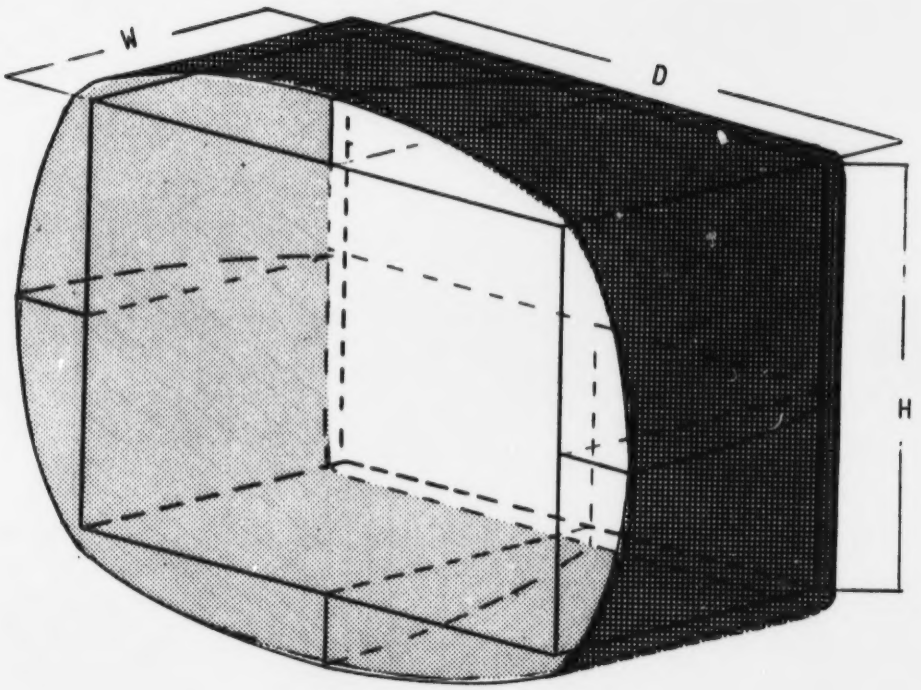

Typical equation:

$$h' = h(0.75 \sin \pi z/_H \cos \pi x/_W + 0.25)$$

Figure 41

VARIATION OF THE SURFACE COEFFICIENTS AT THE INTERNAL SURFACES

similarly $$h' = h\left[(1-\text{const})\ \sin\frac{\pi y}{D}\ \cos\frac{\pi x}{W} + \text{const}\right] \qquad (46)$$

D - depth (y direction)

This distribution reflects the belief that the circulatory flow established in the cell has its maximum velocity at the center of the plates and leaves the corners relatively stagnant.

Extreme conditions were assumed to apply to the external surfaces of the plate. In particular the hold was assumed to be at an elevated temperature due perhaps to the loading of a warm cargo. This extreme was chosen to exaggerate the temperature variations and hence the effects of varying surface coefficients. In the case of the M.V. Arctic, this condition is unlikely to last for as long, as the hold would be rapidly cooled through heat loss through the hull.

The analyses covered the following scenarios.

Hold air assumed constant $20^{\circ}C$

Sea water assumed constant $-2^{\circ}C$

Cell Fluid	External Air Temperature $-55^{\circ}C$		$0^{\circ}C$	
	%	%	%	%
Air	+100	-50	+100	-50
Water	+100	-50	+100	-50
Oil	+100	-50	+100	-50

Table 6 SURFACE COEFFICIENT VARIATION FROM MEAN CALCULATED VALUE

In addition for the water filled cell, the external air temperature was varied through $-20^{\circ}C$ and $-40^{\circ}C$.

The external plate surface coefficients were taken as before to be

Surface exposed to wind and spray 40 $W/m^2\ ^oC$

Surface exposed to sea water 210 $W/m^2\ ^oC$

The latter value is a function of the hull speed and is representative of 2.2 m/s (4.3 knots).

These values were also varied by +100%; -50% to correspond to the extremes used for the internal coefficients.

Surface coefficients internal to the cell were calculated for each of the above scenarios with the mean cell temperature assumed mid-way between the external boundary temperatures. The surface coefficient internal to the hold was also calculated assuming free convection. The values produced by the program FILMC are tabulated in Figures 42 - 45. A description of the variables used can be found in Appendix F.

The plate numbers refer to the following surfaces:

1. Vertical outside face
2. Vertical inside face
3. Stiffener plate surface
4. Top plate
5. Bottom plate
6. Hold side of inside plate

Each of the coefficients calculated was doubled and halved to provide the high and low estimates respectively.

5.2.3 A Discussion of the Results

The temperature variations recorded along the plates are shown in Figures 46 - 58 . Where significant differences between the center of the cell and an edge occur, a dotted line is shown. From the graphical display, it can be seen that the temperature distribution across the plates varies considerably depending on the assumed rate of surface heat transfer, although the mean plate temperature is the average of the end values. Varying the surface coefficients between wide limits has demonstrated that the steady state temperature solution for the case studied provides essentially the same mean plate temperatures.

This analysis verifies two previous assumptions of the macro model,

a) the mean plate temperatures of the frames can be adequately represented by a plate having a

a linear temperature distribution

b) the steady state solution of the mean temperatures does not depend on an accurate assessment of the cell internal surface coefficients.

Clearly, the most important difference is the identification of steep temperature gradients near the edges of the plates in the frames. These gradients depend on the nature of the contained fluid and are highest for the fluids having the largest surface coefficients. The solution is, of course, driven by the original assumption made for the variation of the surface coefficients with distance, and hence only by knowing more accurately the nature of this distribution can the solution be improved. This should be the subject of further research as such temperature gradients may cause undesirable thermal stresses in the plates.

Finally it should be noted that the variations in the surface coefficients will have a marked effect on the time of the transient solution. The above observations are relevant only to a steady state temperature distribution.

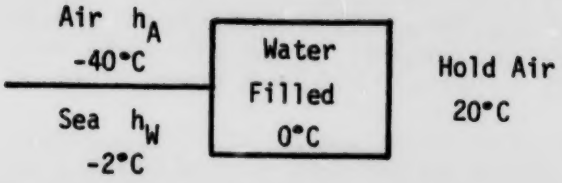

No	Leng.	Del T	Te	Flu	Flo	Srf	Inc	Pr	Gr	Re	Film C
1	1.22	21.00	273.	Wat	Tur	-	Ver	5.8E+00	6.1E+08	3.6E+09	75.07
2	1.22	15.00	273.	Wat	Tur	-	Ver	5.8E+00	4.4E+08	2.5E+09	65.31
3	1.22	5.00	273.	Wat	Lam	-	Ver	5.8E+00	1.5E+08	8.5E+08	46.17
4	1.37	10.00	273.	Wat	Tur	UH	Hor	5.8E+00	4.2E+08	2.4E+09	114.11
5	1.37	9.00	273.	Wat	Tur	UH	Hor	5.8E+00	3.7E+08	2.2E+09	110.18
6	6.00	5.00	273.	Wat	Tur	-	Ver	5.8E+00	1.7E+10	1.0E+11	45.29

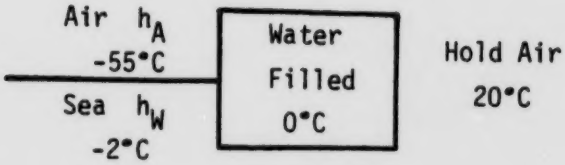

No	Leng.	Del T	Te	Flu	Flo	Srf	Inc	Pr	Gr	Re	Film C
1	1.22	28.50	273.	Wat	Tur	-	Ver	5.8E+00	8.3E+08	4.8E+09	80.69
2	1.22	15.00	273.	Wat	Tur	-	Ver	5.8E+00	4.4E+08	2.5E+09	65.31
3	1.22	5.00	273.	Wat	Lam	-	Ver	5.8E+00	1.5E+08	8.5E+08	46.17
4	1.37	17.50	273.	Wat	Tur	UH	Hor	5.8E+00	7.3E+08	4.2E+09	137.51
5	1.37	9.00	273.	Wat	Tur	UH	Hor	5.8E+00	3.7E+08	2.2E+09	110.18
6	6.00	5.00	273.	Wat	Tur	-	Ver	5.8E+00	1.7E+10	1.0E+11	45.29

Figure 42

FILM COEFFICIENTS FOR WATER FILLED CELL

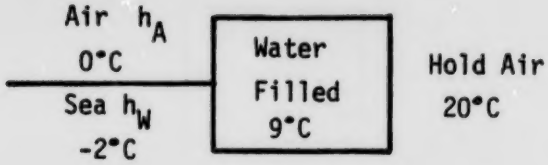

No	Leng.	Del T	Te	Flu	Flo	Srf	Inc	Pr	Gr	Ra	Film C
1	1.22	10.00	282.	Wat	Tur	-	Ver	5.8E+00	2.9E+08	1.7E+09	57.00
2	1.22	6.00	282.	Wat	Tur	-	Ver	5.8E+00	1.7E+08	1.0E+09	48.12
3	1.22	5.00	282.	Wat	Lam	-	Ver	5.8E+00	1.5E+08	8.5E+08	46.17
4	1.37	1.00	282.	Wat	Lam	UC	Hor	5.8E+00	4.2E+07	2.4E+08	14.51
5	1.37	1.00	282.	Wat	Lam	UC	Hor	5.8E+00	4.2E+07	2.4E+08	14.51
6	6.00	5.00	282.	Wat	Tur	-	Ver	5.8E+00	1.7E+10	1.0E+11	45.29

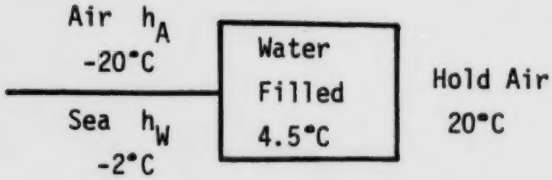

No	Leng.	Del T	Te	Flu	Flo	Srf	Inc	Pr	Gr	Ra	Film C
1	1.22	15.50	278.	Wat	Tur	-	Ver	5.8E+00	4.5E+08	2.6E+09	66.05
2	1.22	11.50	278.	Wat	Tur	-	Ver	5.8E+00	3.4E+08	2.0E+09	59.76
3	1.22	5.00	278.	Wat	Lam	-	Ver	5.8E+00	1.5E+08	8.5E+08	48.17
4	1.37	5.00	278.	Wat	Tur	UH	Hor	5.8E+00	2.1E+08	1.2E+09	90.57
5	1.37	4.50	278.	Wat	Tur	UH	Hor	5.8E+00	1.9E+08	1.1E+09	87.45
6	6.00	5.00	278.	Wat	Tur	-	Ver	5.8E+00	1.7E+10	1.0E+11	45.29

Figure 43

FILM COEFFICIENTS FOR WATER FILLED CELL

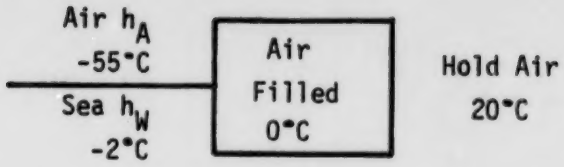

No	Leng.	Del T	Te	Flu	Flo	Srf	Inc	Pr	Gr	Ra	Film C
1	1.22	26.50	273.	Air	Tur	-	Ver	8.2E-01	7.4E+09	6.1E+09	3.41
2	1.22	15.00	273.	Air	Tur	-	Ver	8.2E-01	3.5E+09	3.2E+09	2.75
3	1.22	5.00	273.	Air	Tur	-	Ver	8.2E-01	1.3E+09	1.1E+09	1.91
4	1.37	17.50	273.	Air	Tur	UH	Hor	8.2E-01	6.5E+09	5.3E+09	5.60
5	1.37	9.00	273.	Air	Tur	UH	Hor	8.2E-01	3.3E+09	2.7E+09	4.65
6	6.00	5.00	273.	Air	Tur	-	Ver	8.2E-01	1.5E+11	1.3E+11	1.91

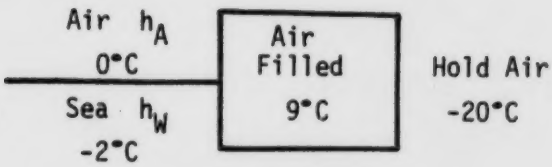

No	Leng.	Del T	Te	Flu	Flo	Srf	Inc	Pr	Gr	Ra	Film C
1	1.22	10.00	282.	Air	Tur	-	Ver	8.2E-01	2.3E+09	1.9E+09	2.50
2	1.22	6.00	282.	Air	Tur	-	Ver	8.2E-01	1.4E+09	1.1E+09	2.01
3	1.22	5.00	282.	Air	Lam	-	Ver	8.2E-01	1.1E+09	9.4E+08	1.99
4	1.37	1.00	282.	Air	Lam	UC	Hor	8.2E-01	5.3E+08	2.7E+08	.59
5	1.37	1.00	282.	Air	Lam	UC	Hor	8.2E-01	5.3E+08	2.7E+08	.59
6	6.00	5.00	282.	Air	Tur	-	Ver	8.2E-01	1.4E+11	1.1E+11	1.09

Figure 44

FILM COEFFICIENTS FOR AIR FILLED CELL

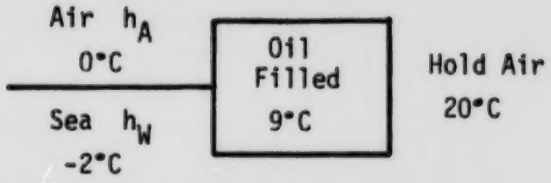

No	Leng.	Del T	Te	Flu	Flo	Srf	Inc	Pr	Gr	Ra	Film C
1	1.22	10.00	282.	Oil	Tur	-	Ver	6.3E+01	6.6E+09	4.1E+11	95.24
2	1.22	6.00	282.	Oil	Tur	-	Ver	6.3E+01	4.0E+09	2.5E+11	71.89
3	1.22	5.00	282.	Oil	Tur	-	Ver	6.3E+01	3.3E+09	2.1E+11	67.66
4	1.37	1.00	282.	Oil	Lam	UC	Hor	6.3E+01	9.4E+08	5.9E+10	13.52
5	1.37	1.00	282.	Oil	Lam	UC	Hor	6.3E+01	9.4E+08	5.9E+10	13.52
6	6.00	5.00	282.	Oil	Tur	-	Ver	6.3E+01	3.9E+11	2.5E+13	67.66

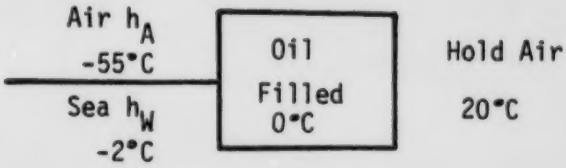

No	Leng.	Del T	Te	Flu	Flo	Srf	Inc	Pr	Gr	Ra	Film C
1	1.22	28.50	273.	Oil	Tur	-	Ver	6.3E+01	1.9E+10	1.2E+12	120.85
2	1.22	15.00	273.	Oil	Tur	-	Ver	6.3E+01	9.9E+09	6.2E+11	97.58
3	1.22	5.00	273.	Oil	Tur	-	Ver	6.3E+01	3.3E+09	2.1E+11	67.66
4	1.37	17.50	273.	Oil	Tur	UH	Hor	6.3E+01	1.6E+10	1.0E+12	205.44
5	1.37	9.00	273.	Oil	Tur	UH	Hor	6.3E+01	8.5E+09	5.3E+11	164.00
6	6.00	5.00	273.	Oil	Tur	-	Ver	6.3E+01	3.9E+11	2.5E+13	67.66

Figure 45

FILM COEFFICIENTS FOR OIL FILLED CELL

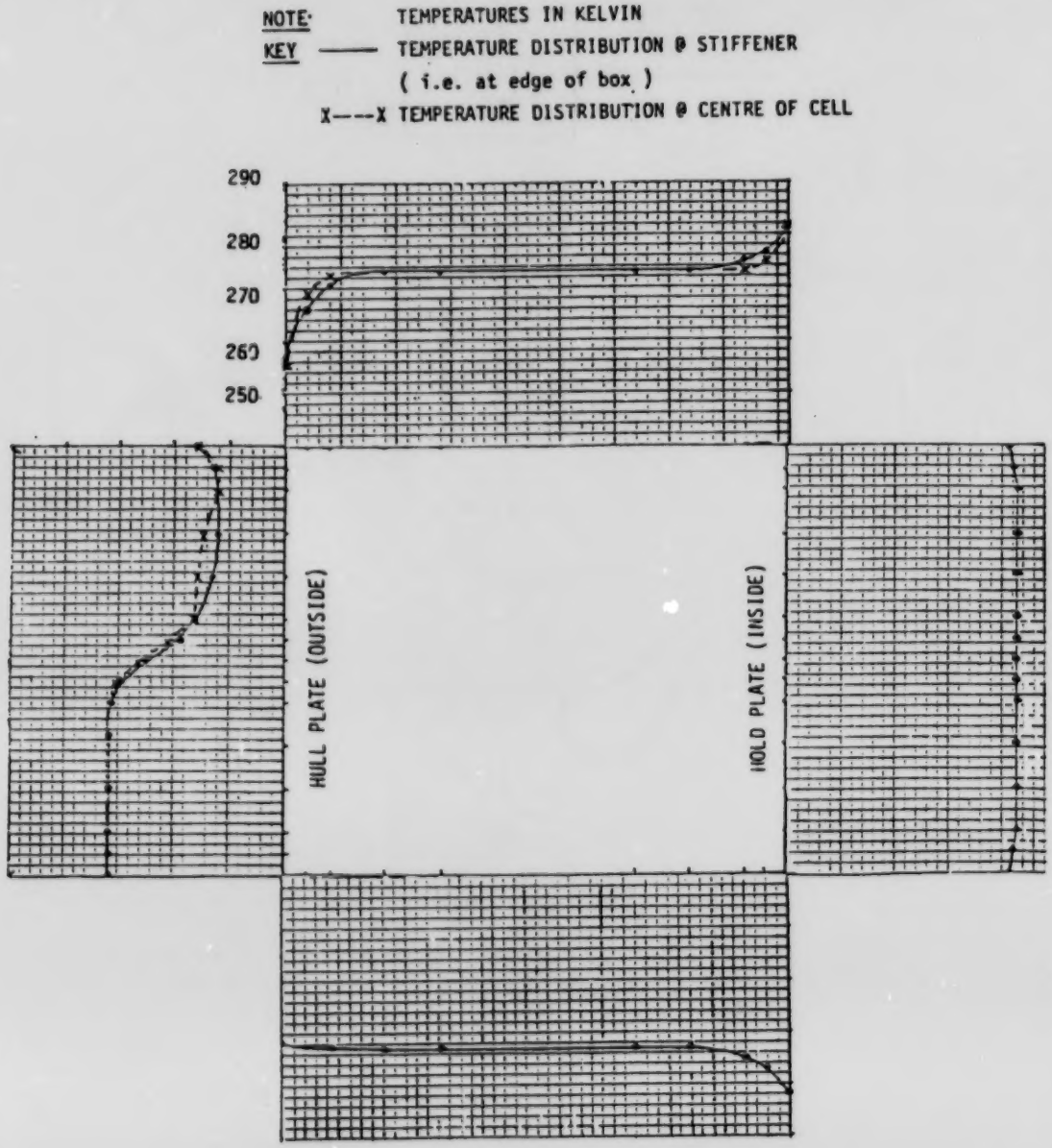

Figure 46

TEMPERATURE DISTRIBUTION FOR OIL FILLED CELL

-55,0,20 - HIGH COEFFICIENTS

NOTE: TEMPERATURES IN KELVIN

KEY —— TEMPERATURE DISTRIBUTION @ STIFFENER
(i.e. at edge of box)

X---X TEMPERATURE DISTRIBUTION @ CENTRE OF CELL

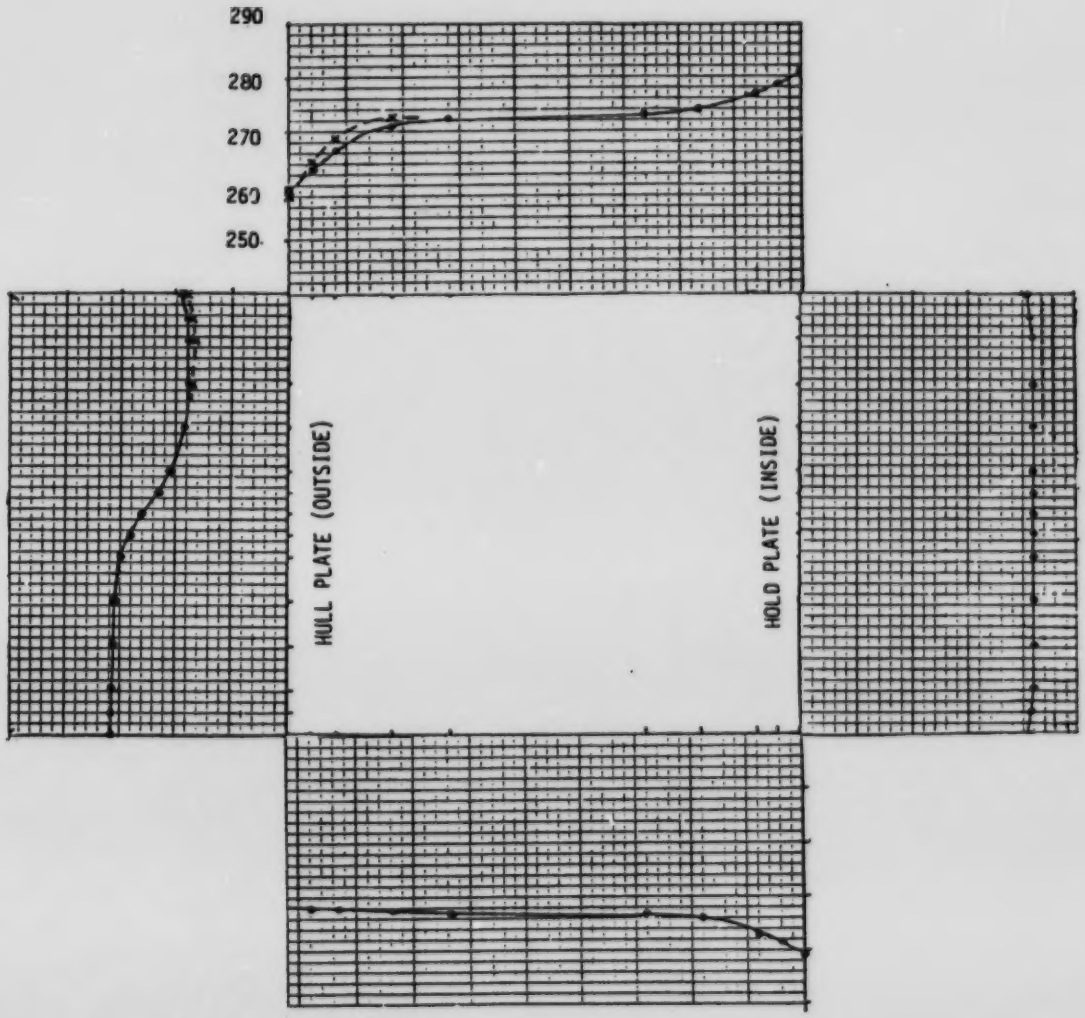

Figure 47

TEMPERATURE DISTRIBUTION FOR WATER FILLED CELL

-40,0,20 - LOW COEFFICIENTS

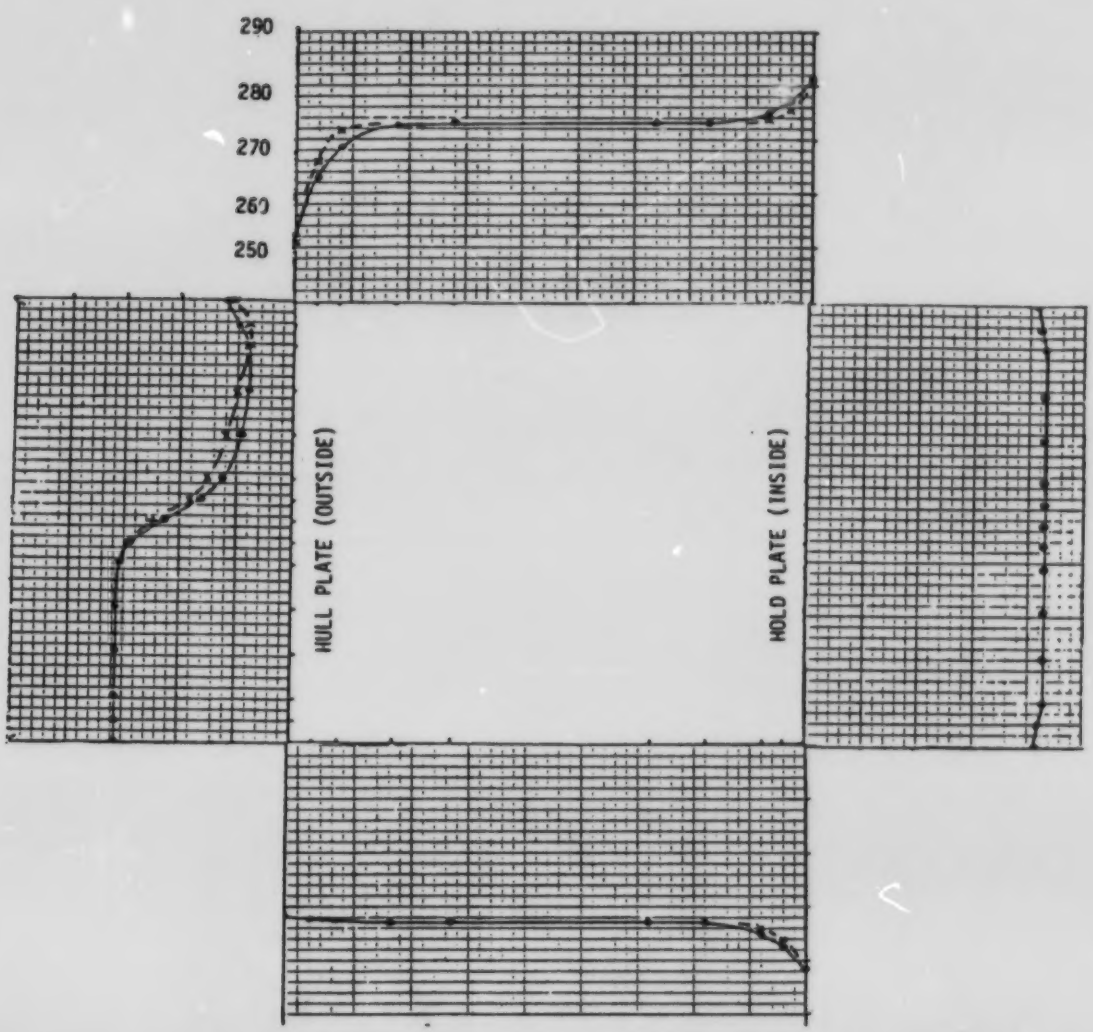

Figure 48

TEMPERATURE DISTRIBUTION FOR WATER FILLED CELL

-55,0,20, - HIGH COEFFICIENTS

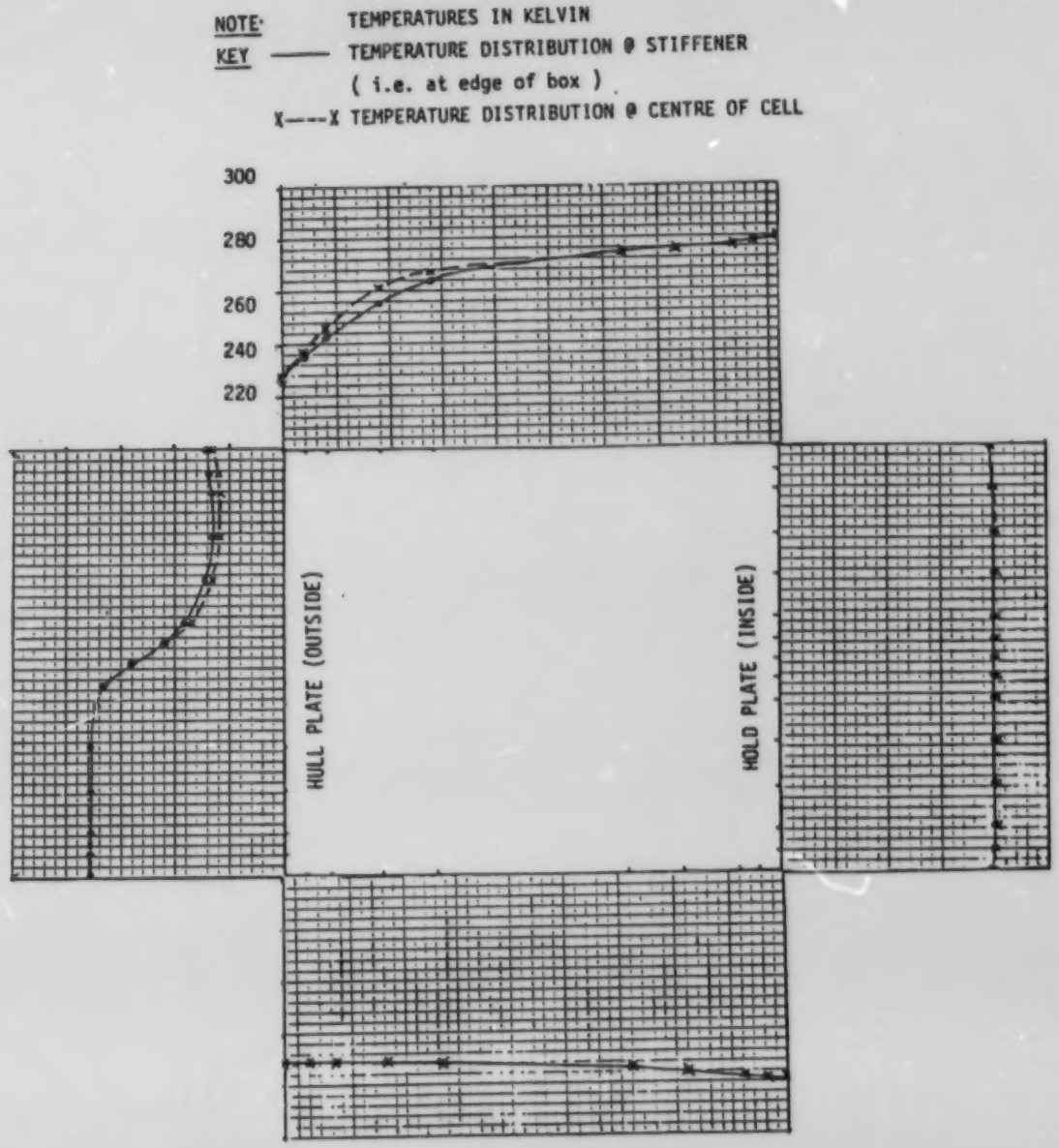

Figure 49

TEMPERATURE DISTRIBUTION FOR AIR FILLED CELL

-55,0,20 - HIGH COEFFICIENTS

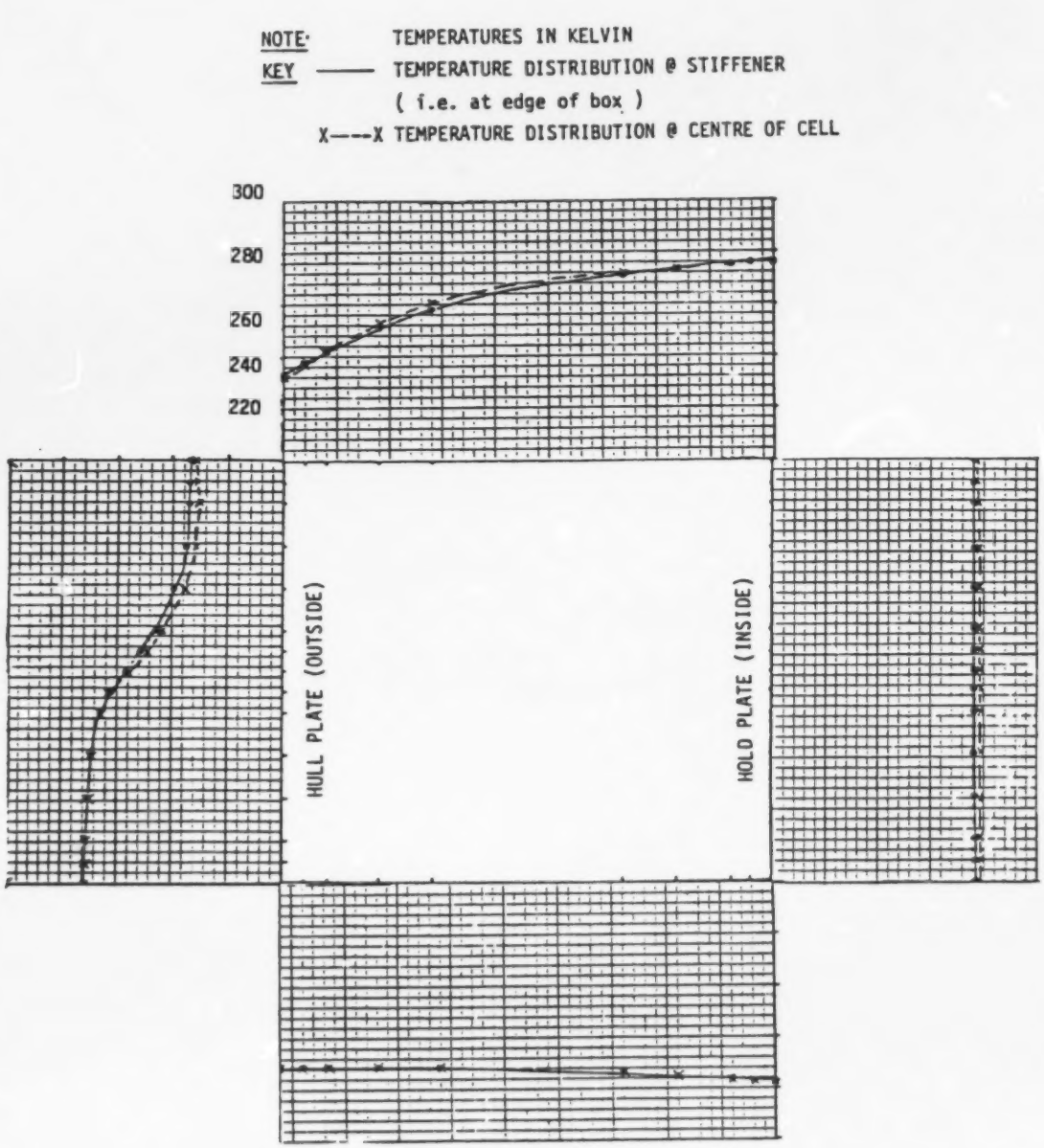

Figure 50

TEMPERATURE DISTRIBUTION FOR AIR FILLED CELL

-55,0,20 - LOW COEFFICIENTS

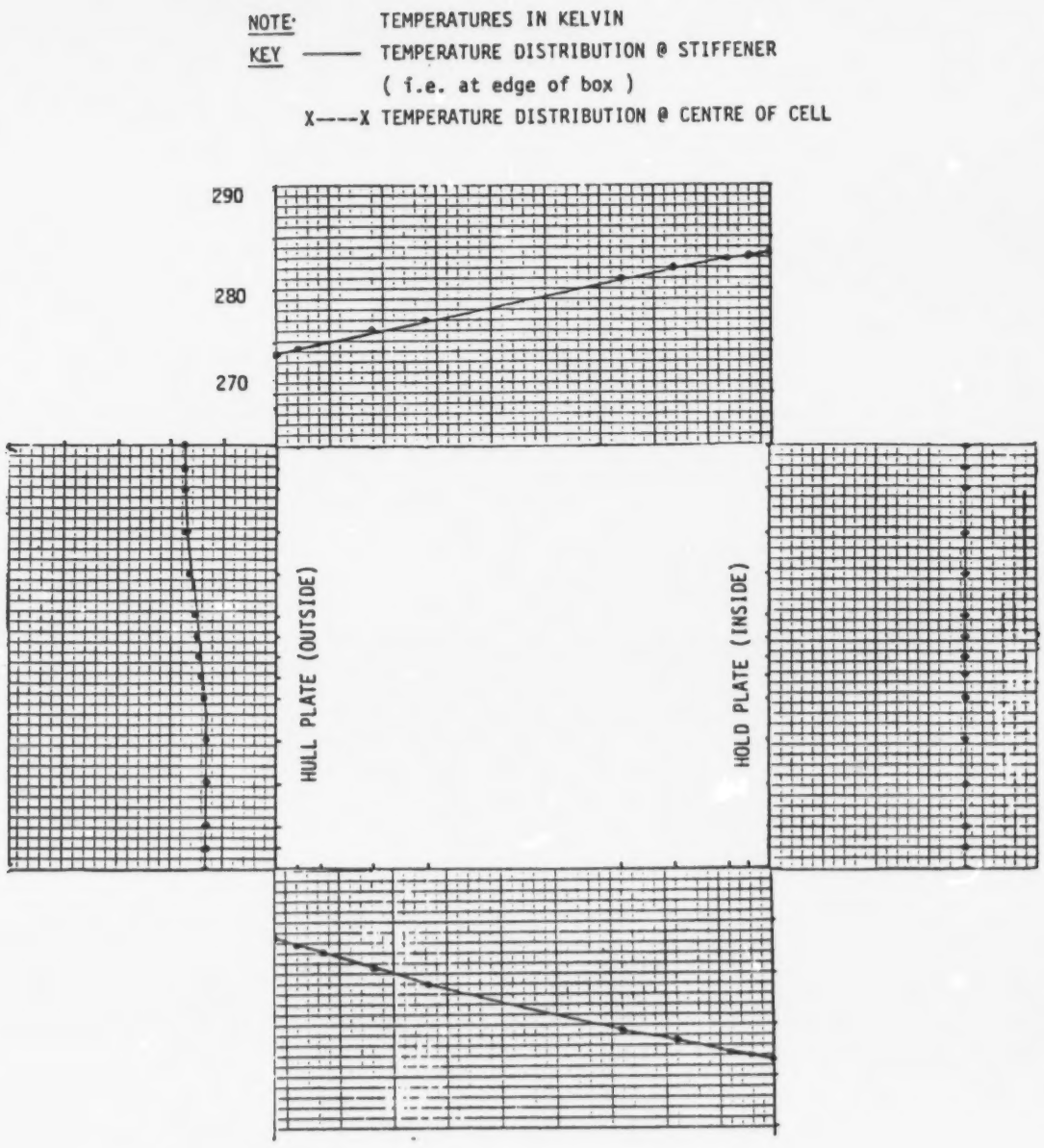

Figure 51

TEMPERATURE DISTRIBUTION FOR AIR FILLED CELL

0,9,20 - LOW COEFFICIENTS

NOTE: TEMPERATURES IN KELVIN

KEY —— TEMPERATURE DISTRIBUTION @ STIFFENER
(i.e. at edge of box.)

X---X TEMPERATURE DISTRIBUTION @ CENTRE OF CELL

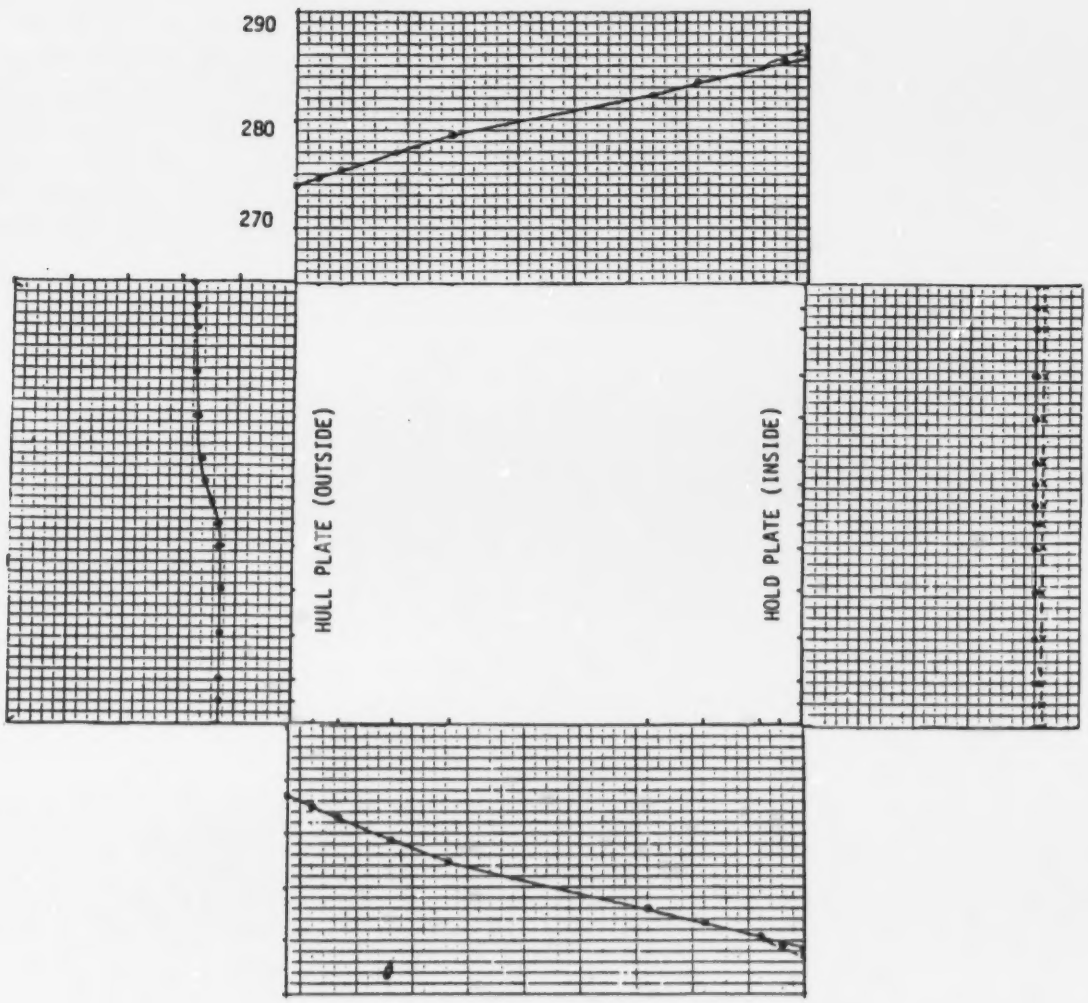

Figure 52

TEMPERATURE DISTRIBUTION FOR AIR FILLED CELL

0,9,20 - HIGH COEFFICIENTS

NOTE: TEMPERATURES IN KELVIN

KEY —— TEMPERATURE DISTRIBUTION @ STIFFENER
(i.e. at edge of box)

X---X TEMPERATURE DISTRIBUTION @ CENTRE OF CELL

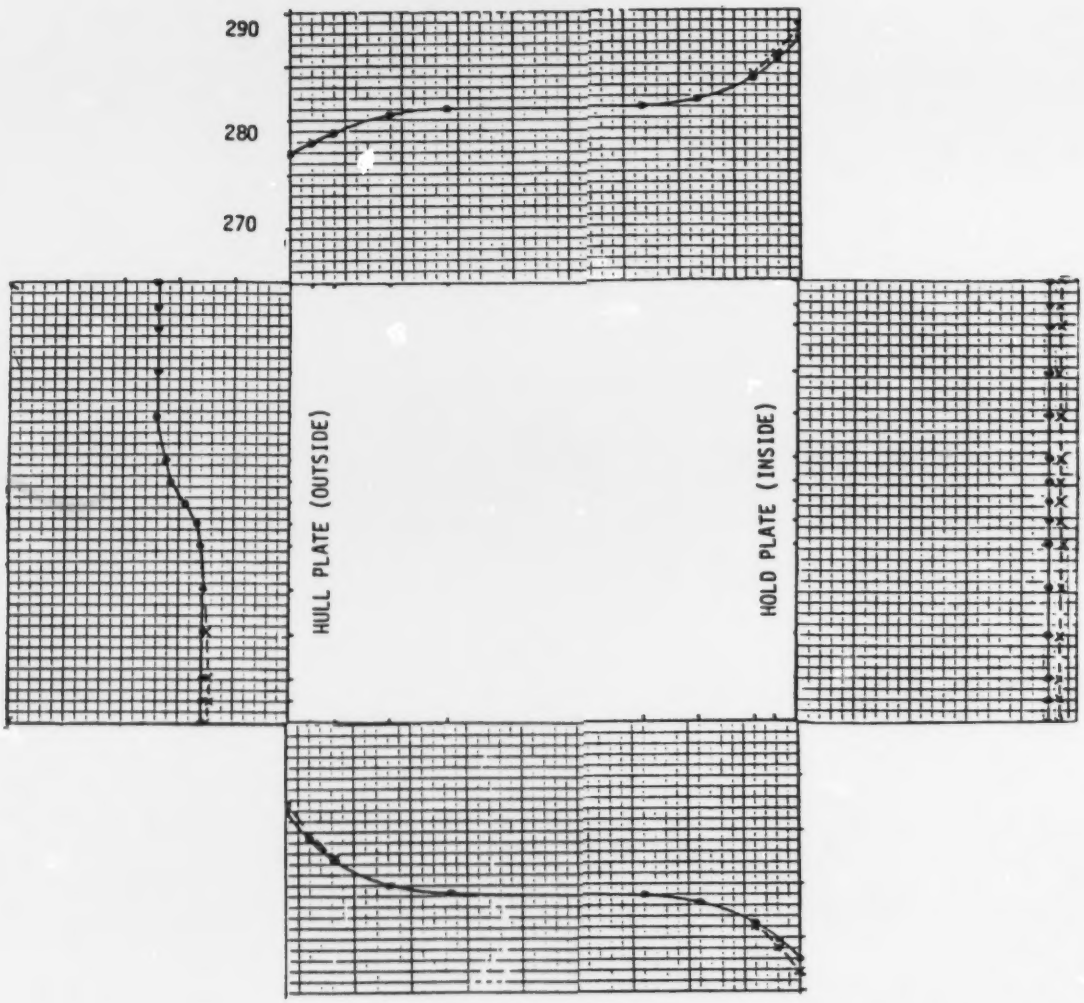

Figure 53

TEMPERATURE DISTRIBUTION FOR WATER FILLED CELL

0,9,20 - HIGH COEFFICIENTS

NOTE: TEMPERATURES IN KELVIN

KEY —— TEMPERATURE DISTRIBUTION @ STIFFENER
(i.e. at edge of box)

X----X TEMPERATURE DISTRIBUTION @ CENTRE OF CELL

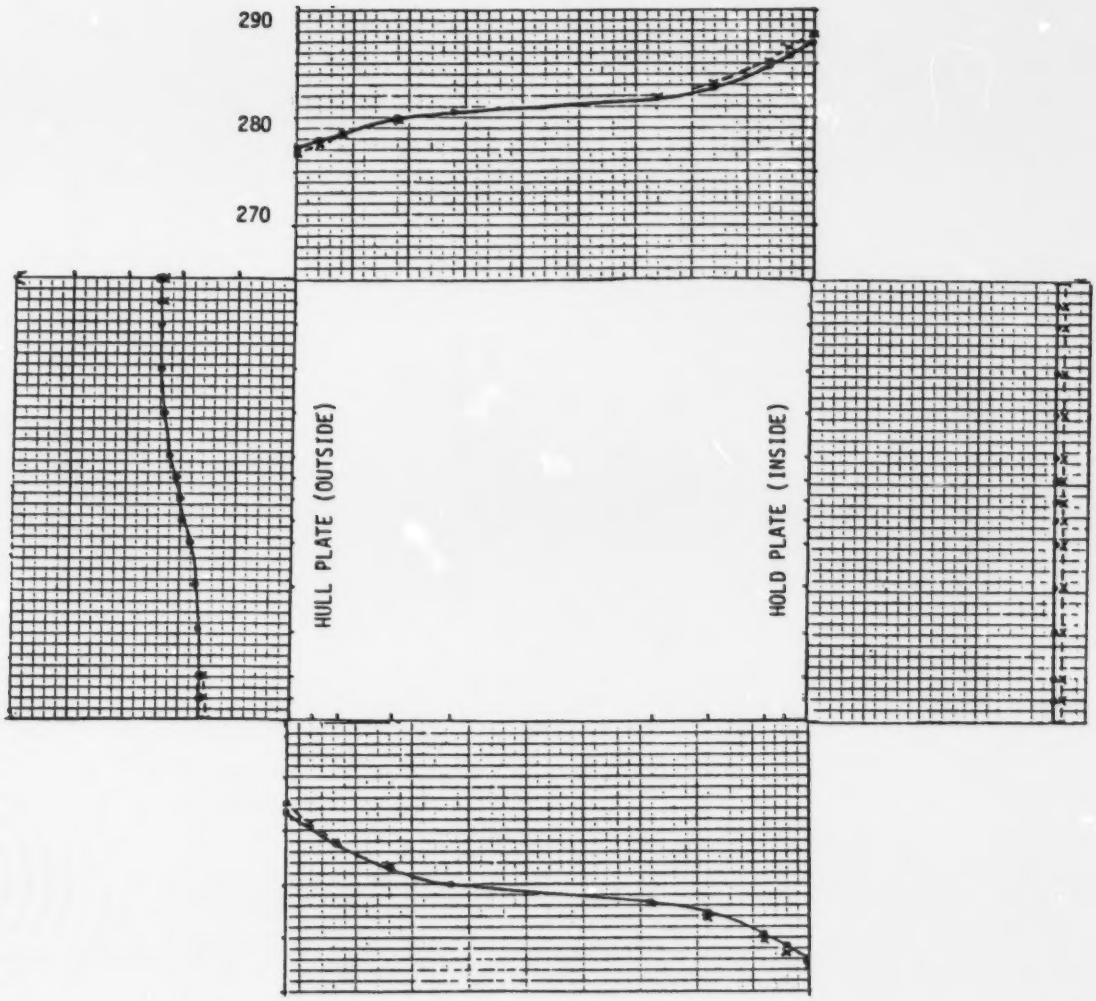

Figure 54

TEMPERATURE DISTRIBUTION FOR WATER FILLED CELL

0,9,20 - LOW COEFFICIENTS

NOTE: TEMPERATURES IN KELVIN

KEY —— TEMPERATURE DISTRIBUTION @ STIFFENER
(i.e. at edge of box)

X---X TEMPERATURE DISTRIBUTION @ CENTRE OF CELL

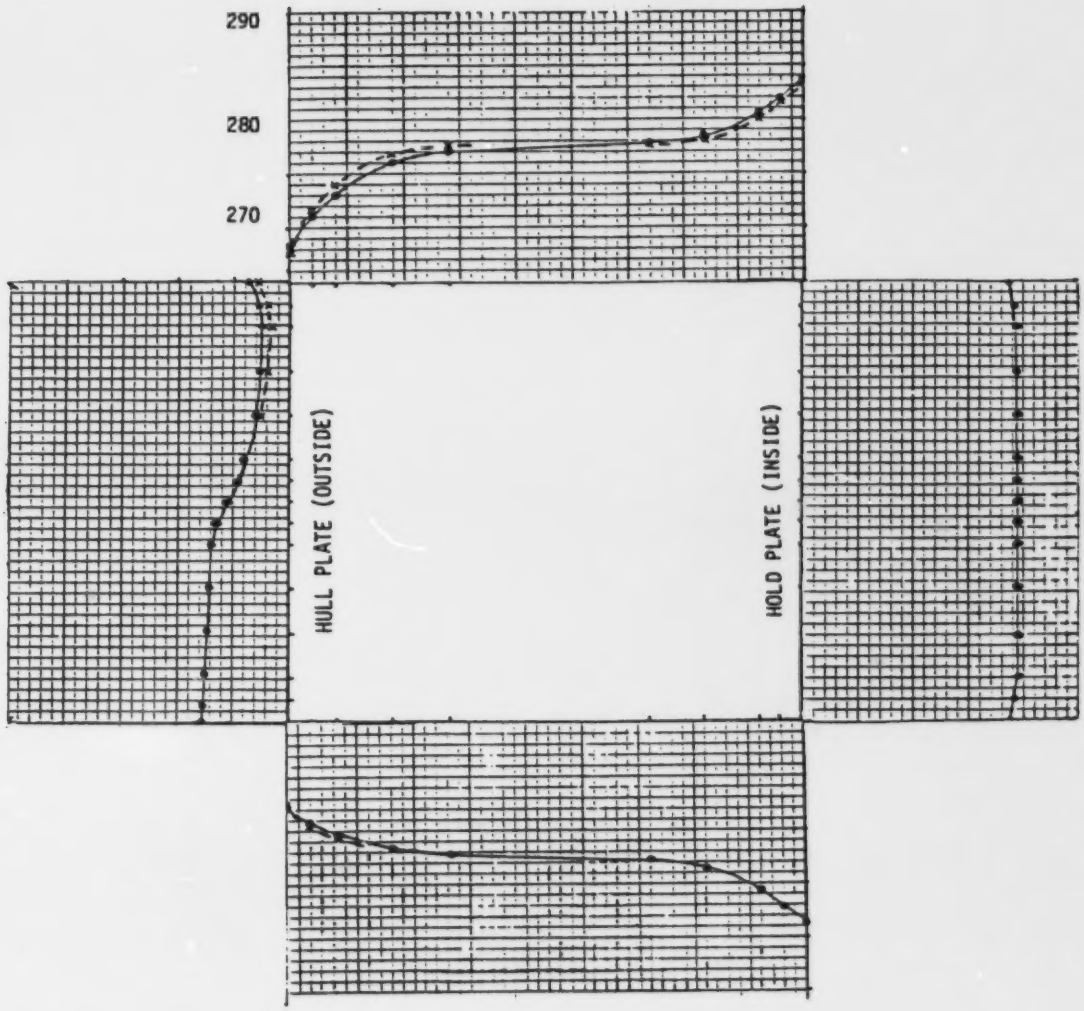

Figure 55

TEMPERATURE DISTRIBUTION FOR WATER FILLED CELL

-20,4.5,20 - LOW COEFICIENTS

NOTE: TEMPERATURES IN KELVIN

KEY —— TEMPERATURE DISTRIBUTION @ STIFFENER
(i.e. at edge of box)

X---X TEMPERATURE DISTRIBUTION @ CENTRE OF CELL

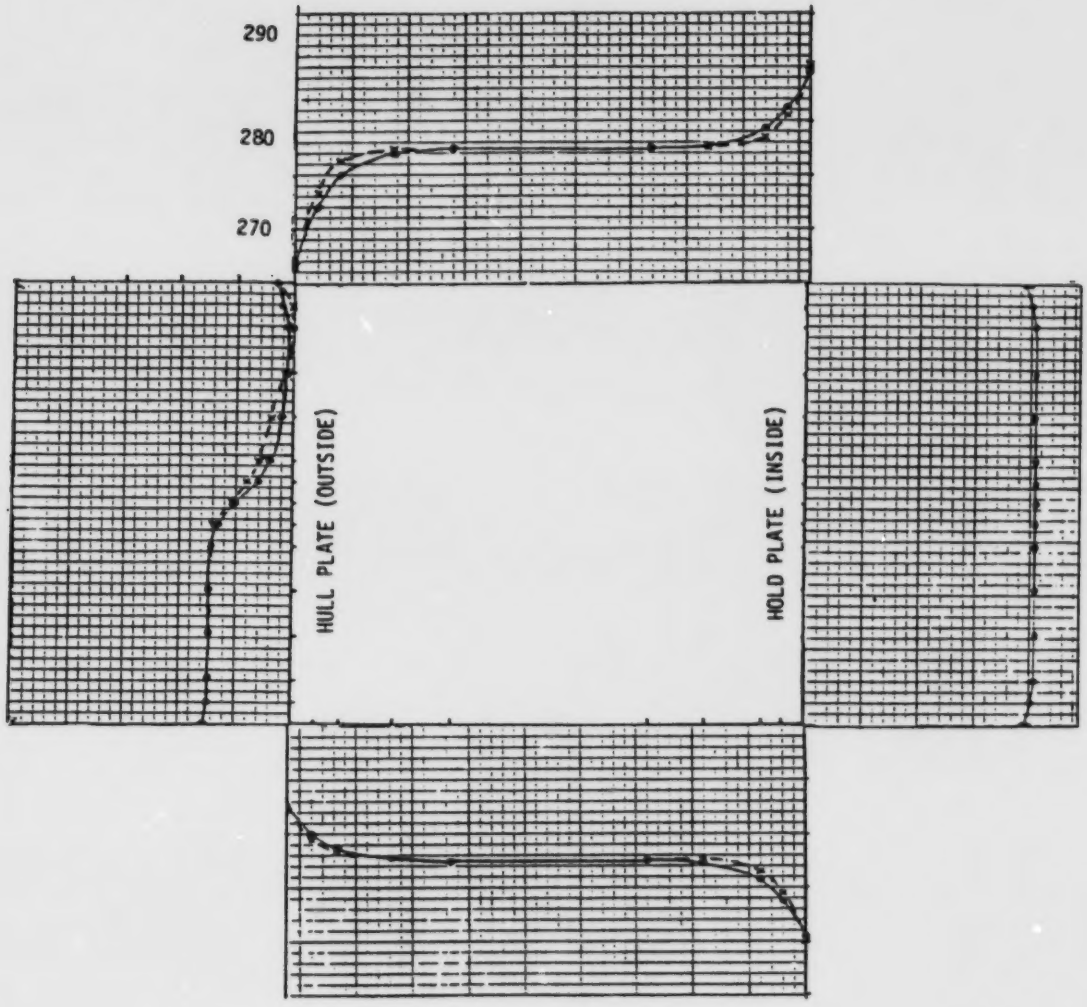

Figure 56

TEMPERATURE DISTRIBUTION FOR WATER FILLED CELL

-20,4.5,20 - HIGH COEFFICIENTS

NOTE: TEMPERATURES IN KELVIN

KEY —— TEMPERATURE DISTRIBUTION @ STIFFENER
(i.e. at edge of box)

X---X TEMPERATURE DISTRIBUTION @ CENTRE OF CELL

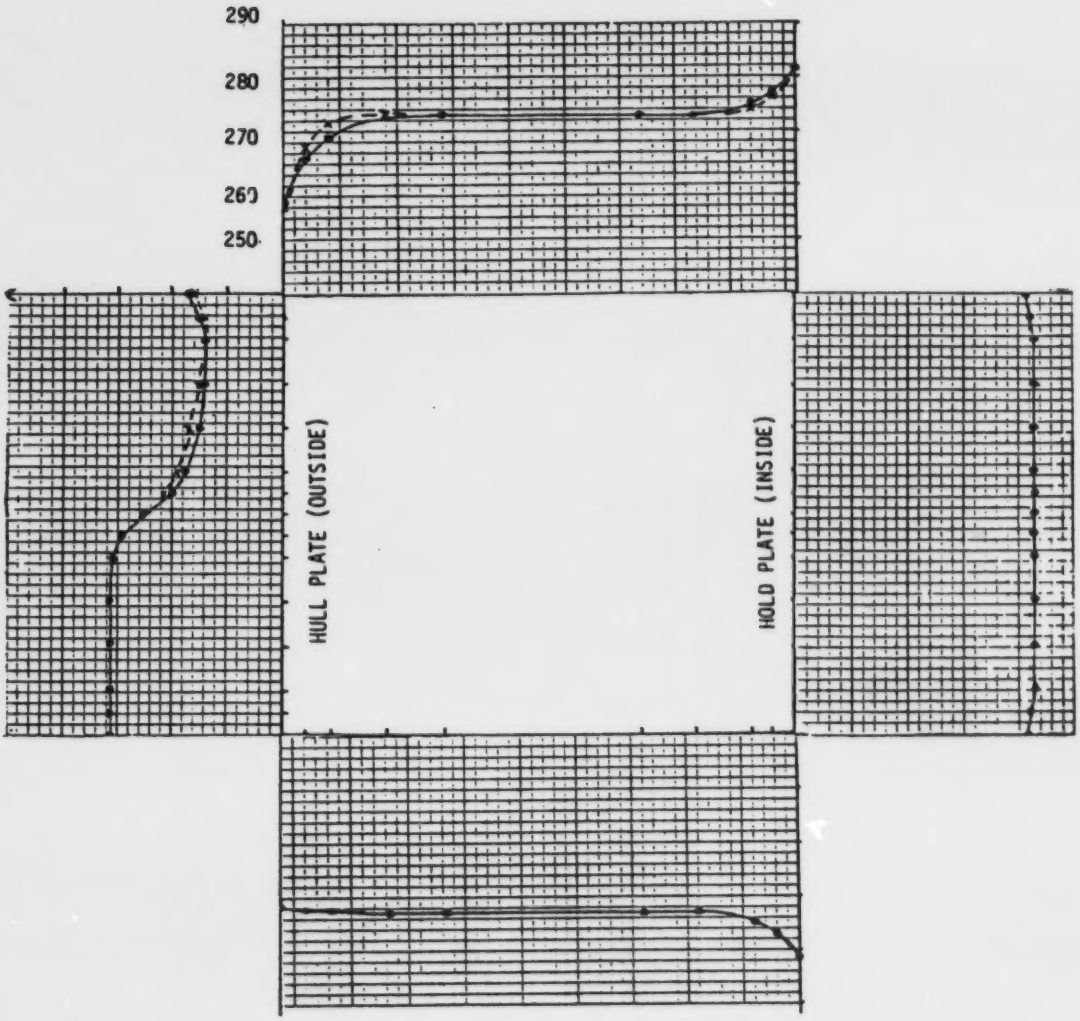

Figure 57

TEMPERATURE DISTRIBUTION FOR WATER FILLED CELL

-40,0,20 - HIGH COEFICIENTS

NOTE: TEMPERATURES IN KELVIN

KEY —— TEMPERATURE DISTRIBUTION @ STIFFENER
(i.e. at edge of box)

X---X TEMPERATURE DISTRIBUTION @ CENTRE OF CELL

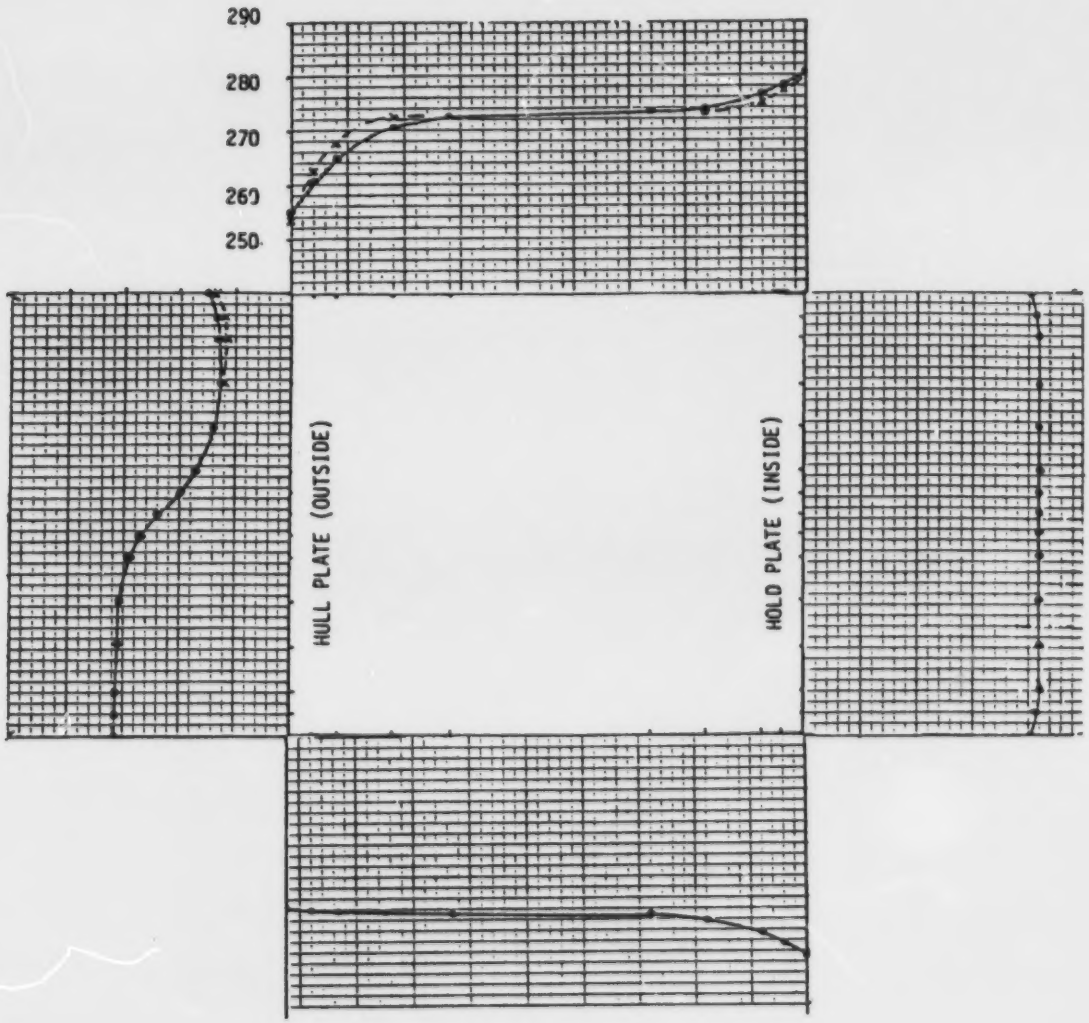

Figure 58

TEMPERATURE DISTRIBUTION FOR WATER FILLED CELL

-55,0,20 - LOW COEFFICIENTS

5.3 Transient Thermal Network Model of a Cell from the M.V. Arctic

5.3.1 Introduction

This second example of the use of a thermal network model employs a more complex idealization to represent a typical cell at the waterline. In this case the upper half of the cell hull plates is exposed to air and the lower is submerged. The cell was assumed to be filled with water initially at the temperature of the Gulf Stream, which in the case of the trip made by the M.V. Arctic in July 1981 was measured at 12.0°C. Heat transfer through the cell and into the ballast water, which is assumed well mixed, is through natural convection and conduction through the hull plates. The hold is also assumed to transfer heat to and from the cell by natural convection. The dimensions of the cell are shown in Figure 59.

The temperatures at a number of points around the cell are of interest, together with their transient response to a change in external conditions. Two external temperature transients have been considered, the first closely approxmates the measured conditions of the July Atlantic crossing reported in Section 6. The external air, hold air and sea water temperatures were varied over an eleven day period and the response of the ballast water and steel temperatures compared to those measured. The second transient assumed the same transatlantic crossing, but with the external air and sea temperatures dropping to -55°C and -2°C respectively as the ship entered ice infested waters. This latter case was run in an attempt to predict the thermal response of the ship to an extreme drop in temperature. It was hoped that a later voyage of the M.V. Arctic would have permitted monitoring with air temperatures substantially below zero; however, as is described in Section 6, this was not possible.

5.3.2 Transient Thermal Network Model

The periphery of the cell is modelled by a series of conducting links as shown in Figure 60 for links 1 to 18 (shown in circles). The top, bottom and sides of the cell are represented by links 11, 12 and 17, 18. The thickness of the plates separating other similar cells is halved, by reason of symmetry. As it was to be assumed that the cell is on the waterline, then considerably more nodes are used along the outside plate to permit the variation of properties and external temperatures and to avoid a poor solution at the sharp transition in temperature. Due to the presence of cut-outs in the horizontal and vertical stiffener plates, only 1/3 of those plates was considered effective in conduction.

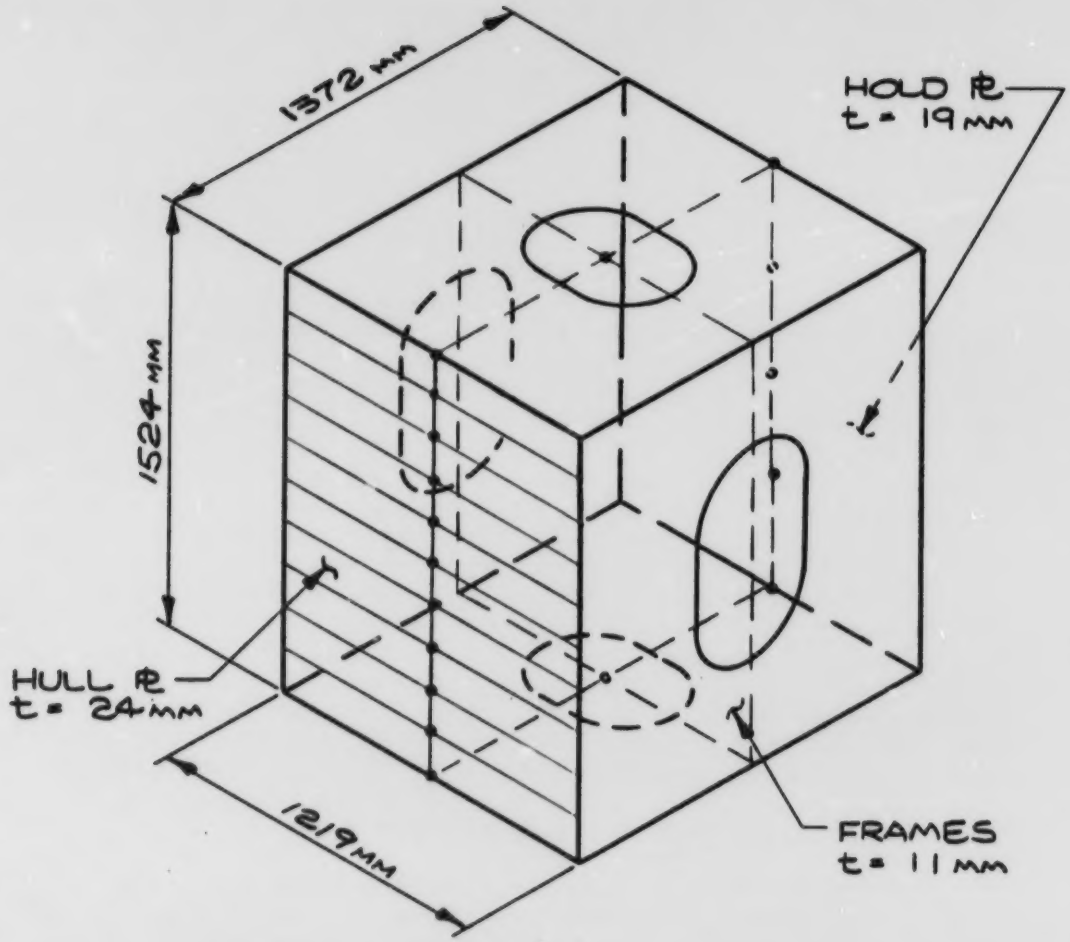

VOLUME = 2.54884 M^3

Figure 59

DIMENSIONS OF A SINGLE CELL
FROM THE M.V. ARCTIC

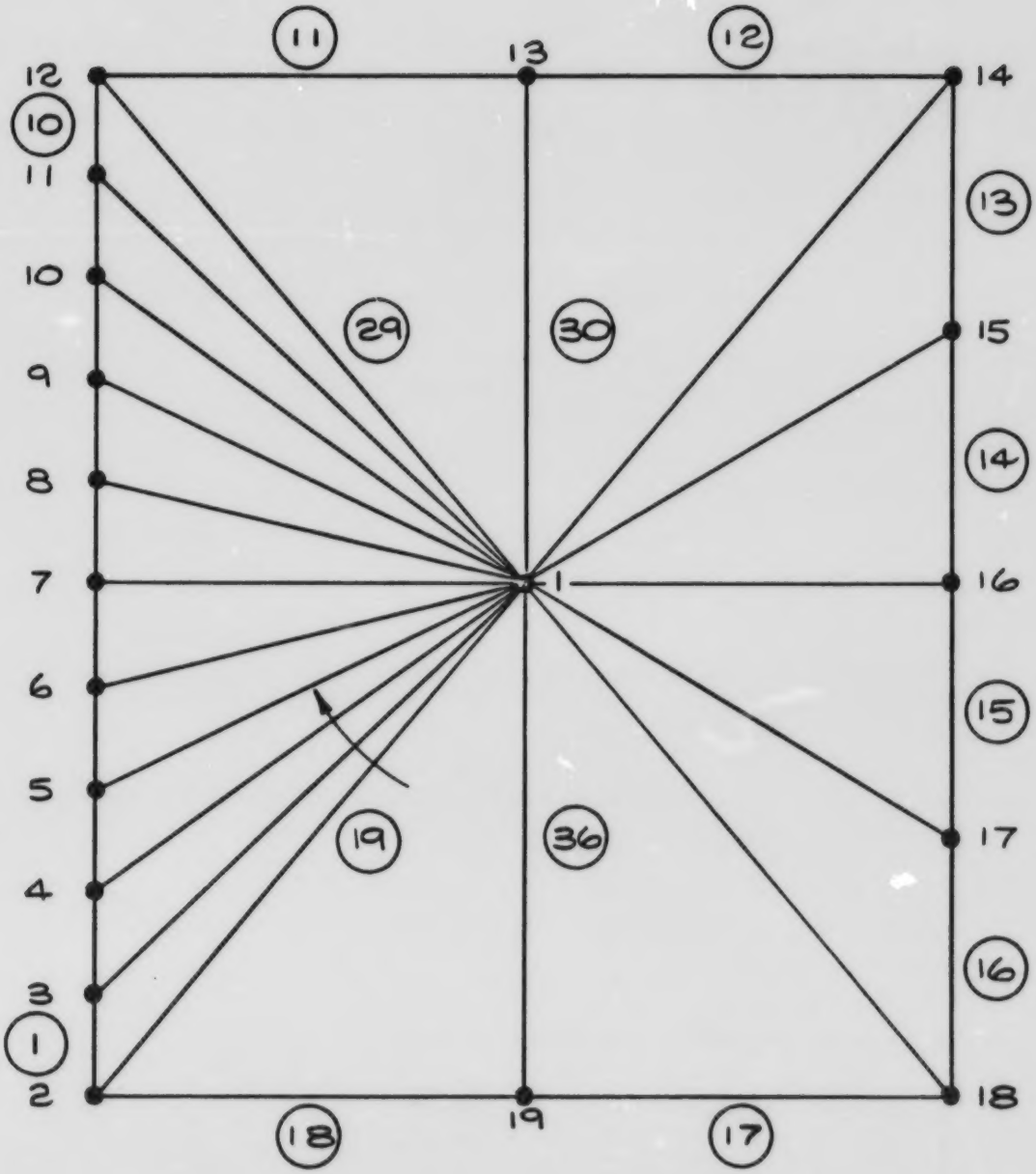

Figure 60

THERMAL NETWORK MODEL OF M.V. ARCTIC CELL

The cross-sectional areas of the conduction links were therefore calculated as follows, from the dimensions of Figure 59:

Front face	$1219 \times 24 \times 10^{-2}$	$= 292.6\ cm^2$
Side plates	$1524 \times 11 \times 10^{-2}/(2 \times 3)$	$= 27.94\ cm^2$
Top and bottom plates	$1219 \times 11 \times 10^{-2}/(2 \times 3)$	$= 22.34\ cm^2$
Inside back face	$1219 \times 19 \times 10^{-2}$	$= 231.6\ cm^2$

The volume of steel to be lumped at each node for the purpose of heat capacity can be calculated from the plate dimensions and the idealization detail based on the 'tributary' area surrounding each node. The side plates are lumped in with the top and bottom plates. The volume V_M represents a typical node in the middle of a plate and the volume V_E, that at an edge.

Volumes for steel

Front face	$V_M = 1219 \times 1524 \times 24/(10 \times 10^3)$	$= 4.54 \times 10^3\ cm^3$
	V_E	$= 2.27 \times 10^3\ cm^3$
Top and bottom face	$V_M = (1219 \times 1372 \times 11)/(4 \times 3 \times 10^3)$	$= 1.533 \times 10^3\ cm^3$
	V_E	$= 7.665 \times 10^2\ cm^3$
Side plates	$V_M = (1524 \times 1372 \times 11)/(2 \times 3 \times 10^3)$	$= 3.833 \times 10^3\ cm^3$
	V_E	$= 1.9167 \times 10^3\ cm^3$
Hold plate	$V_M = (1219 \times 1524 \times 19)/(4 \times 10^3)$	$= 8.824 \times 10^3\ cm^3$
	V_E	$= 4.412 \times 10^3\ cm^3$

The nodal volumes are then as follows:

	cm^3
1 (water volume)	2548840.
2, 12	4953.
3 - 11	4540.
13, 19	5366.
14, 18	7095.
15 - 17	8824.

Film coefficient data for the single cell

External hull to water coefficient = 210 $W/m^2\ ^oC$

Hold air/internal plate = 2 $W/m^2\ ^oC$

Assume for the purpose of calculating the surface coefficient that the fluid to plate $\Delta T = 6^oC$ and the temperature of the fluid is 279 K (6^oC).

The vertical plate length = 1.524 m

The horizontal plate = 1.372 m

The plate on the upper surface is upper surface heated and the lower plate is lower surface cooled. The resulting coefficients from FILMC are shown below.

For the case where the upper part of the cell is exposed to a very low temperature as in the second analysis a revised convection coefficient has been calculated as shown in the second table.

FILM COEFFICIENTS DUE TO FREE CONVECTION

M.V.ARCTIC - SINGLE CELL/1

No	Leng.	Del T	Te	Flu	Flo	Srf	Inc	Pr	Gr	Ra	Film C
1	1.52	6.00	279.	Wat	Tur	-	Ver	5.8E+00	3.4E+08	2.0E+09	48.12
2	1.37	6.00	279.	Wat	Tur	UH	Hor	5.8E+00	2.5E+08	1.4E+09	96.25
3	1.37	6.00	279.	Wat	Lam	UC	Hor	5.8E+00	2.5E+08	1.4E+09	22.41

FILM COEFFICIENTS DUE TO FREE CONVECTION

M.V.ARCTIC - SINGLE CELL/2

No	Leng.	Del T	Te	Flu	Flo	Srf	Inc	Pr	Gr	Ra	Film C
1	1.52	33.00	294.	Wat	Tur	-	Ver	5.8E+00	1.9E+09	1.1E+10	84.95

The internal film coefficients, together with their links to the fluid node, are represented by 'interface' links in the program. The following coefficients and effective areas were used for the case of the ballast water filled cell.

	Node	Film Coefficient	Cross-sectional Area cm^2
Ballast water	to 2	48.10	929.0
Ballast water	to 3-7	48.10	1858.
Ballast water	to 8-11	48.10(84.95)	1858.
Ballast water	to 12	48.10	929.0
Ballast water	to 13	96.25	12545.
Ballast water	to 14, 18	48.10	2322.0
Ballast water	to 15, 17	48.10	4644.0
Ballast water	to 19	22.40	12545.

The external air and water temperatures and internal hold temperatures are set up as a transient loadcase consisting of a background heat load specified through the equation

$$Q = MQ_p(T_b^{n_2} - T_n^{n_2})^{n_1} \qquad (47)$$

In the case of forced fluid (air) convective exchange n_1 and n_2 are unity, M is unity and we need only specify Q_p (the effective surface transfer coefficient) and T_b. T_n is then the calculated temperature of the node.

These conditions are given for all the nodes with the exception of 13 and 19.

Node	Qp(W/k)
2	195090.
3-7	390117.
8-11	74310.
12	37155.
14	4644.4
15-17	9288.8
18	4644.4

The temperatures vary, and are specified at a number of discrete points in time, between which they are assumed to vary linearly.

THERMAL NETWORK ANALYSIS - INPUT DATA FOR TRANSIENT SEQUENCE SOLUTION

Engineer ...A.F
Date ...
Run Identifier ...MV ARCTIC/1 MVAT1

DATA SUMMARY

Number of Nodes in Structure	...	19
Number of Conduction Links	...	36
Number of Conduction Link Interfaces	...	18
Number of Radiation Links	...	0
Highest number of Surface Faces for any one Node	...	0
No of Surfaces having Implicit Radiation Losses	...	0
Number of sets of Bulk Material Properties	...	2
Number of sets of Surface Material Properties	...	0
Number of Background Load Points	...	16
Cases	...	7
Solution Type	...	TRANSIENT SEQUENCE
Number of Transient Sequence Instructions	...	8
Total Transient Time (Hrs/Mins/Secs)	...	0/0/0
Number of Results Outputs	...	0
Problem Bandwidth	...	19
Due to Conduct(i) link no 18		
connecting nodes 1 and 19		

CONDUCTION LINK (HOMOGENOUS) DATA

Data set consists of 18 entries

	Connected Node Names			Link Length	Link Cross Section
1)	2	3		15.24	292.60
2)	3	4		15.24	292.60
3)	4	5		15.24	292.60
4)	5	6		15.24	292.60
5)	6	7		15.24	292.60
6)	7	8		15.24	292.60
7)	8	9		15.24	292.60
8)	9	10		15.24	292.60
9)	10	11		15.24	292.60
10)	11	12		15.24	292.60
11)	12	13		68.60	50.28
12)	13	14		68.60	50.28
13)	14	15		38.10	231.60
14)	15	16		38.10	231.60
15)	16	17		38.10	231.60
16)	17	18		38.10	231.60
17)	18	19		68.60	50.28
18)	19	2		68.60	50.28

BODY DATA

Data set consists of 19 entries

Node Number	Node Name	Volume	No. of Surface Faces	Bulk Properties Identifier
1	WATR	2548840.00	0	BWATER
2	2	4953.00	0	BSHIPST
3	3	4540.00	0	BSHIPST
4	4	4540.00	0	BSHIPST
5	5	4540.00	0	BSHIPST
6	6	4540.00	0	BSHIPST
7	7	4540.00	0	BSHIPST
8	8	4540.00	0	BSHIPST
9	9	4540.00	0	BSHIPST
10	10	4540.00	0	BSHIPST
11	11	4540.00	0	BSHIPST
12	12	4953.00	0	BSHIPST
13	13	5366.00	0	BSHIPST
14	14	7095.00	0	BSHIPST
15	15	8824.00	0	BSHIPST
16	16	8824.00	0	BSHIPST
17	17	8824.00	0	BSHIPST
18	18	7095.00	0	BSHIPST
19	19	5366.00	0	BSHIPST

CONDUCTION LINK (INTERFACE) DATA

Data set consists of 18 entries

	Connected Node Names		Link Length	Link Section	Link Length	Link Section	Interface Conductance	Interface Section
1)	WATR	2	0.00	0.00	0.00	0.00	48.10	929.00
2)	WATR	3	0.00	0.00	0.00	0.00	48.10	1857.70
3)	WATR	4	0.00	0.00	0.00	0.00	48.10	1857.70
4)	WATR	5	0.00	0.00	0.00	0.00	48.10	1857.70
5)	WATR	6	0.00	0.00	0.00	0.00	48.10	1857.70
6)	WATR	7	0.00	0.00	0.00	0.00	48.10	1857.70
7)	WATR	8	0.00	0.00	0.00	0.00	85.00	1857.70
8)	WATR	9	0.00	0.00	0.00	0.00	85.00	1857.70
9)	WATR	10	0.00	0.00	0.00	0.00	85.00	1857.70
10)	WATR	11	0.00	0.00	0.00	0.00	85.00	1857.70
11)	WATR	12	0.00	0.00	0.00	0.00	85.00	929.00
12)	WATR	13	0.00	0.00	0.00	0.00	96.25	12545.00
13)	WATR	14	0.00	0.00	0.00	0.00	48.10	2322.00
14)	WATR	15	0.00	0.00	0.00	0.00	48.10	4644.00
15)	WATR	16	0.00	0.00	0.00	0.00	48.10	4644.00
16)	WATR	17	0.00	0.00	0.00	0.00	48.10	4644.00
17)	WATR	18	0.00	0.00	0.00	0.00	48.10	2322.00
18)	WATR	19	0.00	0.00	0.00	0.00	22.40	12545.00

FIGURE 61
113

Engineers' Identification A.F
Run Time/Date
Run Identifier MV ARCTIC/1 7VAT1
Solution Type TRANSIENT ANALYSIS

PRESCRIBED STARTING POINT TEMPERATURE DISTRIBUTION

Data set consists of 19 entries

Node	Temperature	Node	Temperature
WATR	285	2	285
3	285	4	285
5	285	6	285
7	285	8	285
9	285	10	285
11	285	12	285
13	285	14	285
15	285	16	285
17	285	18	285
19	285		

LOAD CASE SEQUENCE CONTROL INSTRUCTIONS

Data set consists of 8 entries

Blank data (if any) omitted from printout

	Internal Case.X	Radiant Case.X	Instruction Set Background Case.X	Local Time	Output Control	Time Step
1)	0.000	0.000	1.000	0.00	0	-2.00
2)	0.000	0.000	2.000	1440.00	1	720.00
3)	0.000	0.000	3.000	1440.00	1	720.00
4)	0.000	0.000	4.000	2880.00	2	720.00
5)	0.000	0.000	5.000	1440.00	1	720.00
6)	0.000	0.000	6.000	0.00	0	-1.00
7)	0.000	0.000	6.000	7200.00	5	1440.00
8)	0.000	0.000	7.000	1440.00	2	360.00

Background Load Point Index /Temperature Exponents

Load Point	Node Ne	Temp Exponents n1	n2	Load Point	Node Ne	Temp Exponents n1	n2
1)	2	1.000	1.000	2)	3	1.000	1.000
3)	4	1.000	1.000	4)	5	1.000	1.000
5)	6	1.000	1.000	6)	7	1.000	1.000
7)	8	1.000	1.000	8)	9	1.000	1.000
9)	10	1.000	1.000	10)	11	1.000	1.000
11)	12	1.000	1.000	12)	14	1.000	1.000
13)	15	1.000	1.000	14)	16	1.000	1.000
15)	17	1.000	1.000	16)	18	1.000	1.000

Background Load Case 1

Qa	Load Tb	at Node	Qa	Load Tb	at Node	Qa	Load Tb	at Node
195898.0000	285.00	2	398117.0000	285.00	3	398117.0000	285.00	4
398117.0000	285.00	5	398117.0000	285.00	6	398117.0000	285.00	7
74318.0000	285.00	8	74318.0000	285.00	9	74318.0000	285.00	10
74318.0000	285.00	11	37155.0000	285.00	12	4644.4000	285.00	14
9288.0000	285.50	15	9288.0000	285.50	16	9288.0000	285.50	17
4644.4000	285.50	18						

Background Load Case 2

Qa	Load Tb	at Node	Qa	Load Tb	at Node	Qa	Load Tb	at Node
195898.0000	281.00	2	398117.0000	281.00	3	398117.0000	281.00	4
398117.0000	281.00	5	398117.0000	281.00	6	398117.0000	281.00	7
74318.0000	281.00	8	74318.0000	281.00	9	74318.0000	281.00	10
74318.0000	281.00	11	37155.0000	281.00	12	4644.0000	283.50	14
9288.0000	283.50	15	9288.0000	283.50	16	9288.0000	283.50	17
4644.4000	283.50	18						

Background Load Case 3

Qa	Load Tb	at Node	Qa	Load Tb	at Node	Qa	Load Tb	at Node
195898.0000	277.00	2	398117.0000	277.00	3	398117.0000	277.00	4
398117.0000	277.00	5	398117.0000	277.00	6	398117.0000	277.00	7
74318.0000	278.00	8	74318.0000	278.00	9	74318.0000	278.00	10
74318.0000	278.00	11	37155.0000	278.00	12	4644.4000	281.00	14
9288.0000	281.00	15	9288.0000	281.00	16	9288.0000	281.00	17
4644.4000	281.00	18						

Figure 62

Background Load Case 4

Qp	Load Tb	at Node	Qp	Load Tb	at Node	Qp	Load Tb	at Node
195098.0000	275.00	2	390117.0000	275.00	3	390117.0000	275.00	4
390117.0000	275.00	5	390117.0000	275.00	6	390117.0000	275.00	7
74310.0000	276.00	8	74310.0000	276.00	9	74310.0000	276.00	10
74310.0000	276.00	11	37155.0000	276.00	12	4644.4000	278.00	14
9288.8000	278.00	15	9288.8000	278.00	16	9288.8000	278.00	17
4644.4000	278.00	18						

Background Load Case 5

Qp	Load Tb	at Node	Qp	Load Tb	at Node	Qp	Load Tb	at Node
195098.0000	272.00	2	390117.0000	272.00	3	390117.0000	272.00	4
390117.0000	272.00	5	390117.0000	272.00	6	390117.0000	272.00	7
74310.0000	273.00	8	74310.0000	273.00	9	74310.0000	273.00	10
74310.0000	273.00	11	37155.0000	273.00	12	4644.4000	277.50	14
9288.8000	277.50	15	9288.8000	277.50	16	9288.8000	277.50	17
4644.4000	277.50	18						

Background Load Case 6

Qp	Load Tb	at Node	Qp	Load Tb	at Node	Qp	Load Tb	at Node
195098.0000	271.00	2	390117.0000	271.00	3	390117.0000	271.00	4
390117.0000	271.00	5	390117.0000	271.00	6	390117.0000	271.00	7
74310.0000	273.00	8	74310.0000	273.00	9	74310.0000	273.00	10
74310.0000	273.00	11	37155.0000	273.00	12	4644.4000	277.00	14
9288.8000	277.00	15	9288.8000	277.00	16	9288.8000	277.00	17
4644.4000	277.00	18						

Background Load Case 7

Qp	Load Tb	at Node	Qp	Load Tb	at Node	Qp	Load Tb	at Node
195098.0000	271.00	2	390117.0000	271.00	3	390117.0000	271.00	4
390117.0000	271.00	5	390117.0000	271.00	6	390117.0000	271.00	7
74310.0000	288.00	8	74310.0000	288.00	9	74310.0000	288.00	10
74310.0000	288.00	11	37155.0000	288.00	12	4644.4000	288.00	14
9288.8000	288.00	15	9288.8000	288.00	16	9288.8000	288.00	17
4644.4000	288.00	18						

Background Load Case 8

Qp	Load Tb	at Node	Qp	Load Tb	at Node	Qp	Load Tb	at Node
195098.0000	271.00	2	390117.0000	271.00	3	390117.0000	271.00	4
390117.0000	271.00	5	390117.0000	271.00	6	390117.0000	271.00	7
74310.0000	218.00	8	74310.0000	218.00	9	74310.0000	218.00	10
74310.0000	218.00	11	37155.0000	218.00	12	4644.4000	245.00	14
9288.8000	245.00	15	9288.8000	245.00	16	9288.8000	245.00	17
4644.4000	245.00	18						

Figure 63

IDENTIFIER ... SSHIPST DATA REFERENCE ... 1020

Material Density ... 7860.00

			Specific Heat	Conductivity
Upper default temperature			373	373
Lower :	:		100	100
Polynomial coefficients		T^0	448.00E+00	520.00E-01
:	:	T^1	-100.00E-13	-100.00E-14

IDENTIFIER ... SSHIPST DATA REFERENCE ... 1020

			Emissivity	Reflectivity	Absorptivity
Upper default temperature			373	373	373
Lower :	:		100	100	100
Polynomial coefficients		T^0	200.00E-03	550.00E-03	450.00E-03
:	:	T^1	-400.00E-17	-100.00E-16	-100.00E-16

IDENTIFIER ... SWATER DATA REFERENCE ... WATER

Material Density ... 1025.00

			Specific Heat	Conductivity
Upper default temperature			373	373
Lower :	:		3	3
Polynomial coefficients		T^0	180.00E+01	139.00E-03
:	:	T^1	561.00E-02	115.25E-05

Figure 64

The temperature cases considered are as follows:

Case	Time from ballast pick-up (hrs)	Sea Temp (Nodes 2-7)	Air Temp (Nodes 8-12)	Hold Temp (Nodes 14-18)
1	0	285	285	285
2	24	281	281	283
3	48	277	278	281
4	72	275	276	278
5	120	272	275	277
6	144	271	275	277
7	264	271	288	288
8	120	271	218	245

The time in column 2 is the time at which the temperatures are applicable. The first transient assumes cases 1-7 follow in the sequence given which corresponds to the measured temperature/time history. The second transient assumes a rapid drop in temperature to the temperatures of case 8, starting at hour 120 and lasting for 24 hours, after which the temperatures are maintained at this level to the end of the 11 day period.

A listing of the data is given in figures 61 - 64 as printed by the THETA program.

5.3.3 Discussion of the Results

Selected temperature transients have been plotted to illustrate the nature of the thermal response of the ballast water and of the plates surrounding the cell.

In Figure 65 the ballast water temperature is shown for the first analysis labelled MVAT1. The fall in temperature follows closely the change in external conditions. The minimum temperature is 4^{o}C above the sea temperature due to the influence of the higher air temperatures in contact with the cell plates. It is interesting to note the sudden change in temperature that occurs at the end of the voyage when the air temperature rose rapidly. The tick marks on the time scale indicate the points at which the solution is stored. Figure 66 shows the corresponding rate of heat loss or gain during the voyage.

Figure 67 illustrates the different response of the exterior hull plates above and below the water. The Index Number key indicates the order of the graphs in a vertical sequence; plates 7 and 2 are plotted together. Similarly Figure 68 gives the temperature of the plates on the 'hold' side of the cell.

All the above temperature plots follow closely the measured values recorded during the July crossing described in Section 6. This indicates that when taken over a long time scale, the surface coefficients chosen are sufficiently accurate to predict the response, and that the characteristic time for the response of the cell is very short.

The second analysis, labelled MVAT2, illustrates the effect of a rapid drop in temperature. Figure 69 shows that the ballast water temperature comes to rest midway between the sea water and air temperatures. (Note the cell is assumed to be at the waterline with half the hull plates exposed to air). Further, the response of the ballast water lags, by a few hours, the change in air temperature. The hold plate temperatures naturally follow the ballast water and hold ambient temperature, which are the same when the system reaches the steady state. These temperatures are shown in Figure 70. Finally, the heat loss from the ballast water during the cooling transient is shown in Figure 71.

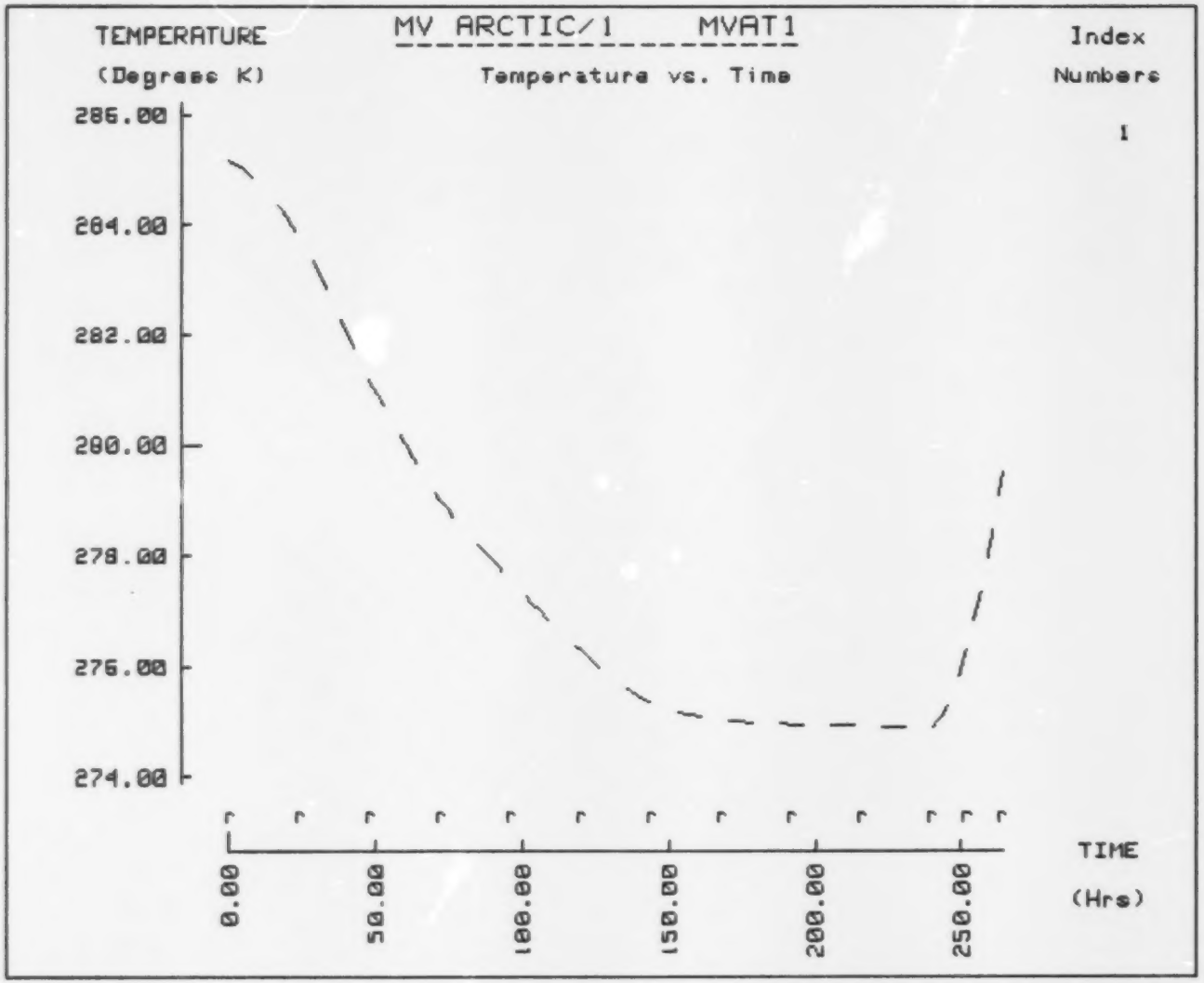

Figure 65

BALLAST WATER TEMPERATURE TRANSIENT

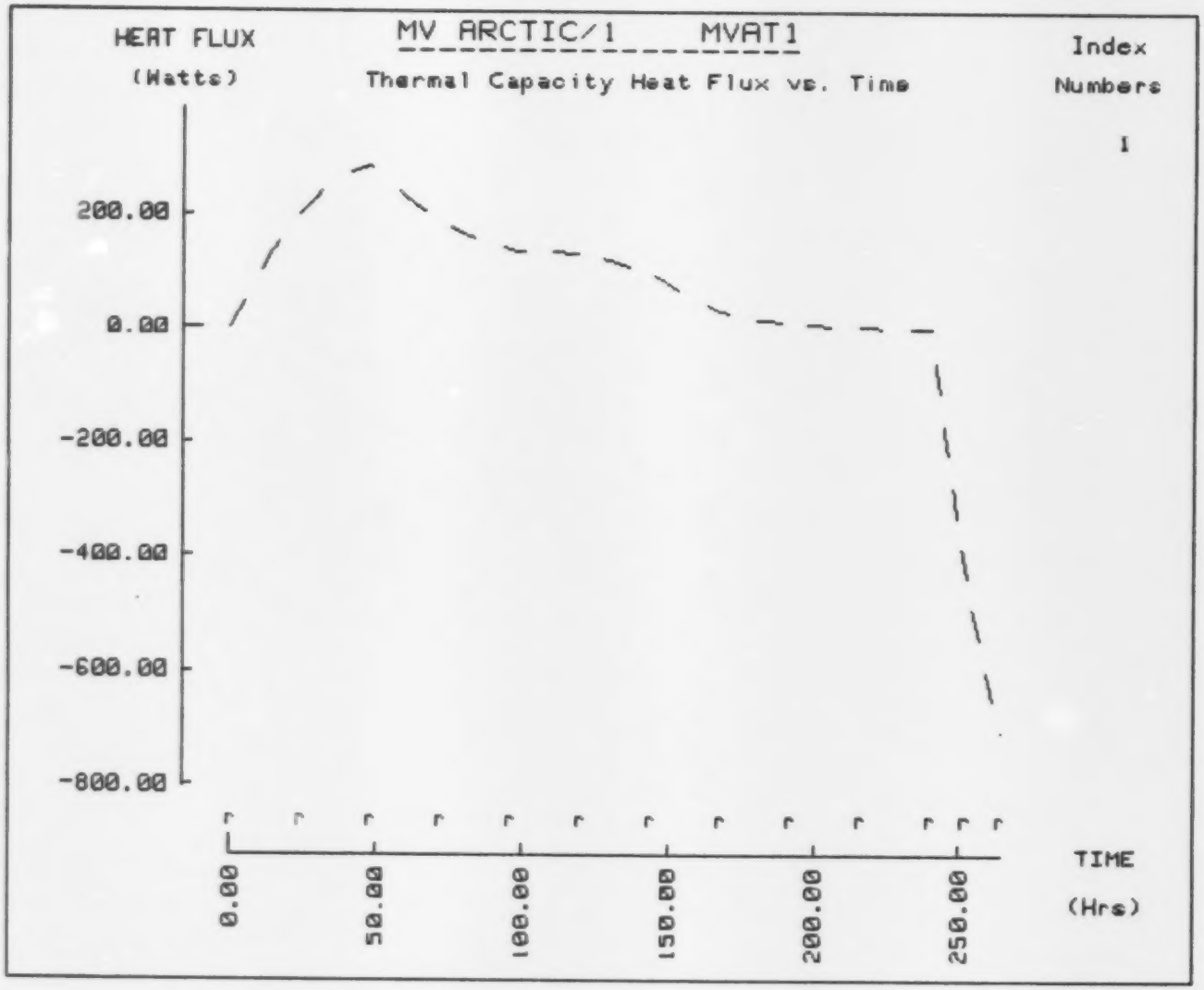

Figure 66

BALLAST WATER HEAT LOSS OR GAIN

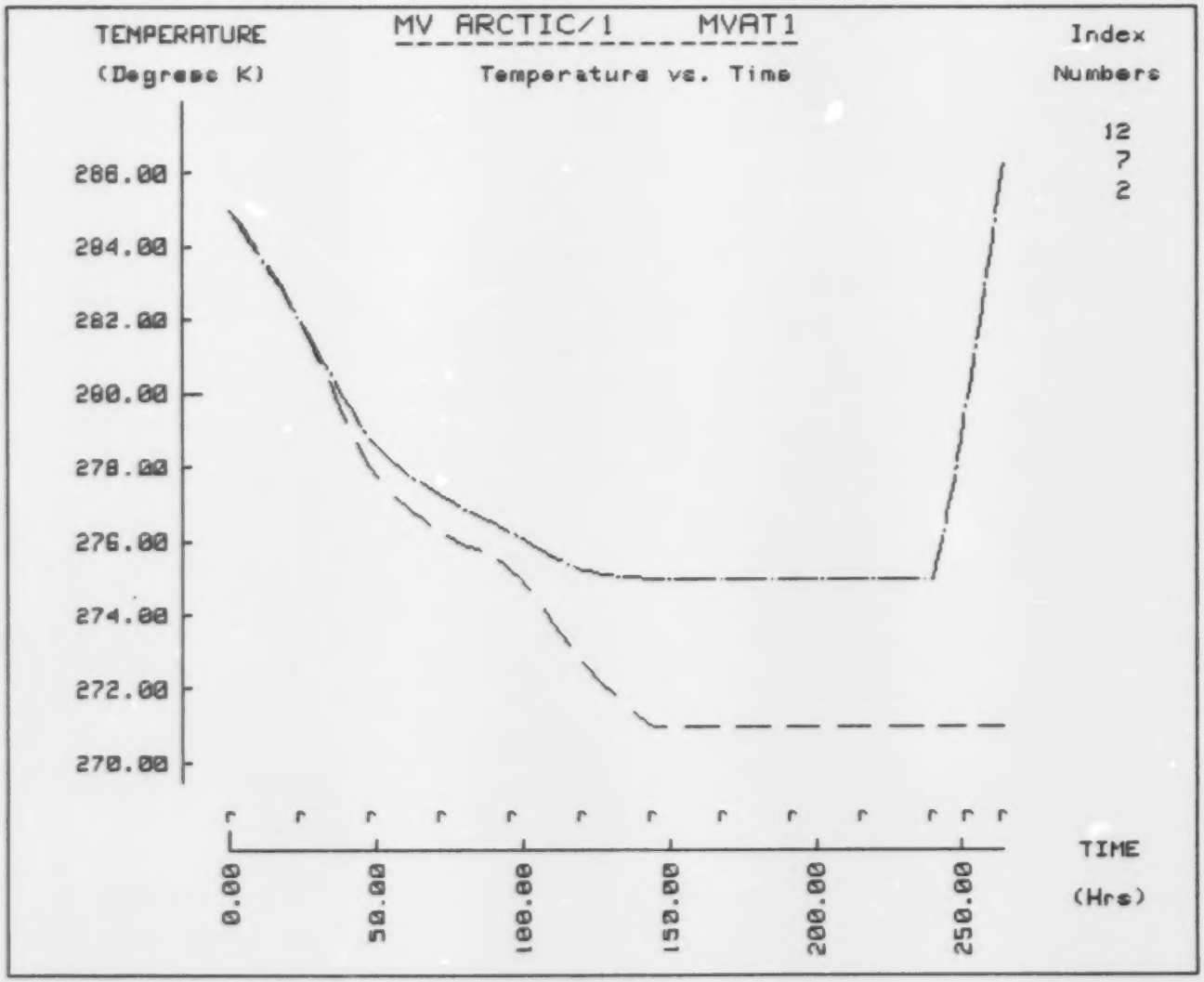

Figure 67

EXTERIOR HULL PLATES TEMPERATURE TRANSIENT

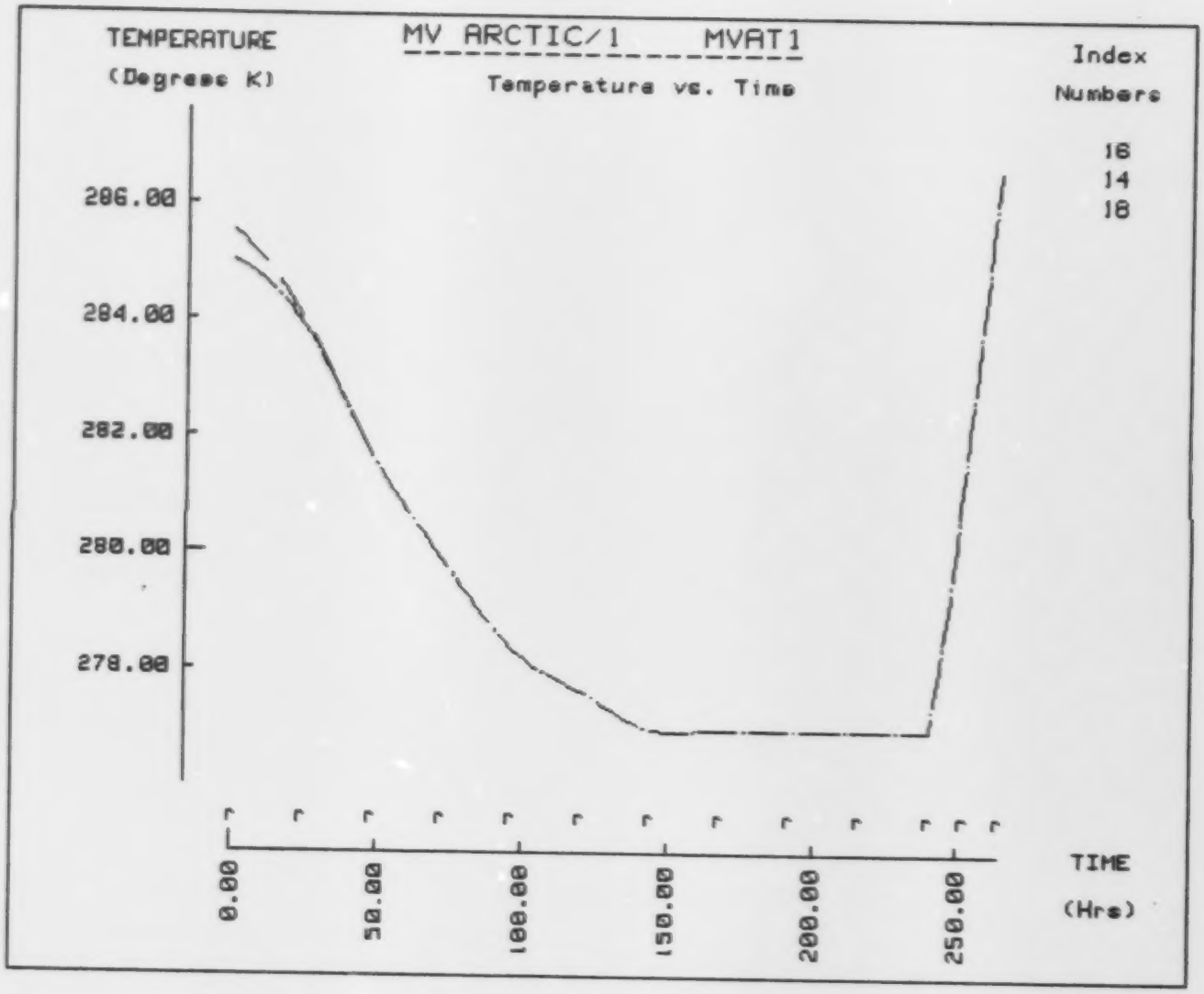

Figure 68

HOLD PLATE TEMPERATURE TRANSIENT

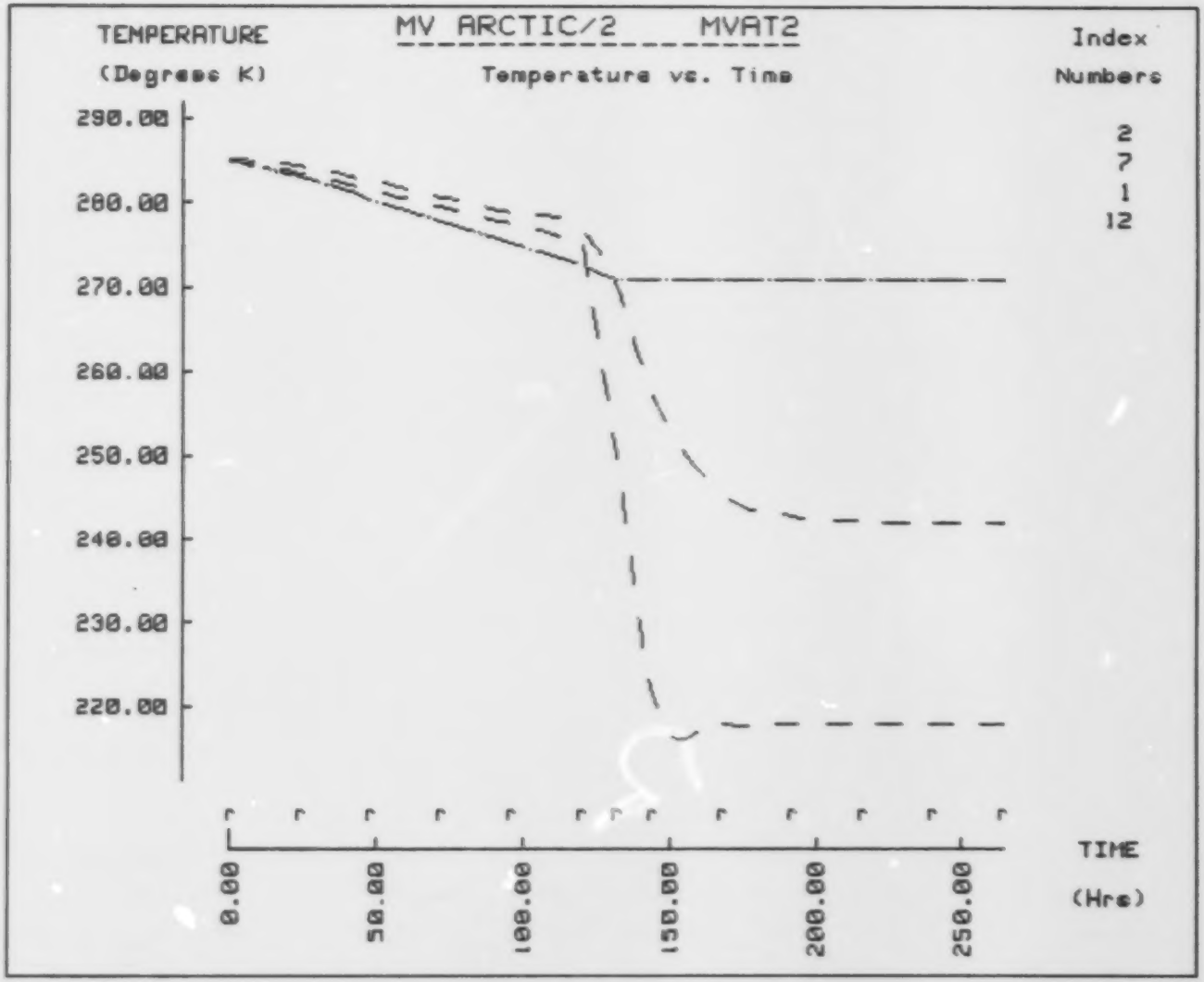

Figure 69

HULL PLATES AND BALLAST WATER TEMPERATURE TRANSIENTS

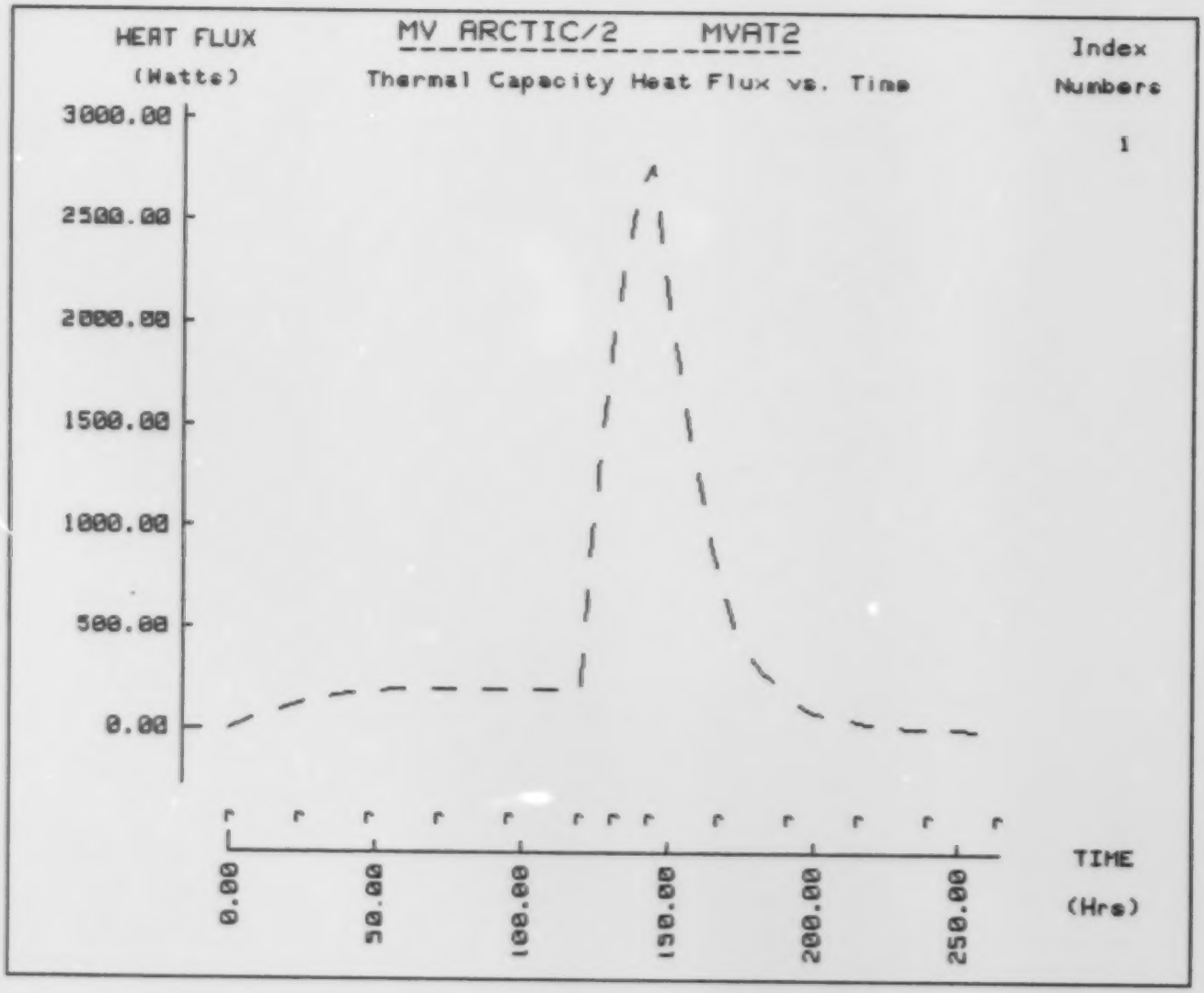

Figure 70

HOLD PLATE TEMPERATURE TRANSIENTS

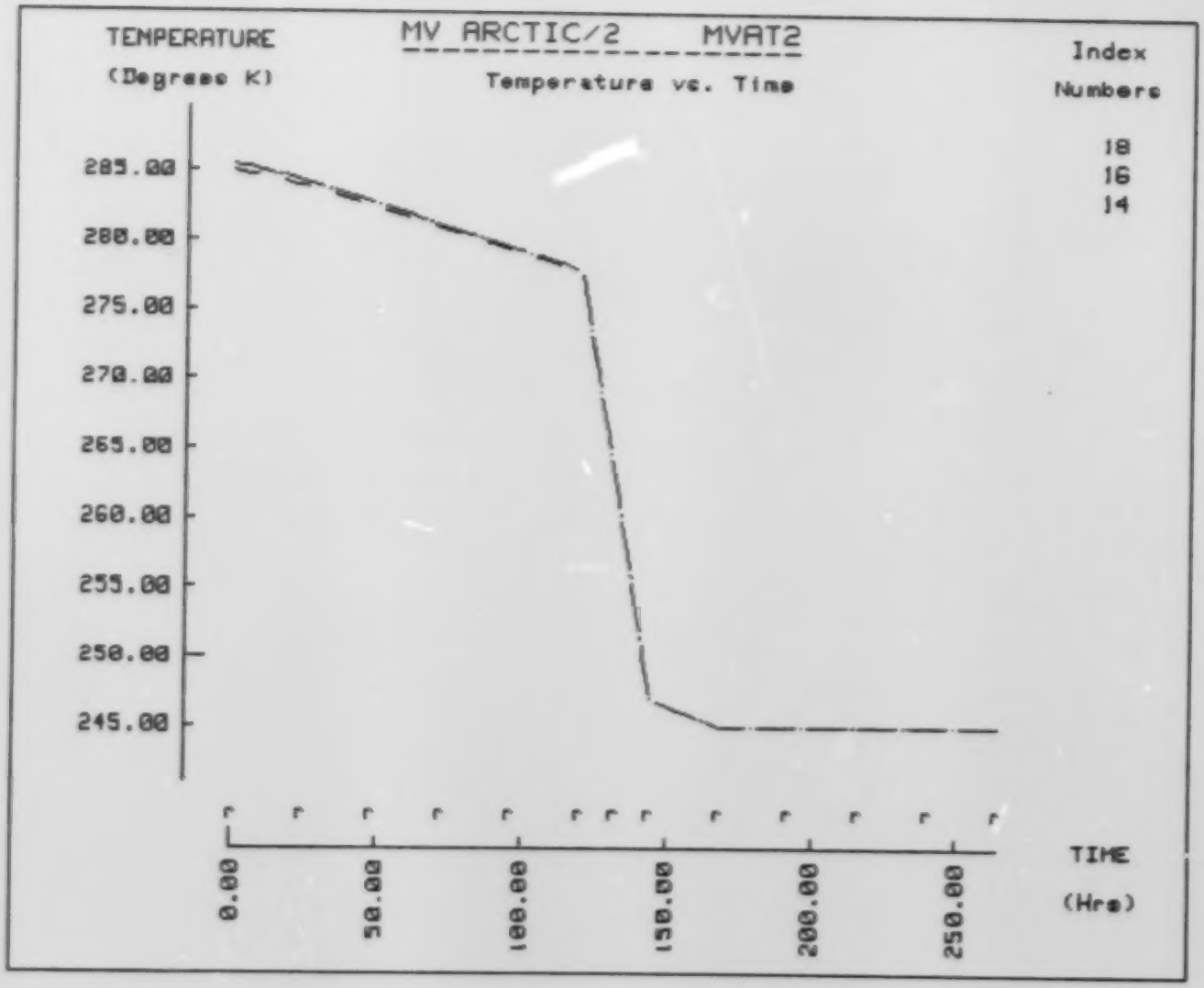

Figure 71

HEAT LOSS FROM THE BALLAST WATER

5.4 Conclusions

In this section several examples have been used to illustrate the possibilities for more detailed analysis of a small section of the ship's hull. By concentrating on a single cell formed by the vertical frames, horizontal stiffeners, and inside hold plates, more questions regarding local temperature variations, non-linear effects and transient variations have been investigated. In view of the complexity of the ship's structure, this is perhaps the only approach that will permit cost effective study of such problems. The modelling of larger sections of the hull with such detail would involve considerable labour and computing cost. The facilities exist in both the ASASHEAT and THETA programs to generate much larger models, where necessary. However, a combination of models similar to those used in this report can be used to study a wide range of heat transfer problems effectively. When radiation or three dimensional effects are important (such as heat transfer into the ballast water), the complexity of the heat transfer links is such that gross assumptions must be made if large sections of the ship are to be studied.

In all the models given in this section the heat transfer through the ship's hull is clearly dependent on the assumption made for the size of the surface coefficients on the interior surfaces of the plates. In the steady-state it affects the nature of the temperature distribution along the plates, which may be an important factor in determining thermal stresses. For the transient case it will determine the rate of heat flow and hence the time that the ship takes to respond to a sudden change in temperature. If a comparison is made for the July, Atlantic crossing of the M.V. Arctic, it is clear from the model and the recorded measurements that the characteristic response time is a matter of hours rather than days. It may also be seen from the transient model that the outside hull plates change temperature more rapidly than the hold plates, in response to a sudden drop in external temperature. This leads to a short lived temperature gradient in the frame to hull connection that has not been investigated here. Such a temperature gradient may be of concern when local thermal stresses are investigated, especially in combination with other, non-thermal, stresses.

The implication of the above conclusions is that where the thermal gradients or heat flow rates are considered important, more work needs be done to establish the surface coefficients more accurately. This should be done by a combination of numerical analysis and measurement as the long term interest would be to calculate these values from a theoretical model.

6. M.V. ARCTIC TEMPERATURE MONITORING

6.1 Introduction

As the analytical study proceeded it rapidly became apparent that the area about which least was known was the mechanism of convective heat transfer within the cells of a double skinned hull. Efforts were made (see section 3.1.3) to calculate by numerical methods applied to the governing fluid flow equations, what the heat transfer coefficients might be. However it rapidly became clear, that for the size of cells typically encountered in a ship, the solution was impossible using the techniques currently at our disposal and that the problem taxed even state of the art techniques currently under development in other research groups. It was therefore necessary to fall back on approximate solutions derived from flow over a flat surface immersed in a fluid.

It was determined by consideration of the cell dimensions and the temperature differences for the air filled cells that the Rayleigh number of a typical cell was of the order of 10^{12}. This suggested that the flow would be turbulent and that the heat transfer would be controlled by a boundary layer on the side walls. Estimates of the Nusselt number that characterizes this heat transfer indicated a theoretical value of about 500, but no experimental support could be found at these high Rayleigh numbers to confirm these predictions. It was therefore concluded that the possibility of experimental work should be investigated.

Two avenues were considered, laboratory model tests and monitoring at full scale in an actual ship. The former approach offers the great advantage of a controlled environment, which permits reliable scheduling, good instrumentation calibration, valid design of experiment, the opportunity to repeat tests and to examine systematically a range of the variables, such as temperature difference and surface emissivity. However, physically modelling the cells requires both geometric and kinematic similarity between model and prototype, which, in this case requires the Rayleigh numbers, $Ra = g\beta L^3 \left(\frac{T_w - T_\infty}{\nu\alpha}\right)$, to be equal. It is clear that even a half scale model would reduce the value of L^3 by a factor of 8, and require that the temperature difference term be increased by a similar factor.

Satisfying the modelling requirements mentioned above would imply maximum temperatures in the model of over 100°C, which would introduce other difficulties. These difficulties include the viscosity dependence upon temperature in an air filled cell, and in the case of water the reversal in the β

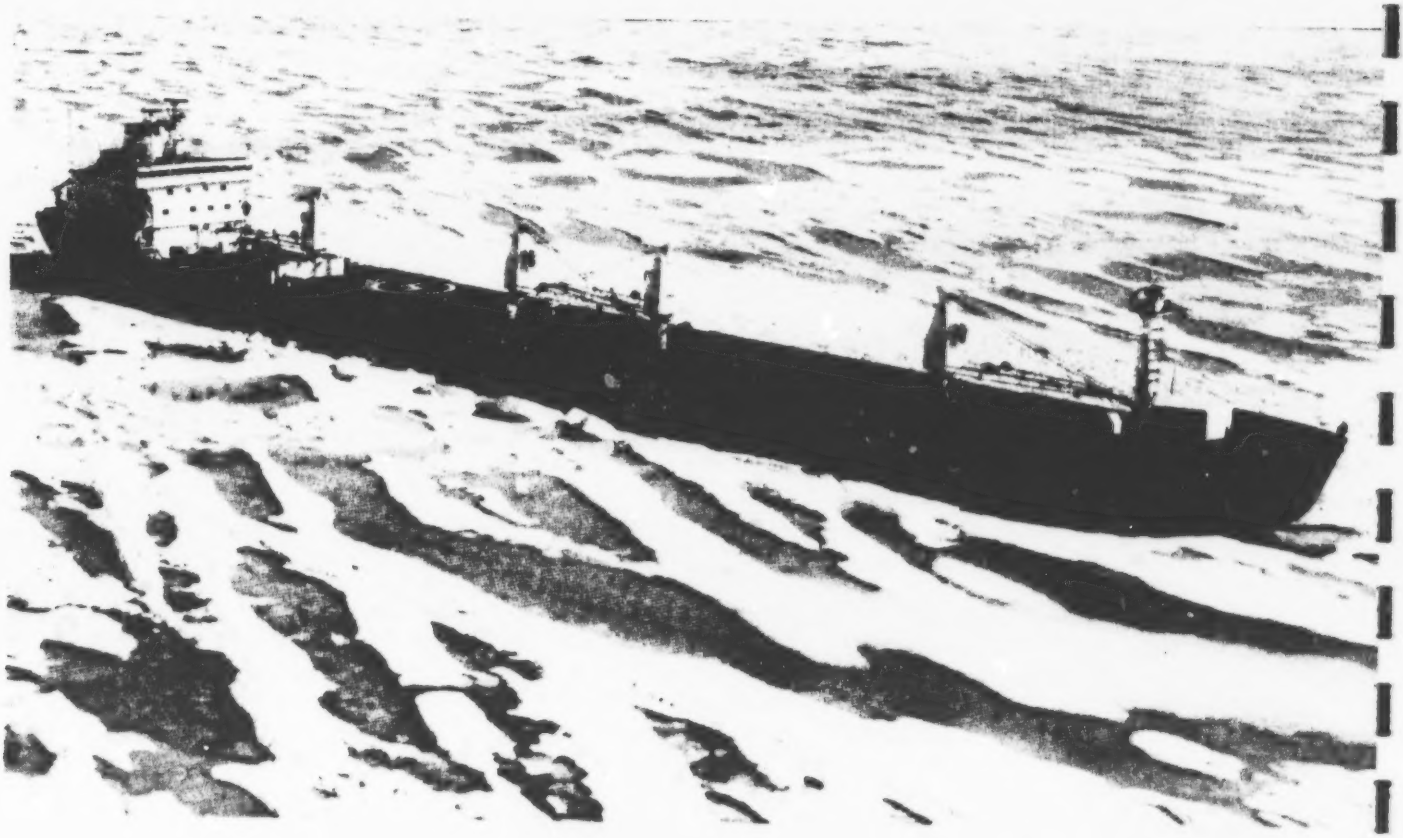

Midship Section

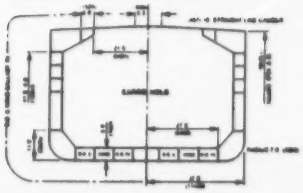

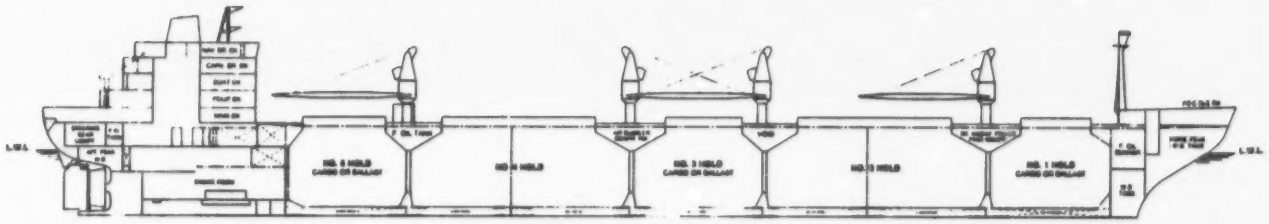

Profile

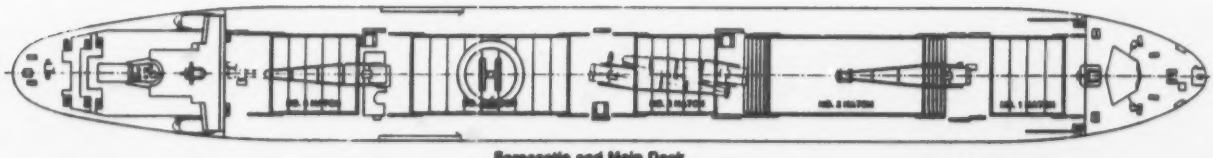

Forecastle and Main Deck

Figure 72 M.V. ARCTIC

value near 4°C together with the upper temperature limit imposed by the discontinuity at the boiling point. While a lower temperature difference could be used, and certain analytical adjustments made to allow for failure to match the Rayleigh numbers, confidence in the result would be limited. Even a scale model would, however, allow good flow visualization studies, offering real assistance to the designer. Laboratory modelling at full scale was considered to be technically satisfactory, but expensive in the case of the large cells representative of very large ships, especially if several cell configurations were to be investigated.

In consequence of the above considerations it was decided, in the first instance, to consider the alternative of monitoring cell thermal response in an actual vessel in Arctic service.

The full scale monitoring posed logistics problems in securing and instrumenting a suitable vessel, but had the advantage of providing results from a real set of circumstances. It was decided that initially any money available would be best spent gathering data from full scale monitoring and that a controlled experiment would have second priority. Added to this a good opportunity arose to participate in an on-going test program aboard the M.V. Arctic during the period from July to November 1981.

The M.V. Arctic is a bulk carrier built to operate as an icebreaker. The vessel is shown in Figure 72. A series of tests has been conducted since the ship was commissioned to establish information on the ice-forces experienced on the vessel's bow. The ship's owners expressed an interest in knowing more about the heat transfer aspects, and offered to let additional instrumentation be added to the ship in July 1981 in readiness for a series of transatlantic runs from European ports to Nanisivik culminating in November 1982.

The instrumentation plan was carried out by Weir-Jones Engineering Consultants Ltd., of Vancouver. A trial run was made from Antwerp to Nanisivik during the first week of July, 1981, and a set of temperature readings successfully obtained for air and sea temperatures ranging from 12°C to -2°C.

Regrettably these were the only results obtained as the ship encountered a severe storm during its next crossing and the ship's captain ordered the wiring, that entered through a man-way cover on the ship's deck, be cut and the cover fastened down. This single action irreparably severed the connection between the thermistors mounted in the hull and the monitoring room. Insufficient money was available

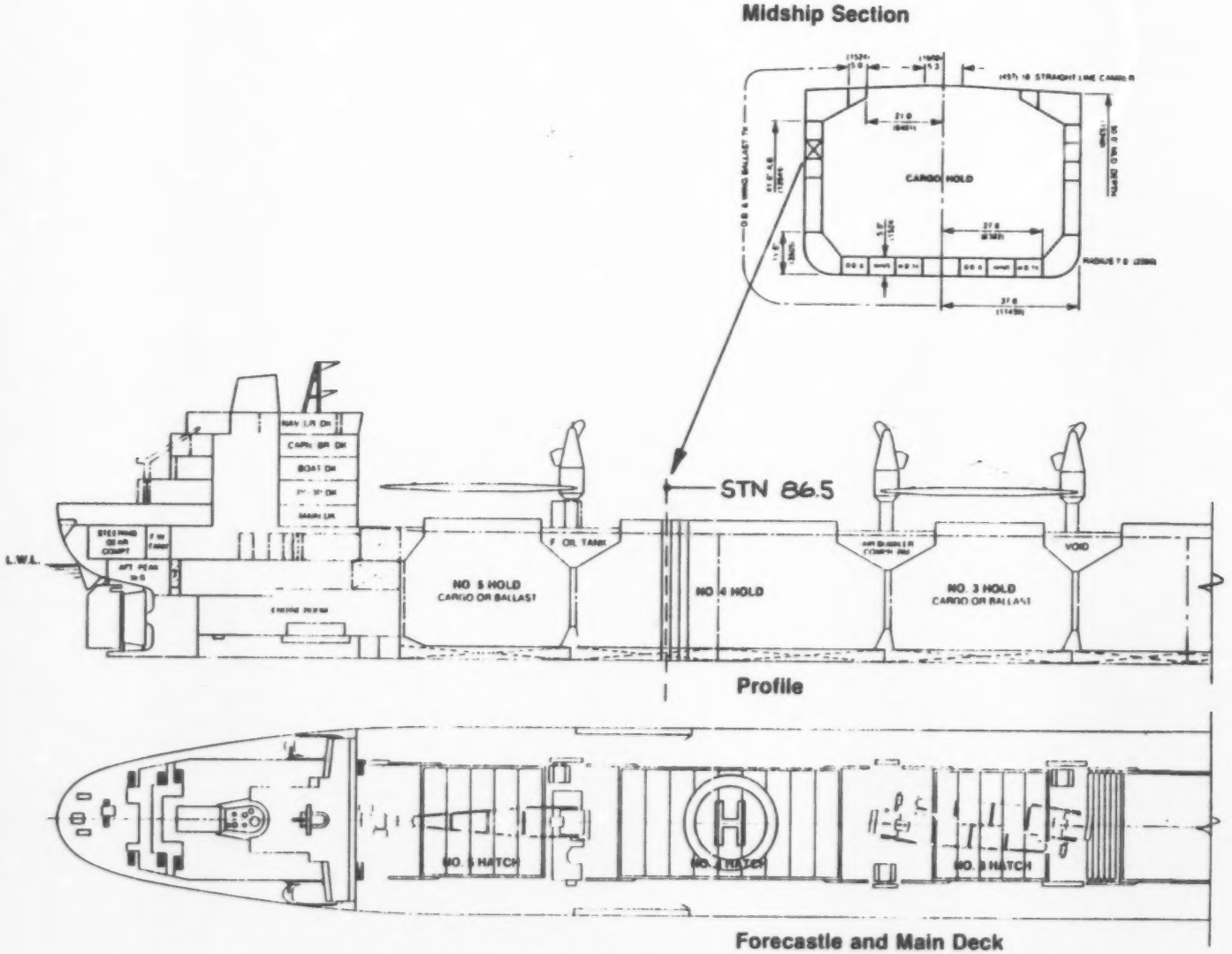

Figure 73 LOCATION OF THE TEST CELLS

to re-do the wiring and thermistor attachments, and it was determined to seek a more lasting and robust system for use at a later date. In the meantime, the only results available are those recorded during the summer crossing. The following sections describe the apparatus used, the positioning of the thermistors, and the temperatures recorded during that voyage.

6.2 Description of the Monitoring Procedure

The objective of the experimental study was to measure temperatures in the outside ballast tanks of the ship in a region removed from the engine room, and where the structure is typical of the standard hull construction. A line of cells was therefore chosen at stations 86-89 which was opposite hold number 4 and in ballast tank number 6. The positions are shown in Figure 73. In particular it was decided to monitor all the plates within two cells both at the same horizontal level. In one cell, all the openings were covered by plates (perforated by a number of holes) so that free motion of the fluid through the cell (air or water) could not take place. In addition to these cells, a number of gauges were mounted above and below the fully monitored cells. Figures 74, 75 and 76 show the relative placement of these gauges. The temperature measurements were made using FENWAL precision thermistors coupled to an automatic data acquisition system. The thermistors were mostly mounted directly on the steel surface following the removal of an area of the protective paint coating. Several thermistors were used to monitor the ballast water and the ambient outside air and hold temperatures. The method of securing the thermistors is shown in Figure 77.

A major problem was encountered in measuring the sea temperature as there was no location where a penetration through the ship's hull could be used to permanently mount a thermistor. Two solutions were tried; the first involved lowering a bucket over the side and the second trailing a 'bird', with a thermistor attached, over the stern of the ship. Neither proved satisfactory and hence the sea water readings are highly erratic. The reason why such areas as the engine cooling water intake could not be used is that heaters are installed to keep the intakes free of ice.

6.3 The Voyage

The ship sailed to Nanisivik under full ballast and hence the monitored cells were full of sea water for the entire trip. The ballast tanks were purposely voided and refilled on entering the Gulf Stream between 9:30-11:00 a.m. on June 28, 1981 which was two days after the ship sailed on June 26. At that time, the ship was about 200 miles

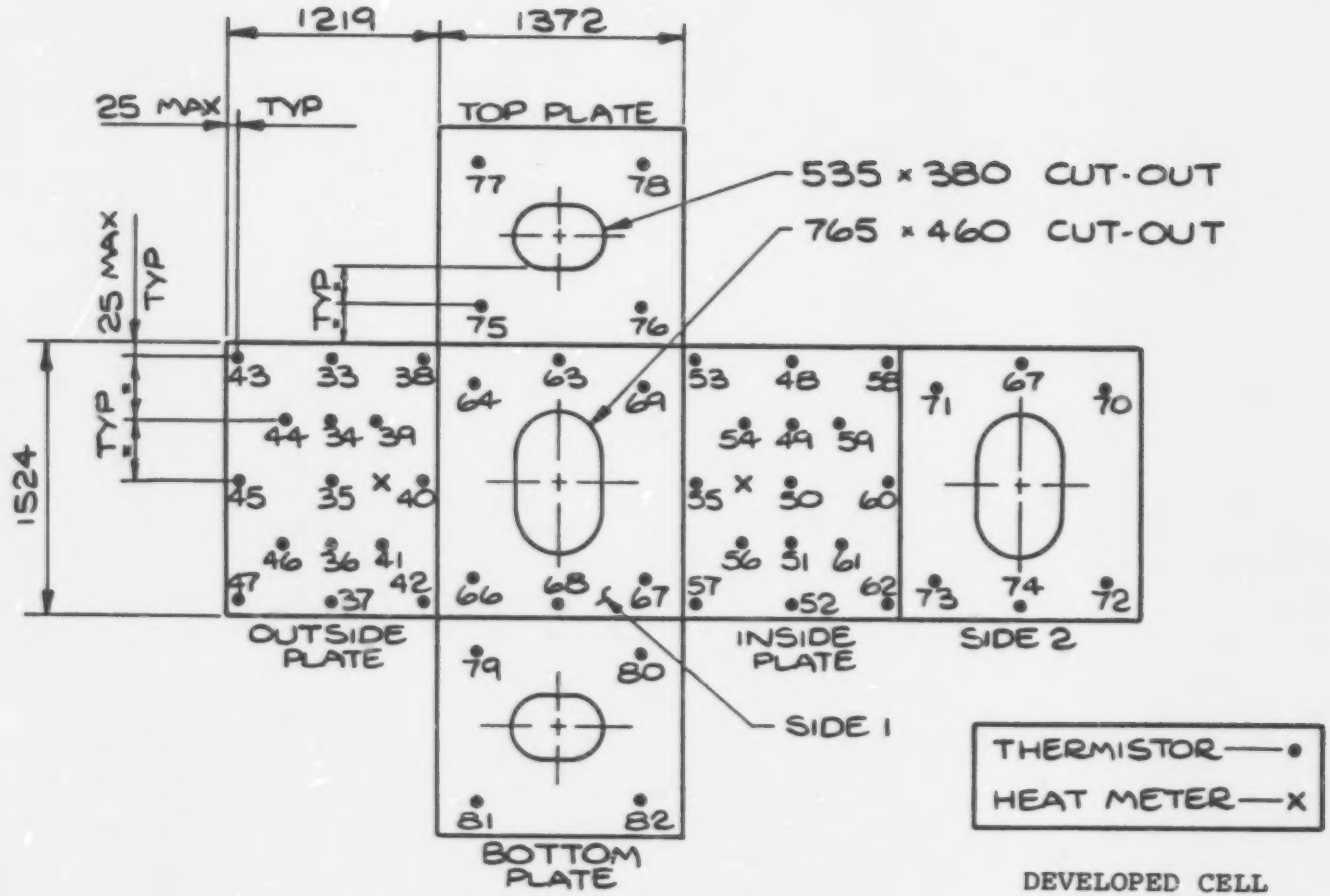

Figure 74

THERMISTOR PLACEMENT MAIN CELL
(50 Thermistors Shown)

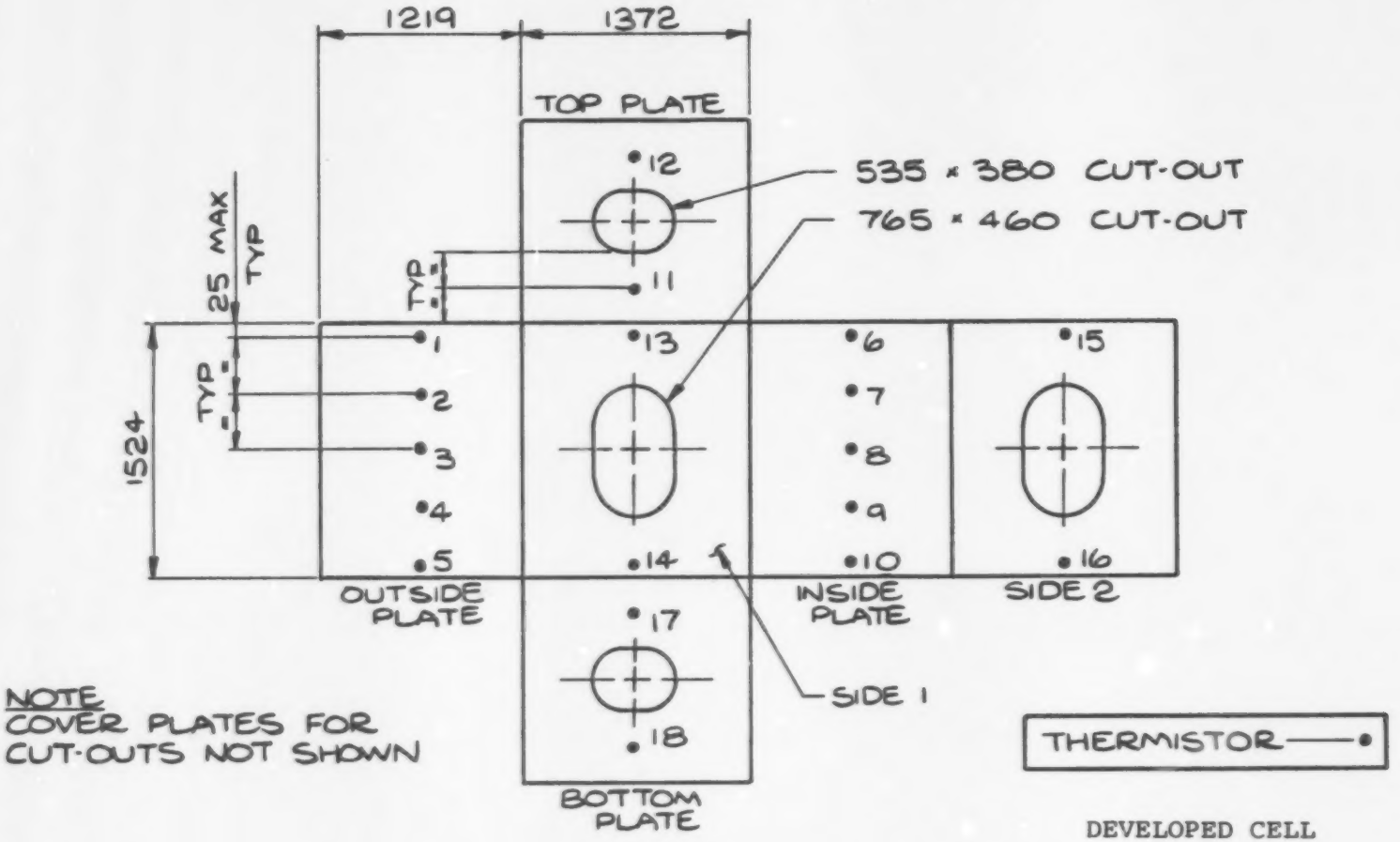

Figure 75

THERMISTOR PLACEMENT TWO BAYS FORWARD OF MAIN CELL
(18 Thermistors Shown)

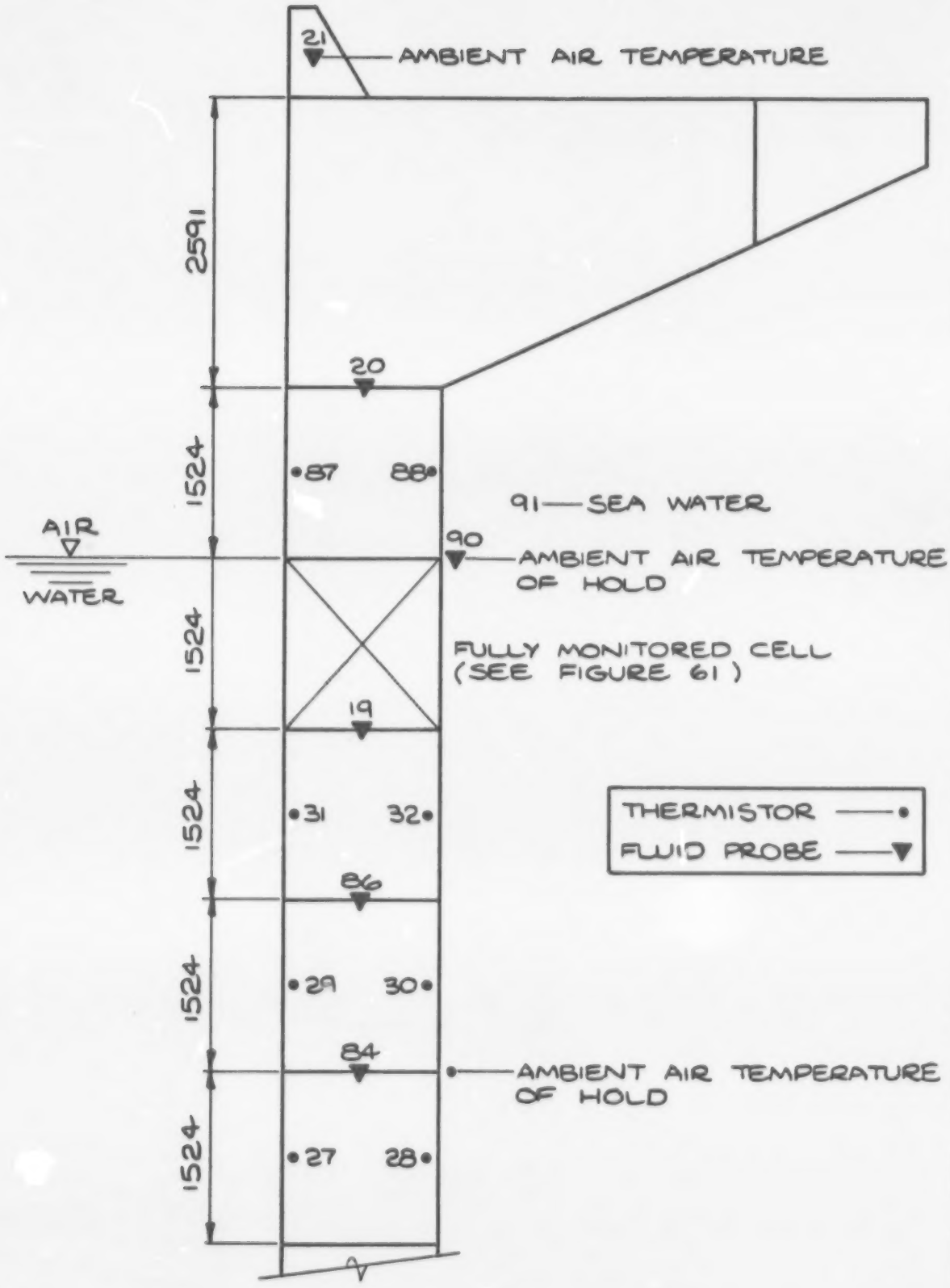

Figure 76

THERMISTOR PLACEMENT IN OTHER THAN MAIN CELL

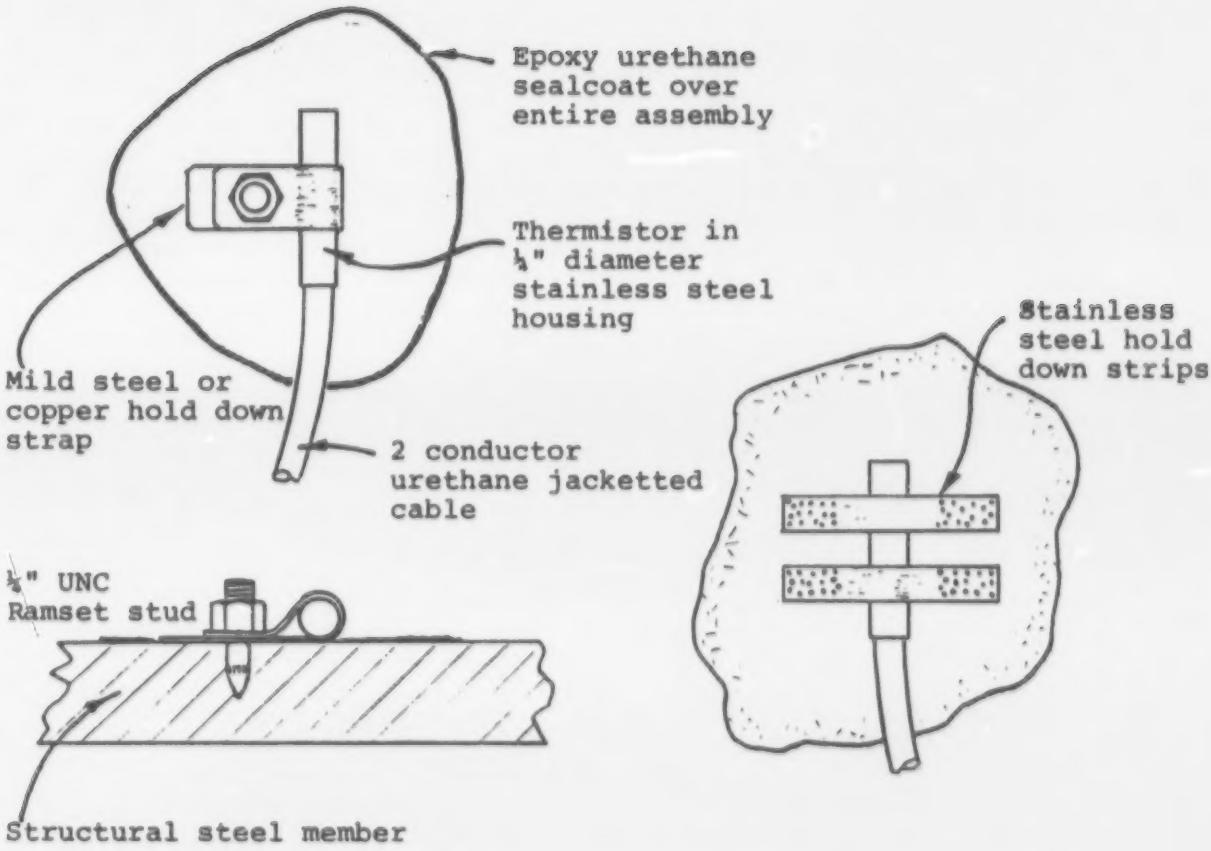
Epoxy urethane sealcoat over entire assembly
Thermistor in ¼" diameter stainless steel housing
Mild steel or copper hold down strap
2 conductor urethane jacketted cable
Stainless steel hold down strips
¼" UNC Ramset stud
Structural steel member

1. PROCEDURE USED ON INTERNAL STRUCTURAL MEMBERS

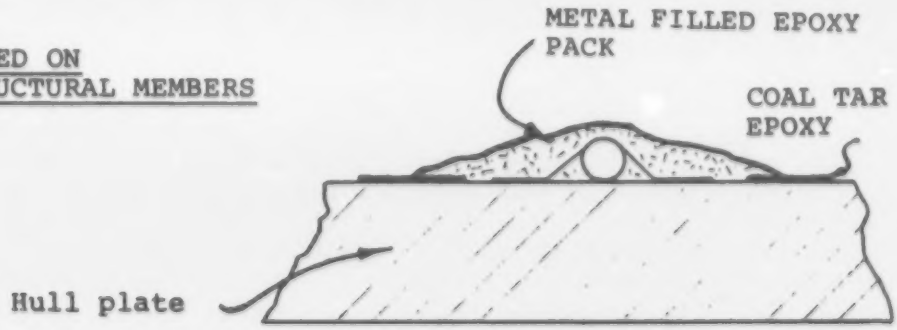

2. PROCEDURE USED FOR HULL MOUNTING

Figure 77

THERMISTOR MOUNTING DETAILS

west of the northern tip of Scotland (58° 47 LAT; 14° 5 LONG). The maximum water temperature recorded at that time was 12°C. The sea and air temperatures fell continuously until the ship encountered ice on July 3, 1981 which coincided with it crossing the Arctic circle just west of Greenland. The ship docked in Nanisivik at 10:00 hrs. on July 9, monitoring was stopped at 21:00 on July 10. As the ship approached the dock, the ballast was dumped; it is estimated that this was done at 03:00 hrs. on the 9th of July. The weather on the 10th of July was unusually hot and the air temperature rose rapidly to a peak well over that previously experienced on the trip. In addition the sun added considerable radiant heating.

A list of the M.V. Arctic positional data as recorded by the satellite navigation system is given in Table 7. This is shown in plotted form in Figure 78, the major tick marks indicate the changing of the date.

6.4 Discussion of the Results

A very good idea of the general temperature levels experienced during the voyage can be gained by reference to Figure 79. Here it can be seen that the majority of the plate temperatures falls in a band that follows the general cooling trend of the voyage. A temperature excursion occurs when the Gulf Stream water is taken on board and subsequently at the end of the voyage when the ballast is dumped and the ambient external air temperature rapidly rises. It is interesting to note that as the voyage progresses, the bandwidth increases indicating a spread in temperature of 4°C. A more detailed examination of the results follows.

The results have been viewed in two ways: a) as a time history, and b) as a spacial variation over the locations monitored. Different information can be obtained from viewing the results from these two perspectives.

1) Because so much trouble was encountered measuring the sea water temperature, it is considered appropriate to fit a curve through the measured data points. This is particularly relevant in the period after the ice was encountered at which stage it can be fairly assumed that the sea temperature remains constant at about 1.5°C. This is illustrated in the sea water temperature plot shown in Figure 80.

2) Consider first the thermistors mounted in the closed cell; a spacial display of the temperatures recorded at a number of time intervals in the voyage is shown in Figures 81 - 85. From these diagrams the following

M.V.ARCTIC POSITIONAL DATA

DATE	TIME	LATITUDE	LONGITUDE
YY-MM-DD	hh:mm:ss	Deg N Min	Deg W Min
81 06 26	07:46:42	91°05.40'	-1°09.39'
81 06 26	09:07:11	93°20.80'	-2°53.34'
81 06 26	21:19:46	95°31.33'	-0°19.06'
81 06 27	00:47:25	97°47.13'	1°50.11'
81 06 27	10:04:07	99°01.75'	2°00.91'
81/06/27	20:04:28	98°44.26'	5°52.22'
81/06/27	20:53:11	98°44.76'	6°49.32'
81 06 27	22:17:11	98°44.99'	7°32.35'
81/06/28	00:02:35	98°45.46'	8°25.93'
81/06/28	03:20:00	98°46.63'	10°05.16'
81/06/28	06:40:42	98°47.10'	11°55.01'
81 06 28	07:40:35	98°47.20'	12°25.73'
81/06/28	09:32:42	98°47.00'	13°19.48'
81/06/28	11:01:32	98°47.02'	14°05.40'
81/06/28	13:16:07	98°46.96'	15°13.51'
81/06/28	15:20:07	98°47.05'	16°16.69'
81/06/28	18:52:35	98°47.04'	18°04.10'
81/06/28	21:47:39	98°48.41'	19°32.82'
81/06/29	23:14:35	98°48.17'	20°16.79'
81/06/29	01:00:00	98°47.98'	21°09.97'
81/06/29	02:10:35	98°48.99'	21°44.69'
81/06/29	03:51:32	98°50.22'	22°35.80'
81/06/29	07:26:35	98°51.78'	24°17.38'
81/06/29	10:42:00	98°51.79'	25°49.14'
81/06/29	15:58:00	98°52.20'	28°20.60'
81/06/29	19:30:07	98°53.08'	30°06.55'
81 06 29	22:51:53	98°53.41'	31°44.69'
81/06/30	02:20:07	98°55.16'	33°25.07'
81/06/30	05:33:39	98°56.92'	34°51.83'
81/06/30	09:37:04	98°56.38'	36°44.71'
81/06/30	12:56:35	98°57.20'	38°17.28'
81/06/30	15:10:07	98°58.88'	39°17.44'
81/06/30	22:03:39	98°53.39'	42°41.27'
81/07/01	01:36:28	99°05.71'	44°29.40'
81 07 01	03:25:04	99°17.97'	45°24.17'
81 07 01	04:42:35	99°24.94'	46°08.22'
81 07 01	08:59:11	99°31.31'	48°16.41'
81 07 01	10:31:04	60°01.98'	49°00.36'
81/07 01	14:22:00	60°53.12'	50°11.51'
81 07 01	15:29:39	61°07.45'	50°33.53'
81/07/01	17:26:49	61°33.48'	51°00.53'
81/07/01	18:58:42	61°53.57'	51°36.80'
81 07 01	20:49:46	62°17.48'	52°11.64'
81/07/02	00:21:39	63°05.43'	53°21.64'
81/07/02	02:07:04	63°29.08'	53°58.05'
81 07 02	04:01:04	63°54.26'	54°10.82'
81/07/02	05:41:39	64°19.74'	54°28.28'
81/07/02	07:51:32	64°49.46'	54°39.83'
81 07 02	09:56:07	65°11.38'	54°40.87'
81/07/02	13:02:00	65°55.08'	55°02.30'
81/07/02	14:24:42	66°17.81'	55°09.79'
81/07/02	15:17:04	66°30.41'	55°15.68'
81 07 02	16:07:39	66°43.59'	55°22.76'
81/07/02	17:01:39	66°57.90'	55°29.35'
81/07/02	18:19:04	67°16.94'	55°37.72'
81/07/02	21:25:04	68°03.23'	55°56.33'
81/07/02	23:34:35	68°36.44'	56°09.49'
81/07/03	01:19:32	69°04.28'	56°22.73'
81 07 03	03:19:39	69°36.76'	56°37.63'
81/07/03	05:24:35	70°08.39'	56°55.62'
81/07/03	07:14:35	70°36.81'	57°10.20'
81/07 03	09:04:07	70°55.71'	57°24.21'
81 07 03	10:52:29	71°23.20'	57°35.32'
81/07/03	13:19:04	72°00.38'	57°47.28'
81/07/03	16:12:00	72°43.73'	58°07.64'
81/07 03	19:14:35	73°32.11'	58°40.00'
81/07/03	20:17:32	73°47.66'	58°49.57'
81/07/03	22:04:07	74°14.21'	59°10.42'
81/07 03	23:51:39	74°31.06'	59°43.71'
81/07 04	00:58:57	74°37.31'	60°06.14'
81/07/04	11:10:35	74°42.40'	60°25.98'
81 07 04	11:49:32	74°45.92'	60°31.80'
81/07/04	13:55:39	75°00.66'	60°59.21'
81/07/04	15:22:20	75°04.10'	61°36.62'
81/07 04	15:39:32	75°04.91'	61°43.07'
81/07/04	17:24:07	75°07.57'	62°42.41'
81/07/04	18:23:32	75°09.04'	63°11.32'
81 07 04	19:09:04	75°10.12'	63°31.58'
81/07/05	00:29:32	75°27.16'	64°42.42'
81/07/05	02:17:04	75°35.13'	70°34.51'
81 07 05	03:15:32	75°40.58'	71°33.92'
81/07/05	04:04:00	75°43.44'	72°16.49'
81/07/05	05:09:04	75°44.66'	73°03.36'
81/07 05	06:49:32	75°39.28'	73°41.55'
81/07 05	10:58:29	75°27.34'	75°19.27'
81/07 05	12:46:29	75°11.17'	76°52.67'
81 07 05	14:03:04	75°02.62'	77°40.89'
81/07 05	19:17:32	74°38.21'	79°47.17'
81/07/05	22:56:21	74°09.94'	82°11.44'
81 07 06	00:37:32	73°56.08'	83°31.90'
81/07 06	12:04:08	73°24.72'	83°18.22'
81/07 06	12:04:08	73°24.72'	83°18.22'
81/07/08	19:10:49	73°23.48'	83°19.19'

Table 7

M.V. ARCTIC POSITION

TICKS indicate measurement points - MAJOR ticks indicate NEW DAY

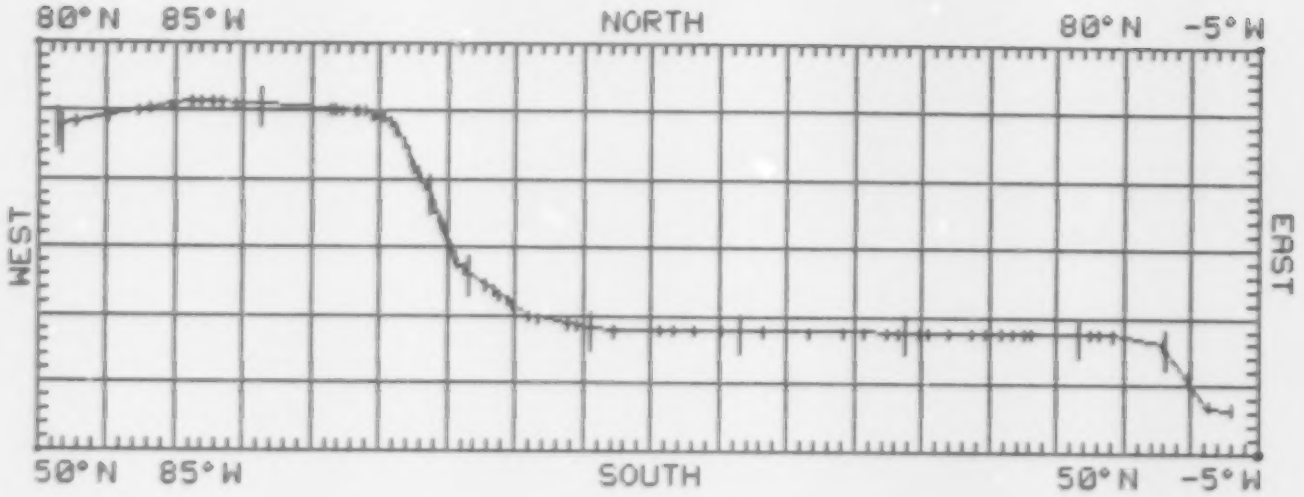

Figure 78

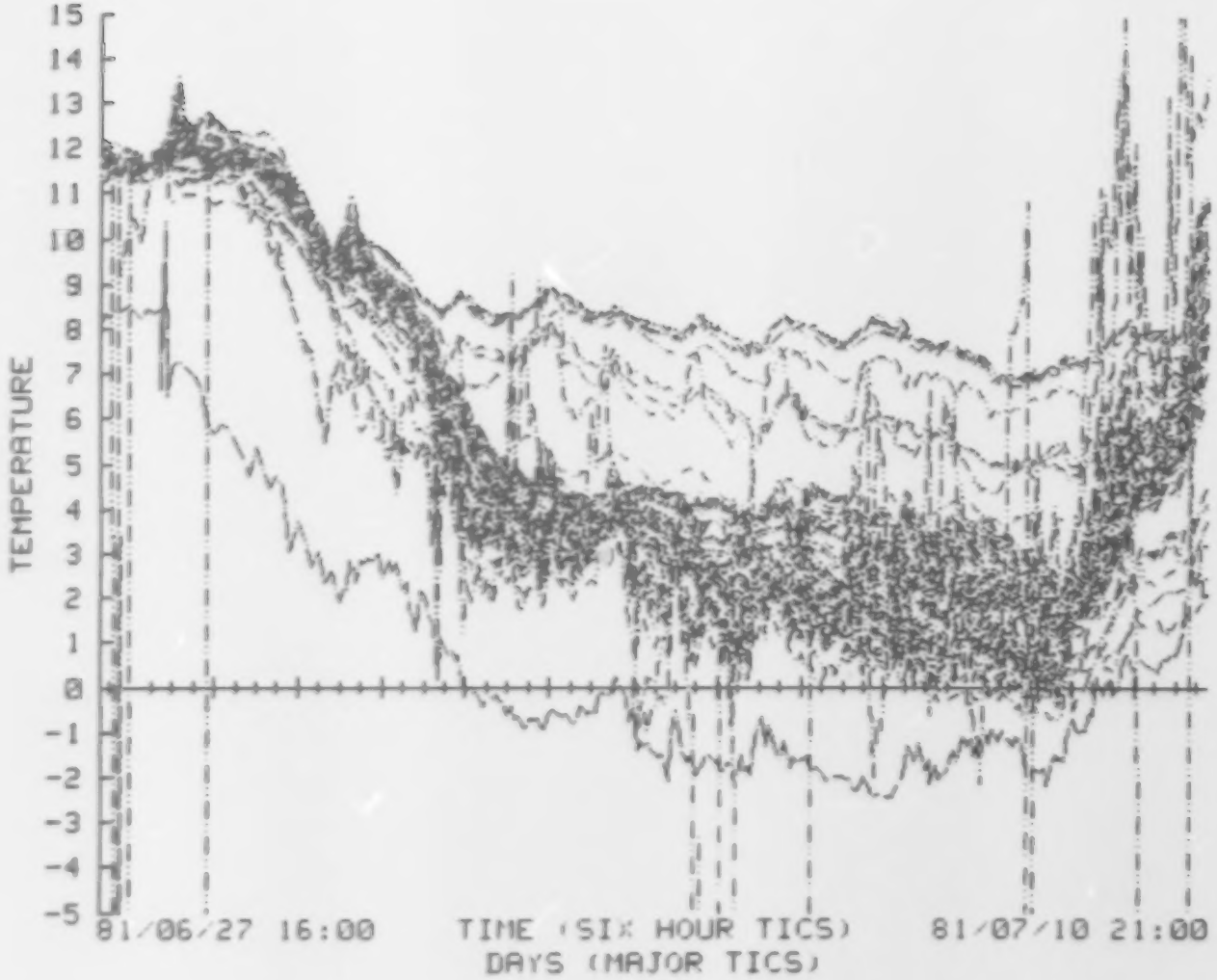

Figure 79

PLATE TEMPERATURE LEVELS

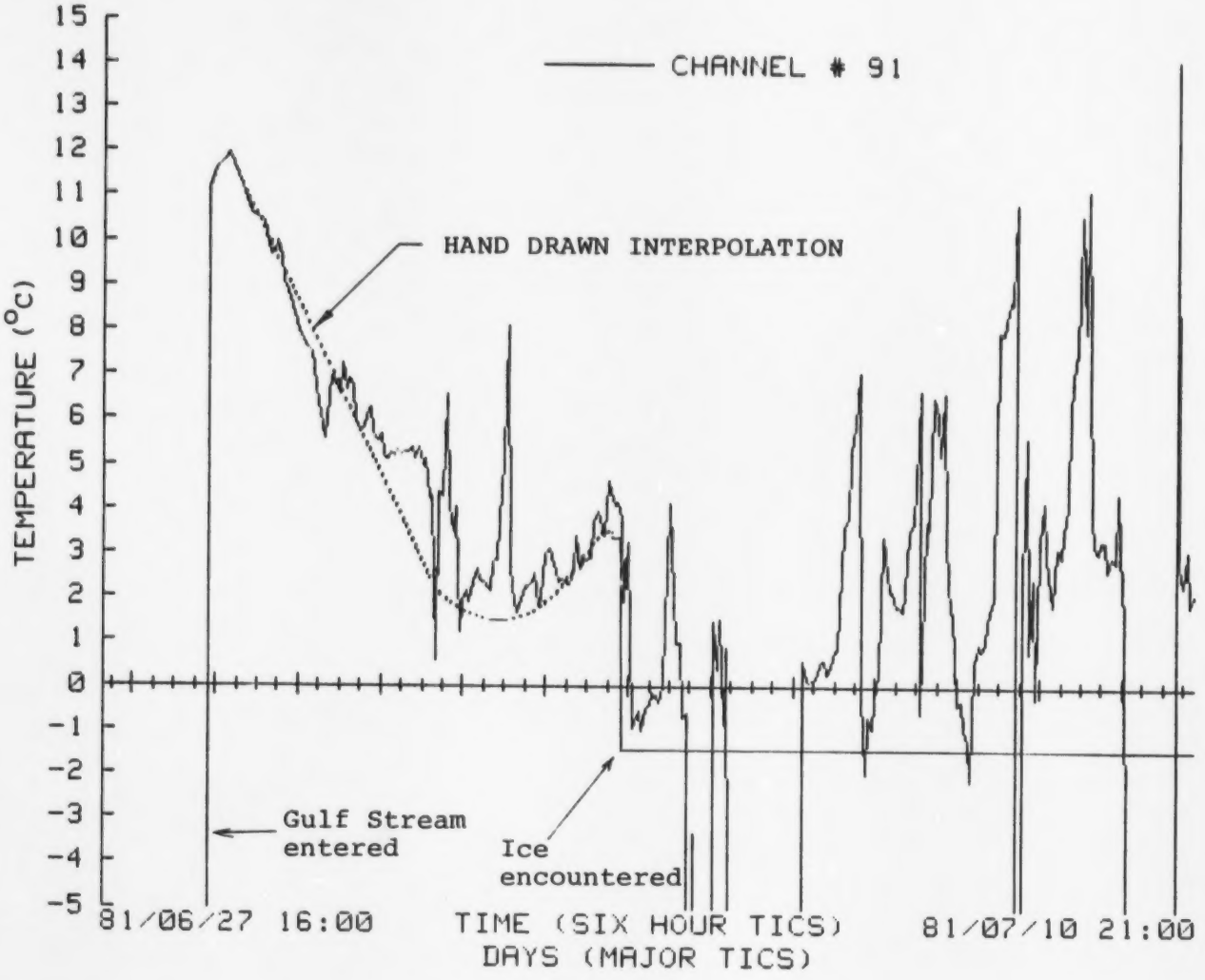

Figure 80

SEA WATER TEMPERATURE

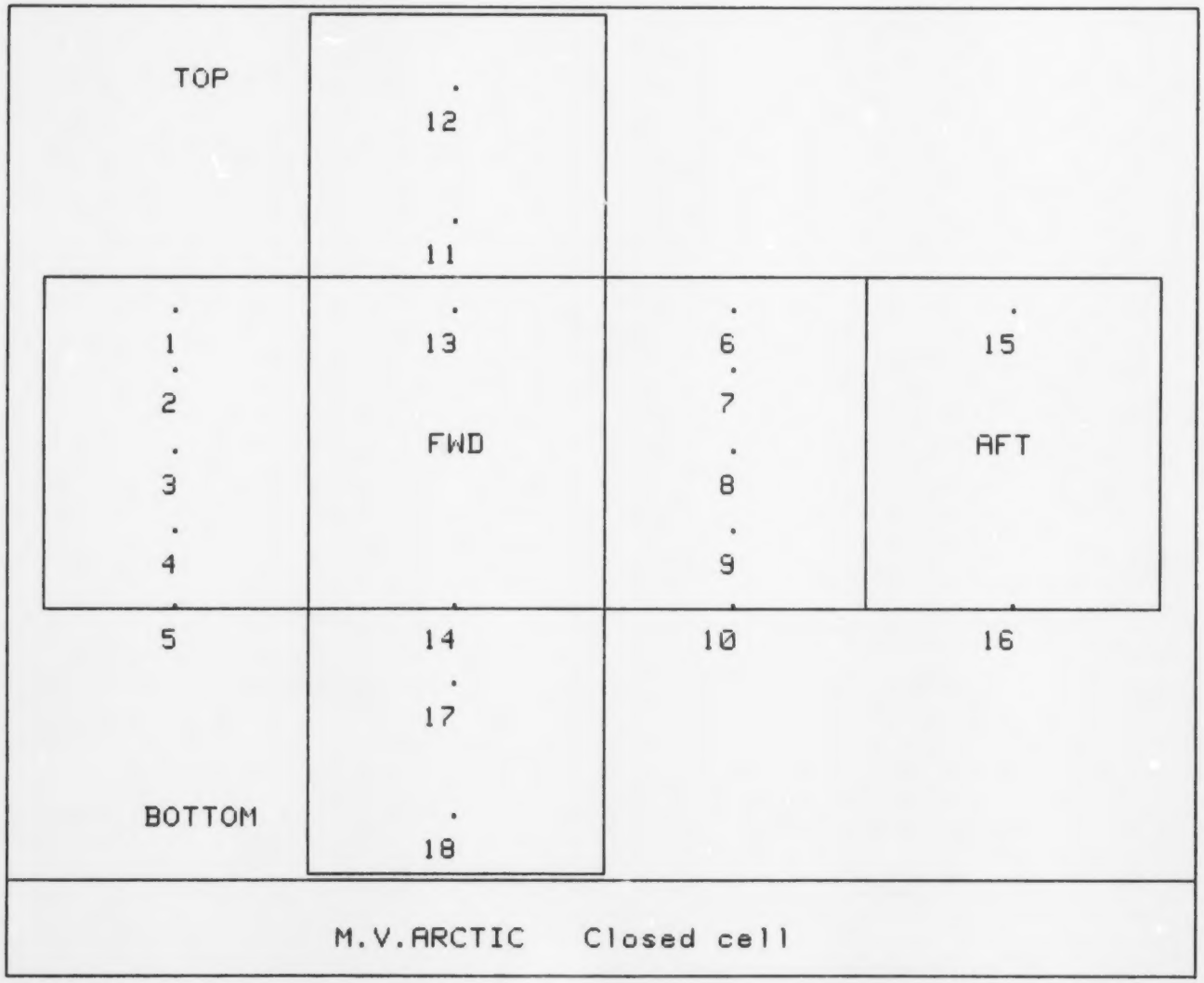

Figure 81

THERMISTOR PLACEMENT FOR THE CLOSED CELL

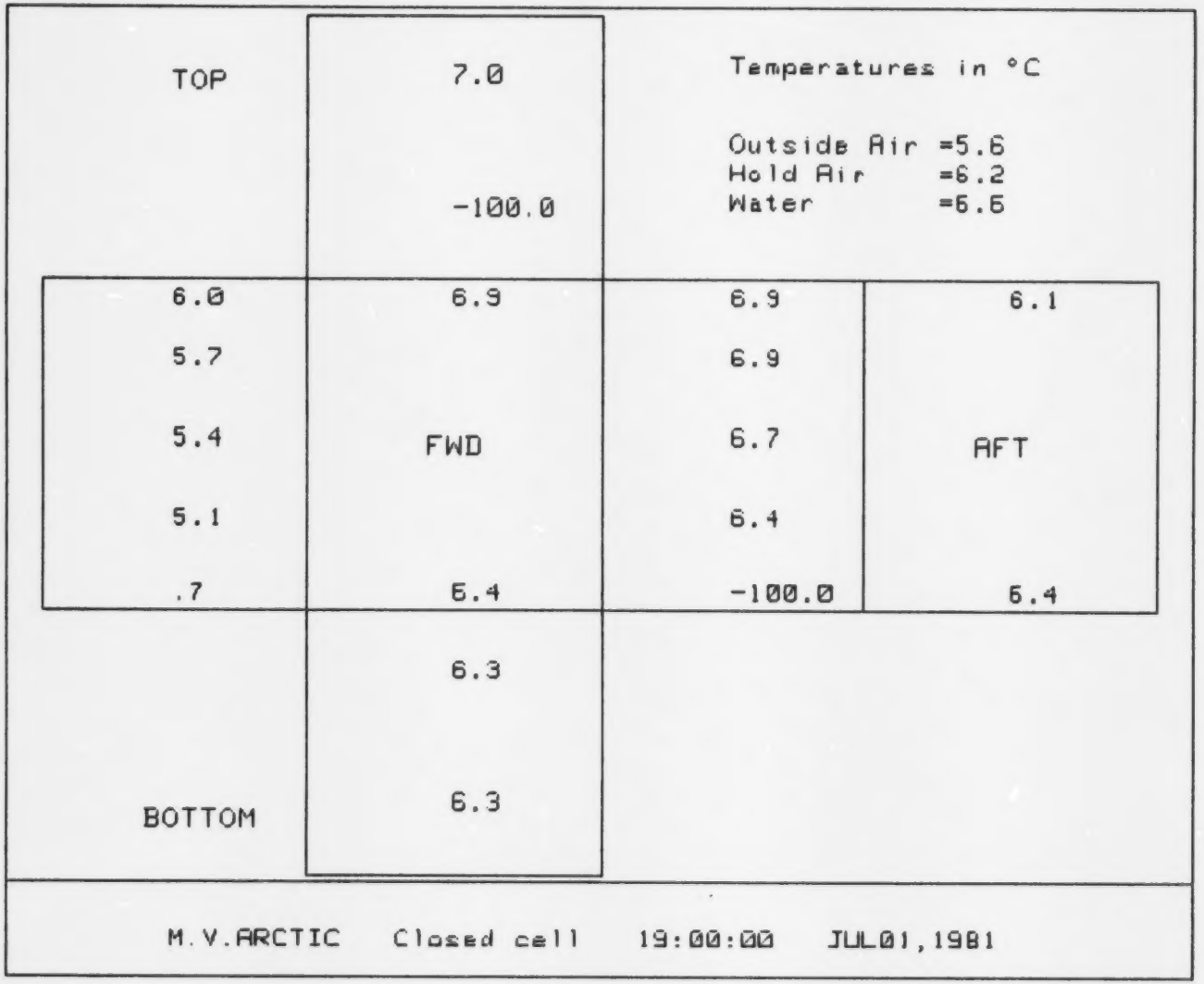
TOP
7.0
-100.0
Temperatures in °C
Outside Air =5.6
Hold Air =6.2
Water =6.6
6.0
5.7
5.4
5.1
.7
6.9
FWD
6.4
6.9
6.9
6.7
6.4
-100.0
6.1
AFT
6.4
6.3
6.3
BOTTOM
M.V.ARCTIC Closed cell 19:00:00 JUL01,1981

Figure 82

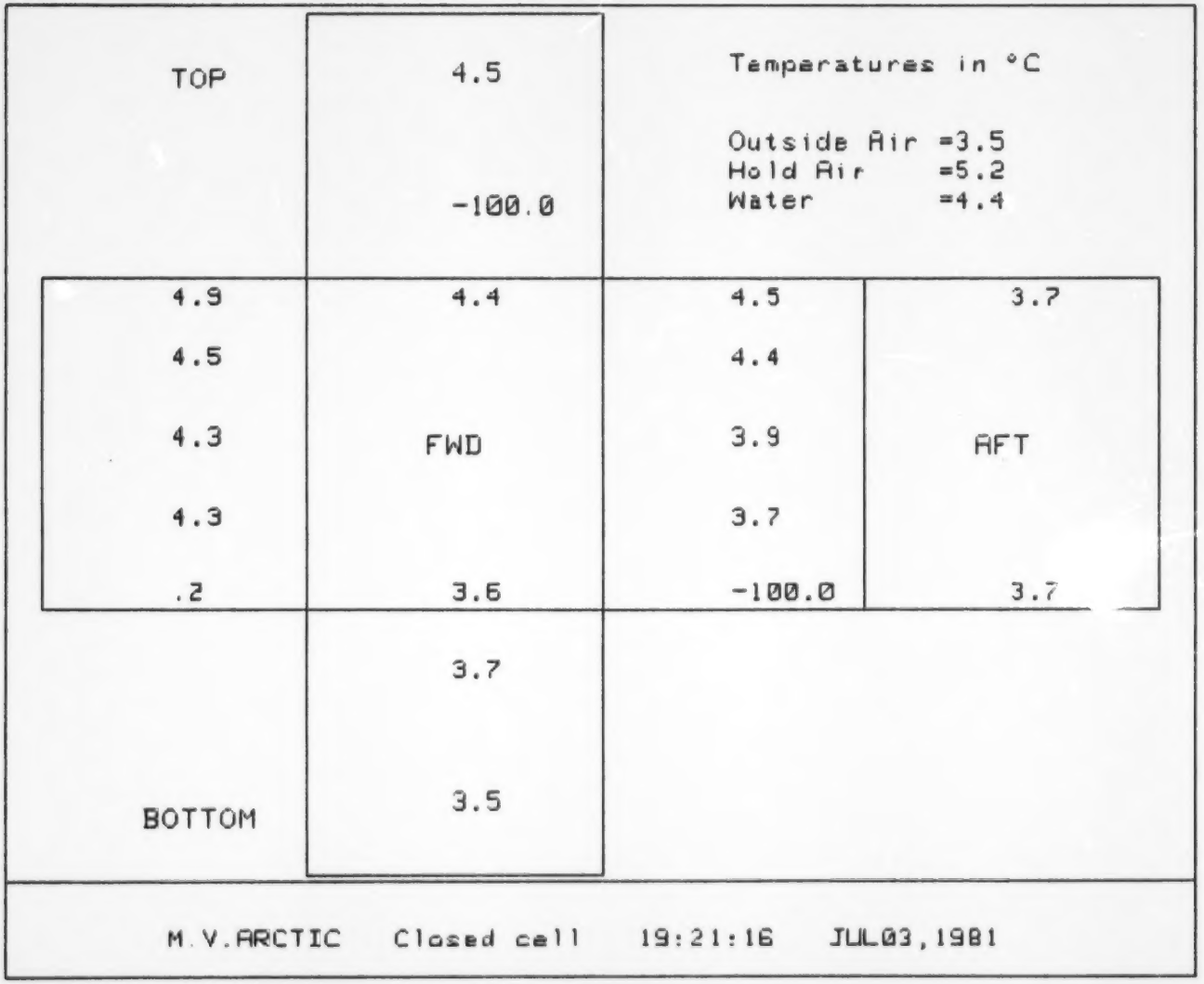
TOP
4.5
-100.0
Temperatures in °C
Outside Air =3.5
Hold Air =5.2
Water =4.4
4.9
4.5
4.3
4.3
.2
4.4
FWD
3.6
4.5
4.4
3.9
3.7
-100.0
3.7
AFT
3.7
BOTTOM
3.5
M.V.ARCTIC Closed cell 19:21:16 JUL03,1981

Figure 83

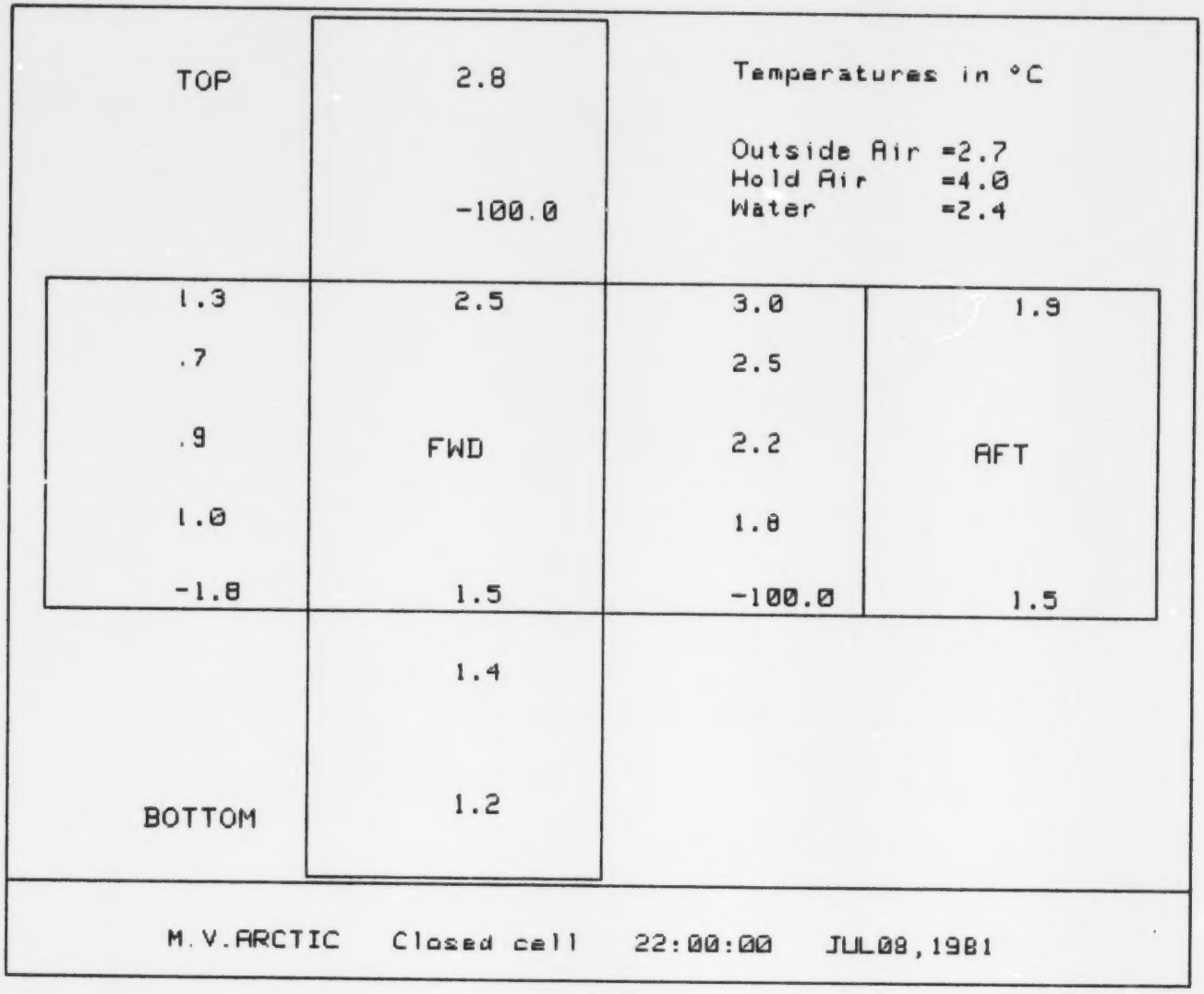
TOP
2.8
-100.0
Temperatures in °C
Outside Air =2.7
Hold Air =4.0
Water =2.4
1.3
.7
.9
1.0
-1.8
2.5
FWD
1.5
3.0
2.5
2.2
1.8
-100.0
1.9
AFT
1.5
1.4
1.2
BOTTOM
M.V.ARCTIC Closed cell 22:00:00 JUL08,1981

Figure 84

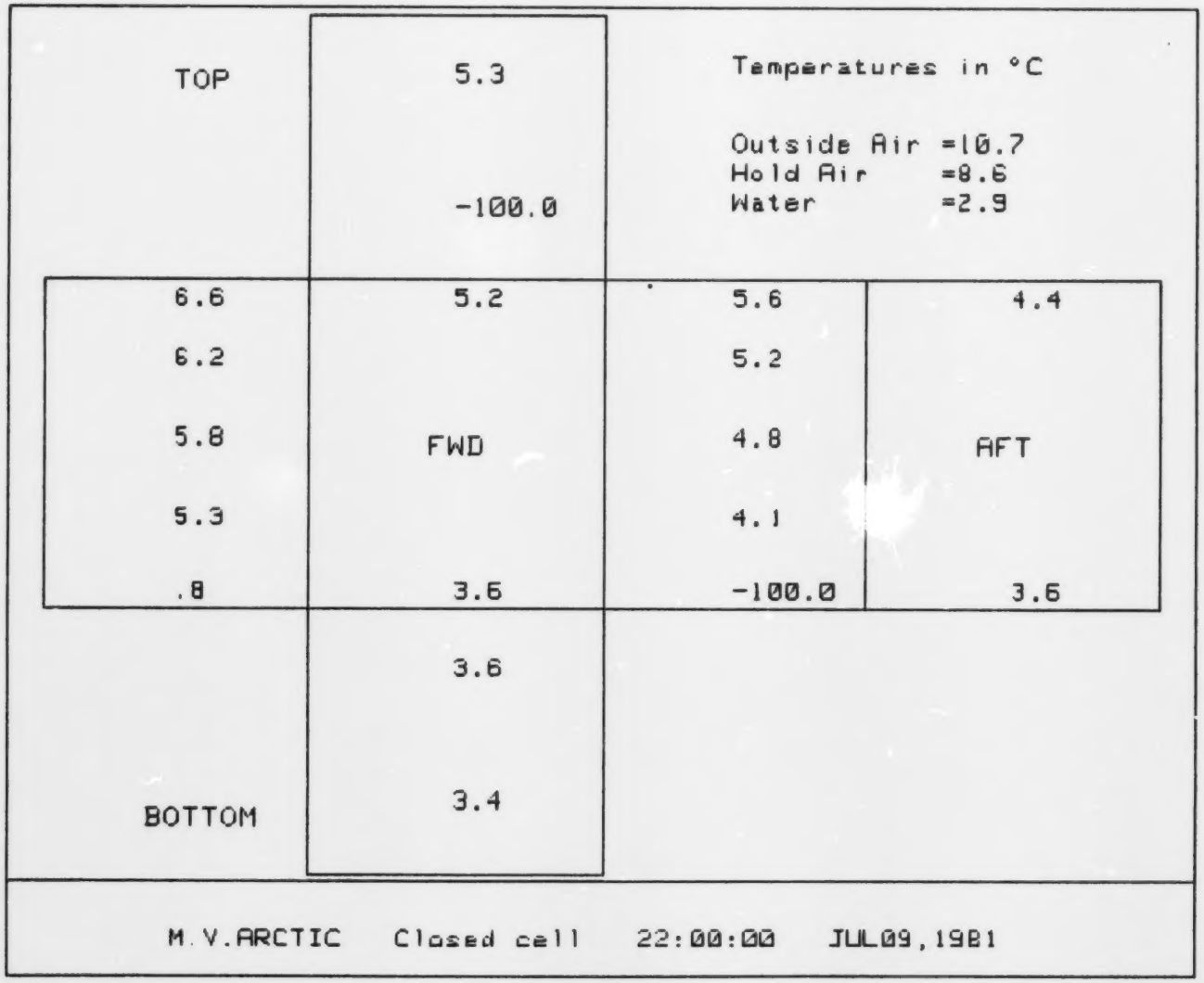
TOP
5.3
-100.0
Temperatures in °C
Outside Air =10.7
Hold Air =8.6
Water =2.9
6.6
6.2
5.8
5.3
.8
5.2
FWD
3.6
5.6
5.2
4.8
4.1
-100.0
4.4
AFT
3.6
3.6
3.4
BOTTOM
M.V.ARCTIC Closed cell 22:00:00 JUL09,1981

Figure 85

observations are made.

a) Thermistors 10 and 11 are not working.
b) Thermistor 5 is reading consistently low.
c) The temperature varies from the top to the bottom of the cell with a $1^{o}C$ difference. The hotter plate being on top, as expected.
d) During the major part of the voyage, the plate on the inside is warmer than the outside by up to $2^{o}C$.
e) The status of d) reversed when the ballast was dumped and the cell rose above the waterline and solar heating occurred on the outside plate.
f) The average temperature can be identified by reference to gauges 12, 18, 8 and 3.

(It is well to remember that the maximum density of water occurs at about $4^{o}C$, and that natural convection is limited in water near this temperature).

3) A time history plot of the four thermistors 12, 18, 8 and 3 of the closed cell is shown in Figure 86. This clearly shows how the outside plate experiences the widest temperature excursions while the inside plate is generally slower to react. The top plate consistently maintains a higher temperature.

4) A number of thermistors was located in positions that would monitor the ballast water temperatures. Figures 87 - 88 show these readings compared to the outside ambient air temperature. Channel 21 is mounted on deck above the cells being monitored and illustrates a cyclic heating and cooling due to day to night temperature swings. Channel 19, which corresponds to a position some 12 inches below the top plate and measures the ballast water temperature, registers consistently higher than the surrounding plates during the major part of the voyage. This appears to be an unexplainable anomaly as the ballast water temperature above this cell (channel #20) is lower. If, by chance, the channels had been reversed such that 19 was the one on top, 20 in the middle and 84 below, then the temperatures would be in a decreasing progression which would be more understandable. This is quite likely to have occurred.

   As can be seen from Figure 76, the location of thermistor 20 is above the sea level and hence would benefit from the higher day time radiant heating from the sun. Channel #86 does not appear on the plot in Figure 88 as it was not functioning.

5) The temperatures in the open cell reflect very closely those measured in the closed cell. The open cell

results for the same four time periods are given in Figures 89 - 93.

6) The thermistors mounted above and below the main cell are numbered in Figure 94 and the temperatures for the same time period are given in Figures 95 - 98. From these temperature distributions, it can be clearly seen that a differential exists between the cells above the sea level and those below. This differential reached a maximum of 5°C just prior to the dumping of the ballast. It is interesting to note that the steel plates and the ballast water above sea level maintain a temperature above the outside air temperature. From the diagram, Fig. 92, dated 22:00 hours, July 8th, the temperatures on the plate next to the hold are much closer to the ballast water temperature than the air temperature of the hold. It appears that the ballast water temperature largely controls the inside plate temperature.

7) Gauges 22 - 26 were not mounted on any plate surface but due to a lack of length in the available wiring were simply laid inside the first cell beneath the deck. The temperatures registered by all these thermistors were consistently above the values in the monitored cell and followed closely the values recorded on channel 19. This confirmed the ballast water temperature in the upper cell was above the values in the area below the sea surface.

8) Finally the temperature transient of the hold air is measured via thermistor #90 and is shown in Figure 99. The hold air is 2 - 3°C above the mean external air temperature and is relatively constant during the period of the voyage when the night to day mean air temperature is itself constant. Its fluctuations are far less than those of the external air temperature, indicating a good seal on the hatch cover, leading only to heat transfer through the hull rather than by mass flow.

6.5 Conclusions

The results reported were obtained for the following set of conditions.

a) Ballast tanks full to deck level, (until last day).
b) Predominately above zero ambient air conditions.
c) A sea temperature falling to just below $0^{o}C$.
d) An empty hold opposite the measured cell.

The following conclusions are drawn from a review of the recorded temperatures.

1) A stable temperature gradient is set up in the ballast water such that the upper levels are considerably warmer than the lower. This condition is unlikely to occur when the ambient air temperature is considerably colder than the sea temperature.

2) The outside plate temperature was maintained at most a couple of degrees above the sea temperature as the vessel sailed through arctic waters. The temperature of the ballast water in the cell just below the sea level, is generally slightly above the outside plate temperature. Hence it is concluded that the ballast water follows closely the falling temperature of the sea. In other words, the thermal resistance of the hull plates and surface coefficients is so small that only a small temperature difference can be maintained.

3) The divergence in the temperature of the ballast water in the upper cell that occurs after day 4 is assumed to have been caused by daytime heating of the upper deck plates.

4) The air temperature measured in the hold remains $4^{o}C$ above the sea temperature and $2^{o}C$ above the average outside air temperature.

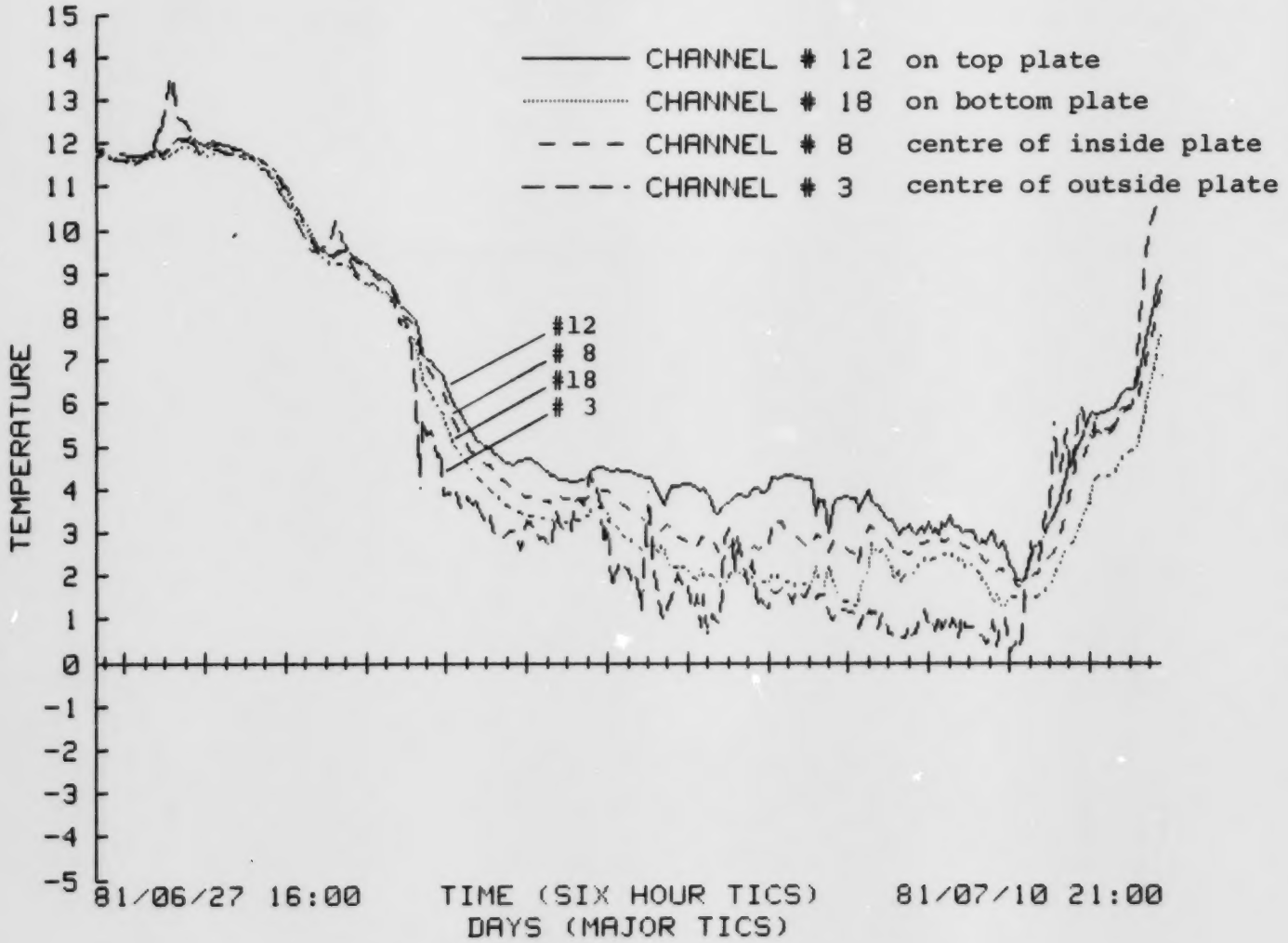

Figure 86

TYPICAL CLOSED CELL PLATE TEMPERATURES

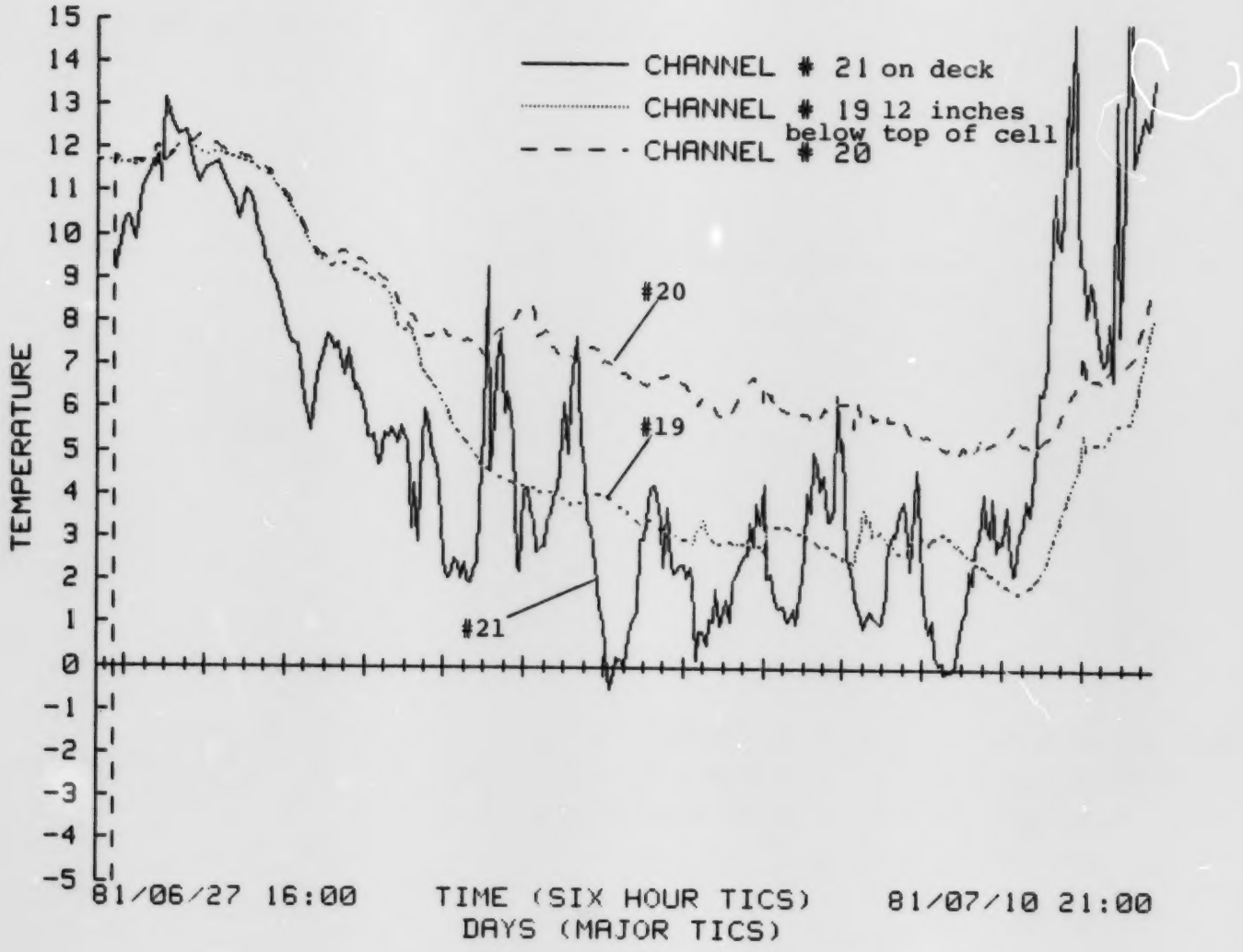

Figure 87

AIR AND BALLAST WATER TEMPERATURES

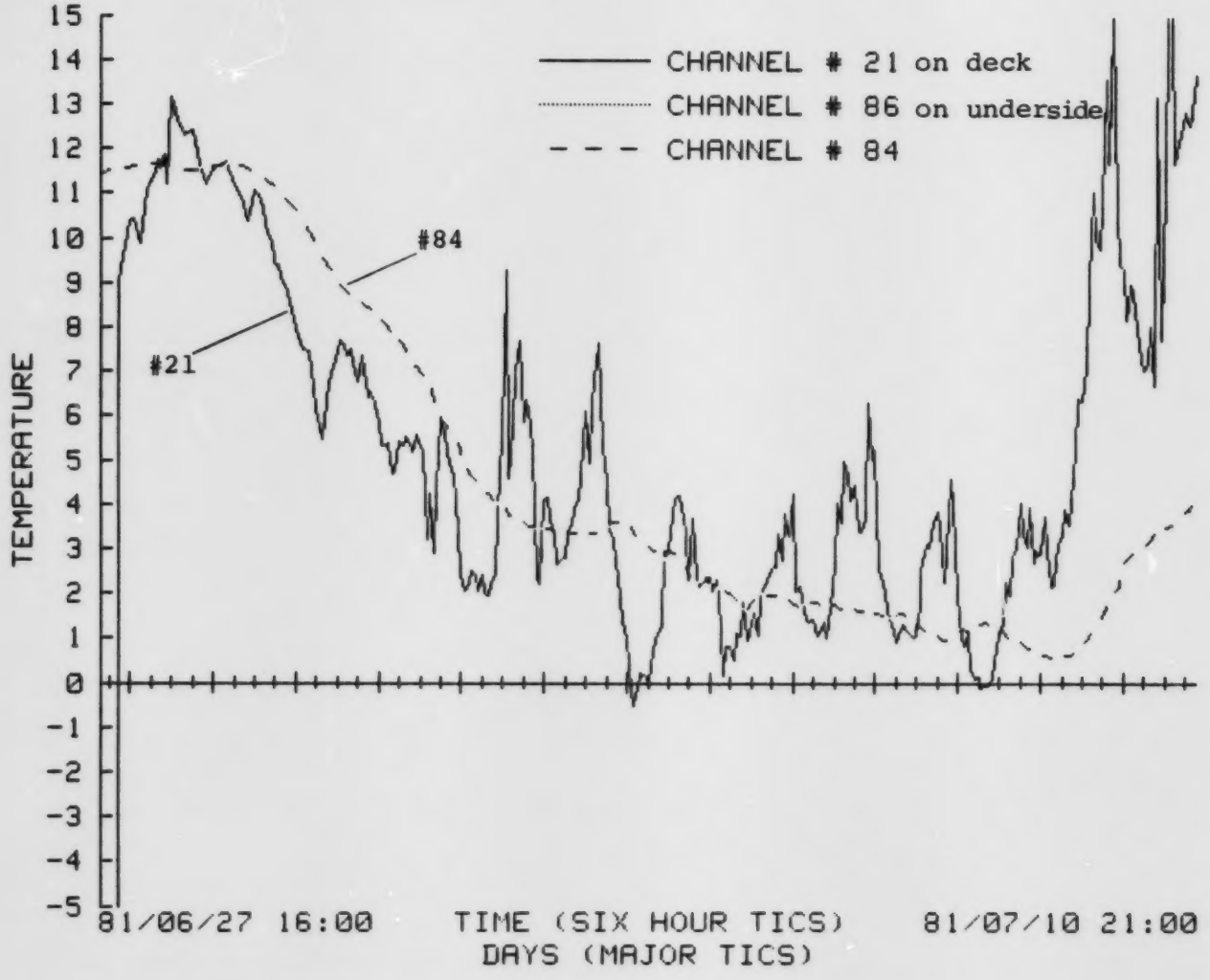

Figure 88

AIR AND BALLAST WATER TEMPERATURES

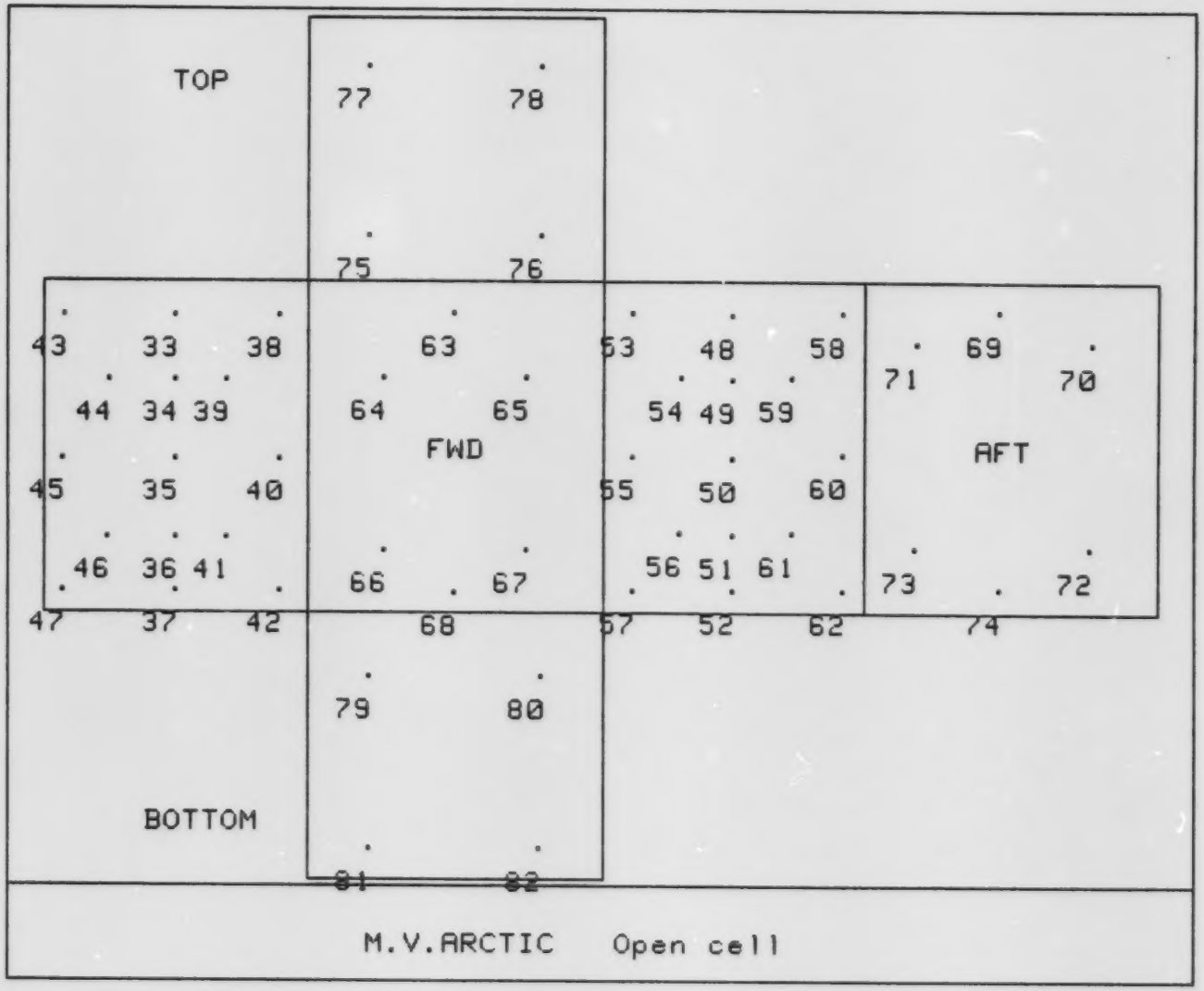

Figure 89

THERMISTOR PLACEMENT FOR THE OPEN CELL

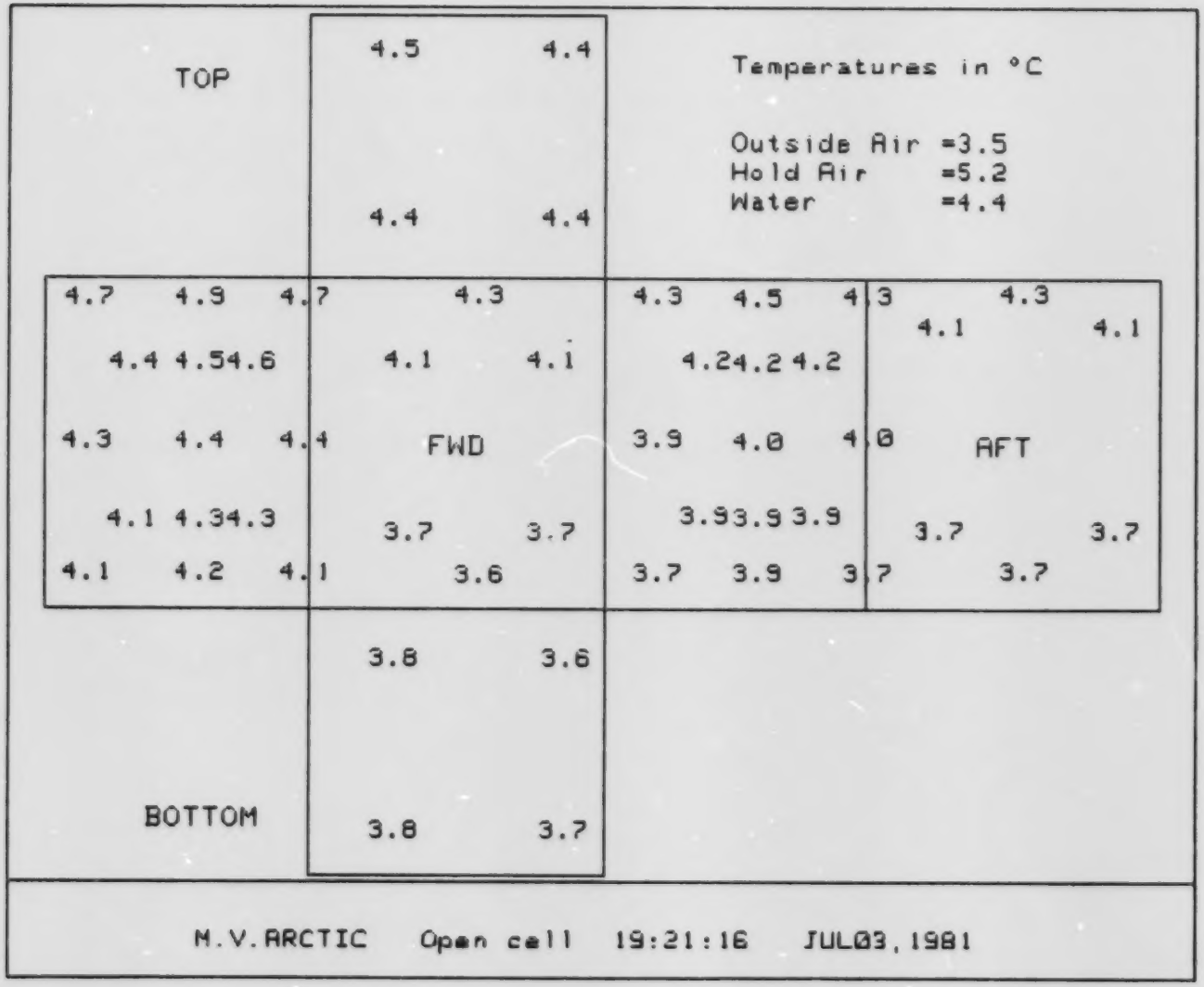
TOP
4.5 4.4
4.4 4.4
Temperatures in °C
Outside Air =3.5
Hold Air =5.2
Water =4.4
4.7 4.9 4.7 4.3
4.4 4.5 4.6 4.1 4.1
4.3 4.4 4.4 FWD
4.1 4.3 4.3 3.7 3.7
4.1 4.2 4.1 3.6
4.3 4.5 4.3
4.2 4.2 4.2
3.9 4.0 4.0 AFT
3.9 3.9 3.9
3.7 3.9 3.7
4.3 4.3
4.1 4.1
3.7 3.7
3.7 3.7
3.8 3.6
BOTTOM
3.8 3.7
M.V.ARCTIC Open cell 19:21:16 JUL03,1981

Figure 90

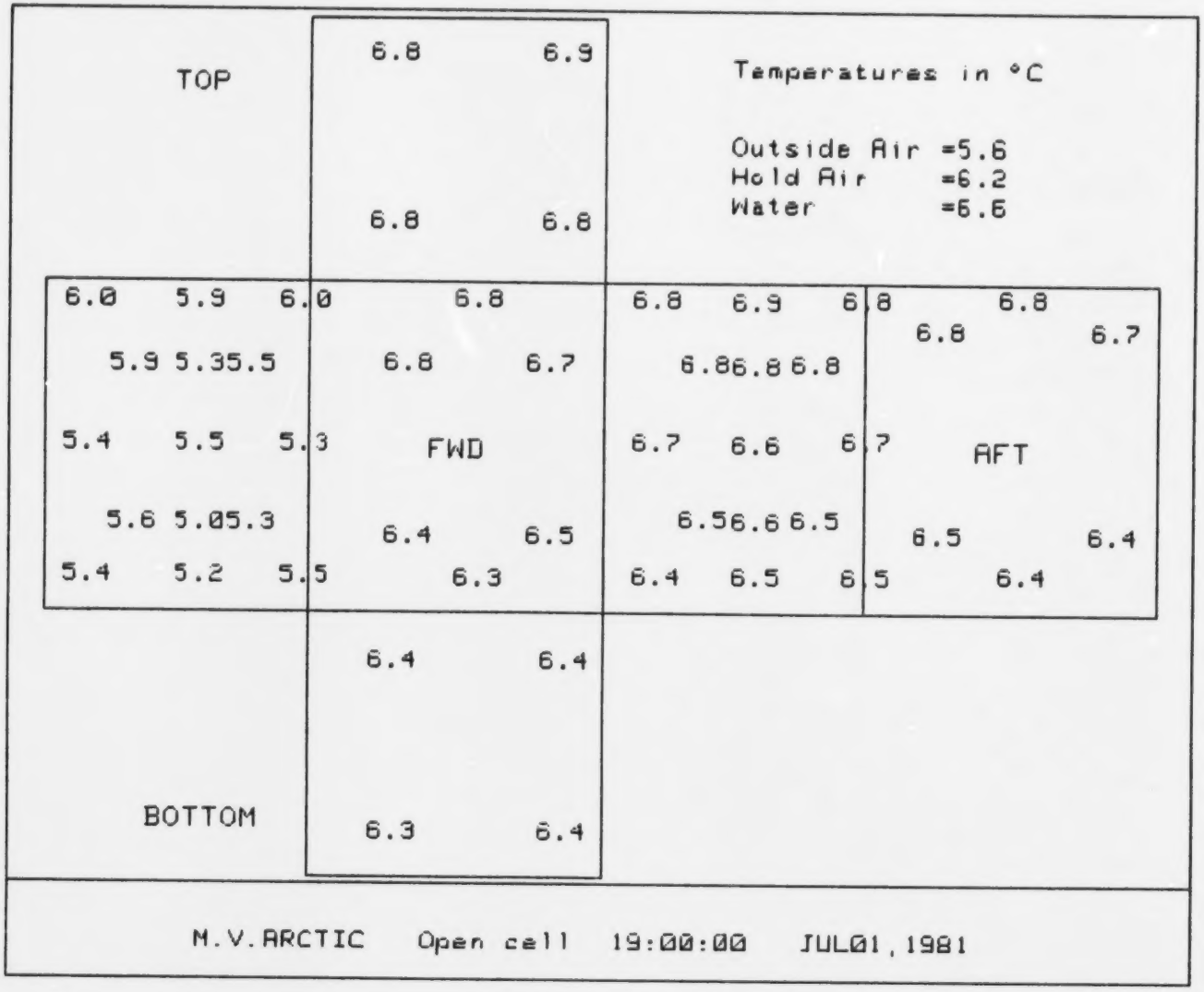
TOP
6.8 6.9
6.8 6.8
Temperatures in °C
Outside Air =5.6
Hold Air =6.2
Water =6.6
6.0 5.9 6.0
5.9 5.3 5.5
5.4 5.5 5.3
5.6 5.0 5.3
5.4 5.2 5.5
6.8
6.8 6.7
FWD
6.4 6.5
6.3
6.8 6.9 6.8
6.8 6.8 6.8
6.7 6.6 6.7
6.5 6.6 6.5
6.4 6.5 6.5
6.8 6.8
6.8 6.7
AFT
6.5 6.4
6.4
6.4 6.4
BOTTOM
6.3 6.4
M.V.ARCTIC Open cell 19:00:00 JUL01,1981

Figure 91

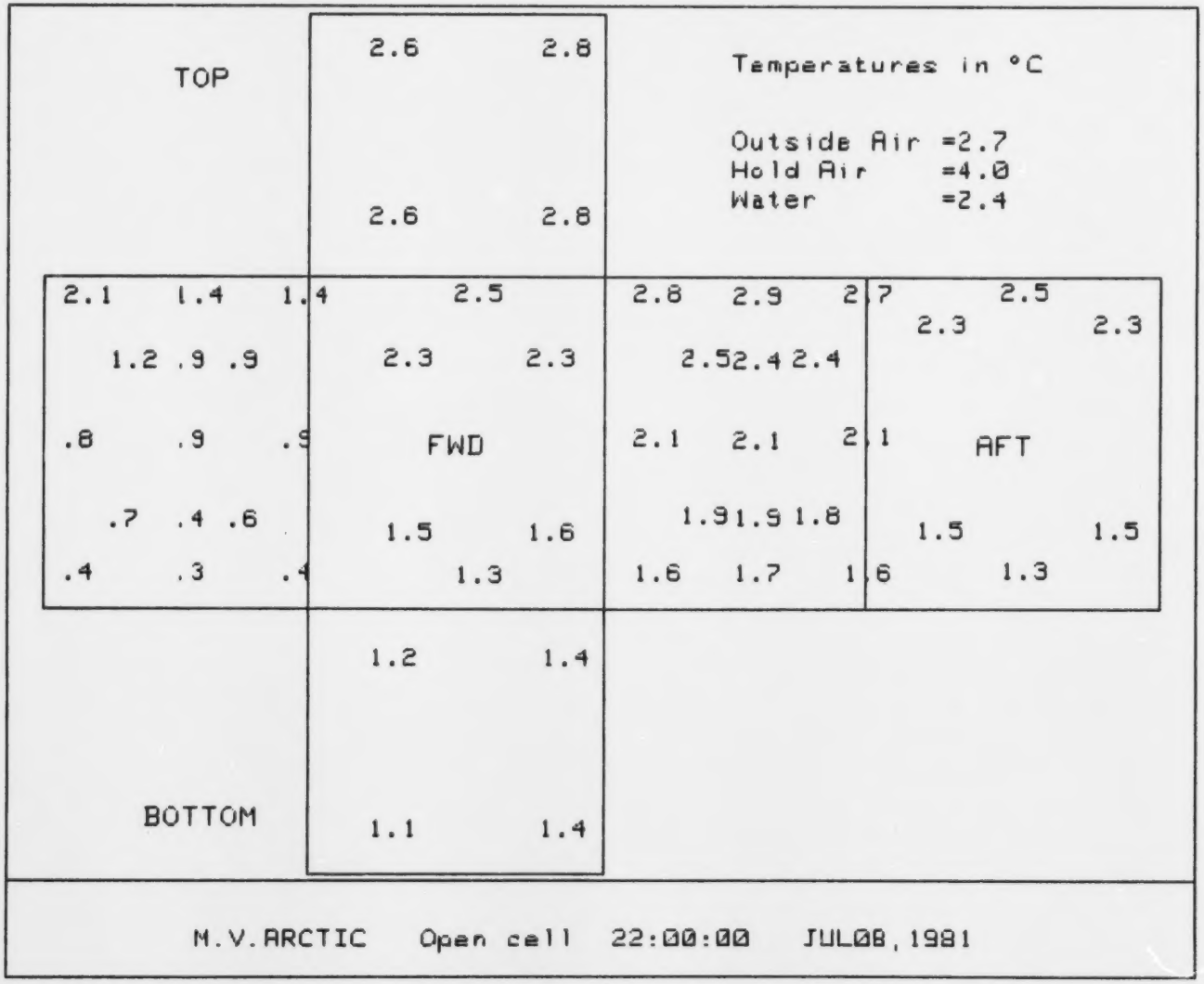
TOP
2.6 2.8
2.6 2.8
Temperatures in °C
Outside Air =2.7
Hold Air =4.0
Water =2.4
2.1 1.4 1.4
1.2 .9 .9
.8 .9 .9
.7 .4 .6
.4 .3 .4
2.5
2.3 2.3
FWD
1.5 1.6
1.3
2.8 2.9 2.7
2.5 2.4 2.4
2.1 2.1 2.1
1.9 1.9 1.8
1.6 1.7 1.6
2.5
2.3 2.3
AFT
1.5 1.5
1.3
1.2 1.4
BOTTOM
1.1 1.4
M.V.ARCTIC Open cell 22:00:00 JUL08,1981

Figure 92

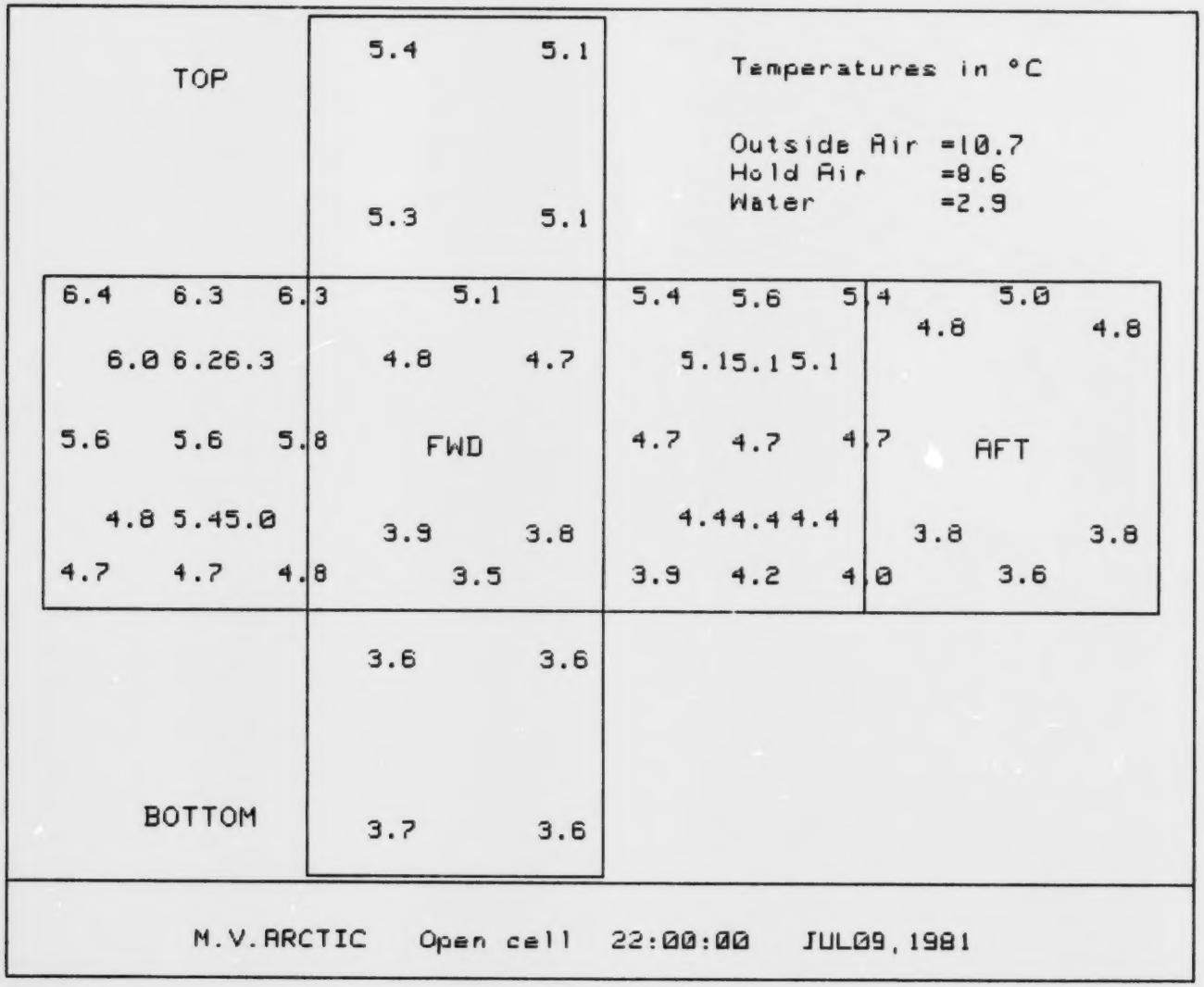
TOP
5.4 5.1
5.3 5.1
Temperatures in °C
Outside Air =10.7
Hold Air =8.6
Water =2.9
6.4 6.3 6.3 5.1
6.0 6.2 6.3 4.8 4.7
5.6 5.6 5.8 FWD
4.8 5.4 5.0 3.9 3.8
4.7 4.7 4.8 3.5
5.4 5.6 5.4 5.0
5.1 5.1 5.1 4.8 4.8
4.7 4.7 4.7 AFT
4.4 4.4 4.4 3.8 3.8
3.9 4.2 4.0 3.6
3.6 3.6
BOTTOM
3.7 3.6
M.V.ARCTIC Open cell 22:00:00 JUL09,1981

Figure 93

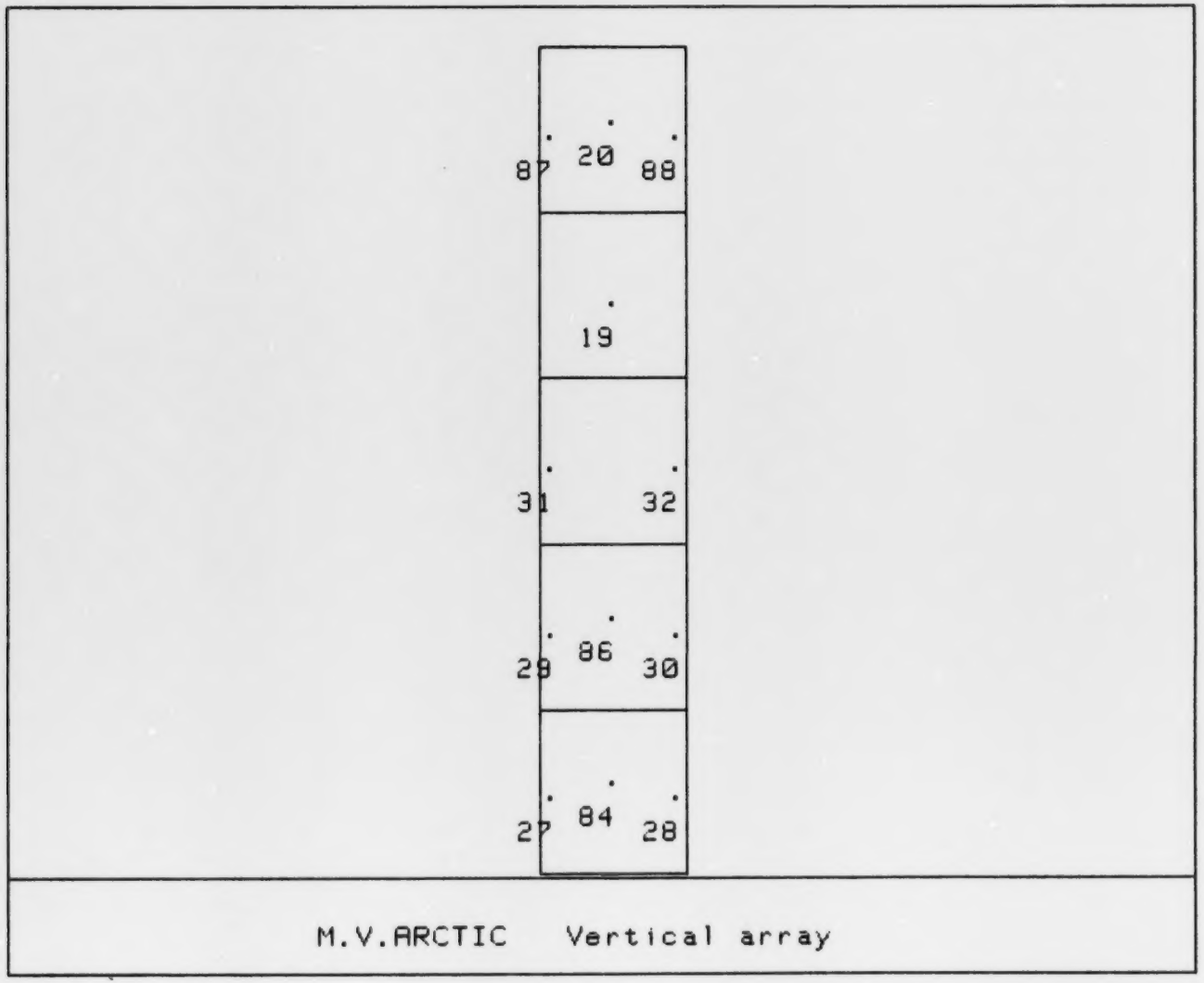

Figure 94

THERMISTOR PLACEMENT VERTICALLY THROUGH THE HULL

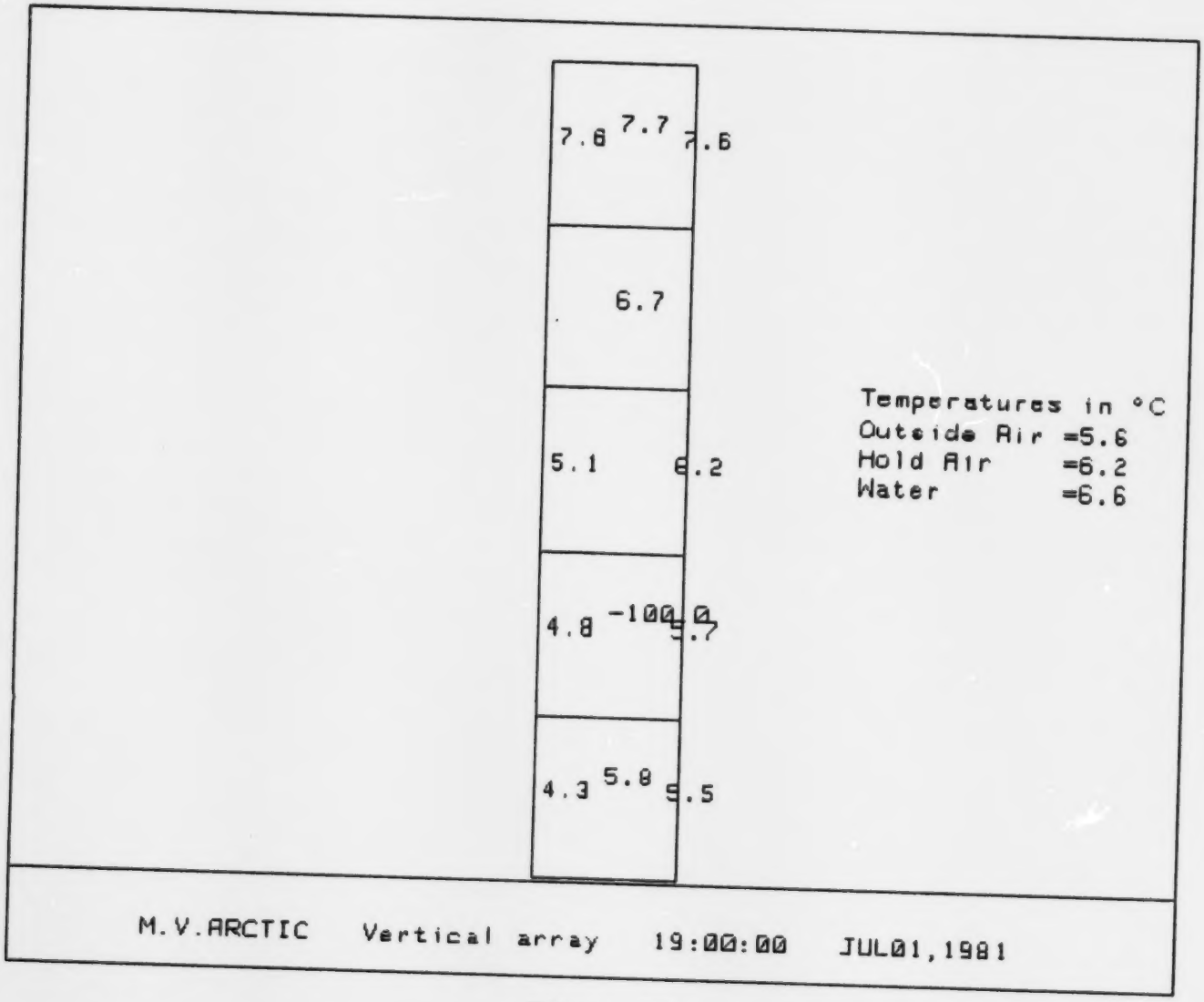
7.6
7.7
7.6
6.7
5.1
6.2
4.8
-100.0
5.7
4.3
5.8
5.5
Temperatures in °C
Outside Air =5.6
Hold Air =6.2
Water =6.6
M.V.ARCTIC Vertical array 19:00:00 JUL01,1981

Figure 95

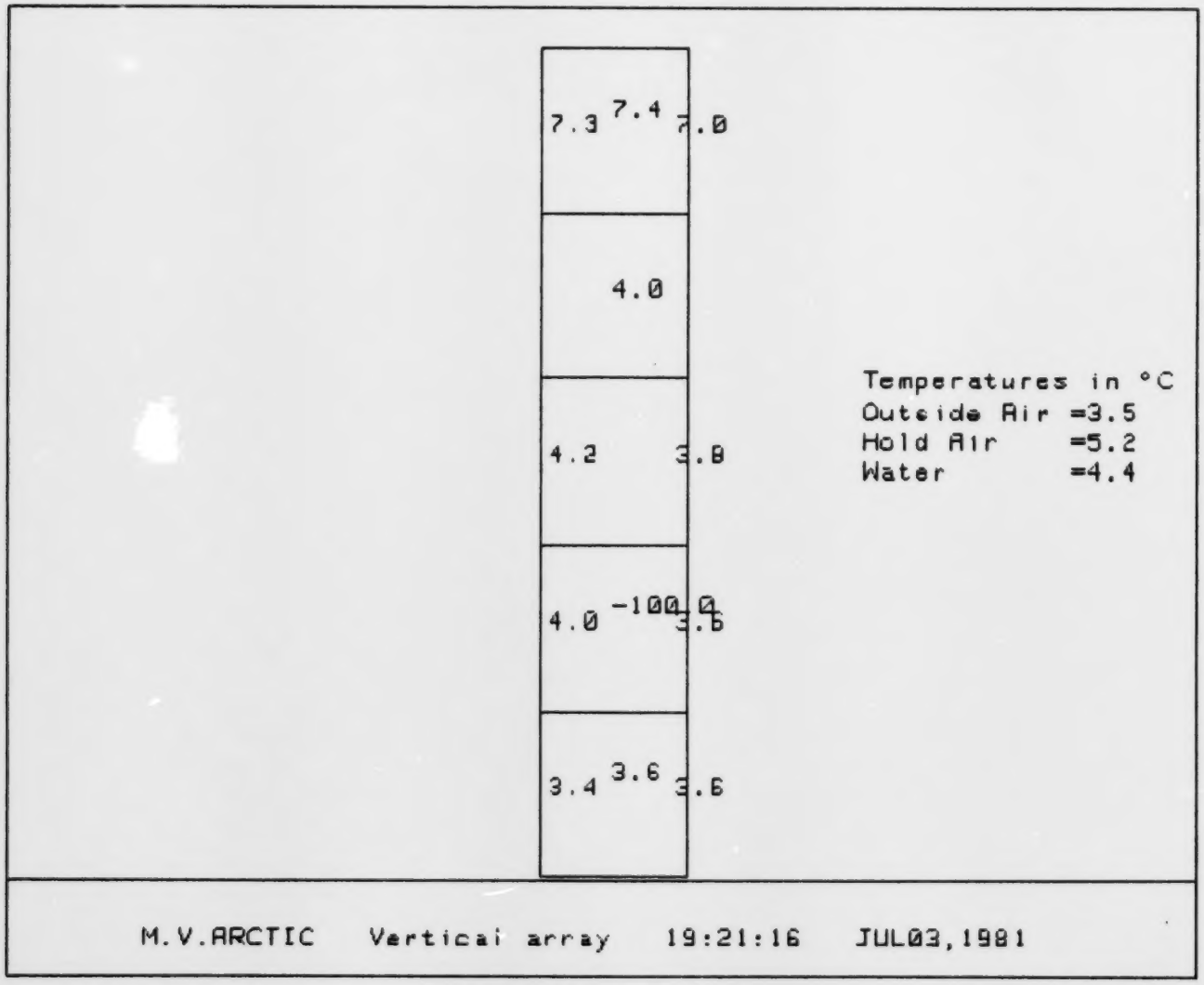
7.3
7.4
7.0
4.0
4.2
3.8
4.0
-100.0
3.6
3.4
3.6
3.6
Temperatures in °C
Outside Air =3.5
Hold Air =5.2
Water =4.4
M.V.ARCTIC Vertical array 19:21:16 JUL03,1981

Figure 96

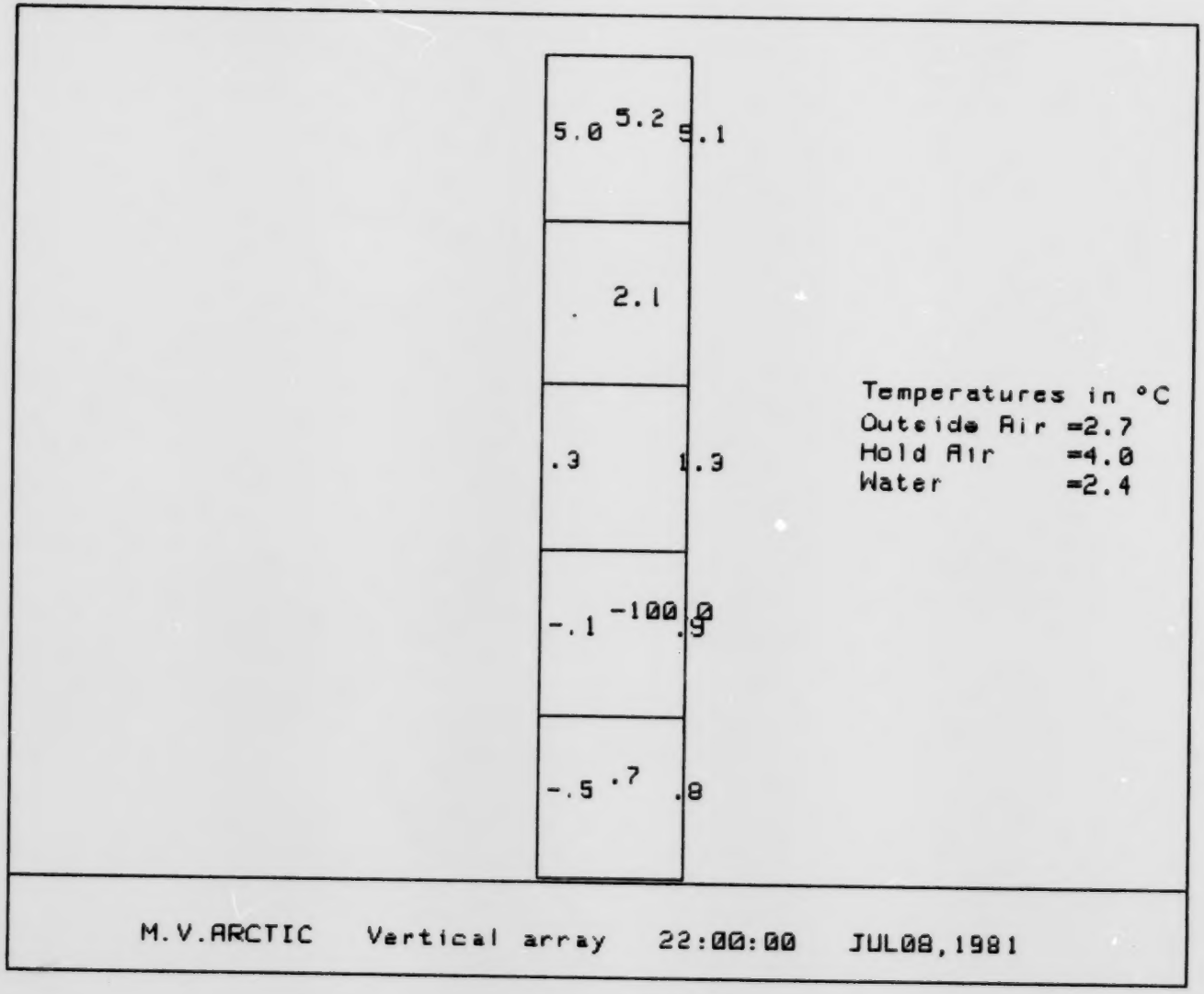
5.0
5.2
5.1
2.1
.3
1.3
-.1
-100.0
.9
-.5
.7
.8
Temperatures in °C
Outside Air =2.7
Hold Air =4.0
Water =2.4
M.V.ARCTIC Vertical array 22:00:00 JUL08,1981

Figure 97

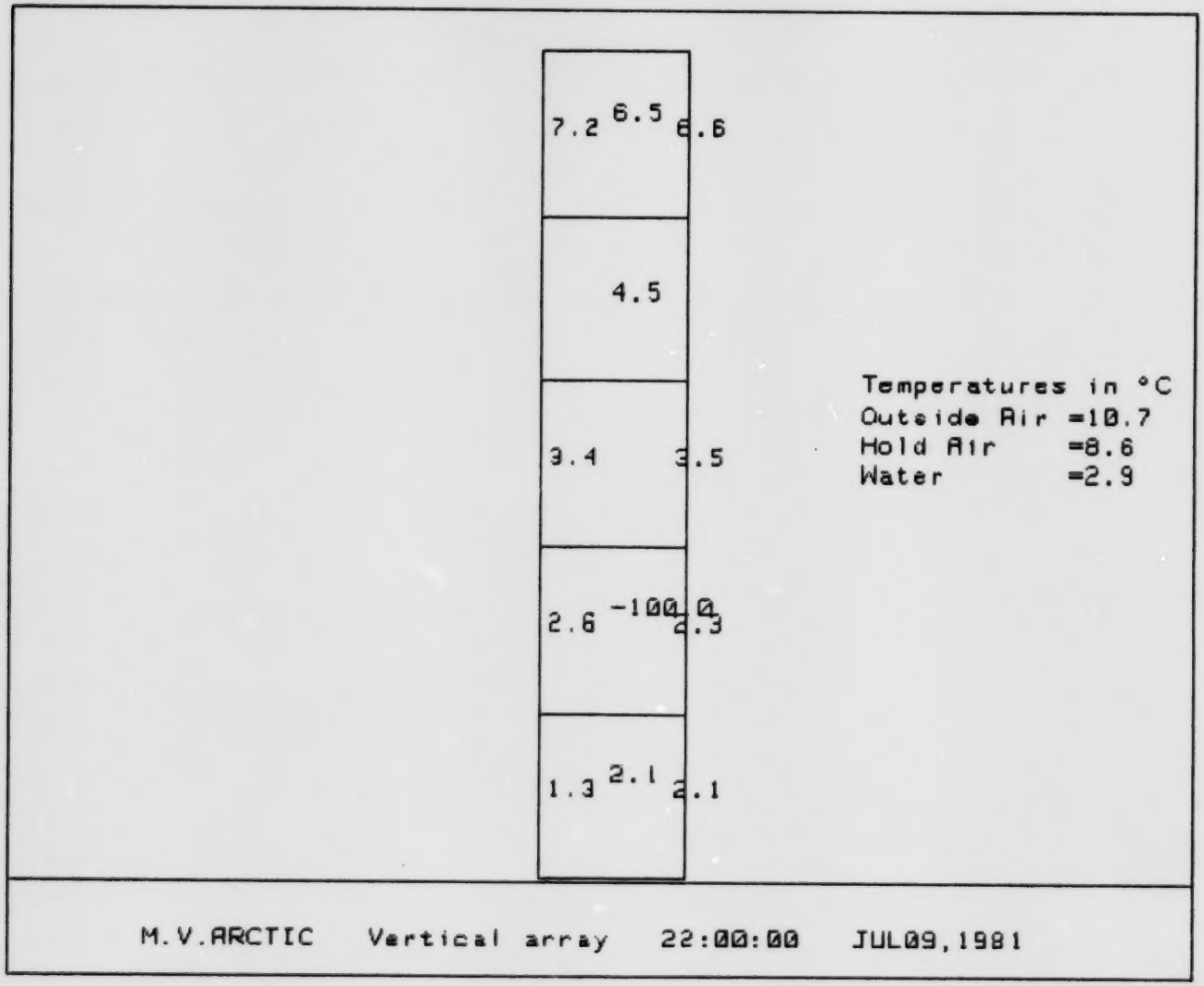
7.2
6.5
6.6
4.5
3.4
3.5
2.6
-100.0
2.3
1.3
2.1
2.1
Temperatures in °C
Outside Air =10.7
Hold Air =8.6
Water =2.9
M.V.ARCTIC Vertical array 22:00:00 JUL09,1981

Figure 98

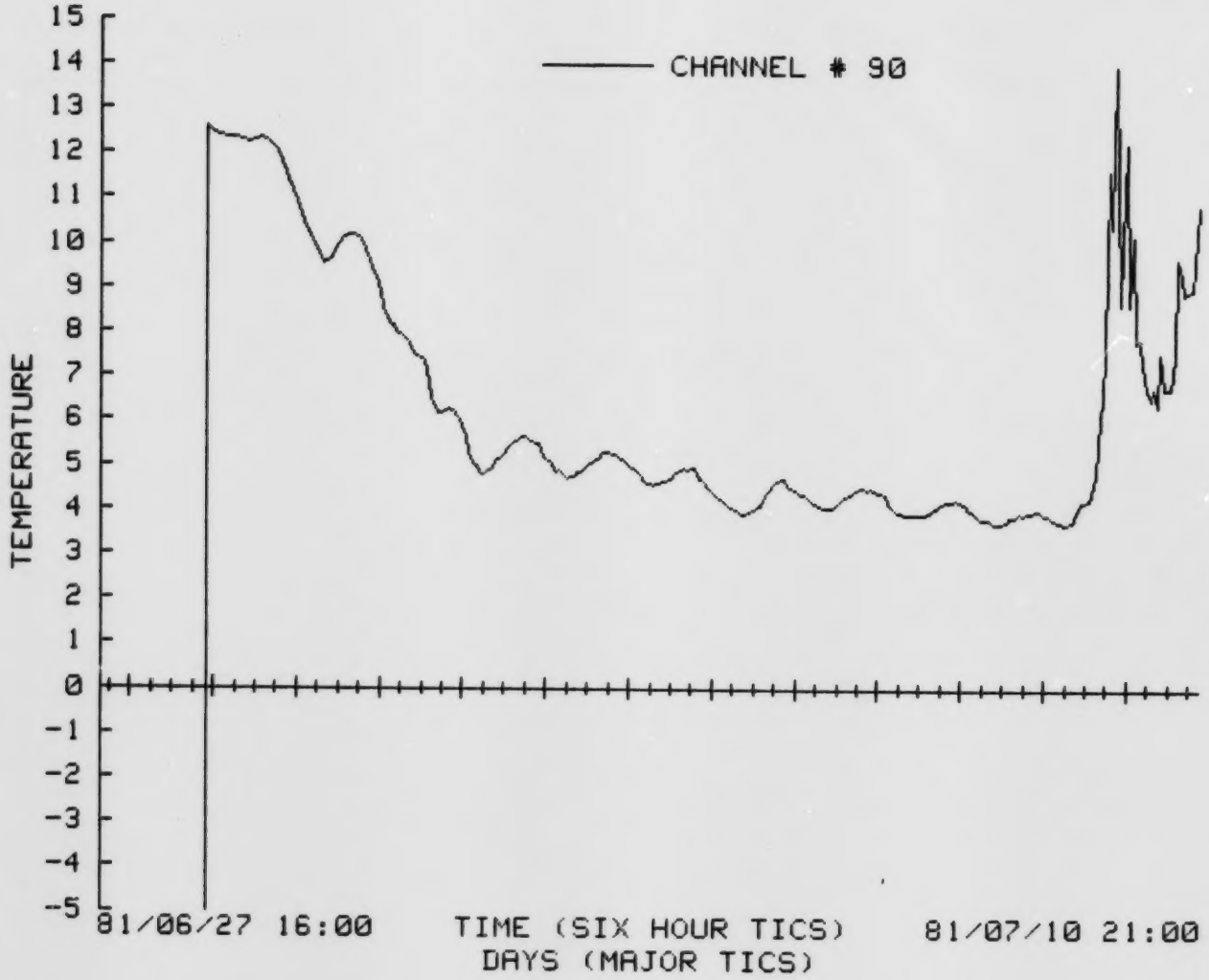

Figure 99

HOLD TEMPERATURE TRANSIENT

7. GENERAL DISCUSSIONS AND RECOMMENDATIONS

7.1 General Discussion

The work reported here centred around the development of analytical tools for the evaluation of heat flow and temperature predictions in ship's hulls. Because of the complex nature of the problems, both geometrically and with respect to the heat flow mechanisms, computer based numerical methods have been used. The primary goal was to develop a general purpose tool suitable for the analysis of any hull configuration. The finite element method was chosen as the basis for the program because of its ability to conveniently handle general structural shapes. An existing finite element program, ASASHEAT, was taken in preference to developing a new code. However, some extensions were made to enable the modelling of the convective and radiative heat transfer at plate surfaces encountered in typical ship's hulls. The modified program was subsequently used to analyze three hull sections of different ships.

The ASASHEAT program is available for general use and can model the heat transfer processes in any type of hull configuration. The accuracy of the resulting predictions are, of course, only as good as the data input and the sophistication of the model. Experience and a knowledge of heat transfer fundamentals are required to obtain reliable results. The analysis of the conduction of heat through the metal plates can be made far more accurately than the analysis of the convective heat transfer. The former simply requires a refined mesh to represent the plates whereas the latter involves the correct analysis of the effect of fluid flow, which is more difficult to predict. In the case of an air filled cell a contribution due to radiation must be included but even this is easier to predict than the convective component. Hence the solution to a problem involving pure conduction could be accurate to 2-3% whereas for a problem dependent primarily on convective heat transfer errors of 20% or more might occur.

The importance of convective heat transfer internal to the hull was recognized and various attempts made to estimate the coefficients of heat transfer at the plate surfaces. An attempt to model the natural convection by a computer based numerical method failed, due to problems associated with the turbulent nature of the flow. Classical methods based on the consideration of a simple plate surface immersed in a fluid were eventually used to approximately predict the coefficients. The monitoring of the heat transfer process within a ship's hull was only partially successful due to environmental difficulties. It is therefore considered that the weakest link in the modelling is the prediction of the fluid heat transfer mechanism and as it was demonstrated that this could account for 50% of the heat flux, this is considered an important area for further research.

Results reported for some typical hull sections should be considered simply representative of the type of analysis that is possible using the ASASHEAT program. This report does not provide formulas for the solution of heat transfer in ship's hulls but describes computer based methods that are capable of solving more complex problems.

In addition to the macro models some local modelling was performed on single cell sections to illustrate the potential for obtaining local temperature gradients. Another program based on a thermal network approach and capable of including the non-linear effects of radiation and temperature dependent convection coefficients was used to investigate the effects of these phenomena.

All the computer based tools described in this report are available and can be used in the manner illustrated or in a variety of other ways, to solve a range of heat transfer problems in ships. The facilities are flexible but the major prerequisite is that an idealization, similar to those used in the report, be constructed to represent the particular problem to which a solution is required. This means that some assumptions must be made and that the appropriate choice of model is an important determinant of the solution accuracy.

7.2 Overall Conclusions

The overall conclusion of this report, concisely stated, is that a satisfactory analytical methodology has been demonstrated for the prediction of the temperature distributions throughout the hull of a ship in Arctic waters. However the numerical values predicted are dependent upon a knowledge of the physical data, including the convective heat transfer surface coefficients. The prediction of these coefficients, for both air and water filled cells, is beyond the effective range of current analytical tools for the cell dimensions and temperatures involved in cold water ships, and for the reasons discussed in the report the confidence level in the results of an experimental approach using smaller-than-full-scale tests would be low.

7.3 Recommendations for Future Work

An attempt to obtain data at real scale from an operating vessel showed that, although useful as a check on empirical coefficients, this approach was expensive, not subject to scheduling and did not allow repeatability. The results were limited to the configuration tested, and were thus unsuitable for the prediction of the coefficients in new and substantially different hull designs. On the other hand knowledge of the operating conditions encountered in the Arctic are needed to assist in the calibration of any

results obtained by analysis. To this end it was felt a more carefully designed, long term monitoring system for the M.V. Arctic should be considered. Appendix I contains a summary of a cost proposal solicited from Weir-Jones Engineering Consultants to provide a system that would repeat the tests attempted in July 1981 but with the ability to reactivate the apparatus on demand and at short notice so that a research program could be operated over an extended period. This form of research should be paralleled by a similar program in the laboratory which would permit the shortcomings described above to be overcome.

In these circumstances it is recommended that tests should be conducted on full scale cells in a laboratory, under planned and controlled conditions, to provide the information on the heat transfer coefficients necessary to complement the analytical procedures presented here, and hence provide a complete design process at a high level of confidence. Such full scale laboratory testing would assess not only the convection effects, but also the effects of ice accumulation, white frost deposits, and the special conditions near the sea water level line and near the cell water level line. A more detailed consideration of this option is given in Appendix J.

Finally a third, analytical option is open for future research. State of the art techniques for modelling two dimensional turbulent flow are now available in computer software that could provide better estimates than were previously possible by the techniques used in this report. It is recommended that this avenue also be explored to investigate the convective fluid processes.

REFERENCES

1. Basic Heat Transfer, M.N. Ozisik, McGraw-Hill, New York, 1977

2. Heat Transfer, A.J. Chapman, MacMillan Co., New York, 1960

3. Thermal Insulation Report, Society of Naval Architects, New York, TRB 4-7, 1974

4. Heat Transfer in an Oil Tank on Board the Danish Motor Tanker "Esso Aarkus", Danish Ship Research Institute, December 1971

5. Thermal Analysis for Complex Structural Systems, J.F. Cox, D.F. Cameal, Marine Technology Vol. 8, No. 4, Oct. 1971

6. Structural Analysis Including Thermal Effects for Icebreakers, E.W. Kiesling, Southwest Research Institute TCG 17961-A, June 1967

7. Heat Losses from Oil Tanker Cargoes, R.J. Saunders, C.Eng., British Ship Research Association

8. The Heating of High Viscosity Oils by Natural Convection using Horizontal Tubular Grids, C.B. Lamb, British Ship Research Association, J. Inst. of Petroleum, Vol. 57, Sept. 1971

9. Experimental Studies on Heat Transfer Coefficients and Effective Length of Tank Heating Coils in Vessels, Kurihara, Armagata and Mackowa, J.S.N.A. West Japan No. 40, July 1970

10. Finite Element Analysis of Free Convection Flows, B. Tabarrok and R.C. Lin, Int. J. Heat and Mass Transfer, Vol. 20 #9, 1977

11. Maximum Density Effects in the Free Convection of Liquids in a Closed Cell, Robillard and Vasseur, Can. J. Civil Eng., December 1979

12. ASASHEAT User's Manual, H.G. Engineering Ltd., June 1982

13. THETA User's Manual, H.G. Engineering Ltd., April 1982

14. THETA: A Desktop Computer Solution for Non-Linear Time Dependent Heat Flow Problems, P.J. Moir and J.R. Stoker (copies available from H.G. Engineering Ltd.)

15. Arctic Resources by Sea, Northern Associates Holdings Ltd., 1973

16. Heat Transmission, W.H. McAdams, 3rd ed. McGraw Hill Book Company, New York, 1954

17. An Analysis of Turbulent Free Convection Heat Transfer, F.J. Bayley, Proc. Inst. Mech. Eng. London 168: 361 (1955)

18. An Investigation of Turbulent Natural Convection in Air at Low Pressure Along a Vertical Heated Plate, C.Y. Warner and V.S. Arpaci, Int. J. Heat Mass Transfer 11: 347-406 (1968)

19. Heat Transfer and Flow Instability of Natural Convection over Upward-Facing Horizontal Surfaces, R. Ishiguro and T. Abe, Proc. Sixth International Heat Transfer Conference, Toronto, August 1978

20. The Influence of Aging Factors on the Emissivity of Reflective Insulations, F.C. Hooper and W.T. Moroz, A.S.T.M. Bulletin, #182, May 1952.

APPENDICES

APPENDIX A

Formulation of the Heat Flow Model using the Finite Element (F.E.) Method

The equation governing steady state heat conduction in three dimensions can be written

$$\frac{\partial}{\partial x}\left(kx\ \frac{\partial T}{\partial x}\right)+\frac{\partial}{\partial y}\left(ky\ \frac{\partial T}{\partial y}\right)+\frac{\partial}{\partial z}\left(kz\ \frac{\partial T}{\partial z}\right)+Q=0 \qquad (1)$$

where $T(x,y,z)$ = Temperature function

kx, ky, kz = Heat conductivity coefficients

Q = The rate of heat generation

The Euler theorem from the calculus of variations states that if the integral

$$\pi=\int_V f\left(x, y, z, T, \frac{\partial T}{\partial x}, \frac{\partial T}{\partial y}, \frac{\partial T}{\partial z}\right) dxdydz \qquad (2)$$

is to be minimized over the region V, then the necessary and sufficient conditions for this minimum is that the unknown function T (x, y, z) should satisfy the equation.

$$\frac{\partial}{\partial x}\left\{\frac{\partial f}{\partial(\partial T/\partial x)}\right\}+\frac{\partial}{\partial y}\left\{\frac{\partial f}{\partial(\partial T/\partial y)}\right\}+\frac{\partial}{\partial z}\left\{\frac{\partial f}{\partial(\partial T/\partial z)}\right\}-\frac{\partial f}{\partial T}=0 \qquad (3)$$

By comparison between equations (3) and (1) it can be seen that an equivalent formulation of equation (1) is that the volume integral taken over the whole region be minimized.

$$\pi=\int_V \tfrac{1}{2}\left\{kx\left(\frac{\partial T}{\partial x}\right)^2+ky\left(\frac{\partial T}{\partial y}\right)^2+k_z\left(\frac{\partial T}{\partial z}\right)^2\right\} dV-\int Tq^B\ dV$$

$$-\int_S T^s q^s\ ds-\sum_i T^i\ Q^i \qquad (4)$$

where

q^B is the rate of heat generation/unit volume

q^s is the rate of heat transfer per unit surface area

Q^i are concentrated heat flow inputs

subject to T (x, y, z) obeying the physical boundary conditions which may be

1) Prescribed temperature Tp

2) Prescribed heat flux $q_p = - kn \frac{\partial T}{\partial \eta}$

3) Convective loss $h (T - T) = kn \frac{\partial T}{\partial \eta}$

when n is the normal to the surface

h is the surface (film) coefficient

k_n is the conductivity assuming

kx = ky = kz = kn

Taking the differential w.r.t. T

$$\frac{\partial \pi}{\partial T} = \int_v \left\{ kx \frac{\partial T}{\partial x} \cdot \frac{\partial}{\partial T} \left(\frac{\partial T}{\partial x} \right) + ky \frac{\partial T}{\partial y} \cdot \frac{\partial}{\partial T} \left(\frac{\partial T}{\partial y} \right) + kz \frac{\partial T}{\partial z} \cdot \frac{\partial}{\partial T} \left(\frac{\partial T}{\partial z} \right) \right\} dV - \frac{\partial}{\partial T} \left(T \right) q^B \, dV$$

$$- \int_s \frac{\partial}{\partial T} \left(T^s \right) q^s \, ds - \sum_i \frac{\partial}{\partial T} \left(T^i \right) Q^i \qquad (5)$$

which may be re-written

$$\frac{\partial \pi}{\partial T} = \int_v \frac{\partial}{\partial T} T'^T K T' dv - \int_v \frac{\partial}{\partial T} (T) q^B dv -$$

$$\int_s \frac{\partial}{\partial T} (T^s) q^s ds - \sum_i \frac{\partial}{\partial T} (T^i) Q^i \qquad (6)$$

where $T'^T = \left\{ \frac{\partial T}{\partial x} \quad \frac{\partial T}{\partial y} \quad \frac{\partial T}{\partial z} \right\}$

and $K = \begin{bmatrix} Kx & 0 & 0 \\ 0 & Ky & 0 \\ 0 & 0 & Kz \end{bmatrix}$

If the body is approximated as an assemblage of finite elements connected at nodal points on the element boundaries, then it can be assumed that the temperature at any points in an element m is a function of the nodal point temperatures

$$T^m = H^m T \qquad (7)$$

where H is the shape function and T a vector containing the nodal point temperatures. It also follows that

$$T'^m = B^m T \qquad (8)$$

where B is a matrix of shape function derivatives with respect to the element coordinate system.

Now if $\frac{\partial}{\partial T} (T)$ is considered as a virtual quantity in equation (6) then all such terms can be replaced by $\overline{T}$, hence (6) becomes

$$\int_v K T' dv = \int_v \overline{T} q^B dv + \int_v \overline{T}^s q^s ds + \sum_i \overline{T}^i Q^i \qquad (9)$$

Using equations (7) and (8) the heat flow equilibrium equations corresponding to the nodal temperatures of the element assemblage can be derived.

$$\sum_m \int T \; K \; T' \, dv^m = \sum \int \bar{T}^m \, q^{BM} dv^m + \sum \int \bar{T}^{sm} q^{sm} ds^m + \sum \bar{T}^i Q^i \qquad (10)$$

where m = 1,2 ... number of elements.

Substituting into equation (10) from (7) and (8)

$$= \bar{T}^T \left\{ \sum_m \int_{v^m} B^{mT} K^m B^m \, dv^m \right\} T = \bar{T}^T \left\{ \sum_m \int_{v^m} H q^{Bm} \, dv^m \right\} + \bar{T}^T \left\{ \sum \int H^{smT} q^{sm} \, ds^m \right\} + \bar{T}^T Q \qquad (11)$$

By proposing a virtual temperature theorem analogous to the virtual displacement theorem in structural analysis, which states: If a virtual temperature perturbation is applied to a body then the resulting heat flow by conduction is equal to the total heat input to the body if the system was initially in thermal equilibrium, and equation (11) must be true for any virtual temperature difference, hence

$$K T = Q_T \qquad (12)$$

where K is the conductivity matrix

$$K = \sum_m \int_{V^m} B^{mT} K \; B^m \, dV^m \tag{13}$$

and Q is the total nodal point heat flow input

$$Q_T = Q_B + Q_s + Q_c \tag{14}$$

where

$$Q_B = \sum_m \int_{V^m} H^{mT} q^{Bm} \, dV^m \tag{15}$$

which expresses the nodal equivalent heat input due to q^B heat generation/unit volume

$$Q_s \quad \sum_m \int_{V^m} H^{smT} \, q^{sm} \, ds^m \tag{16}$$

which expresses the nodal equivalent heat input due to q^s surface heat flux

and Q_c is a vector of nodal heat inputs.

If heat flow changes with time a term must be included which takes account of the rate at which heat is stored.

The rate of heat absorption is given by

$$q^c = c \dot{T} \tag{17}$$

where q^c can be thought of as being part of the rate of heat generated per unit volume

c is the heat capacity

For element m

$$\dot{T}^m = H^m \dot{T} \tag{18}$$

Substituting into equation (15)

$$Q_B = \sum_m \int_{V^m} H^{mT} \left\{ q^{Bm} - c^m H^m \dot{T} \right\} dV^m \tag{19}$$

The heat flow equation now becomes

$$C\dot{T} + KT = Q_T \tag{20}$$

where the heat capacity matrix is

$$C = \sum_m \int_{V^m} H^{mT} c^m H^m \, dV^m \tag{21}$$

Time-Stepping Solution Procedure for Transient Problems

Given equation (20) and suitable boundary conditions, a solution may be sought by taking incremental time steps.

In the ASASHEAT program a direct integration method is used that is unconditionally stable.

The incremental scheme is

$$\left[\frac{2}{\Delta t} C + K_{n+1}\right] T_{n+1} = Q_n + Q_{n+1} + \left[\frac{2}{\Delta t} C - K_n\right] T_n \qquad (22)$$

where Δt is the time step from t_n to t_{n+1}.

The Treatment of Convective Boundary Conditions

Normal boundary conditions such as prescribed temperatures, nodal heat inputs etc., are easily dealt with. However the inclusion of surface convection requires special consideration because the rate of heat transfer is proportional to the temperature difference between the surrounding fluid, which is known, and the surface temperature which is unknown.

Given a surface convecting heat to a fluid

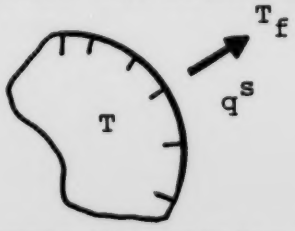

the heat flow across the boundary is

$$q^s = h\ (T - T_f) \qquad (23)$$

where h is the heat transfer coefficient.

In terms of the finite element approximation of the already stated analysis

$$K\,T = \int_S h\,H^T H\,ds\,T_f - \int_S h\,H\,H\,ds\,T \qquad (24)$$

where the second term on the right hand side contains the unknown temperatures T.

In steady-state analysis where h is obviously independent or in transient analysis when h is constant, this term can be moved to the left hand side to form an augmented conductivity matrix.

$$\left(K + \int_S h\,H^T H\,ds\right) T = \int_S h\,H^T H\,ds\,T_f \qquad (25)$$

The Treatment of Radiation Boundary Conditions

In general the surface flux due to radiation to a background ambient temperature is given by

$$q^r = \sigma\varepsilon\,(T^4 - T_A^4) \qquad (26)$$

where σ = Boltzmann's constant

ε = Emissivity constant for the surface

T_A = The ambient background temperature

To enable this non-linear condition to be incorporated into the finite element approximation the radiation coefficient has to be linearised

$$q^r = \sigma\varepsilon(\tilde{T}^3 + T_A^3)\quad (T - T_A)$$

$$= \alpha\,(T - T_A)$$

where α is now an equivalent surface coefficient and can be handled as a convective surface coefficient and $\tilde{T}$ is an estimate of the surface temperature.

The current version of the ASASHEAT program permits an iteration to be automatically used in the steady-state solution or at each time step. Under these circumstances the value of α is performed at each iteration. Convergence is determined from a comparison of the Euclidean norm with a given tolerance

$$\frac{\left\{ \sum_{m=1}^{\text{nodes}} \left[T_m^{(i)} - T_m^{(i-1)} \right]^2 \right\}^{\frac{1}{2}}}{\left\{ \sum_{m=1}^{\text{nodes}} \left[T_m^{(i)} \right]^2 \right\}^{\frac{1}{2}}} \leqslant \text{Tolerance}$$

where i refers to the iteration number.

If the inequality is not satisfied the program reiterates.

APPENDIX B

Extensions to the ASASHEAT Program Developed for the Solution of Fabricated Plate Structures

There are in general three components to the heat transfer model; conduction, radiation and convection. The latter two may be included in the conduction model as boundary conditions to the surfaces of the conduction medium. In the fabricated plate type of structure each surface of a plate may be subject to this condition with a different coefficient on each surface associated with a different ambient temperature. A typical plate is shown below.

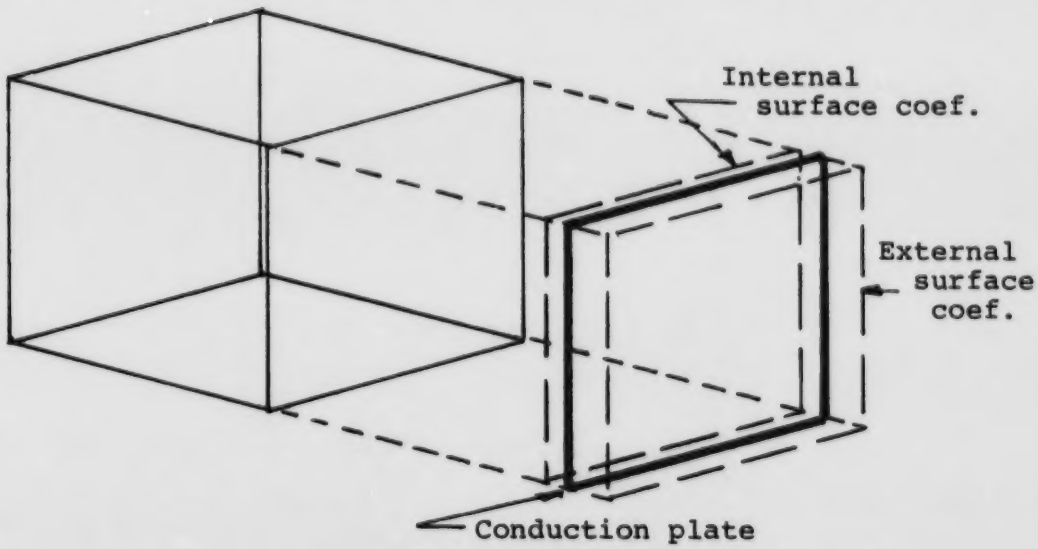

Figure 100
TYPICAL PLATE FABRICATED CELL

The ASASHEAT program has been extended to incorporate this particular boundary condition on all plate type finite elements in the library. The elements used in this analysis include

ASASHEAT Name	Type
TRM3	Triangular 3 noded plate
QUM4	Quadrilateral 4 noded plate
TRM6	Triangular 6 noded plate having additional nodes at the mid-point of each side
QUM8	Quadrilateral 8 noded plates having additional nodes at the mid-point of each side.

Equation 12 of Appendix A expressed the general heat flow relation for the model

$$K\,T = Q_T \qquad \ldots(1)$$

The facility described above may be obtained by the particular case of this equation as stated in equation 24 of Appendix A. For any of the above elements this may be written

$$K\,T = \int_S h_I\,(T_{fI} - T)\,H^T H\,ds + \int_S h_E\,(T_{fE} - T)\,H^T H\,ds \qquad \ldots(2)$$

where h_I = the surface coefficient on the 'internal' face

T_{fI} = the fluid temperature associated with the 'internal' coefficient

h_E = the surface coefficient on the 'external' face

T_{fE} = the fluid temperature associated with the 'external' coefficient

The surface coefficient may also vary over the element. There is no special significance associated with the words 'internal' and 'external' other than that they designate opposite sides of the plate.

As stated in Appendix A, equation (25), implementation of equation (2) leads to the modification of two areas of the program; first an augmentation of the conductivity matrix and second as an addition to the right hand side vector of heat fluxes. Use of this facility and of the ASASHEAT program in general is illustrated in Appendix C.

APPENDIX C

Example and Validation Model for ASASHEAT

The following example illustrates the use of the ASASHEAT program for the analysis of a plate having surface coefficients on both faces. The problem selected was that of a cantilever plate with a prescribed temperature at one edge and all other surfaces with a uniform film coefficient and ambient temperature. The dimensions are illustrated in Figure 101.

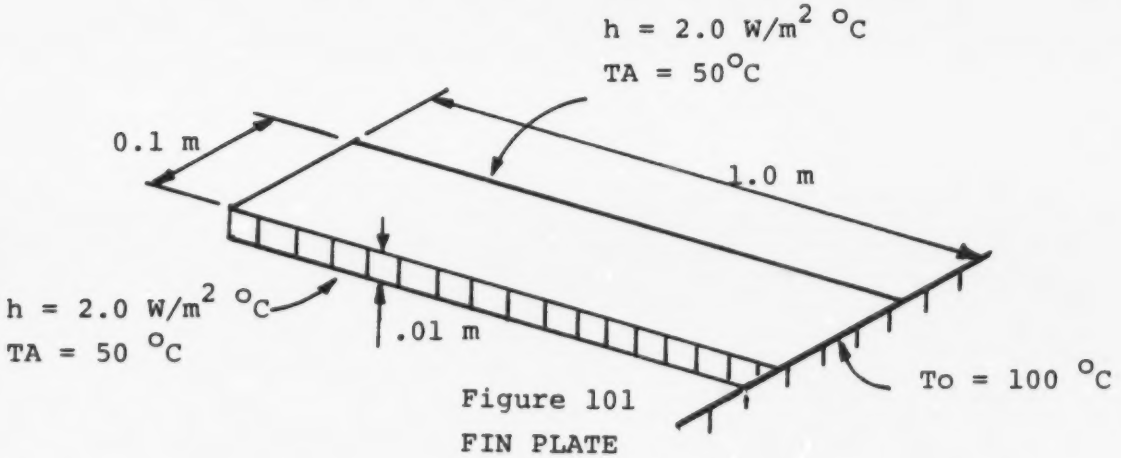

Figure 101
FIN PLATE

The plate was subdivided into ten equal divisions as shown in Figure 102. Three different idealizations using the four node quadrilateral, three node triangular and eight node quadrilateral elements were used to model the plate. These idealizations and their associated nodes are shown in Figure 102. A typical data file for this example is given in Figures 103 and 104.

The steady-state solution of the temperature distribution (1) is given by the expression:

$$T(x) = T_\infty + \frac{\cosh m(L-x) + (\frac{h}{mK}) \sin hm\ (L-x) \times (T_o - T_\infty)}{\cosh mL + (\frac{h}{mk}) \sin hmL}$$

where $T(x)$ = the temperature a distance x from the prescribed temperature

T_∞ = the ambient temperature

$m = \frac{Ph}{kA}$

P = the perimeter of cross-section of the plate

h = the surface heat transfer coefficient

k = the plate material conductivity

A = the plate cross-sectional area

L = the length of the plate

For this example the values of the above were set as follows:

$L = 1m$; $A = .001m^2$; $P = .2m$

$k = 51.922\ W/m^oC$; $h = 2.0\ W/m^{2o}C$

$T_\infty = 50^oC$ $T_o = 100^oC$

Hence $m^2 = \frac{.20 \times 2.0}{51.922 \times .001} = 7.7039$

$m = 2.776$

$\frac{h}{mk} = \frac{2.0}{2.776 \times 51.992} = .01386$

and

$$T(x) = 50 + \left[\frac{\cosh 2.776(1-x) + .0139 \sinh 2.776(1-x)}{\cosh 2.776 + .0139 \sinh 2.776} \right] \times 50$$

$$= 50 + 6.12 \left(\cosh 2.776(1-x) + .0139 \sinh 2.776(1-x)\right.$$

therefore the tip temperature $T(L) = 56.12^{\circ}C$.

A comparison between the computed results and the above solution is shown graphically in Figure 105. The three different solutions were indistinguishable from the classical solution at all points.

A number of other checks on the program's execution were made but because a rigorous comparison was not available they were not included.

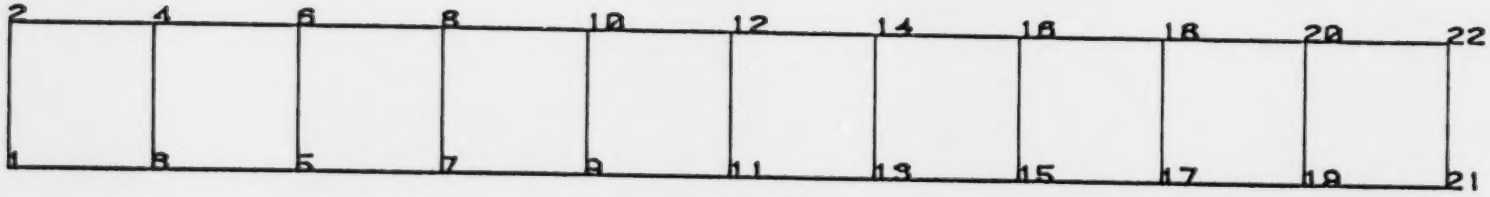

QUM4 ELEMENTS

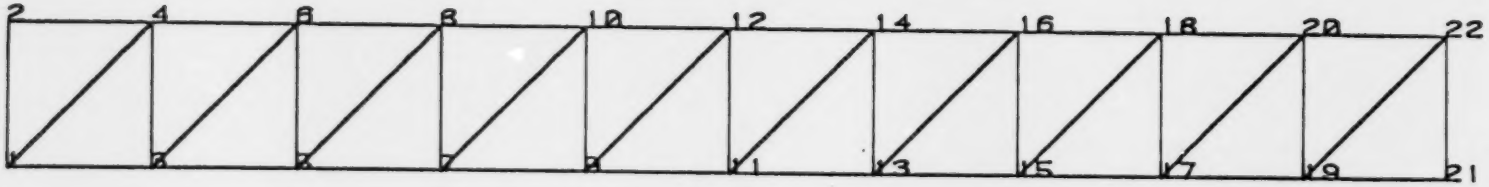

TRM3 ELEMENTS

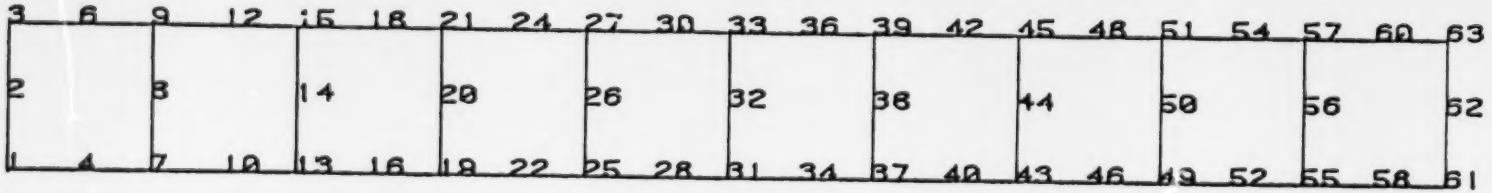

QUM8 ELEMENTS

Figure 102

THREE FINITE ELEMENT IDEALIZATIONS OF THE FIN PLATE

```
NAME = DATFIN4

JOB      HEAT     FIN4
TITLE                    TEST CASE #4  FIN(TRM3)
OPTIONS NOBL TWOD END
          COOR
          CART
          1                .0000      .0000      .0000
          3                .1000      .0000      .0000
          5                .2000      .0000      .0000
          7                .3000      .0000      .0000
          9                .4000      .0000      .0000
         11                .5000      .0000      .0000
         13                .6000      .0000      .0000
         15                .7000      .0000      .0000
         17                .8000      .0000      .0000
         19                .9000      .0000      .0000
         21               1.0000      .0000      .0000
          2                .0000      .1000      .0000
          4                .1000      .1000      .0000
          6                .2000      .1000      .0000
          8                .3000      .1000      .0000
         10                .4000      .1000      .0000
         12                .5000      .1000      .0000
         14                .6000      .1000      .0000
         16                .7000      .1000      .0000
         18                .8000      .1000      .0000
         20                .9000      .1000      .0000
END      22               1.0000      .1000      .0000
          ELEM
          0    0 TRM3(1) (   1) (   2) (   4) (   1) (   1)
          0    0 TRM3(1) (   3) (   4) (   6) (   1) (   1)
          0    0 TRM3(1) (   5) (   6) (   8) (   1) (   1)
          0    0 TRM3(1) (   7) (   8) (  10) (   1) (   1)
          0    0 TRM3(1) (   9) (  10) (  12) (   1) (   1)
          0    0 TRM3(1) (  11) (  12) (  14) (   1) (   1)
          0    0 TRM3(1) (  13) (  14) (  16) (   1) (   1)
          0    0 TRM3(1) (  15) (  16) (  18) (   1) (   1)
          0    0 TRM3(1) (  17) (  18) (  20) (   1) (   1)
          0    0 TRM3(1) (  19) (  20) (  22) (   1) (   1)
          0    0 TRM3(1) (   1) (   4) (   3) (   1) (   1)
          0    0 TRM3(1) (   3) (   6) (   5) (   1) (   1)
          0    0 TRM3(1) (   5) (   8) (   7) (   1) (   1)
          0    0 TRM3(1) (   7) (  10) (   9) (   1) (   1)
          0    0 TRM3(1) (   9) (  12) (  11) (   1) (   1)
          0    0 TRM3(1) (  11) (  14) (  13) (   1) (   1)
          0    0 TRM3(1) (  13) (  16) (  15) (   1) (   1)
          0    0 TRM3(1) (  15) (  18) (  17) (   1) (   1)
          0    0 TRM3(1) (  17) (  20) (  19) (   1) (   1)
END       0    0 TRM3(1) (  19) (  22) (  21) (   1) (   1)
```

Figure 103

ASASHEAT INPUT DATA

```
          MATE
END       1       ISO .5192E 02 .4480E 03 .7830E 04 .0000E 00
          GEOM
END       1       TRM3 .1000E-01
          BOUNDARY CONDITIONS
          EX F
          E       2.0000 ( 10) (   1,   2) (   4,   2) (   3,   2)
END       E       2.0000 ( 10) (   1,   2) (   2,   2) (   4,   2)
          EX T
          E      50.0000 ( 10) (   1,   2) (   4,   2) (   3,   2)
END       E      50.0000 ( 10) (   1,   2) (   2,   2) (   4,   2)
          IN F
          E       2.0000 ( 10) (   1,   2) (   4,   2) (   3,   2)
END       E       2.0000 ( 10) (   1,   2) (   2,   2) (   4,   2)
          IN T
          E      50.0000 ( 10) (   1,   2) (   4,   2) (   3,   2)
END       E      50.0000 ( 10) (   1,   2) (   2,   2) (   4,   2)
          PRESCRIBED TEMPERATURES
END          100.000 (   2)(   1,   1)
          FILM COEFFICIENT
END       E       2.0000 (  1) (  21) (  22)
          AMBIENT TEMPERATURES
END          50.000 (   2)(  21,   1)
          END OF DATA
```

NODE	TEMPERATURE	NODE	TEMPERATURE	NODE	TEMPERATURE	NODE	TEMPERATURE
1	.10000E 03	7	.72050E 02	13	.60360E 02	19	.56336E 02
2	.10000E 03	8	.72012E 02	14	.60345E 02	20	.56323E 02
3	.87978E 02	9	.66931E 02	15	.58396E 02	21	.56098E 02
4	.87925E 02	10	.66902E 02	16	.58385E 02	22	.56041E 02
5	.78889E 02	11	.63133E 02	17	.57088E 02		
6	.78840E 02	12	.63112E 02	18	.57080E 02		

1ASASHEAT 12:30 MAY 08,'80 TEST CASE #4 FIN(TRM3)

Figure 104

ASASHEAT INPUT DATA AND RESULTS

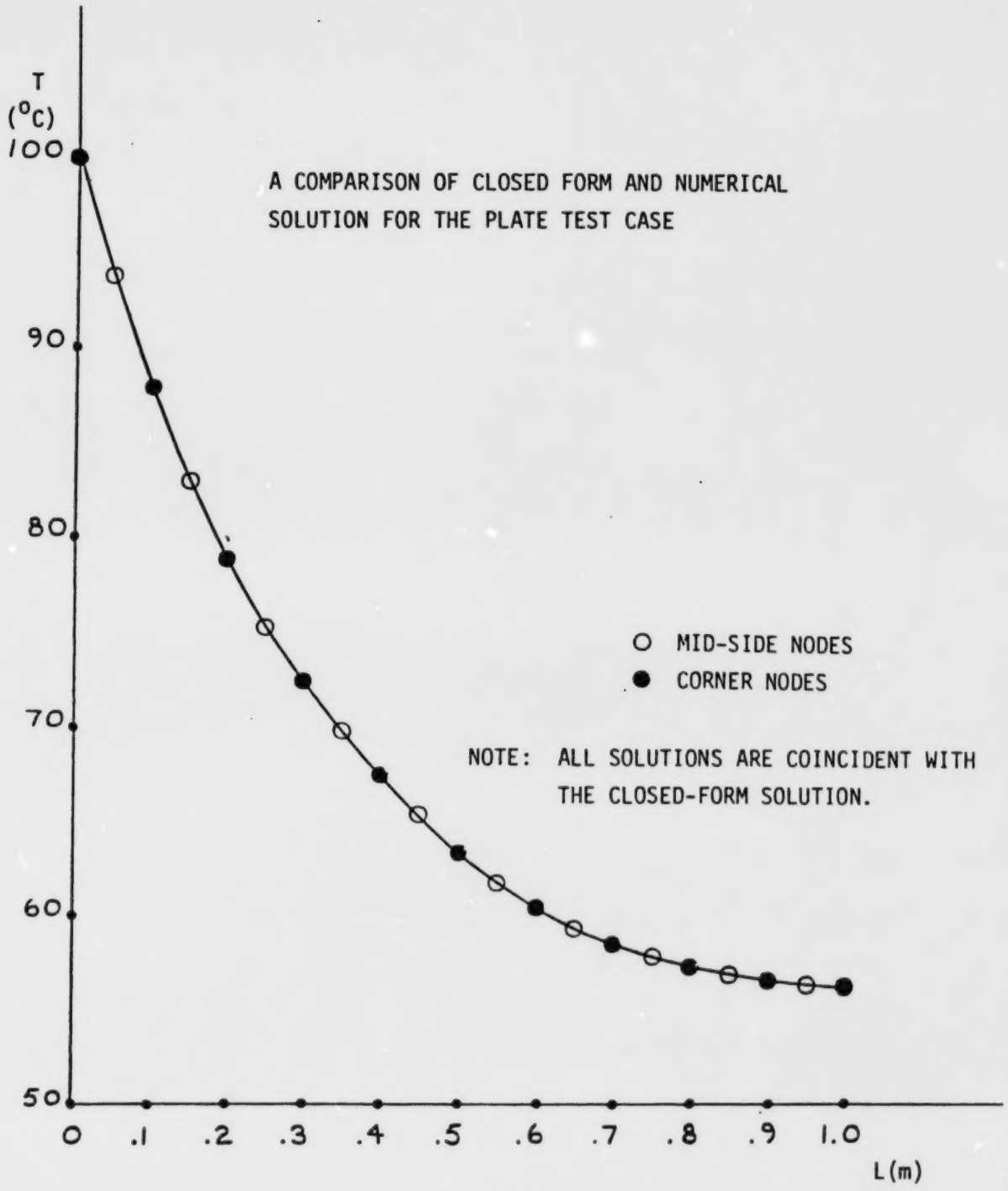
A COMPARISON OF CLOSED FORM AND NUMERICAL SOLUTION FOR THE PLATE TEST CASE
T
(°C)
100
90
80
70
60
50
MID-SIDE NODES
CORNER NODES
NOTE: ALL SOLUTIONS ARE COINCIDENT WITH THE CLOSED-FORM SOLUTION.
0
.1
.2
.3
.4
.5
.6
.7
.8
.9
1.0
L(m)

Figure 105

APPENDIX D

Theoretical Background to Modelling Closed Cell Convection

The program used in section 3.1.3 to model closed cell convection by the finite element method follows the detailed description given in (Ref. 10). A summary of the essential equations and the method are given below for completeness.

The problem of two dimensional steady-state flow of an incompressible fluid driven by buoyancy forces is considered. The latter forces are assumed to be sufficiently accurately described by the Boussinesque approximation.

$$\frac{d\rho}{\rho_o} = -\beta dT \quad B, \text{ thermal expansion coefficient} \qquad - (1)$$

It is assumed that the density changes are ignored in the inertia terms of the equilibrium equations and the continuity equation. It is further assumed that dissipation due to viscous forces in the equilibrium equations does not contribute significantly to the energy transport equation.

Under these assumptions the conservation of mass, momentum and energy may be expressed as

$$\frac{\partial u}{\partial x} + \frac{\partial v}{\partial y} = 0 \qquad - (2)$$

$$u \frac{\partial u}{\partial x} + v \frac{\partial u}{\partial y} = - \frac{1}{\rho} \frac{\partial p}{\partial x} + g\left(\frac{\rho - \rho_o}{\rho_o}\right) + \nu \nabla^2 u \qquad - (3)$$

$$u \frac{\partial v}{\partial x} + v \frac{\partial v}{\partial y} = - \frac{1}{\rho_o} \frac{\partial p}{\partial y} + \nu \nabla^2 v \qquad - (4)$$

$$u \frac{\partial T}{\partial x} + v \frac{\partial T}{\partial y} = \alpha \nabla^2 T \qquad - (5)$$

and from equation 1

$$\frac{\rho - \rho_o}{\rho_o} = -\beta (T - T_o) \qquad - (6)$$

where the symbols are as defined in Appendix H and

$$\nabla^2 = \frac{\partial^2}{\partial x^2} + \frac{\partial^2}{\partial y^2}$$

The subscript o denotes a reference temperature which is taken as the mean of the hot and cold temperatures, see Figure 106.

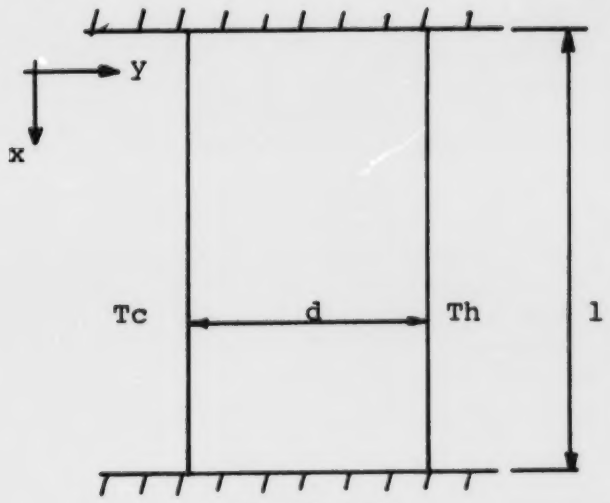

Figure 106

THE CLOSED CELL

It is convenient to put the equations into non-dimensional form by introducing the following dimensionless parameters

$$X = x/d, \quad Y = y/d \quad \theta = \frac{T-To}{T_n - T_o} \qquad -$$

$$U = ud/\nu, \quad V = vd/\nu \quad P = pd^2/\rho_o \nu^2 \qquad - (7)$$

A further transformation is made by introducing the stream function ψ

$$U = \frac{\partial \psi}{\partial Y}, \quad V = -\frac{\partial \psi}{\partial X} \qquad - (8)$$

and the vorticity

$$\omega = \frac{\partial V}{\partial X} - \frac{\partial U}{\partial Y} \qquad - (9)$$

It can be shown that the governing equations in terms of the new variables reduce to

$$\frac{\partial \psi}{\partial Y}\frac{\partial \theta}{\partial X} - \frac{\partial \psi}{\partial X}\frac{\partial \theta}{\partial Y} = \frac{1}{Pr}\nabla^2\theta \qquad - (10)$$

$$\frac{\partial \psi}{\partial Y}\frac{\partial \omega}{\partial X} - \frac{\partial \psi}{\partial X}\frac{\partial \omega}{\partial Y} = \frac{Gr}{2}\frac{\partial \theta}{\partial Y} + \nabla^2\omega \qquad - (11)$$

$$\nabla^2\psi = -\omega \qquad - (12)$$

These together with appropriate boundary conditions constitute a definition of our problem. Equations 10-12 form a set of quasilinear elliptic equations for which ψ, ω and θ will be continuous in the spacial domain. The equations may be solved by the following iterative procedure.

1. Initially the stream function is assumed as zero everywhere and equation 10 is solved for θ. This solution describes the temperature distribution for pure conduction.

2. This temperature distribution (and the associated stream function when non zero) are substituted into equation 11 from which a distribution of vorticity is obtained.

3. Finally the vorticity distribution is used in equation 12 to obtain an improved distribution for the stream function.

The iterative cycle is repeated until the values of ω for two consecutive calculations are within prescribed limits.

The solution to each equation is obtained by using a finite element approach to express the differential equation as a series of linear equations in terms of the parameters ψ, ω and θ at the corners of a mesh of triangular elements covering the domain.

Each equation has the form

$$\frac{\partial^2 \phi}{\partial x^2} + \frac{\partial^2 \phi}{\partial y^2} + \bar{S}\ (X,Y) = 0 \qquad - (13)$$

where ϕ represents the stream function, temperature and vorticity and $\bar{S}$ (X, Y) takes different forms in each case. If $\bar{S}$ (X, Y) is considered to be prescribed them equation 13 is the Euler-Lagrange equation for the following functional

$$I = \int_A \left\{ \frac{1}{2} \left[\left(\frac{\partial \phi}{\partial X} \right)^2 + \left(\frac{\partial \phi}{\partial Y} \right)^2 \right] - \bar{S}\ (X, Y)\ \phi \right\} dA \qquad - (14)$$

It can be shown that extremisation of I yields equation 13 and the general boundary condition

$$\frac{\partial \psi}{\partial n}\ \delta\phi = 0 \qquad - (15)$$

where n is a vector normal to the boundary of the region. For equation 14 to be integrable ϕ must be continuous everywhere in the domain hence in the finite element discretisation of the domain the functions chosen to represent the variable ϕ must be continuous within and across element boundaries. Let

$$\phi\ (X,Y) = \left[N\ (X,Y) \right] \left\{ q \right\} \qquad - (16)$$

where N is a 1 x 3 matrix of interpolation functions and $\left\{ q \right\}$ denotes the value of ϕ at each node of a triangular element. Typical functions for N are given (Ref. 20). Substituting from equation 16 into equation 14 we obtain the following discrete form of I.

$$I = \sum_{e=1}^{M} \int_{A_e} \left\{ \frac{1}{2} \{q\}^t \left(\left\{ \frac{\partial N}{\partial X} \right\} \left[\frac{\partial N}{\partial X} \right] + \left\{ \frac{\partial N}{\partial Y} \right\} \left[\frac{\partial N}{\partial Y} \right] \right) q \right.$$

$$\left. - \bar{S}(X,Y) \left[N \right] \{q\} \right\} dA \qquad - (15)$$

where e denotes an element, and M is the total number of elements.

The result of integrations in equation 15 will yield discrete equations of the following form

$$I = \sum_{e=1}^{M} \frac{1}{2} \{q\}^t \left(\left[K_e \right] \{q\} - \{Qe\} \right)$$

expressing this in terms of a global vector of nodal parameters $\bar{q}$ the functional I may be written

$$I = \frac{1}{2} \{\bar{q}\}^t \left[\bar{K} \right] \{\bar{q}\} - \bar{q}^t \bar{Q} \qquad - (16)$$

where the global matrices will be obtained by adding the element matrices. Extremisation of I with respect to $\bar{q}$ yields the discrete equations for the system

$$\left[\bar{K} \right] \{\bar{q}\} = \{ \bar{Q} \} \qquad - (17)$$

For the three equations (10) - (12) the previous formulations yield three sets of discrete equations.

$$\left[\bar{K}_\theta \right] \{ \bar{q}_\theta \} = \{ \bar{Q}_\theta \ (\psi) \} \qquad - (18)$$

$$\left[\bar{K}_\omega \right] \{ \bar{q}_\omega \} = \{ \bar{Q}_\omega \ (\psi, \theta) \} \qquad - (19)$$

$$\left[\bar{K}_\psi \right] \{ \bar{q}_\psi \} = \{ \bar{Q}_\psi \ (\omega) \} \qquad - (20)$$

These equations are coupled in a non-linear manner through the vectors on the right hand side. They are solved in an iterative manner as described previously.

The Nusselt number which characterizes heat flow through the surface of the cell walls is calculated from the following integral

$$Nu = \frac{1}{2\alpha} \int_0^{\alpha} \frac{\partial \theta}{\partial Y} \, dX, \quad \alpha = \text{aspect ratio} \qquad - (21)$$

In the case of the solution provided by the finite element method the above integral is evaluated from the nodal temperatures at the edge and one element width in from the edge (see Figure 107).

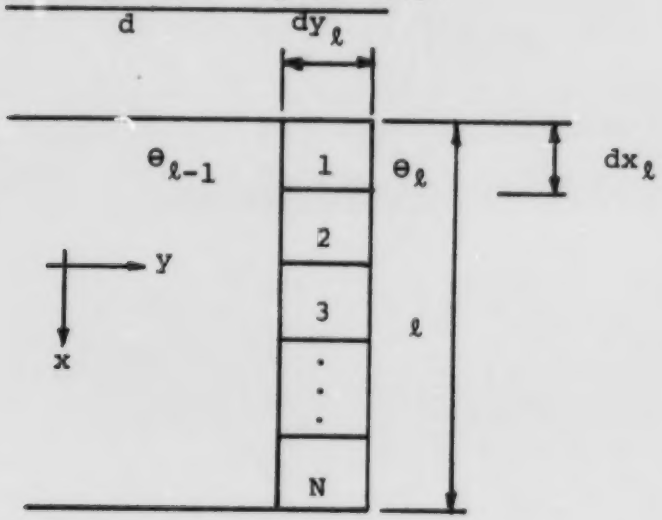

Figure 107

ELEMENTS AT THE EDGE OF THE MESH

The

$$Nu = \frac{d}{2\ell} \sum_{\ell=1}^{N} \left[\frac{\theta_\ell - \theta_{\ell-1}}{dy_{\ell/d}} \quad dx_{\ell/d} \right]$$

$$= \frac{d}{2\ell} \sum_{\ell=1}^{N} \left[\frac{\theta_\ell - \theta_{\ell-1}}{dy_\ell} \quad dx_\ell \right]$$

APPENDIX E

Calculation of Surface Convection Coefficients for the Plates of the L.N.G. Finite Element Model

External Surfaces Exposed to Sea, Wind and Spray

The heat flow on the external surfaces in the extreme case of no radiant absorption is dominated by the convection to the air or sea water. The convection coefficients are governed by the ship's speed, wind speed and spray. It was decided that as these factors provided a wide range of alternative values the best compromise was to adopt the values recommended in the Thermal Insulation Report produced by SNAME (Ref. 3). For decks and hull plates exposed to the weather at temperatures ranging from -12°C to -23°C the surface coefficient recommended is 40 W/m^2 °C. For plates exposed to sea water under cooling conditions, the recommended surface coefficient is 210 W/m^2 °C.

If it is assumed that the forced turbulent convection can be calculated from the following expression

$$\frac{hL}{L} = 0.036\ (Re)^{0.8}\ (Pr)^{1/3}$$

then the external surface coefficients are relevant to a wind speed of approximately 40 m/s (89 mph). However including the effect of sea spray in this probably means the equivalent velocity is actually lower as the wetting will tend to increase the heat transfer.

Internal Surfaces of Air Filled Cells

The internal hold is filled with LNG at -162°C and the wall is insulated with material that has an equivalent surface coefficient of 0.15 W/m^2 °C. From this it was estimated that the internal steel might have an equilibrium temperature of -90°C.

The properties of air are assumed to vary linearly with temperature. The calculations were performed according to the theory stated in section 3.1.4.

For vertical plates $h = 0.1k \left[\frac{g\beta\Delta T}{\nu\alpha} \right]^{1/3}$

For horizontal plates $h = 0.2k \left[\frac{g\beta\Delta T}{\nu\alpha} \right]^{1/3}$

For inclined plates $h = 0.1k \left[g\beta\Delta T \frac{\cos\theta}{\nu\alpha} \right]^{1/3}$

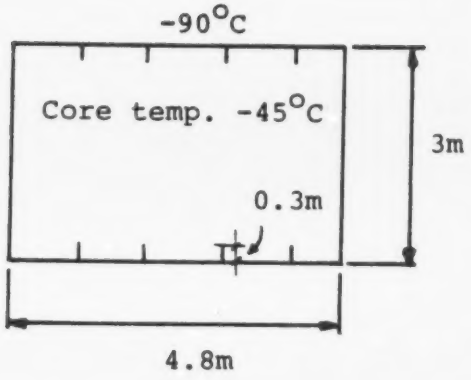

Figure 108
A TYPICAL CELL ON THE BOTTOM OF THE HULL

Assume temperature at the top of the lower stiffeners = $-10^{o}C$

Assume temperature at the bottom of the upper stiffeners = $-80^{o}C$

Horizontal surfaces

Assume $\Delta T = 10^{o}C$

For the lower surface (heating - unstable) $h \doteq 1.25\ W/m^2\ ^{o}C$

For the upper surface (cooling - stable) $h \doteq 1.43\ W/m^2\ ^{o}C$

Vertical surfaces

Assume $\Delta T = 10^{o}C$
Properties taken at $-45^{o}C$
For the vertical surfaces $h \doteq 0.66\ W/m^2\ ^{o}C$

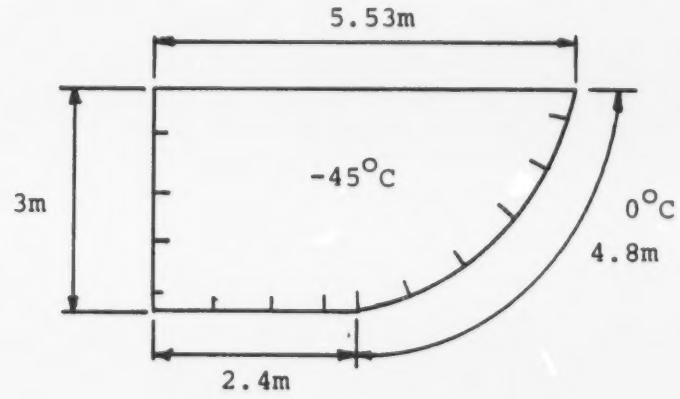

Figure 109
A TYPICAL BILGE CELL

Assume $\Delta T = 10^{o}C$ and properties evaluated at $-45^{o}C$

For the lower surface $h \doteq 1.25\ W/m^2\ ^{o}C$

For the inclined plates $h \doteq 0.55\ W/m^2\ ^{o}C$

For the vertical surface $h \doteq 0.66\ W/m^2\ ^{o}C$

For the top surface (assuming heat flux upward) $h \doteq 1.32\ W/m^2\ ^{o}C$

For the side cells

Vertical surfaces

Assume $\Delta T = 10^{o}C$

Evaluating properties at about $-10^{o}C$

For the right vertical surface $h \doteqdot 0.63\ W/m^2\ ^{o}C$

Evaluating properties at about $-45^{o}C$

For the left vertical surface $h \doteqdot 0.66\ W/m^2\ ^{o}C$

Hence, as these values are close assume they apply throughout the vertical cells.

APPENDIX F

A Program for the Evaluation of Plate Convection Coefficients by Classical Methods

The evaluation of the formulas for the surface convection coefficients from existing theory, described in section 3.1.4, can be considerably speeded up by the use of a computer. As many alternative values were required for use in the analysis models described in the report a BASIC program was written to accomplish this task.

This appendix contains a listing of the program, called FILMC, a description of the data requirements and subsequent results output. The program currently runs on a Hewlett-Packard 9845 desktop computer.

Data Input

The user is permitted to choose a compact or prompted form of input, the former being preferred when the input data is to be repeated for a large number of plates.

Program prompt: DO YOU WANT EXPERT(0) OR BEGINNERS(1) INPUT?

Response: 0 or 1

If the data has previously been created in a former run it may, at this point, be read back and edited when the user requests the "EXPERT" form of input.

Program prompt: HAVE YOU GOT DATA TO BE INPUT FROM FILE?

Response: Y or N

If the response is Y.

Program prompt: ENTER FILENAME OF STORED DATA (&MSUS)

Response: Filename and device on which it resides

A number of values are prompted for as follows:

Variable	Description	Units
L	The typical length of plate	Metres
Dt	The estimated boundary layer temperature difference	^{o}C
Te	The mean temperature of the fluid	^{o}C

Fluid. A flag to select the fluid type

1. Air
2. Water
3. Oil
4. Other

If 1, 2 or 3 are selected the following default properties are assigned by the program

Pnu	Kinematic viscosity	m^2/s
Alpha	Diffusivity	m^2/s
Beta	Expansion coefficient	^{1}/deg.C
Grav	Gravitational constant	m/s^2
K	Conductivity	W/m.degC

If the response is 4 then these values must be input.

Prompt: Enter Pnu, Alpha, Beta, Grav, Conductivity for material.

Finally the orientation of the plate and the temperature of the fluid relative to the plate must be stated.

Variable	Description	Units
Orientation	Vertical, horizontal or inclined	-

For horizontal plates the following choice has to be made

Flow	A cooler upper surface or a warmer upper surface	-

For the inclined plates the angle of inclination is also required.

Finally the program will prompt for more data.

Program prompt: Another case?...Yes(1), No(2)

Response: 1 or 2

If the input process is complete then the data may be stored.

Program prompt: DO YOU WANT TO STORE THE INPUT DATA?
Response: Y or N

Program prompt: ENTER FILENAME FOR STORED DATA (&MSUS)
Response: Filename and device on which it is to be stored.

The results may then be printed in a tabular form.

Results output

The results table is comprised of the following variables.

Variables	Description
No	The number of the plate (sequentially assigned)
Leng	The length of the plate
Del T	The estimated boundary layer temperature difference
Te	The mean temperature of the fluid
Flu	The fluid type
Flo	The nature of the flow (turbulent or laminar)
Srf	The nature of the temperature gradient between the plate and the fluid (see input variable Flow).

Variable	Description
Inc	The inclination of the plate
Pr	The Prandtl number
Gr	The Grashoff number
Ra	The Raleigh number
Film C	The film coefficient ($W/m^2.K$)

Film C has been evaluated according to the formula specified in sections 3.1.4.1 - 3.1.4.3.

The physical values assumed for the standard fluid type are as follows:

	Air	Water	Fuel Oil
Kinematic Viscosity	$\left[(T-100)/200x.16+.02\right]x10^{-4}$	$7.81x10^{-7}$	$4.4x10^{-6}$
Diffusivity	$\left[(T-100)/200x.2+.02\right]x10^{-4}$	$1.34x10^{-7}$	$7.03x10^{-8}$
Expansion coeff.	$1/T$	$1.0x10^{-6}$	$7.2x10^{-4}$
Conductivity	$\left[(Te-110)/190x14.8+10.1\right]x10^{-3}$	.583	.13946

Examples of the output are given in Section 5.2.

```
10    L=15
20    PRINTER IS 16
30     PRINT SPA(L-3);"*****************************************************",LIN
(1)
40     PRINT SPA(L);"FFFFFFFF    II   LL        MM       MM    CCCCCCC"
50     PRINT SPA(L);"FFFFFFFF    II   LL        MMM     MMM   CCCCCCCC"
60     PRINT SPA(L);"FF          II   LL        MMMM   MMMM   CC"
70     PRINT SPA(L);"FFFFFF      II   LL        MM  MM  MM   CC"
80     PRINT SPA(L);"FFFFFF      II   LL        MM  MM  MM   CC"
90     PRINT SPA(L);"FF          II   LLLLLL    MM  MM  MM   CCCCCCCC"
100    PRINT SPA(L);"FF          II   LLLLLL    MM  MM  MM    CCCCCCC"
110    PRINT LIN(1);SPA(L-3);"*****************************************************
**",LIN(2)
120    PRINT SPA(L);"          PROGRAM TO CALCULATE SURFACE "
130    PRINT SPA(L);"    FILM COEFFICIENTS DUE TO FREE CONVECTION "
140    PRINT SPA(L);"           AT THE SURFACE OF A PLATE ",LIN(2)
150    !          Written by D.Ruby 12/80 - H.G.ENGINEERING LTD
160    !          Theory by Prof B. Taborrak - U. of T.
170    DIM A$(100)[80],M$[3],F$[3],O$[3],S$[3],I$[40],Istore$(100)[40],Typ$[3],T
it$[80]
180    INTEGER Fluid,P1
181    STANDARD
190    In=0
200    Ipos=0
210    Maxdata=100
220    P1=0
230    BEEP
240    INPUT "DO YOU WANT EXPERT(0) OR BEGINNERS(1) INPUT",In
250    IF In THEN 510
260    LINPUT "HAVE YOU GOT DATA TO BE INPUT FROM FILE",Y$
270    IF Y$[1,1]="N" THEN 380
280    LINPUT "ENTER FILENAME OF STORED DATA (&MSUS)",File$
290    ASSIGN #1 TO File$,X1
300    IF X1 THEN 350
310    READ #1;Nump1
320    REDIM Istore$(Nump1)
330    READ #1;Istore$(*)
340    REDIM Istore$(Maxdata)
341    GOTO Start_exp
350    DISP ,"FILE NOT FOUND "&File$&" "
360    WAIT 1000
370    GOTO 280
380 Start_exp:   P1=P1+1
381    IF (Y$[1,1]="Y") AND (P1)Nump1) THEN 400
390    IF Y$[1,1]="Y" THEN I$=Istore$(P1)
400    P1$=TRIM$(VAL$(P1))
410    PRINT ,PAGE,"ENTER FOR PLATE NUMBER "&P1$&" "
420    Ipos=0
430    EDIT "L,DT,Te,Fluid,Orientation,Flow,Z - ( END to finish )",I$
440    Istore$(P1)=I$
450    IF I$[1;3]="END" THEN 1850
451    L=FNVal(I$,Ipos)
460    Dt=FNVal(I$,Ipos)
461    Te=FNVal(I$,Ipos)
470    Fluid=FNVal(I$,Ipos)
480    Orientation=FNVal(I$,Ipos)
490    Flow=FNVal(I$,Ipos)
500    Z=FNVal(I$,Ipos)
510 Start_nov:   IF In THEN INPUT "Enter typical plate length(m) and the B.L. te
mperature difference(DegC)",L,Dt
520    IF In THEN INPUT "Is the fluid Air(1),Water(2),Oil(3),or Other(4)?",Fluid
521    IF In THEN INPUT "Enter the mean temperature of the fluid",Te
522    Te=Te+273
```

```
523     IF In THEN P1=P1+1
530     F$=""
540     O$=""
550     M$=""
560     IF Fluid>4 THEN 2700
570     ON Fluid GOTO 590,670,750,820
580     ! CONSTANTS FOR AIR
590     M$="Air"
600     Pnu=((Te-100)/200*.16+.02)*1E-4    !  m^2/s
610     Alpha=((Te-100)/200*.2+.02)*1E-4   !  m^2/s
620     Beta=1/Te          !  1/deg.C
630     Grav=9.81          !  m/s
640     K=((Te-110)/190*14.8+10.1)*1E-3    !  w/m.deg.C
650     GOTO 850
660     ! CONSTANTS FOR WATER
670     M$="Wat"
680     Pnu=7.81E-7        !  m^2/s ~ kinematic viscosity
690     Alpha=1.34E-7      !  m^2/s ~ diffusivity
700     Beta=1.0E-6        !  1/deg.C ~ expansion coefficient
710     Grav=9.81          !  m/s^2
720     K=.583             !  w/m.degC ~ conductivity
730     GOTO 850
740     ! CONSTANTS FOR OIL
750     M$="Oil"
760     Pnu=4.4E-6         !  m^2/s ~ kinematic viscosity
770     Alpha=7.03E-8      !  m^2/s ~ diffusivity
780     Beta=7.2E-4        !  1/m.deg.C
790     Grav=9.81          !  m/s^2
800     K=.13946           !  w/m.degC
810     GOTO 850
820     LINPUT "Enter new fluid type - (3 characters)",Typ$
830     INPUT "Enter Pnu,Alpha,Beta,Grav,Conductivity for material ",Pnu,Alpha,Be
ta,Grav,K
840     M$=Typ$[1,3]
850     ! CALCULATE THE PRANDTL NUMBER
860     Pr=Pnu/Alpha
870     ! CALCULATE THE GRASHOF NUMBER
880     Gr=Grav*Beta*L^3*Dt/Pnu^2
890     ! CALCULATE THE RAYLEIGH NUMBER
900     Ra=Gr*Pr
910     ! WALL ORIENTATION
920     BEEP
930     IF In THEN INPUT "Is the wall vertical(1),horizontal(2),or inclined(3)",O
rientation
940     IF Orientation>3 THEN 930
950     ON Orientation GOTO 970,1120,1370
960     ! VERTICAL WALL
970     O$="Ver"
971     S$=" - "
980     IF Ra<1.0E5 THEN 1740
990     IF (1.0E5<Ra) AND (Ra<1E9) THEN 1020
1000    IF (1E9<Ra) AND (Ra<1E14) THEN 1060
1010    GOTO 1740
1020    F$="Lam"
1030    C=.59
1040    N=1/4
1050    GOTO 1090
1060    F$="Tur"
1070    C=.1
1080    N=1/3
1090    H=C*K/L*Ra^N
1100    GOTO 1770
1110    ! HORIZONTAL WALL
```

```
1120   O$="Hor"
1130   BEEP
1140   IF In THEN INPUT "Is the flow upper surface heated(1),or upper surface co
oled(2)?",Flow
1150   IF Flow>2 THEN 1140
1160   ON Flow GOTO 1170,1220
1170   S$=" UH"
1180   IF Ra<1E6 THEN 1740
1190   IF (Ra>1E6) AND (Ra<2E7) THEN 1280
1200   IF (Ra>2E7) AND (Ra<3E12) THEN 1320
1210   GOTO 1740
1220   S$=" UC"
1230   IF Ra<3E5 THEN 1740
1240   IF Ra>3E12 THEN 1740
1241   F$="Lam"
1250   C=.27
1260   N=1/4
1270   GOTO 1090
1280   F$="Lam"
1290   C=.54
1300   N=1/4
1310   GOTO 1090
1320   F$="Tur"
1330   C=.2
1340   N=1/3
1350   GOTO 1090
1360   ! INCLINED WALL
1370   O$="Inc"
1380   BEEP
1390   IF In THEN INPUT "Is the flow upper surface heated(1),or upper surface co
oled(2)?",Flow
1400   IF Flow>2 THEN 1390
1410   ON Flow GOTO 1420,1470
1420   S$=" UH"
1430   IF Ra<1E6 THEN 1740
1440   IF (Ra>1E6) AND (Ra<2E7) THEN 1540
1450   IF (Ra>2E7) AND (Ra<3E20) THEN 1590
1460   GOTO 1740
1470   S$=" UC"
1480   IF Ra<3E5 THEN 1740
1490   IF Ra>3E12 THEN 1740
1491   F$="LAM"
1500   C=.27
1510   N=1/4
1520   D=1
1530   GOTO 1640
1540   F$="Lam"
1550   C=.54
1560   N=1/4
1570   D=1
1580   GOTO 1640
1590   F$="Tur"
1600   C=.1
1610   N=1/3
1620   D=8
1630   GOTO 1640
1640   DEG
1650   IF In THEN INPUT "Angle of inclination?",Z
1660   IF (-90<Z) AND (Z<0) THEN 1680
1670   IF (90>Z) AND (Z>0) THEN 1700
1680   H=K/L*C*(Ra*COS(Z))^N
1690   GOTO 1770
1700   H=K/L*C*(Ra*(COS(Z)+D*SIN(Z)))^N
```

```
1710   GOTO 1770
1720   ! COEFFICIENT
1730   BEEP
1740   INPUT " Value of Ra does not lie within set limits...Re-calculate?...Yes(
1),No(2)",Again
1750   IF Again>2 THEN 1960
1760   ON Again GOTO 420,1810
1770   A$(P1+3)=""
1780   OUTPUT A$(P1+3)[1,80] USING Form;P1,L,Dt,Te,M$,F$,S$,O$,Pr,Gr,Ra,H
1790   Case=1
1800   IF NOT In THEN GOTO Start_exp
1810   IF In THEN INPUT "Another case?...Yes(1),No(2)",Case
1820   IF Case>2 THEN 1810
1830   ON Case GOTO 380,1940
1840 Form:   IMAGE 3X,"|",DD,"|",2(DD.DD,"|"),DDD.,"|",4(3A,"|"),3(MD.DE,"|"),4D
.2D,"|",1X
1850   LINPUT "DO YOU WANT TO STORE THE INPUT DATA",Y$
1860   IF Y$[1,1]="N" THEN 1940
1870   EDIT "ENTER FILENAME FOR STORED DATA - (&MSUS) ",File$
1880   ASSIGN #1 TO File$,X1
1890   IF NOT X1 THEN PURGE File$
1900   CREATE File$,1,P1^40+4
1910   ASSIGN #1 TO File$
1920   REDIM Istore$(P1)
1930   PRINT #1;P1,Istore$(*)
1940   LINPUT "OUTPUT TO 'S' FOR SCREEN,'I' FOR INTERNAL AND 'E' FOR EXTERNAL PR
INTER",Y$
1941   PRINTER IS 16
1945   IF Y$[1,1]="I" THEN PRINTER IS 0
1950   IF Y$[1,1]="E" THEN PRINTER IS 10
1960   LINPUT "ENTER TITLE TO PRECEED TABLE ((75 Chars)",Tit$
1970   L=(80-LEN(TRIM$(Tit$)))/2
1980   N=P1
1990   A$(1)="    ***************************************************************
********"
1992   A$(3)="    ***************************************************************
********"
2010   A$(2)="   |No|Leng.|Del T| Te |Flu|Flo|Srf|Inc|    Pr  |    Gr  |    Ra
| Film C|"
2030   A$(N+4)="    ***************************************************************
**********"
2040   PRINT LIN(1);SPA(18);" FILM COEFFICIENTS DUE TO FREE CONVECTION ";LIN(2
)
2050   PRINT SPA(L);TRIM$(Tit$);LIN(1)
2060   FOR I=1 TO N+4
2070   PRINT A$(I)[1,75]
2090   NEXT I
2100   STOP
2110   DEF FNVal(I$,Ipos)
2120   Jpos=POS(I$[Ipos+1],",")+Ipos
2121   IF Ipos=Jpos THEN Jpos=LEN(I$)+1
2130   Val=VAL(I$[Ipos+1,Jpos-1])
2140   Ipos=Jpos
2150   RETURN Val
2160   FNEND
```

APPENDIX G

Technical Basis of THETA Program

The background of the THETA program is described in references (13 & 14). A summary of the theoretical basis and numerical algorithms is given below.

Solution of Equilibrium Equations

From the heat flow properties of the elements can be assembled the thermal equilibrium equations for the entire system which have the form

$$C\dot{T} + KT = Q \qquad (1)$$

where C is the heat capacity matrix
K is the heat conduction matrix
Q is the vector of nodal heat inputs
T is the unknown temperature vector
$\dot{T}$ is the unknown temperature derivatives vector with rexpect to time

Depending on the problem type, several different categories of solution are outlined.

Steady States with Constant Conductivities

In the case of a steady state solution, time derivatives are zero, and Equation 1 reduces to the set of linear simultaneous equations

$$KT = Q \qquad (2)$$

Steady States with Temperature Dependent Conductivities

In this case the heat conduction matrix can be expressed as

$$K = K_1 + K_n(T) \qquad (3)$$

where K_1 refers to the linear components of conductivity and K_n to the non-linear terms which are functions of the unknown temperatures T. Any radiation effects appear wholly in K_n, introducing terms containing T^3.

The equilibrium equations can now only be solved iteratively, starting with some guess at the temperature distribution, say T_o, in order to calculate a better estimate T_1 using

$$K_1 T_j = Q - K_n(T_{j-1})T_{j-1} \tag{4}$$

where T_j is the jth iteration to the required temperatures. T_o could be taken as the mean equilibrium temperature calculated from an approximation to the overall heat transfer across the system boundary, or a better estimate obtained by application of Equation 2. Equation 4 may be solved repeatedly until successive iterations give temperature estimate within some preset tolerance. T^3 terms introduced by radiation conductors may cause divergence unless corrective measures are taken.

Transients with Constant Conductivity and Specific Heat

Equation 1 may be recast as

$$C\dot{T} + KT = Q(t) \tag{5}$$

in which nodal heat inputs Q are now some function of time t.

A practical solution procedure is to assume that over a small time interval $dt = t_i - t_{i-1}$ the temperature derivatives are constant so that

$$\dot{T} = \frac{1}{dt}(T_i + T_{i-1}) \tag{6}$$

and at the end of the time interval

$$\frac{1}{dt} C(T_i - T_{i-1}) + KT_i = Q(t_i) \tag{7}$$

which can be recast to give

$$(\frac{1}{dt} C + K)T_i = Q(t_i) + \frac{1}{dt} CT_{i-1} \tag{8}$$

Knowing then a temperature distribution at some time t_{i-1} and the heat inputs at some time $t_i = t_{i-1} + dt$ the temperature distribution at time t_i can be obtained from the solution of the linear simultaneous equations 8. By considering a sequence of consecutive time intervals, the time history of the temperature distribution may be computed. For equal time intervals each solution involves the identical matrix on the left hand side of Equation 8, and only the right hand side is changing. Consequently, if we choose to solve the equations by the Choleksy process, we can preserve the triangular factor of the left

hand side as generated during the first solution, so that most of the arithmetic involved in solving for subsequent right hand sides is avoided and the solution process considerably speeded up.

Transients with Temperature Dependent Conductivity

Substituting K in Equation 8 using Equation 3 gives the relationship which transforms temperatures T_{i-1} at the beginning of a time step into T_i at the end as

$$(\frac{1}{dt} C+K_1)T_i = Q(t_i)+\frac{1}{dt} CT_{i-1}-K_n(T_i)T_i \quad (9)$$

As with Equation 4, the right hand side term is a non-linear function of the unknown temperatures T_i, and must be solved iteratively starting with some estimate $T_{i,o}$ of temperatures T_i, provided say by the solution to Equation 8. Successively better approximations $T_{i,j}$ may be obtained by solving

$$(\frac{1}{dt} C+K_1)T_{i,j} = Q(t_i)+\frac{1}{dt} CT_{i-1}-K_n(T_{i,j-1})T_{i,j-1} \quad (10)$$

repeatedly, until within acceptable limits $T_{i,j}$ $T_{i,j-1}$

Transients with Temperature Dependent Conductivity and Specific Heat

Non-linear specific heat effects require further terms to be included on the right hand side of Equation 9, which if $C=C_1+C_n(T)$ can be written as

$$(\frac{1}{dt} C_1+K_1)T_i=Q(t_i)+\frac{1}{dt} C_1T_{i-1}-K_n(T_i)T_i+\frac{1}{dt} C_n(T_i)(T_i-T_{i-1}) \quad (11)$$

An iterative scheme similar to Equation 10 enables the temperatures T_i to be calculated from known values T_{i-1}, taking account of property non-linearities.

Convergence may be assisted by incorporating into the left hand side of the equation terms approximating to the non-linear components, for example

$$(\frac{1}{dt} C_1+\frac{1}{dt} C_n(T_a)+K_1+K_n(T_a)) \quad (12)$$

may be used in which T_a is an approximate estimate of the required temperature vector. T_a may in its simplest form be a user's estimate of the average temperature level of the solution, or more elegantly but at the expense of

an additional solve operation, T_a may be estimated as

$$(\frac{1}{dt}C_1+K_1)T_a = Q(t_i) \tag{13}$$

Formation of Conductivity Links

The forms of the individual link equations which are combined to make up the heat conduction matrix K for the entire system are cast such that the left hand side includes an approximatin to non-linear terms, balanced by appropriate correction terms on the right hand side.

Taking the example of heat conduction through the body of the system between nodes a and b, then

$$\frac{kA}{L}\begin{bmatrix} 1 & -1 \\ -1 & 1 \end{bmatrix}\begin{bmatrix} T_a \\ T_b \end{bmatrix} = \begin{bmatrix} Q_a \\ Q_b \end{bmatrix} \tag{14}$$

where the link conductivity depends on material conductivity k, link cross section area A and length L. Taking $K_o=k_oA/L$, where k_o is material conductivity based on an original temperature estimate, and $K_c = k_cA/L$, where k_c is the material conductivity based on the previous temperature estimate is given by

$$\begin{bmatrix} K_o & -K_o \\ -K_o & K_o \end{bmatrix}\begin{bmatrix} T_{aj} \\ T_{bj} \end{bmatrix} = \begin{bmatrix} H_a-K_cT_{a,j-1}+K_oT_{a,j-1}+K_cT_{b,j-1}-K_oT_{b,j-1} \\ H_b-K_cT_{b,j-1}+K_oT_{b,j-1}+K_cT_{a,j-1}-K_oT_{a,j-1} \end{bmatrix} \tag{15}$$

After repeated solutions of this equation, updating the right hand for K_c but maintaining the left hand side containing K_o, successive temperature estimates approach each other and correction terms balance out.

APPENDIX H

The following pages summarize some of the useful facts concerning the major symbols and their units, as used in this report. It was discovered during the process of this work that due to the three systems of units in common use, S.I., Metric and Imperial, that there was ample opportunity for error when performing the calculations. Table 8 states the preferred S.I. units of the main quantities used in the analysis and Table 9 shows the equivalent units for the other two systems. Tables 10-11 state the conversion factors between S.I. and the other systems and Table 12 gives some commonly used values for the materials encountered in the analytical models of this report. It was thought that the definition of the various dimensionless groups would also be useful and they are shown in Table 13. Finally, radiation emissivity values are given in Table 14 for a number of typical surfaces encountered in the analysis of ships hulls under Arctic conditions.

NOMENCLATURE

Commonly used symbols:

ρ	Density
g	Gravitational constant
β	Expansion coefficient of air
T	Temperature
L	Characteristic length
Gr	Grashof number
h	Surface coefficient
K	Conductivity
Nu	Nusselt number
q	Heat flux
A	Area
f	View factor
σ	Stefan-Boltzman constant
Pr	Prandtl number
δ	Velocity boundary layer thickness
δ_t	Thermal boundary layer thickness
u	Fluid velocity (parallel to x-axis)
gv	Fluid velocity (parallel to y-axis)
P	Pressure
μ	Viscosity
Cp	Specific heat
R	Universal gas constant

ν	Kinematic viscosity
Re	Reynolds number
θ	Dimensionless temperature change
α	Thermal diffusivity
c	1st constant in formula for Nusselt number
n	2nd constant in formula for Nusselt number
d	Constant in formula for surface coefficients
$\hat{f}_{12}$	Factor in calculation of radiation
F_{12}, F_{12}	Configuration factors for radiation
ε	Emissivity from a surface
H	Matrix of shape functions
B	Matrix of shape function derivatives
ψ	Stream function
ω	Vorticity
Bi	Biot number

Preferred Units (SI)

Length	- Metre (m)
Mass	- Kilogram (kg)
Temperature	- K ($0^{\circ}C$ = 273.15 K)
Density	- kg/m^3
Quantity of heat	- Joules (J)
Heat flow	- Joules/Second (W)
Surface heat flux (flux density)	- W/m^2
Internal heat flux	- W/m^3
Heat capacity	- J/kg
Thermal conductivity	- $W/m \cdot K$
Specific heat	- $J/kg \cdot K$
Surface coefficient of heat transfer	- $W/m^2 \cdot K$
Dynamic viscosity	- $kg/m \cdot s$ $(N \cdot S/m^2) = Pa \cdot s$
Kinematic viscosity	- m^2/S
Stefan-Boltzmann	- $W/(m^2 \cdot K^4)$

Table 8

PARAMETER		IMPERIAL	SI	METRIC
Temperature	(T)		K or ^{o}C	^{o}C
Quantity of heat	(Q)	Btu	Joules (J)	cal
Heat flow	(q)	Btu/hr.	W (J/sec)	cal-kg/hr
Heat capacity	(C)	Btu/lb.	J/kg	cal/g
Thermal conductivity	(k)	Btu/hr·ft.^{o}F	W/m · K	cal/s·cm ^{o}c
Coefficient of heat transfer	(h)	Btu/hr·ft.^{2} ^{o}F	W/m^{2}· K	cal/s·cm^{2} ^{o}C
Radiant intensity	(I_e)		W/sr	
Thermal resistance		hr ^{o}F/B.t.u.	K/W	^{o}C s/cal
Thermal resistivity Thermal diffusivity	(k/ρc)	ft^{2}· hr	m·K/w	
Specific heat	(c)	Btu/lb^{o}F	J/(kg · K)	cal/g ^{o}C
Kinematic viscosity	ν	H^{2}/hr	m^{2}/S	cm^{2}/S

Table 9

HEAT TRANSFER UNITS

(Equivalents in other common systems)

IMPERIAL	SYMBOL	S.I.
^{o}F	T	$(^{o}F - 32) \times \frac{1}{1.8}$ ^{o}C
		$K = {}^{o}C + 273.15$
1 Btu	Q	1055.04 J
1 Btu/hr	q	0.2931 W
1 Btu/hr·ft^2	q/A	3.154 W/m^2
1 Btu/lb	C	2326 J/kg
1 Btu/hr·ft ^{o}F	k	1.7303 W/m^{o}C
1 Btu/lbm ^{o}F	Cp	4186.7 J/kg ^{o}C
1 Btu/hr·ft^2 ^{o}F	h	5.677 W/m^2 ^{o}C
lbm/ft^3	ρ	16.019 kg/m^3
lbm/ft-hr	μ	4.134 x 10^{-4} kg/m·s
ft^2/hr	ν	2.58 x 10^{-5} m^2/s

Table 10

CONVERSION FACTORS BETWEEN OTHER COMMON UNITS AND S.I.

If the original units are Imperial

METRIC	SYMBOL	S.I.
^{o}C	T	^{o}C
1 cal	Q	4.1868 J
1 kcal/hr	q	1.163 W
1 cal/g	C	4186.8 J/kg
1 cal/s m ^{o}C	k	4.1868 W/m ^{o}C
1 cal/g ^{o}C	C_p	4186.8 J/kg ^{o}C
1 kcal/hr m^2 ^{o}C	h	1.163 W/m^2 ^{o}C
stoke $(\frac{cm^2}{s})$	ν	1 x 10^{-4} m^2/s

Table 11

CONVERSION FACTORS BETWEEN OTHER COMMON UNITS AND S.I.
If the original units are Metric

	Steel (1020)	Sea Water 20°C	Ice 0°C	Air* (0°C)	Marine Diesel Fuel
Conductivity k W/m °C	52.	0.5686	2.	2.4×10^{-2}	0.138 (15°C)
Specific Heat Cp J/kg °C	448.	3900.	2086	1031.	-
Density ρ kg/m^3	7860.	1025.	920.	1.293	917.88
Diffusivity $(\frac{k}{\rho c_p})$ m^2/s	14.8×10^{-6}	0.142×10^{-6}	1.04×10^{-6}	1.8×10^{-5}	-
Linear Expansion α 1/°C	$15. \times 10^{-6}$	-	51×10^{-6}	-	-
Cubic expansion α 1/°C	-	2.1×10^{-4}	-	3.66×10^{-3}	7.2×10^{-4} (15 °C)
Kinematic viscosity ν m^2/s	-	9.7×10^{-7}	-	1.3×10^{-5}	$1.7\text{-}4.4 \times 10^{-6}$ (6.7°C)

Table 12

COMMONLY USED VALUES OF HEAT TRANSFER CONSTANTS

* Properties vary linearly as a function of temperature.

Group	Symbol	Formula	Application	Physical Significance
Fourier	Fo	$kt/c\rho L^2$	Conduction, unsteady	Ratio of heat diffusion to heat storage
Nusselt	Nu	hL/k	Convection, natural and forced	Ratio of characteristic length to equivalent laminar film thickness
Prandtl	Pr	$\mu c/k$	Convection, natural and forced	Ratio of diffusivity of heat to that of momentum
Grashof	Gr	$L^3\rho^2\beta g\Delta T/\mu^2$	Convection, natural	(Bouyancy forces) x (inertial forces) (viscous forces)^2
Graetz	Gz	$\dot{M}c/kL$	Convection, laminar	
Reynolds	Re	$\rho VL/\mu$	Convection, forced	Ratio of inertial to viscous forces
Stanton	SE	$h/\rho Vc$ (= Nu/Re Pr)	Convection, forced	Ratio of heat flow through wall to heat flow along wall
Rayleigh	Ra	Gr. Pr.	Convection, natural	

Table 13

DIMENSIONLESS GROUPS USED IN THERMOPHYSICAL ANALYSIS

where $\dot{M}$ = mass flow rate kg/(s)
V = velocity m/(s)
ΔT = temperature difference K

SUBSTRATE AND SURFACE	EMISSIVITY	
Rolled steel plate, rough, oxidized	0.96	
Rolled steel plate, rough, painted, all colours	0.94	
Rolled steel plate, rough, aluminized lacquer	0.65	
Rolled steel plate, rough, white paints	0.18	(solar absorptivity)
Rolled steel plate, rough, non-white paints	0.70	(solar absorptivity)
Rolled steel plate, white-frost covered	0.80	
Aluminum plate, weathered, oxidized	0.32	
Galvanized iron and steel	0.25	
Water and clear ice surfaces	0.97	

Table 14 EMISSIVITY VALUES FOR VARIOUS HULL SURFACES

Note: In the analysis used in this report, and in many engineering applications, Kirchhoff's Law is extended to the assumption of the equality of the surface emissivities and absorptivities for total hemispherical radiation, as well as for directionally and spectrally similar radiation. The emissivity values shown are chosen to be compatible with this assumption. Except as noted the values apply to low temperature, rather than solar radiation.

APPENDIX I

Summary of a Proposal for a Long Term Temperature Monitoring System on Board the M.V. Arctic

The following is a summary of a cost proposal solicited from Weir-Jones Engineering Consultants Ltd., under this contract, for the re-instrumentation of the M.V. Arctic to provide temperature measurements in cells adjacent to the ship's hull plates. The objective is to provide a monitoring system capable of measuring steel surface temperatures, water or air temperatures within the ship and ambient air and water temperatures outside the hull.

System Specification

The temperature sensors would be thermistors encapsulated in a stainless steel tube sealed to the end of an Arctic grade two conductor grease blocked cable. The sensors would be mechanically attached to the tank plating and coated to minimize corrosion. All cabling would be marked with the sensor number. The sea water and hold air sensors would be fitted with penetrators from the instrumented ballast tank to satisfy the criteria of reliability, accuracy and durability. These penetrators would be fitted with isolation ball valves permitting zero leakage sensor removal.

The sensor cables would be led through a deck penetrator located at the same frame as the instrumented cell and routed through a combination of flexible and rigid metal conduit supported at four foot spacing by U-bolts through the bulwark stays approximately six inches below the bulwark top. The chosen route should minimize potential hazards to the cabling due to seas, fuelling lines, mooring lines etc., while also minimizing inconvenience to ships operating personnel, in particular avoiding tripping hazards. The cabling would penetrate the poop front using an approved sealing gland. The gland would be fitted to a welded pipe base, entering the laboratory "ante-room" below the deckhead.

The data acquisition system would consist of a data logger with two wire resistance capability connected to a desktop computer. The desktop computer would acquire and verify the data, perform sensor calibration and linearization to temperature units, store the data on magnetic tape, and provide back-up paper records of the data.

Insofar as the monitoring system proposed involves four penetrations of the ship and new equipment on deck, involvement of regulatory bodies will be required in finalization of designs and/or inspection work. In particular the Montreal representatives of Lloyd's Register of Shipping and the CSI/Coast Guard will need contacting for approval.

A drawing illustrating details from the system described above is given in Figure 110.

Installation Cost Summary

Sensors (100)	$ 5,270.
Cable, Penetrators etc.	6,750.
Total Capital Cost	$12,020.
Mobilization/Demobilization Documentation	$ 5,775.
Installation	$ 8,250.
Expenses	$ 4,200.
Sub total	$30,245.
Contingencies @ 10%	3,025.
TOTAL	$33,270.

These costs are projected for early 1984, and do not include costs for dockside work.

Measurement Costs/Trip

System Rental/Month	$ 3,150.
Mobilization/Demobilization	$ 1,100.
Operation (one technologist)	$ 7,700.
Expenses (assuming accommodation aboard ship)	$ 3,544.
	$15,494.

The measurement costs presume a minimum passage time between Antwerp and Nanisivik of two weeks.

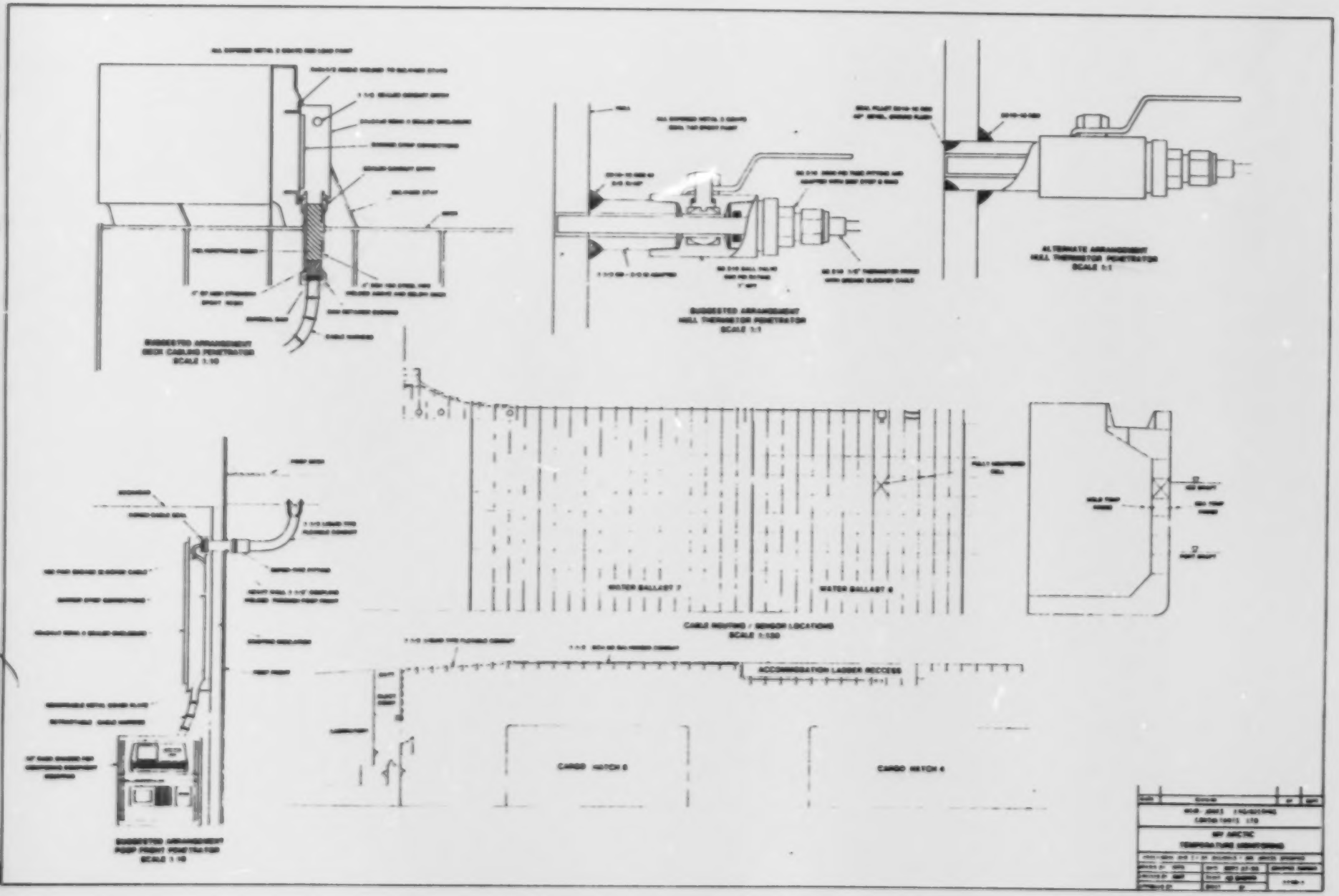

Figure 110 Temperature Monitoring System

APPENDIX J

Recommendations for the Design of a Laboratory Apparatus for the Determination of the Heat Transfer Coefficients in a Ship's Hull

We have made a preliminary approach to the design of an experiment necessary for the determination of the significant physical factors involved in the heat transfer processes under consideration. This has included consideration of the test cell, its boundary surface temperature control subsystems, the necessary instrumentation, and the range of the variables to be investigated.

A basic test cell, built to full scale size but using plate thicknesses of about 20 mm, should be satisfactory because the conduction in the walls is a relatively small factor and can be scaled with good confidence. This would represent a cell of nearly cubical shape, about 2 m in each dimension, and suitable for testing in air filled, water filled, or partially water filled conditions. This basic cell could be modified to include stiffeners of various types, and other details of hull cells to deal with special hull points, where the basic cell would not be representative. Each such basic cell is estimated to cost about $50,000.

The basic instrumentation would require a set of about 125 thermocouples, 10 heat meters, and moveable anemometers of at least two types. A data acquisition and recording system would have to be made available during test runs. The cost of the instrumentation, in the first instance, but not including the data acquisition system, would be about $20,000 to $30,000.

A test facility, able to supply substantial refrigeration to the outer hull wall through either circulating ice water or air, would be required and a corresponding heat source on the inner hull side. This facility might be a part of an existing laboratory, or developed specially for the purpose. The cost might be on the order of $50,000 to $100,000 depending upon the control methods and flexibility required.

The first step in examining this proposal for a full scale test facility would be to make a study of the specific design requirements for the test apparatus, and prepare a preliminary design specification. This study would include the following tasks.

(1) Make preliminary drawings and write specifications for the test cell or cells required to model the actual segments of the double hull designs proposed.

(2) Draw up flow diagrams, control specifications and equipment size specifications for the test cell.

(3) Draw up the instrumentation and recorder requirements.

(4) Draw up the detailed design of the experiments proposed, including the length of each test, the number of tests in a series, the number of technicians and engineers required during the tests, the precision required of the observations, the number of observations to be made during a test, and the manner in which the data would be reduced, analyzed and displayed.

(5) Draw up estimated costs for both the apparatus and the operation of each test.

(6) Investigate the advantages of various sites for the tests, including existing government, university and private laboratories.

Such a study and report would provide a rational foundation upon which future planning and decision-making could be based.